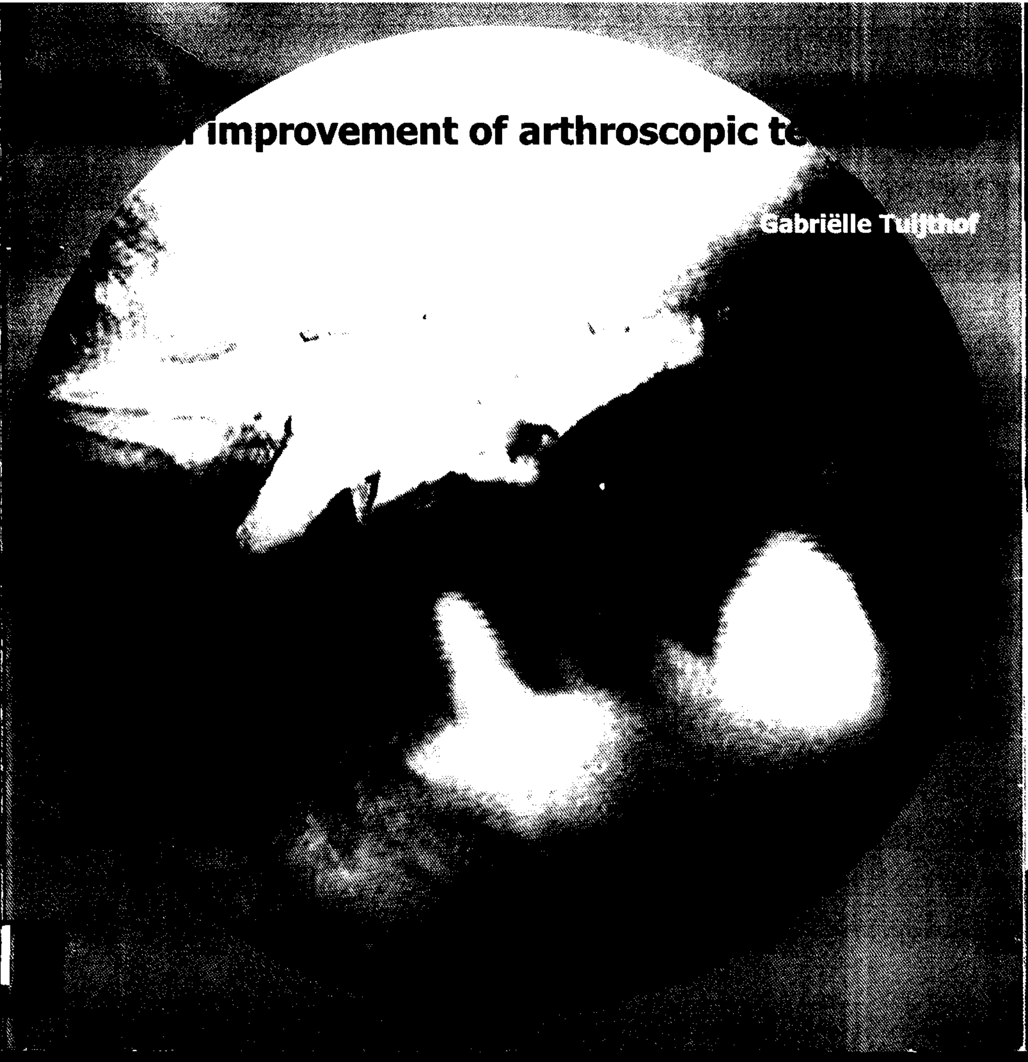

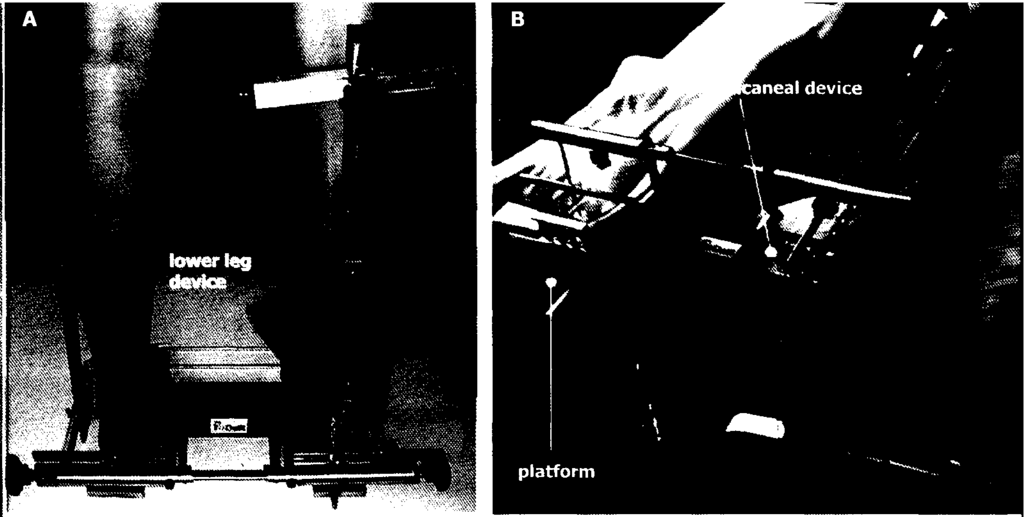

Figure 4.1.2

A. Photograph of a person standing in the measurement system.

B. Photograph of a person lying in prone position in the measurement system.

Figure 4.3.4

C. Close up of the tip.

D. Flexible shaverblade inserted in the shaver holder.

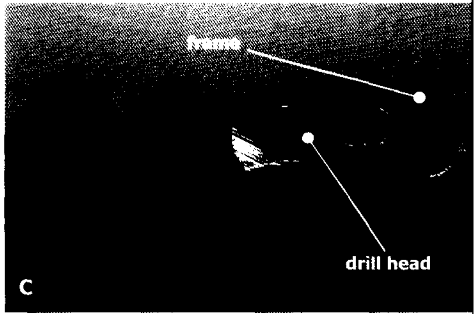

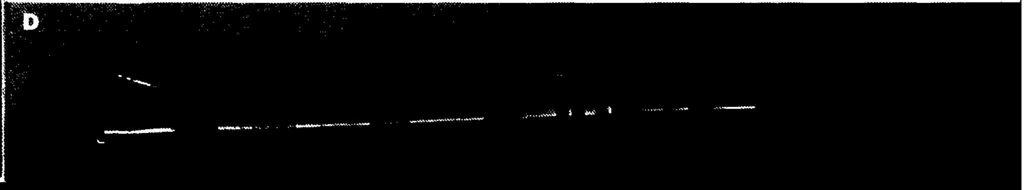

Figure 4.2.6.

A. Photograph of the drilling device clamped onto the working bench to simulate the drilling process. To simulate the milling process the drilling device was clamped at a 90°-angle with the pushing direction of the working bench.

B. Five different drills that were tested. From left to right: standard mill used for the machining of metals (5.5 mm), cylindrical drill of a conventional shaverblade (5.5 mm Stonecutter Acromionizer blade, Smith and Nephew Company, Hoofddorp, the Netherlands), spherical drill (5.5 mm), conical drill (diameter ranging from 2.5 to 5.5 mm), and prototype (5.5 mm). The prototype consists of a hollow tube with a sharp edge.

C. Example of a drilling experiment.

D. Example of a milling experiment.

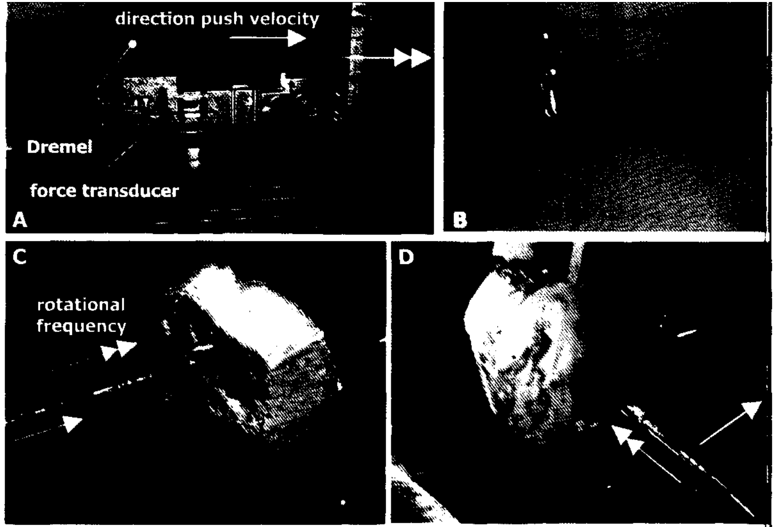

Figure 4.2.3

A. Photograph of the inferior side of a talus showing the axes of the ellipse ($l_{ellipse1}$ and $l_{ellipse2}$).

B. Photograph the superior side of a calcaneus showing the crest line (l_{crest}), crest angle, and the locations of the portals. The alternative crest angle (φ_3) is defined as the angle between the crest line and the axis along the medial side of the calcaneus.

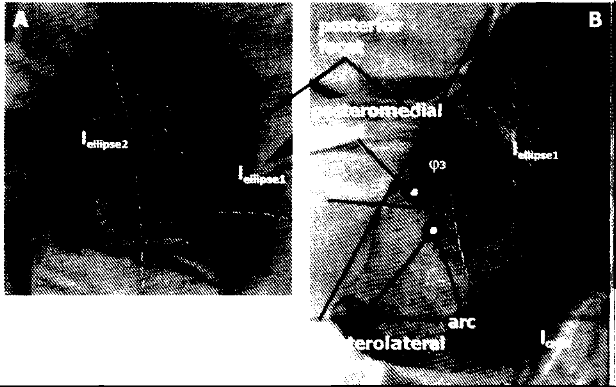

Figure 4.3.6

A. Photograph of the posterior side of one cadaver ankle showing the posterior facet. Half of the posterior facet (till the top of the joint) is machined with the flexible instrument. This resulted in a smooth surface and equally removed portions of tissue on both surfaces.

B. Photograph of the posterior side of the second cadaver ankle showing the posterior facet. The photograph shows that the major part of the joint surface of the calcaneus is machined, but the majority of joint surface of the talus contains still cartilage.

C. Photograph of the second cadaver ankle, showing the subtalar joint space height after machining the joint with the flexible shaverblade.

D. Photograph of the second cadaver ankle showing the flexible shaverblade inserted in the posteromedial portal.

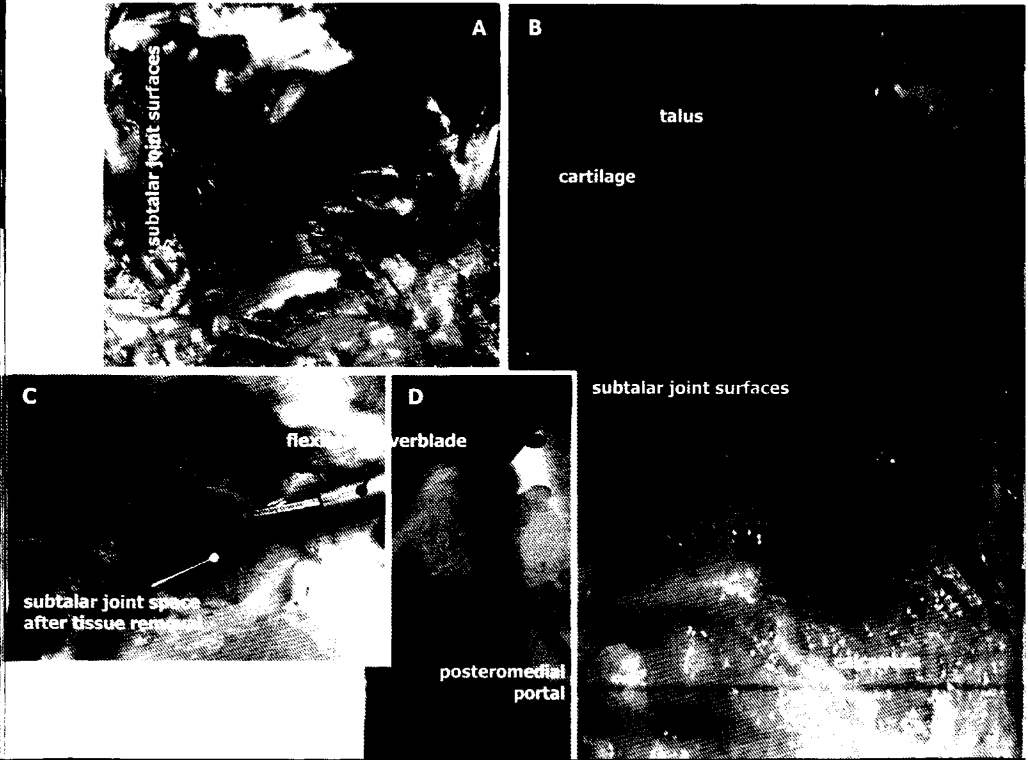

Stellingen behorende bij het proefschrift

Technical improvements of arthroscopic techniques

Gabriëlle Tuijthof

1. Dat er geen consensus bestaat over de optimale stand van de achtervoet ten opzichte van het been van een individuele patiënt is niet verwonderlijk omdat er geen eenduidige en reproduceerbare maat voor deze stand bestaat. *(dit proefschrift)*

2. Het is verwonderlijk dat er consensus bestaat over de absolute noodzaak van een helder zicht tijdens arthroscopische operaties, terwijl er geen consensus is over optimale spoelingscondities of eenduidige richtlijnen. *(dit proefschrift)*

3. Alle subtalaire arthrodeses zijn via een minimaal invasieve techniek uit te voeren in het bijzonder indien de achterste benadering wordt benut.

4. Voor een aantal ziektebeelden zouden arthrodeses overbodig zijn als men beschikt over geschikte prothesen.

5. In tegenstelling tot de beitelmethode waarbij twee platte botoppervlakken gemaakt worden tijdens het uitvoeren van een arthrodese bevordert het aanbrengen van minimaal letsel, waaronder het congruent houden van de oppervlakken, de vergroeiing van de botten.

6. Het loont de moeite om niet te voortvarend aan de slag te gaan als ingenieur.

7. Dankzij de vergrijzing van de populatie vraagt de orthopedie een versnelde ontwikkeling.

8. In tegenstelling tot in de laparoscopie is de ontwikkeling van ergonomische handvatten voor arthroscopie nog niet begonnen.

9. Niettegenstaande de derde wet van Newton is het verschil in tackelen of getackeld worden opmerkelijk groot: de lekkerste tackels maak je zelf.

10. Ondanks dat vrouwen beter in staat zijn over hun gevoelens te communiceren hebben lesbiennes korte relaties.

Deze stellingen worden verdedigbaar geacht en zijn als zodanig goedgekeurd door de promotoren

Prof. Dr. Ir. H.G. Stassen

Prof. Dr. C.N. van Dijk

Technical improvement of arthroscopic techniques

Gabriëlle J.M. Tuijthof

MISIT

Technical improvement of arthroscopic techniques

Gabriëlle Tuijthof

Proefschrift

Ter verkrijging van de graad van doctor
aan de Technische Universiteit Delft,
op gezag van de Rector Magnificus prof. dr. ir. J.T. Fokkema,
voorzitter van het College voor Promoties,
in het openbaar te verdedigen op 24 juni 2003 om 16:00 uur
door Gabriëlle Josephine Maria TUIJTHOF,
werktuigbouwkundig ingenieur,
geboren te Teheran (Iran)

Dit proefschrift is goedgekeurd door de promotoren:

Prof. dr. ir. H.G. Stassen
Prof. dr. C.N. van Dijk

Toegevoegd promotor:
Ir. P.V. Pistecky

Samenstelling promotiecommissie:

Rector Magnificus,	voorzitter
Prof. dr. ir. H.G. Stassen,	Technische Universiteit Delft, promotor
Prof. dr. C.N. van Dijk,	Universiteit van Amsterdam, promotor
Ir. P.V. Pistecky,	Technische Universiteit Delft, toegevoegd promotor
Prof. dr. A. van Kampen,	Katholieke Universiteit Nijmegen
Dr. H. Weinans,	Erasmus Universiteit Rotterdam
Prof. dr. F.C.T. van der Helm,	Universiteit Twente
Prof. ir. A. Beukers,	Technische Universiteit Delft

Dr. ir. J.L. Herder heeft als begeleider in belangrijke mate aan de totstandkoming van dit proefschrift bijgedragen.

Title: Technical improvement of arthroscopic techniques. PhD-thesis, Delft University of Technology, Delft, The Netherlands, datum: 24 juni 2003.
Author: Gabriëlle Josephine Maria Tuijthof.
Design: HD ontwerp, Tilburg.

ISBN: 90-370-0200-5
Printed by: Drukkerij Damen, Werkendam.

To my father

Who stimulated my interest in the world of technology and design.

Reader's guide

This thesis describes the improvement of arthroscopic techniques. Readers who are interested in the approach that was applied throughout the work are advised to read Chapter 2 for the general introduction, and Sections 5.1, and 6.1 for more specific analyses. The work presented addresses three seperate topics: the development of a new arthroscopic technique for performing a subtalar arthrodesis *(Chapter 3 and 4)*, the optimization of arthroscopic view *(Chapter 5)*, and the development of a steerable punch *(Chapter 6)*. Each of these chapters can be read independently. Furthermore, nearly all sections are based on papers, which has the advantage that they can also be read separately. The consequence is that there is often a small overlap, when reading a chapter completely. Chapter 7 will tie all chapters together and evaluates the design approach in this thesis.
Readers without a medical or an orthopaedic background are strongly advised to read Section 1.2 and all introductions of the three seperate topics. There, the necessary medical information to comprehense the rest of the work is briefly given. If additional detailed infomation is desirable, the literature, which is given per chapter, can be consulted. An elaborate list of terms is added in which the medical terms that are used in this thesis are clarified.
For readers without a technical background it was attempted to describe the principles as clear as possible supported by drawings, and formulas were built up step by step. Again it is advised to consult the literature if additional information is required. An elaborate list of symbols was set up to prevent confusion.

Contents

1. Introduction

1.1 Arthroscopy

In the past twenty-five years orthopaedic surgery has made a tremendous progress by means of the development of minimally invasive surgery.[1-3] The minimally invasive field of orthopaedic surgery is called arthroscopy which is derived from the Greek words arthro- *(= joint)* and skopein *(= to examine)*. This implies that the operation is performed through small incisions in the skin, and that the operation area is visualized by means of an arthroscope *(Figures 1.1.1 and 1.1.2)*. The main difference between an open orthopaedic and an arthroscopic procedure is the size of the incision through which the operation is carried out. This difference has great impact on every aspect of the procedure. As is indicated in numerous documents[1,5-8] the main advantage of endoscopic surgery is the quicker recovery of the patient due to the shorter operation time as well as the facts that the patient does not have to be hospitalized, the risk of wound infections is diminished, and the patient can be completely recovered within a couple of weeks due to less trauma to healthy tissues. However, the arthroscopic techniques require good surgical skills and knowledge of the anatomy. Especially, the limited workspace within joints, the limited choice of available access locations in combination with indirect sight, and less available degrees of freedom of the instruments due to the incision make the performance of a treatment difficult.[9]

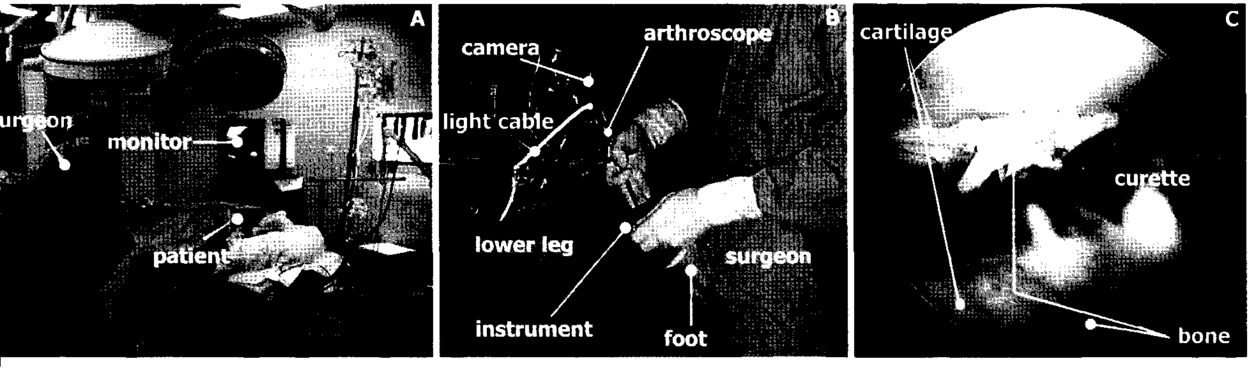

Figure 1.1.1
A) An overview picture of the operation room.

B) Close up of an operation on the ankle joint performed with a two-portal approach.

C) Example of a typical arthroscopic view of a subtalar joint that is located in the hindfoot. The white cartilage can be clearly seen as well as the magnification of the view, which can be derived from the size of the curette which is 3.5 mm.

To be able to perform an arthroscopic operation a number of instruments and devices has been developed, which can be divided in a basic set of instruments and equipment, and additional instruments that are used for specific procedures. In the following chapters, any specific procedure *(subtalar arthrodesis, meniscectomy)* that is addressed to will be described in the chapter in question. The basic instrument set used for arthroscopic procedures will be described here, followed by an introduction to specific arthroscopic treatments in which important characteristics are elucidated.

Basic instruments

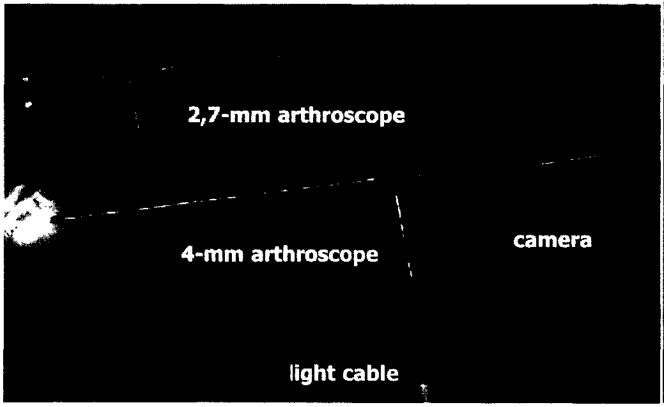

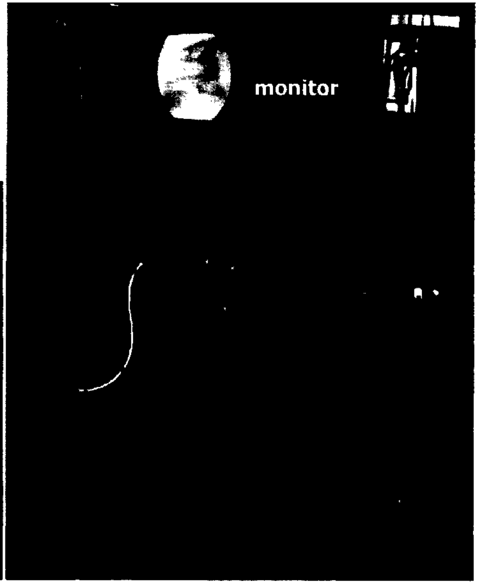

Figure 1.1.2
Arthroscopes (diameter 2.7 and 4 mm), light cable, camera, and monitor.

Arthroscope, light cable, camera and monitor *(Figure 1.1.2)*
To visualize the interior of a joint a 30°-angled arthroscope is usually used. Due to its angled viewpoint the arthroscope can be used as a periscope. For operations in larger joints *(knee, shoulder)*, a 4-mm arthroscope is used, whereas for small joint surgery *(wrist, elbow, and toe)* a 2.7-mm arthroscope is used. For the ankle joint both 4-mm and 2.7-mm scopes can be routinely used. A light source is integrated in the scope to illuminate the operation area, and a camera is attached to the scope that projects the 2D-images on a monitor.

Probe, punch, curette, and forceps *(Figure 1.1.3)*
The probe is an important instrument that gives tactile information on the condition of tissues to the surgeon. It is accomplished by visual inspection of the tissue that is being probed. The punch is used for the cutting of tissues other than bone, for example ligaments, menisci, and

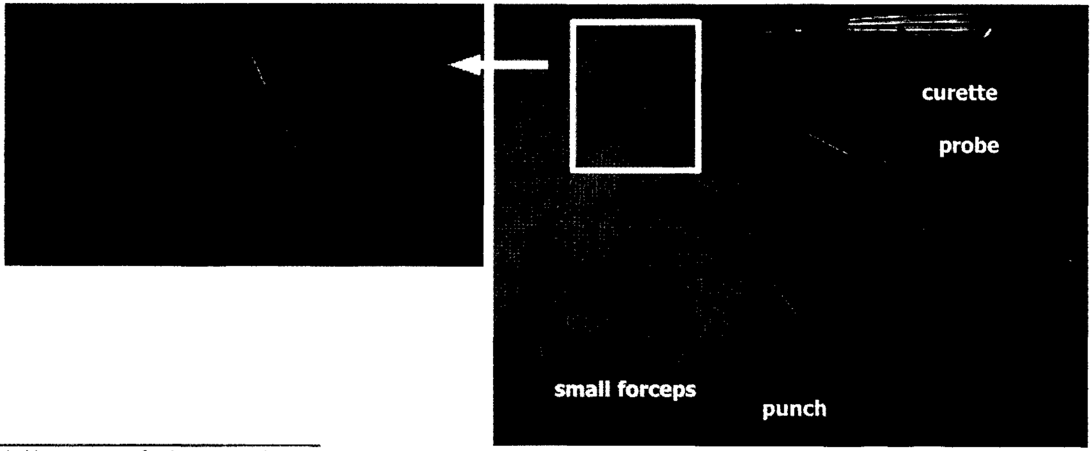

Figure 1.1.3
Probe (diameter is 3.5 mm), punch, curette, and forceps.

adhesions. A large number of punches is available that have a slightly different end-effector *(Chapter 5)*. The curette is used for the removal of cartilage tissue. With a forceps relatively large pieces *(about 10mm³)* can be removed from a joint.

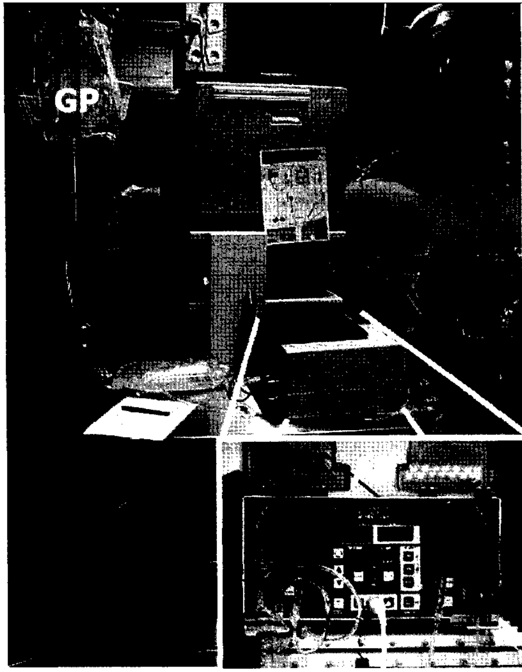

Figure 1.1.4
Color illustration see cover. Two types of irrigation systems: the gravity pump (GP), and an automated pump (AP). More specific information can be found in Chapter 5.

Irrigation system *(Figure 1.1.4)*
An irrigation system serves to irrigate a joint from blood and debris with liquid and to achieve distention of a joint by the liquid pressure during the operation. Several types of irrigation systems are available, of which the gravity pump is the most commonly used pump and operates by the pressure difference generated by a height difference between a liquid reservoir and the joint. Automated pumps aim at facilitating the irrigation process in order to give the surgeon the opportunity to focus on the treatment itself. The automated pumps consist of one or two volumetric pumps that are controlled by a feedback controller that uses the pressure at a certain location as control input. In Chapter 4 both types of irrigation systems will be elucidated in detail.

Sheath and cannula *(Figure 1.1.5)*
The arthroscope is inserted in a sheath that protects it when moving the arthroscope around in a joint. A separate cannula is used in the large joints *(knee, shoulder)* as a separate in- or outflow channel for faster irrigation. The combination of the sheath and cannula provides the in- and outflow of irrigation liquid to the joint.

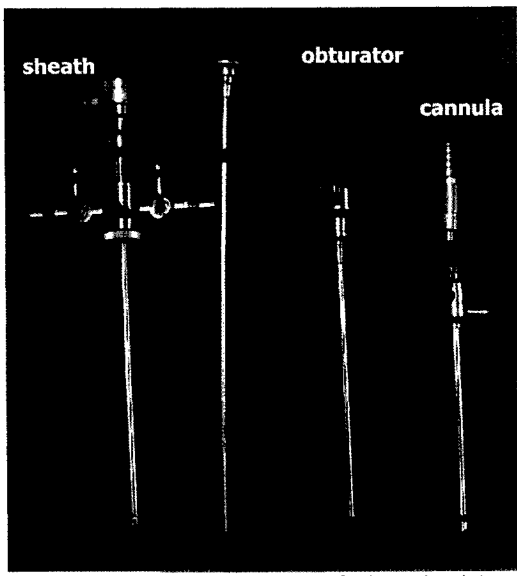

Figure 1.1.5
Sheath (inner diameter is 4.5 mm and outer diameter is 5 mm) and cannula.

Shaver and suction punch *(Figure 1.1.6)*
The shaver is a cutting device with which soft tissue as well as bony tissue can be cut, and immediately removed by suction. The shaver consists of two concentrically placed tubes of which the inner tube can rotate with a variable speed. Suction can be performed with a separate suction device when using the gravity pump. In several automated pumps the suction is integrated in the pump. The tissue is tensioned in the shaver

Figure 1.1.6
Shaver system with different shaverblades (diameters range from 1.9 to 5.5 mm), and suction punch (diameter is 5.2).

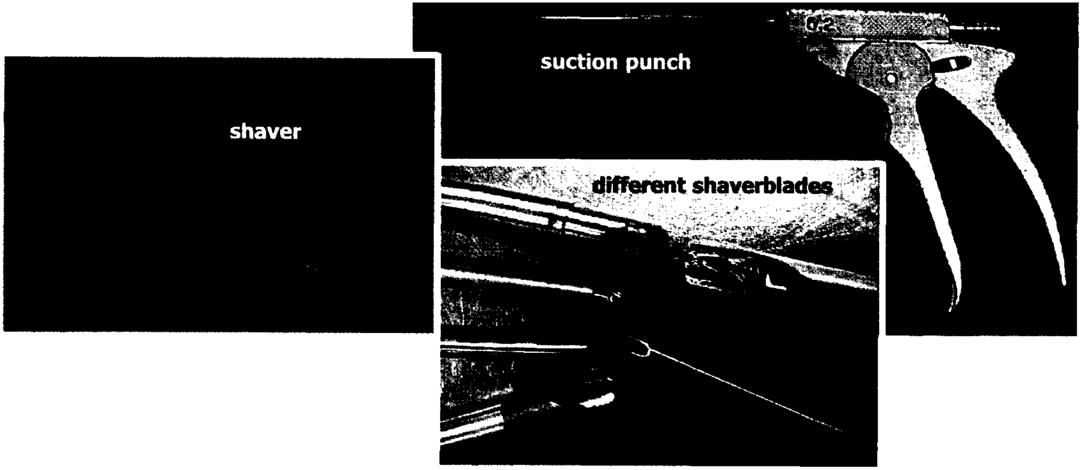

by means of suction, which enables easy cutting. This facility is missing in a punch which sometimes gives difficulty to cut soft tissue. To solve this problem a suction punch has been developed, but the pieces cut with this device are often too large for easy suction.

Tourniquet *(Figure 1.1.7)*
The tourniquet is placed proximally around the upper leg when operation takes place below the hip joint. By pressurizing this device, the blood supply to the extremity is blocked and less bleedings occur during an operation.

Figure 1.1.7
Tourniquet.

Arthroscopic treatments
Treatments in arthroscopy can be roughly categorized in removal surgery and reconstruction surgery. Examples of removal surgery are the meniscectomy[10], and the removal of loose bodies *(bone fragments)* and adhesions. A meniscectomy is a procedure in which the damaged parts of menisci, located in the knee joint, are removed *(Chapter 5)*.
The procedures belonging to the category of removal surgery can be divided in an opening phase in which access is created to the joint, and the joint is visually inspected to verify the

diagnosis. This is followed by the treatment *(tissue removal)* phase, and a closing phase in which the joint is irrigated and the incisions are sutured. Examples of reconstruction surgery are the cruciate ligament reconstruction, tendon transplantation, and rotator cuff repair.[11-13] The cruciate ligament is located in the knee joint, and serves to resist loads on the knee joint. The ligament can be torn, caused by trauma, and reconstructed again with the help of an autograft or an allograft. The autografts most often used are the middle 1/3 of the patella tendon or part of the hamstrings. In cases of posterior tibial tendon dysfunction *(located medially of the ankle joint)*, one of the possible treatments is transplantation of the peroneal tendons to restore the muscle balance around a joint. The rotator cuffs consist of three muscle/tendon structures, and shoulder dysfunction occurs when they are damaged.

The procedures belonging to the reconstruction surgery category can be divided in five phases. The first phase consists of the same opening phase as for removal surgery. In the second phase the reconstruction is prepared, followed by the reconstruction itself in the third phase, and in the fourth phase verification of the intended reconstruction takes place. The last phase is the closing phase which is the same as for removal surgery. The description of specific techniques for joints or pathologies can be found in handbooks[4,7,8,10,14], and the different techniques will be described in the chapter in question.

1.2 Development of arthroscopic instruments

As was stated by Sjoerdsma[15], there are two main groups of people involved in the development of surgical techniques and instruments. There is the group of experimental orthopaedic surgeons who try to solve problems experienced in clinical practice. They suggest only little adjustments or they give advice on using a certain technique usually published in a technical note.[11,16-20] In addition to this, it is common in orthopaedics to present the development of new portal placements, and the testing of new devices *(for example electrosurgical devices, lasers, anchors, or knot tying)* as new developments. However, in most articles of this kind, no attention is paid to the construction or conceptual design of the actual instrument. An aspect may be that surgeons do not have a sufficient technical background to specify the inconveniences they encounter into technical specifications and designs. Finally, surgeons are usually so used to their techniques that they cannot always indicate inconveniences.

Another group that introduces new techniques in the field of arthroscopy is the community of manufacturers of arthroscopic instruments. These companies sometimes receive feedback of the clinical practice from their salesmen, who mostly lack an engineering background, and they can merely transmit the problems signaled by the surgeons. In addition to this, the main interest of the companies is to make profit which leads to the development of techniques that are profitable like implant *(hip and knee prostheses)*[21] or fixation techniques[22]. In addition to this, less attention will be paid to other techniques as for instance small joint arthroscopy or soft tissue endoscopy.[5,23] To reduce the costs of development, the existing instruments are often slightly adjusted or devices are developed that stem from existing technology which is applied to the surgical field.[24,25] This bears the risk that devices are brought to the market that do not fulfill the requirements of the surgeon or to which insufficient attention is paid to the human-machine interaction. Examples are the large number of punches with only slightly different end-effectors

(Chapter 5), and the introduction of laser technology. The laser systems have high potential, but are not always rewarding, because these systems are difficult to use when sufficient technical background or training is missing.[26,27]

In literature, a report was found on instrument-related complications in which for example the fabrication methods are addressed.[28] A number of these complications is solved, nowadays. However, from personal communication and the great number of technical notes, it can be stated that surgeons still endure inconveniences when operating. These can be solved by the development of simple mechanical instruments once the actual problem is analyzed.

1.3 Goal and approach

As appears from Section 1.2, in the development of arthroscopic instruments sufficient communication between the users and the developers or manufactures is missing, leaving unsolved problems indicated by surgeons or developing instruments with limited use. The point of attention in this thesis will be the improvement of the techniques and the instruments used in arthroscopy. To achieve improvements, the philosophy is emphasized that developments should be guided by the clinical practice and by the requirements of the surgeons. The opinion is that starting a thorough analysis of the requirements or inconveniences from scratch will lead to the development of useful and simple instruments that can be straightforwardly handled. If the arthroscopic techniques are improved and are facilitated according to the needs of the surgeon, it is expected that an operation can be performed more safe, efficient *(defined as fast while performing a minimum number of actions)*, accurate, and with less damage of healthy tissue. This will result in a quicker recovery of the patient. Furthermore, the development of useful mechanical instruments will be necessary even if complete joints could be replaced in the future by means of tissue engineering, or when computer aided surgery will be used in daily practice. Telemanipulators also need useful mechanical end-effectors. Finally, mechanical instruments will also be necessary to perform joint replacement.

In this thesis, a straightforward method is presented to take into account the human-machine interaction in every stage of the development of an instrument or technique. This method implies that the surgeons are closely involved in the design process, to point out problem areas, and to share their experience with the currently available techniques. This method is called clinically driven approach and is further developed in Chapter 2. With the help of the application of the clinically driven approach, it was possible to accentuate the problem definitions.

In addition to this, once problem areas are assessed by the clinically driven approach, the focus of attention will be another aspect of the human-machine interaction. The anatomic variability amongst the population has stochastic characteristics for which the average and standard deviations are important parameters to define the range of variations and orders of magnitude for design criteria. Stochastic processes are opposed to deterministic processes which are routinely used in engineering and do not have to deal with matters as probabilities. In consumer product design, the engineer also has to deal with variations of human beings *(ergonomics, anthropometry, and even psychology)*, and therefore this approach was adapted. To derive actual technical values for the set up of design criteria, it is necessary to build up a database with data on technical characteristics of joints and tissues that are sufficiently accurate, but easy to assess. With this approach, it is aimed at the creation of simple technical innovation. It is believed that in this stage continuous feedback with the actual users, leads to an effective and useful contribution to the treatment of patients undergoing arthroscopic surgery. In this thesis, the proposed method is shaped and is applied to three identified problem areas: **the development of a new arthroscopic technique for performing a subtalar arthrodesis, the optimization of arthroscopic view, and the development of a steerable punch**. Each problem area is investigated from different levels ranging from the set up of a new arthroscopic technique to the design of an instrument for one specific treatment. Technical improvements are assessed by the development of instruments.

1.4 Structure

As was indicated, the concept of the clinically driven approach is further depicted in Chapter 2. This resulted in the identification of six problem areas within the arthroscopic field. It was decided to investigate three problem areas in this thesis: the development of a minimal access technique for subtalar arthrodesis, the optimization of arthroscopic view, and the development of a steerable punch for the performance of a meniscectomy. Chapter 3 addresses the subtalar arthrodesis procedure. The current limitations of the subtalar arthrodesis techniques are established by means of a literature study in combination with observations made during the attendance of several operations. From this analysis a strategy for a new arthroscopic technique was set up, and the required instruments that have to be developed in order to implement the technique are pointed out. In Chapter 4, a start is made with the implementation of the proposed technique. For two of these instruments, a measurement system to measure the preoperative and the peroperative alignment of the hindfoot and an instrument for cartilage removal, design criteria were set up with the help of the dimensions derived from the hindfoot and working loads derived from experiments on bony and cartilage tissue. For each instrument several concepts were set up that lead to the fabrication of a prototype for each instrument that was tested in the laboratory. Chapter 5 concentrates on the optimization of arthroscopic view. In this chapter, research is performed to elucidate the behavior of the irrigation systems for which guidelines are defined to optimize irrigation. In addition to this, a new sheath is developed that enables quicker irrigation of a joint. The last problem area considers the meniscectomy. In Chapter 6, design criteria are derived for a new cutting instrument that increases the reachability in the knee joint. Not only attention is paid to the tip of the instrument, but also to the handle of this instrument, since the surgeon has to control two degrees of freedom (cutting and steering) when using this instrument. Finally, overall conclusions on the performed research are drawn and suggestions for future research are indicated in Chapter 7.

References

1. LaPorta G. Turrisi JS. The history and clinical application of arthroscopy. *Clin Podiatr Med Surg* 1987; 4: 829-834.

2. van Dijk, C. N. Beweegredenen, de patient als bron van inspiratie. Inaugural . 14-3-2002. University of Amsterdam, Amsterdam.

3. Scholz J. Kuhling T. Turczynsky T. Advantages of arthroscopy of the knee joint. *Biomed.Tech.(Berl)* 1992; 37: 11-13.

4. van Dijk CN. Hindfoot Endoscopy. *Sports Medicine and Arthroscopic Review* 2000; 8: 365-371.

5. van Dijk CN. Kort NP. Scholten PE. Tendoscopy of the posterior tibial tendon. *Arthroscopy* 1997; 13: 692-698.

6. Howell JR. Handoll HH. Surgical treatment for meniscal injuries of the knee in adults. *Cochrane.Database.Syst.Rev.* 2000; CD001353.

7. Lundeen RO, ed. *Manual of ankle and foot arthroscopy.* New York: Churchill Livingstone, 1992. ISBN 0-443-08694-X.

8. Parisien JS, ed. *Current Techniques in Arthroscopy.* New York: Thieme, 1998. ISBN 0-86577-738-1.

9. Breedveld P. Stassen HG. Meijer DW. Jakimowicz JJ. Manipulation in laparoscopic surgery: overview of impeding effects and supporting aids. *J Laparoendosc.Adv.Surg Tech.A* 1999; 9: 469-480.

10. Sisk TD. Arthroscopy of knee and ankle. In: Crenshaw AH, ed. *Campbell's operative orthopedics.* St. Louis: CV Mosby Company, 1987;2547-2608. ISBN 0-8016-1065-6.

11. McGuire DA. Hendricks SD. Grinstead GL. Use of an endoscopic aimer for femoral tunnel placement in anterior cruciate ligament reconstruction. *Arthroscopy* 1996; 12: 26-31.

12. Moreland JR. Westin GW. Further experience with Grice subtalar arthrodesis. *Clin Orthop* 1986; 207: 113-121.

13. Pollock JH. Carrell B. Subtalar extra-articular arthrodesis in the treatment of paralytic valgus deformities. *J Bone Joint Surg Am* 1964; 46: 533-541.

14. van Dijk CN. Scholte D. Arthroscopy of the ankle joint. *Arthroscopy* 1997; 13: 90-96.

15. Sjoerdsma W. Surgeons at work: time and actions analysis of the laparoscopic surgical process. Delft University of Technology, 1998: 77-91.

16. Kumar VP. Satku K. The A-O femoral distractor for ankle arthroscopy. *Arthroscopy* 1994; 10: 118-119.

17. Lajtai G. Aitzetmuller G. Unger F. Orthner E. Half pipe cannula for shoulder arthroscopy. *Arthroscopy* 2001; 17: 224-225.

18. Thal R. A knotless suture anchor. Design, function, and biomechanical testing. *Am J Sports Med* 2001; 29: 646-649.

19. Kurita K. Ogi N. Toyama M. Maki I. Ike M. Single-channel thin-fiber and Nd:YAG laser temporomandibular joint arthroscope: development and preliminary clinical findings. *Int J Oral Maxillofac.Surg* 1997; 26: 414-418.

20. van Dijk CN. Verhagen RA. Tol HJ. Technical note: Resterilizable noninvasive ankle distraction device. *Arthroscopy* 2001; 17: E12.

21. European joint implant market to see 5.6% annual compound growth by 2006. Orthopaedics Today International 5(2), 37-38. 2002. Thorofare, NJ, Slack Inc.

22. Barber FA. Herbert MA. Click JN. Suture anchor strength revisited. *Arthroscopy* 1996; 12: 32-38.

23. van Dijk CN. Kort NP. Tendoscopy of the peroneal tendons. *Arthroscopy* 1998; 14: 471-478.

24. Dario P. Carrozza MC. Marcacci M. D'Attanasio S. Magnami B. Tonet O. Megali G. A novel mechatronic tool for computer-assisted arthroscopy. *IEEE Trans.Inf.Technol Biomed.* 2000; 4: 15-29.

25. Lyyra T. Jurvelin J. Pitkanen P. Vaatainen U. Kiviranta I. Indentation instrument for the measurement of cartilage stiffness under arthroscopic control. *Med.Eng Phys* 1995; 17: 395-399.

26. Fanton GS. Khan AM. Monopolar radiofrequency energy for arthroscopic treatment of shoulder instability in the athlete. *Orthop Clin N Am* 2001; 32: 511-23, x.

27. Polousky JD. Hedman TP. Vangsness CT, Jr. Electrosurgical methods for arthroscopic meniscectomy: A review of the literature. *Arthroscopy* 2000; 16: 813-821.

28. Metcalf RW. Instrument-related complications. In: Sprague NF, ed. *Complications in arthroscopy.* New York: Raven Press, 1989; 75-86. ISBN 0-88167-523-7.

2. Design of arthroscopic instruments: a clinically driven approach

This chapter is based on the article *Design of arthroscopic instruments: a clinically driven approach*, by G.J.M. Tuijthof, C.N. van Dijk, J.L. Herder, P.V. Pistecky, which is submitted to the Journal of Knee Surgery, Sports Traumatology, Arthroscopy.

Keywords: arthroscopy, interview, clinically driven approach, evaluation

Abstract: In this paper, a clinically driven approach is used as the starting point for the development of arthroscopic instruments, and the approach can be divided in two phases. Phase 1 is a combination of observations and discussions with a limited number of surgeons that resulted in the definition of clinically relevant research topics. Phase 2 consists of an interview which aims an analysis of the general opinion on arthroscopy, and which assigns a priority ranking in the topics. Six research topics were defined: optimization of a clear view during operations, development of soft-tissue endoscopy, development of a minimal access technique for subtalar arthrodesis, optimization of the treatment of osteochondral defects, development of multifunctional instruments, and the assessment of quality of the procedure. Based on the collected information it is concluded that the surgeons are satisfied with the current arthroscopic techniques. A majority gives priority to the optimization of cartilage treatment and the design of a steerable instrument. A minority gives priority to the expansion of arthroscopic techniques.

Introduction

Arthroscopy is becoming more complex due to the continuous development of techniques and instruments that enables the performance of more difficult procedures. If the available technology is chosen as the starting point to develop surgical instruments *(technology driven approach),* there is a risk that instruments are developed that do not fulfill the needs of the surgeon.[1] Furthermore, endoscopic instruments are frequently introduced without proper clinical testing, or even without evident clinical need.[2] The development of surgical instruments is therefore preferably done by a clinically driven approach.[2-4] The clinically driven approach can be best described as a design process where the physician *(in this case the orthopaedic surgeon)* and the designer *(in this case the engineer)* first analyze in close collaboration the specific needs and problems independent of a technical solution.[5] For a successful analysis, it is important that the orthopaedic surgeon and the engineer learn to communicate and to understand the background of their respective disciplines. Such a thorough multidisciplinary problem analysis guarantees that research and development are performed for clinically relevant topics and that instruments are designed that fulfill the requirements of orthopaedic surgeons.[6-8] To the knowledge of the authors, the clinically driven approach has not been recommended before for the design process of arthroscopic instruments.

To be able to communicate effectively with the orthopaedic surgeon and to start the clinically driven approach the engineer has a number of tools at his disposal. These are observations during operations, discussions, interviews, questionnaires and brainstorm sessions. The goal of this chapter is to elucidate the clinically driven approach as it was applied to the arthroscopic field using observations, discussions and an interview. These tools were also evaluated. The expectation was that observations from a person who is not experienced in the common practice of arthroscopy are essential to start a discussion. It was expected that the observer could possibly detect problem areas that an experienced surgeon does not experience as such, because he is used to the situation. Furthermore, it was expected that discussions with individual surgeons were essential to define the specific needs and problems. Lastly, from the interview it was expected that this tool would be essential to reach a larger population of orthopaedic surgeons in order to prevent instruments being developed according to the preferences of only one particular surgeon.

Materials and methods

The clinically driven process was divided into two phases. In Phase 1, 70 arthroscopic operations were attended at seven different hospitals. In Table 2.1, the specific procedures and the number of attended procedures are given. Each operation has been recorded on video or documented in a so-called feedback report. Feedback reports were used consisting of a general section, an instrument section, an observation section, and a concluding section *(Table 2.2)*. The purpose of the feedback reports was threefold. Firstly, a detailed database for general purposes was built up. Secondly, the reports were used as a start of the analysis of arthroscopic operations. Thirdly, the reports were also used in discussions with surgeons to identify clinical problem areas.
In Phase 2, an interview was set up to ask a larger population of orthopaedic surgeons for their opinion on arthroscopy in general and problems with certain techniques or instruments in particular. The interview consisted of three sections: (I) open questions, (II) structured questions about clinical problem areas that were already defined as a result of Phase 1, and (III) indication of a priority ranking of these problem areas. The interview questions are presented in Table 2.3. The surgeons were questioned orally. The Dutch Society of Arthroscopy was asked for a list of fifteen surgeons who are considered to be experts in the field of arthroscopy. Eleven of them agreed to participate. There were nine orthopaedic and two general surgeons distributed amongst peripheral and academic hospitals. The average surgical experience of this group was

type of procedure	number
ankle adhesions	12
subtalar or triple arthrodesis **open procedure**	4
jumper's knee	2
cruciate ligament reconstruction	2
meniscectomy	33
knee diagnostic and adhesions	7
shoulder	1
wrist	5
others	4

Table 2.1
Number and type of procedures that were attended and analyzed.

10 years *(varying from six months to sixteen years)* and the surgeons perform an average of 330 arthroscopic operations a year *(varying from 120 to 700 arthroscopic operations a year)*. This number is about 60% of the total number of operations that the arthroscopists perform each year.
In addition to the opinions of experts in the arthroscopic field, a number of other criteria was taken into account to decide which clinically relevant topics to start researching in. These criteria were: scientific and engineering relevance, availability of a clinical partner, facilities, technical expertise in the research group, milestone after four years, personal interest, and competition with industry.

Table 2.2
Example of a feedback report.

Feedback report

Date:	16 June 1999
Hospital:	IJsselland Hospital
Type procedure:	Knee arthroscopy (adhesions)
Duration:	50 minutes
Surgeon:	Dr. Surgeon

Instrument set:

Name	Brand	Reusable	Function	D(mm)	Shape/picture	Number
Arthroscope (30°)	Storz	Yes	Visualization operation field	4	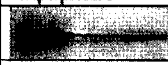	1
Needle		Yes	Positioning of portals	1		1
Sheath		Yes	Protection scope and inflow of irrigation fluid	4.5		1
Obturator		Yes	Save insertion of sheath	4	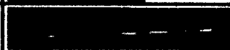	1
Cannula		yes	Outflow of irrigation fluid	5	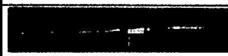	1
Probe		Yes	Feeling of tissue	2	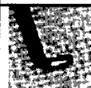	1
Shaver		Yes	Cutting and removal of soft tissue	4		1
Punch		yes	Cutting of soft tissue	3.4		1

Portal placement:

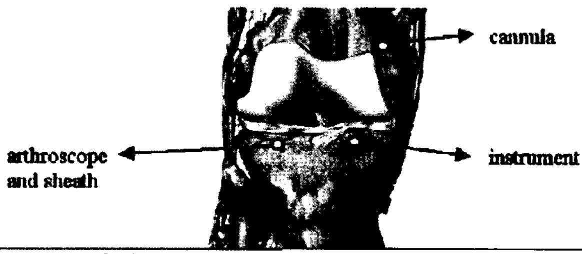

Feedback report

Date:	16 June 1999
Hospital:	IJsselland Hospital
Type procedure:	Knee arthroscopy (adhesions)
Duration:	50 minutes
Surgeon:	Dr. Surgeon

Observations:

Diagnosis/Pathology:
This patient has had an anterior cruciate ligament reconstruction and hispopliteus tendon is torn. At the moment, he has serious functional limitations of his knee joint. He is able to flex the knee by only 20 degrees.

Description procedure :
Firstly, the surgeon inspects the knee joint to establish the intra-articular condition of the knee joint. It is difficult to insert the canula and sheath. After the sheath is inserted the knee can be flexed until 40 degrees. After inspection it is diagnosed that indeed adhesions cause the serious function limitation. These adhesions are cut with a punch and a shaver. Finally, the knee can be flexed until 90 degrees. The menisci are in tact. However, due to the adhesions there is minor cartilage damage. This cannot be treated.

Ergonomics:
The surgeon operated while sitting in a chair and the monitor is placed in direction with his viewpoint. From an ergonomical point of view this is a good posture.

Questions/Conclusions/Ideas:

Questions:
Which options are available to treat osteochondral defects?
Is it possible to treat all locations in the joint where osteochondral defects are present?

Instrument usage:
The shaver and punch are continuously interchanged during the operation, while they in fact have the same function. What is your opinion on an instrument in which the shaver and punch are integrated? This would allow for less instrument exchanges.

Results

The results of Phase 1 *(combination of observations and discussions)* and Phase 2 *(interview)* will be given simultaneously. The reason for this is that from Phase 1 a total of six clinically relevant research topics is defined, each of which is addressed in Section II of the interview.

Section I. Open questions

Nine of the eleven arthroscopists sometimes experience discomfort during arthroscopic operations. The main causes are malfunction of instruments, poor view inside the joints caused by debris or synovial tissue, compactness of the joints and improper functioning of irrigation systems.

The arthroscopists are satisfied with the current instrument set. However, there are still wishes

Table 2.3
Questions that were asked during the interview, translated from Dutch.

Section I:

How many years are you a practicing orthopaedic surgeon?
Do you have a specialization in the field of arthroscopy? If so, which procedure?
What is the number of arthroscopic procedures that you perform per year?
What percentage is this of the total number of procedures that you perform per year?

Do you experience annoyances during certain arthroscopic operations? If so, what are the annoyances?
Which factors cause these annoyances?
Are there certain instruments that do not function well? If so, what is the problem?
Are there procedures for which an arthroscopic technique is desired? If so, which ones?
What are the current limitations that make it impossible to perform the procedure arthroscopically?

Section II:
How often is the view unclear during an operation? What are the causes?
How often is the overview insufficient? What are the causes?
Would the arthroscopic operations be easier to perform if the view was optimized? If so, what is the reason?

What is the number of soft tissue endoscopy procedures that you perform per year?
What are the most difficult phases in the procedure(s)?
Does soft tissue endoscopy offer advantages over the current open techniques? If so, on what conditions?

What is the number of subtalar arthrodeses that you perform per year?
What are the most difficult phases in the open technique?
Why is there no arthroscopic technique so far?
Do you think that an arthroscopic technique for the subtalar arthrodesis would be beneficial? If so, on what conditions?

What technique do you use to treat osteochondral defects?
What is the number of osteochondral defect treatments that you perform per year?
How often is it impossible to treat an osteochondral defect because of technical limitations?

Which instruments are present in your basic set?
How often do you perform an instrument exchange during a normal procedure?
What is usually the reason to interchange the instruments?
What is your opinion on instruments with curved end-effectors?
What is you opinion on a punch with a steerable end-effector?
Is it true that the major part of the treatments consists of the removal of tissue?
What is your opinion on a universal cutter with which soft and hard tissue can be removed?
What is your opinion on an instrument with a combined scope and forceps?

How do you judge if the protocol for a certain procedure is performed thoroughly?
What is your opinion on a method to determine the percentage of meniscus tissue that has to be removed during a meniscectomy?
Which items would you want to know during a meniscectomy?
Could you indicate for which arthroscopic procedures it is desired to establish its success more accurately? What would you want to measure during these procedures?

Section III:
Could you indicate which of the topics discussed in Section II have your priority?

for improvements, predominantly for fixations and to access the posterior side of joints.
The general opinion of the interviewed arthroscopists is that there are a few areas in arthroscopy that can be explored. Three arthroscopists expected changes through the development of soft-tissue endoscopy, an improved operation for rotator cuff ruptures and improved instruments for cartilage transplantations. Restrictions in performing arthroscopic operations are the lack of manipulation space and the limited possibilities to insert implantations.

Section II. Questions related to clinical problem areas defined in Phase I

1. *Optimization of a clear view in joints*

From our observations during operations, it appeared that the view in a joint is often suboptimal.[9-11] In particular during difficult operations and crucial actions, the view is often impeded. An optimal method to create and to maintain a clear view during operations has not yet been formulated.
All surgeons interviewed agreed that a good view is crucial for a safe and fast operation. The interview revealed that the view is most often impeded during meniscectomies and shoulder arthroscopies. The causes are: bleedings, malfunction of irrigation systems, improper functioning of the camera, the scope or the light cable, synovial tissue in front of the camera, and compactness of the joints.

2. *Development of soft-tissue endoscopy*

In soft-tissue endoscopy a treatment takes place in artificial cavities in the body, e.g. around tendons.[12,13] This is a relatively new field and the arthroscopic equipment is not always apt to this type of procedures. It is for example important to keep the intra-articular pressure on a constant and appropriate level to avoid collapse of the cavity or excessive liquid extravasation.
The most frequently performed procedure is the acromioplasty *(an average of 18 per surgeon per year)*, followed by the endoscopic carpal tunnel release *(4 per surgeon per year)*. Difficulties during an acromioplasty are the creation of a clear view and the determination of the correct amount of bone removal. 80% of the arthroscopists interviewed regards soft-tissue endoscopy to be advantageous if a clear view can be created in the artificial cavities, and if they are able to build up experience.

3. *Development of a minimal access method for subtalar arthrodesis*

The open procedure for subtalar arthrodesis gives unsatisfactory results, whereas the available arthroscopic techniques demand very high surgical skills.[14-16] In the discussions with several surgeons they indicated a tendency to perform more operations in small joints. The subtalar joint is one of the joints that is hard to access with the current straight instruments.
The determination of the amount of hindfoot correction, and the access to the joint are identified as the most difficult steps in the open procedure. 80% of the surgeons expects potential advantages of an endoscopic method. The main advantage would be that the neurovascular structures in the foot and ankle could be saved. This new minimal access technique should have a steep learning curve. In addition to this, instruments have to be developed to perform eventually a correction via the minimal access approach.

4. *Optimization of the treatment of osteochondral defects*
During observations and discussions with surgeons it became clear that some osteochondral defects cannot be treated adequately, because the location deep inside the joint cannot be reached. The treatment of osteochondral defects is done according to different methods.[17-19] 70% of the arthroscopists performs debridement and drilling. They indicate that these methods sometimes cannot be performed due to lack of proper instruments to reach the location. 30% of the subjects performs cartilage transplantation. The difficulty of this technique is the placement of the transplant exactly in a correct position.

5. *Instruments*
It was noticed that for certain treatments, e.g. meniscectomy procedures, quite a number of instruments is needed with exactly the same function, but with a slightly different shape. The arthroscopists interviewed indicated that they had to exchange instruments on an average of 8 times per operation, because they either needed an instrument with another function or could not reach the location with the instrument.[2] To enlarge the efficiency and safety of the operations, several suggestions were made for the development of instruments.[5,20-23] These suggestions are: the combination of a scope with a forceps *(50% of the arthroscopists were positive)*, a universal cutter that can cut soft and hard tissue *(all arthroscopists were positive)*, and a punch with a steerable tip *(all arthroscopists were positive)*.

6. *Quality of operations*
The interview indicates that surgeons base their judgment on the quality of operations on their experience. Quality is here defined as the verification of the preoperatively planned outcome of the procedure with the actual outcome. If this result could be quantified, it would be possible to set up an objective quality measure. This measure can be preoperatively applied to plan the treatment actions and postoperatively to judge the results of the outcome due to the operation.[24,25] To determine quantitative measures of quality, criteria and measurements are necessary. Depending on the choice of the quality measure, variables have to be indicated for which measurement instruments or procedures have to be developed.
The arthroscopists interviewed judge the outcome of their treatment by visual inspection or by pressing tissue. Examples of factors that could improve the quality of arthroscopic operations are the determination of the percentage of meniscal tissue that has to be removed, the size of a cartilage defect and the amount of bone resection for an acromioplasty. Furthermore, surgeons indicate the need for a national registration system of all arthroscopic operations that are performed.

Section III. Priority ranking

The arthroscopists were asked to give a priority ranking of the proposed research topics. The results are given in Table 2.4, in which each number stands for the number of arthroscopists who marked that category. The three proposals for instrument development are indicated separately.

priority ranking	none	barely	average	high	very high
clear view	0	2	4	4	1
soft-tissue endoscopy	1	4	3	3	0
minimal access technique for subtalar arthrodesis	2	3	3	3	0
treatment of osteochondral defects	0	0	0	8	3
punch with a steerable tip	0	1	2.5	5.5	2
universal cutter	0	3	2	4	2
combination of scope with forceps	0	3	4.5	2.5	1
measurement method for operation quality	0	1	4	4	2

Table 2.4
Priority ranking of the research topics. Each surgeon was allowed to place one mark at a research topic. Some surgeons placed a mark in between two categories and that score was divided in two.

Discussion

The objective and quantified observations of operations performed by the engineer provided detailed technical knowledge of arthroscopic techniques and were used to perform time-action analyses on certain operation phases.[5,24] A regular observation was the fact that the surgeon is used to perform the operations with the available equipment, and therefore he often does not recognize certain problems or does not experience them as problems anymore.[2] However, discussions with surgeons were needed to document clinical needs and ideas. Therefore, by applying a combination of observations and a discussions, an environment was created where the advantages of both tools were used to integrate the knowledge of engineers and surgeons, and to define clinical problem areas. A similar phenomenon occurred during the interviews where the arthroscopists had some difficulty in answering open questions concerning arthroscopy. For three of the interviewed arthroscopists a combination of the observation tool and interview tool was applied. Feedback by means of the observations, made the surgeons reconsider their answers.

Only a few surgeons were involved in Phase 1, and therefore these topics are colored with their specific interests and expertise. When starting a clinically driven approach, this has to be recognized. Therefore, Phase 2 was started to reach a larger population of surgeons. It is proposed to use more than 11 surgeons for this purpose. This is based on the observation that most arthroscopists have a specialization within arthroscopy and their professional attitude varies also.

With the results and the additional criteria, the choice was made to start with the development of a minimal access technique for the subtalar arthrodesis procedure. The main reasons were that the senior surgeon has ample experience with ankle arthroscopy, the research group has ample experience in the design of mechanic instruments, and there is little competition with the industry. Furthermore, an instrument developed for the subtalar joint can probably also be used in other small joints. Research is also initiated to improve the visualization of joints and to develop a sideways steerable punch, because these two topics were given a high priority.

Conclusions

This paper describes a clinically driven approach to identify clinically problem areas by a two-phase clinically driven approach. This approach worked well to set up a fruitful communication between surgeons and engineers. The available tools were applied in an advantageous manner. In Phase 1, a combination of observations and discussions with surgeons resulted in the definition of clinically relevant research topics. In Phase 2, the interview tool could best be used as a subsequent phase of the clinically driven approach, because detailed questions have to be asked to come to results. The study resulted in the choice to focus on a minimal access technique for subtalar arthrodesis, to optimize the view in joints and to develop a sideways steerable punch.

References

1. Grimbergen CA. Jaspers JEN. Herder JL. Stassen HG. Development of laparoscopic instruments. *Min Invas Ther & Allied Technol* 2001; 10: 145-154.

2. Boer KT den. Jong T de. Dankelman J. Gouma DJ. Problems with laparoscopic instruments; opinions of experts. *J Laparoendosc Adv Surg Tech A* 2001; 11: 149-156.

3. Grimbergen CA. Dankelman J. Stassen HG. Man-machine systems aspects of minimally invasive surgery and interventional techniques. The Delft-Amsterdam cooperation. *Min Invas Ther & Allied Technol* 1998; 10.

4. Stassen HG. Technical assessment of new technology. 1997. Amsterdam. Proceedings of the First Annual Symposium on New Interventional Technology in an Era of Evidence Based Medicine. 1997.

5. Sjoerdsma W. Surgeons at work: time and actions analysis of the laparoscopic surgical process. Delft University of Technology, 1998: 77-91.

6. Stassen HG. Biomedical engineering: an interesting multidisciplinary human-machine systems field with many problems and challenges. Johannsen G. 507-516. 18-9-2001. Kassel, Germany. IFAC, 8th IFAC/IFIP/IFORS/IEA Symposium on analysis, design, and evaluation of human-machine systems.

7. Stassen HG. The influence of new technology on the human-machine interaction in biomedical engineering: a challenge or a problem? 99-107. 2000. Aachen, Germany. 7th IFAC-symposium on automated systems based on human skill.

8. Stassen HG DJGC. Open versus minimally invasive surgery: a man-machine system approach. *Transactions of the institute of measurement and control* 1999; 21: 151-162.

9. Ampat G. Bruguera J. Copeland SA. Aquaflo pump vs FMS 4 pump for shoulder arthroscopic surgery. *Annals of the Royal College of Surgeons of England* 1997; 79: 341-344.

10. Noyes FR. Spievack ES. Extraarticular fluid dissection in tissues during arthroscopy. *Am J Sports Med* 1982; 10: 346-351.

11. Ogilvie-Harris DJ. Weisleder L. Fluid pump systems for arthroscopy: a comparison of pressure control versus pressure and flow control. *Arthroscopy* 1995; 11: 591-595.

12. van Dijk CN. Kort NP. Tendoscopy of the peroneal tendons. *Arthroscopy* 1998; 14: 471-478.

13. van Dijk CN. Kort NP. Scholten PE. Tendoscopy of the posterior tibial tendon. *Arthroscopy* 1997; 13: 692-698.

14. Lundeen RO. Arthroscopic fusion of the ankle and subtalar joint. *Clin Podiatr Med and Surg* 1994; 11: 395-406.

15. Parisien JS. Arthroscopy of the posterior subtalar joint. In: Parisien JS, ed. *Current Techniques in Arthroscopy.* New York: Thieme, 1998;161-168. ISBN 0-86577-738-1.

16. Tasto JP, Laimins PD. Recent advances in ankle arthroscopic techniques. In: Parisien JS, ed. *Current techniques in arthroscopy.* New York: Thieme, 1998;181-194. ISBN 0-86577-738-1.

17. Chen FS. Frenkel SR. Di Cesare PE. Repair of articular cartilage defects: Part I. Basic science of cartilage healing. *Am J Orthop* 1999; 28: 31-33.

18. Chen FS. Frenkel SR. Di Cesare PE. Repair of articular cartilage defects: Part II. Treatment options. *Am J Orthop* 1999; 28: 88-96.

19. Tol JL. Struijs PAA. Bossuyt PMM. Verhagen RAW. van Dijk CN. Treatment strategies in osteochondral defects of the talar dome: a systematic review. *Foot & Ankle Int* 2000; 21: 119-126.

20. Balazs M. Feussner H. Hirzinger G. Omote K. Ungeheuer A. A new tool for minor-access surgery. *IEEE Engineering in medicine and biology* 1998; 45-48.

21. Faraz A. Payandeh S. Synthesis and workspace study of endoscopic extenders with flexible stem. *Journal of Mechanical Design* 1997; 119: 412-414.

22. Hashimoto D. Development of ojigi electrocautery and other ojigi instruments. *Min Invas Ther & Allied Technol* 1997; 6: 287-290.

23. Schurr MO. Melzer A. Dautzenberg P. Neisius B. Trapp R. Buess G. Development of steerable instruments for minimal invasive surgery in modular conception. *Acta Chir Belg* 1993; 93: 73-77.

24. Boer KT den. Straatsburg IH. Schellinger AV. Wit LTh de. Dankelman J. Gouma DJ. Quantitative analysis of the functionality and efficiency of three surgical dissection techniques. *J Laparoendosc Adv Surg Tech A* 1999; 9: 389-395.

25. Boer KT den. Wit LTh de. Davids PHP. Dankelman J. Gouma DJ. Analysis of the quality and efficiency of learning laparoscopic skills. *Surg Endosc* 2001; 15: 497-503.

3. Subtalar arthrodesis: analysis for a new technique

In this chapter the development of a new technique is presented to perform a subtalar arthrodesis by means of a minimally invasive approach. The subtalar joint is located in the hindfoot *(Figure 3.0.1)*. When a surgeon performs an arthrodesis, the joint is fused. On the one hand, this identified problem area did not receive a high priority from the interviewed surgeons *(Chapter 2)* because the operation is not performed frequently *(426 procedures in 2000 in the Netherlands)*.[1] On the other hand, a minimal access technique for this procedure would potentially be beneficial for the patient, the participating surgeon has ample experience with arthroscopic ankle joint surgery, and this project offers technical challenges. These challenges are that the shape of the subtalar joint is complex, and that the new arthroscopic instruments designed to facilitate the reachability in this joint could probably also be used to enable easy arthroscopic access in other joints (e.g. joints in the foot or wrist).

Sections 3.1 to 3.3 are based on the paper *Subtalar arthrodesis: current limitations and criteria for a new technique*, by G.J.M. Tuijthof, C. N. van Dijk, and P.V. Pistecky, which is submitted to Foot & Ankle International.[2] In Section 3.1, the anatomy and function of the subtalar joint and the procedure for subtalar arthrodesis are elucidated in more detail. In addition to this, observations from clinically practice are included. A literature overview of the open and arthroscopic subtalar arthrodesis techniques is given, as well as the current limitations *(Section 3.2)*. The analysis from Sections 3.1 and 3.2 made it possible to set up a strategy for a new subtalar arthrodesis technique *(Section 3.3)*. The chapter is concluded with a discussion in Section 3.4.

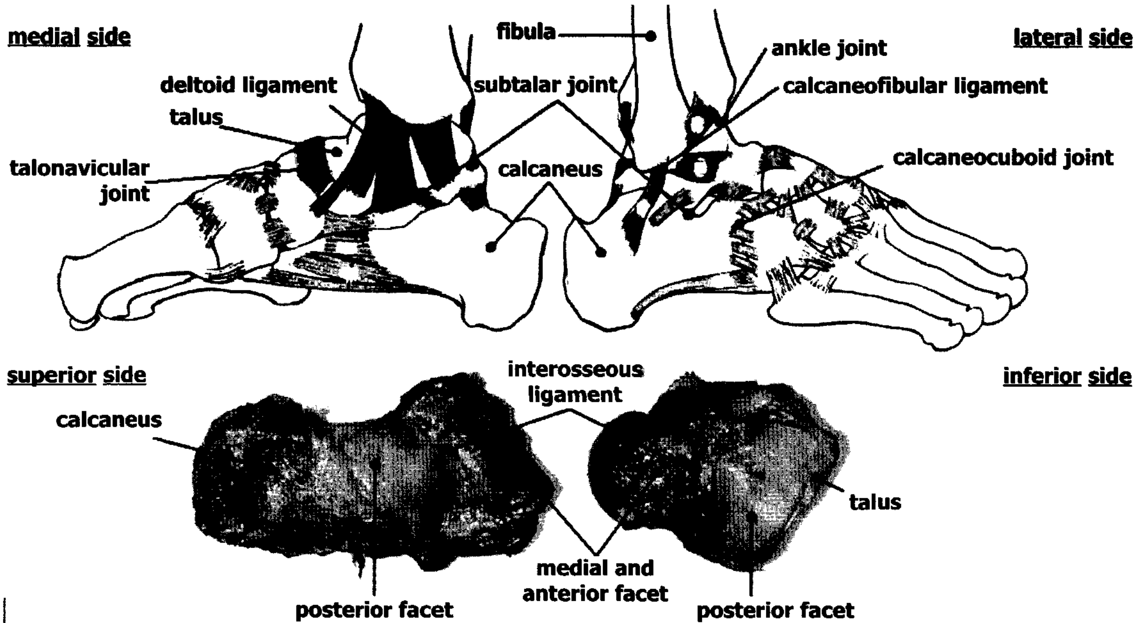

Figure 3.0.1
Bones en ligaments forming the hindfoot, whereby the focus is on the subtalar joint. The calcaneus, and talus as well as the three facets of the subtalar joint are shown in detail. Anatomic illustration is based on Sesam Atlas[76].

3.1 Subtalar joint and arthrodesis

Subtalar joint

Hindfoot motion is possible through the subtalar, talonavicular and calcaneocuboid joint *(Figure 3.0.1)*. The subtalar joint consists of three separate articulations of the calcaneus and talus.[3] The curvature of the subtalar joint is complex and it may be considered as convex and concave ovoid surfaces.[4] This type of curvature makes it difficult to visualize the posterior facet completely when performing open as well as arthroscopic surgery. The orientation of the subtalar joint axis results in a spatial motion of the subtalar joint, which is referred to as either pronation or supination *(Figure 3.1.1)*. According to Isman and Inman[5], the average angle between the subtalar joint axis and the horizontal plane is 42°, and the average angle between the subtalar joint axis and the midline of the foot is 23°, but there is a remarkable variation amongst the population. The subtalar joint allows the foot to rotate medially or laterally while remaining vertical and it helps in the prevention of foot slippage.[6] The motion of the subtalar joint is started on heel contact.[7] The eccentric position of the body weight and the center of heel contact causes a torque about the subtalar joint. The joint moves into eversion which is a quick passive motion that stresses the surrounding ligaments of the subtalar joint.[8] When the subtalar joint is in eversion, the axes of the transversal joints are parallel, which allows the forefoot to be flexible.[8] Inversion of the subtalar joint occurs at heel rise of the foot. The axes of the transversal tarsal joints are divergent at this moment and allow the midfoot to act as a lever to raise the body.

Indications

Subtalar arthrodesis is known to be an accepted surgical procedure for isolated subtalar problems unresponsive to conservative treatment. The categories of problems requiring a subtalar arthrodesis include degenerative joint disease after calcaneal fracture, foot deformities occurring with poliomyelitis and cerebral palsy, subtalar dislocation or instability, different types of arthritis isolated to the subtalar joint, dysfunction of tendons around the ankle joint and failure of previous subtalar arthrodesis.[9-14] Osteoarthritis is a pathology that mainly takes place in older people, whereas foot deformities and dysfunctional tendons usually occur at young ages. Calcaneal fractures mainly result from falls from height and motorcycle accidents. Approximately three-quarters of the calcaneal fractures *(2% of all bone fractures)* are intra-articular and

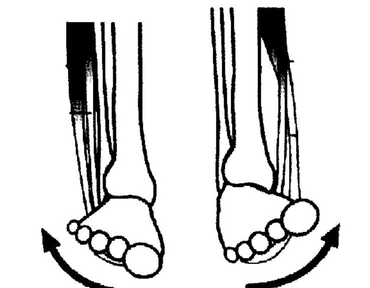

Figure 3.1.1
Movements of the ankle that are possible through the presence of the subtalar joint.

Figure 3.1.2
Picture of the lateral incision that is made to access thesubtalar joint. A lamina spreader is inserted in the joint to create more working space. The surgeon holds a chisel in his hand with which he removes cartilage from the subtalar joint surfaces.

eventually require a subtalar arthrodesis.[15] The patients in this group are aged between 25 and 45 years. The reasons of performing a subtalar arthrodesis are pain relief, correction of instability, and restoration of the function and alignment of the deformed hindfoot. In the early years, a triple arthrodesis was performed to alleviate the painful symptoms. For children, an advantage of performing a subtalar arthrodesis instead of a triple arthrodesis is that the former hardly interferes with the growth of the child's foot.[9] Furthermore, surgeons sometimes prefer a subtalar arthrodesis over a triple arthrodesis, because the foot remains more flexible than the rigid foot after a triple arthrodesis.[13,16] It is indicated that a subtalar arthrodesis causes more stress on neighboring joints. Some believe that this could lead to progressive osteoarthritis in these joints, but so far this is not the case.[17]

General procedure

The general subtalar arthrodesis procedure can be described as follows: access is created to the subtalar joint, cartilage is removed, correction of the foot is performed, the calcaneus is fixed to the talus and the wound is closed. Access is usually achieved from the lateral side via an 8 to 10 cm incision over the subtalar joint area, whereby the patient lies in a lateral decubitus position with the effected leg on top *(Figure 3.1.2)*. The subtalar joint is exposed with a lamina spreader. The cartilage and subchondral bone layers of the subtalar joint are removed with the help of a chisel and curettes. After the surface layers are prepared a guide wire is placed through the subtalar joint and to verify the fixation position fluoroscopy can be used *(Figure 3.1.3)*. A cannulated screw is placed along the guide wire, which is then removed. The gaps in the subtalar joint are filled with bone grafts, and the incision is sutured.

Analysis from clinical practice[18]

Five open subtalar or triple arthrodesis operations were attended, performed by four different surgeons, and one arthroscopic subtalar arthrodesis performed by another surgeon on a cadaver

Figure 3.1.3
A) *Picture of a Steinmann pin inserted through the subtalar joint.*
B) *Fluoroscopic picture of the subtalar joint to verify the location of a guide wire.*

ankle was attended. A number of comments can be made with regards to the observations and discussions with the surgeons in question.

The main indications to perform a subtalar arthrodesis are posttraumatic or rheumatoid arthritis and the main reason to perform a subtalar arthrodesis is pain relieve. The surgeon determines the alignment during an operation by visual inspection, for which he uses the following guidelines for a correct foot position: when the foot is at an angle of 90° with the lower leg, the hindfoot should be in slight valgus position and the forefoot should be flexible enough to allow for both abduction as well as adduction.[19] Both the amount of malalignment preoperatively, and the correction postoperatively are controlled with a lateral weightbearing radiograph. Peroperatively, the joint is preliminary fixated with a guide wire. When the position is checked bone grafts are inserted in the gaps present in the former joint. It is indicated that the method to determine the alignment of the hindfoot is not very accurate, and is performed by visually inspection only.

When the hindfoot is severely deformed it is of no use to preserve the contour of the joint to keep the biomechanics in tact. Bone is removed in thicker layers to ensure enough flexibility for fixation in an anatomically correct position. In cases where not only the subtalar joint is fused but also other joints, a minimal access technique would be useful if all joints can be accessed arthroscopically. In this case it is probably useful to develop 3D-visualization support to define more accurately the direction for bone removal in the joints. In cases where there is no malalignment, the preservation of the surfaces of the subtalar joint is important when performing a subtalar arthrodesis. In these cases it will be advantageous to perform an arthroscopic subtalar arthrodesis. However, this requires high surgical skills, because orientation in the joint and portal placement are difficult, and the removal of cartilage is time consuming. The surgeons indicate that the subtalar joint space is usually about 2 mm, which forces them to use small straight instruments. The limitations of these instruments are that they cannot follow the surface contour, they are fragile, and the small shaver suction passages get blocked. In addition to this, it is very difficult to create smooth congruent surfaces which is important for optimal fusion.

3.2 State of the art and current limitations

Introduction

By means of a clinically driven approach problem areas in the field of arthroscopy were assessed *(Chapter 2)*.[20] One of the projects implies the development of surgical instruments for arthroscopic operations. From our research[21], it was indicated that a minimal access technique for the subtalar arthrodesis could definitely have advantages over the current open procedures for the patients, and that this new technique should be easy to learn and to perform.

The goal of this section is threefold. Firstly, a thorough literature study is performed to analyze the different existing techniques for subtalar arthrodesis. Secondly, from this analysis general limitations of the procedures are pointed out, so that factors can be defined that influence the outcome of a subtalar arthrodesis. Thirdly, analyzing the techniques from a technical viewpoint with the help of these factors, a strategy will be presented *(Section 3.3)* that can lead to an easy-

to-perform and reproducible minimal access technique.
A search was done for literature on the following topics: biomechanics of the subtalar joint, open and arthroscopic arthrodesis techniques, and arthroscopy of the subtalar joint. Since the project goal is to develop a new operation technique, it is not claimed to give a complete review of all articles about subtalar arthrodesis, but the review mainly concentrates on articles that present new techniques or articles that often appear in reference lists of articles about subtalar arthrodesis.

Review: techniques, results, complications, and limitations

Techniques

The general subtalar arthrodesis technique can be described as follows: access is created to the subtalar joint, cartilage is removed, correction of the foot is performed, the calcaneus is fixed to the talus and the wound is closed. In order to be able to analyze the different approaches and techniques, it is proposed to subdivide the subtalar arthrodesis procedure into separate phases. These phases are: measurement of malalignment, access, cartilage removal, correction, fixation and postoperative care. Table 3.2.1 provides an overview of this subdivision on open and arthroscopic techniques for subtalar arthrodesis along with the literature sources. Additional sections to the phases are pathology and type of bone graft, and the access phase is divided into the sections: patient position, location of incision and distention method. For brevity, only the first author and date of publication are mentioned in the phases of Table 3.2.1; and only phases of the arthrodesis technique are taken into account that are explicitly described or referred to, e.g. the Grice- procedure. Not all articles indicated in Tables 3.2.1 and 3.2.2 are explicitly mentioned in the text. If an author is mentioned twice or more in certain phases, he uses each of those items, e.g. Burton et al.[22] use both Steinmann pins and fluoroscopy to establish fixation. If a category contains the term 'all other authors or not mentioned explicitly in the text' it means the most authors do not explicitly mention this item, but it is assumed that they perform the standard actions that all techniques require and that they do not use additional tools other than those explicitly mentioned. Fixation is sometimes performed with more than one screw, this is indicated between brackets. The number of weeks of nonweightbearing is added between brackets if this is explicitly mentioned in the paper. Open subtalar arthrodesis techniques give rise to a significant number of complications and the procedure has some major technical limitations. As arthroscopy is becoming a widely accepted approach in orthopaedic surgery, several surgeons have successfully performed arthroscopic subtalar arthrodesis.[23-26] According to these authors, an arthroscopic approach causes significantly less morbidity and enhances proprioception, shortens length of hospitalization, the possibility of early motion and weightbearing, less complications, and allows careful resection of the cartilage, leaving the geometry of the joint intact. These authors are also included in Table 3.2.1 and indicated by the names printed in bold face. Instead of incisions they use portals to reach the joint, as is indicated separately.

Results and complications

In order to derive factors which are important in the different phases of the operation to reach an optimal outcome, the results and the complications were analyzed, too. Table 3.2.2 gives the results in chronological order. In the first column, the first author and publication date are mentioned, followed by the number of operated feet and patients. The term clinical result is defined as an objective outcome assessed by the surgeon. The percentages indicating a positive clinical result are given *(fourth column)*. Patient satisfaction indicates the subjective opinion of the patient about the outcome of the arthrodesis. The percentages of patients that were satisfied or satisfied with minor reservations are presented in the fifth column. Combined scales contain both objective and subjective criteria to judge the outcome, e.g. the AOFAS-scale *(American Orthopaedic Foot and Ankle Society)*.[27] The results of combined scales are given in the sixth column, where the maximum AOFAS-scale scoring is 94 points.[27] Furthermore, about half of the papers mention explicitly whether or not the patient has residual pain since this is an important reason to perform an arthrodesis in the first place. The percentages of patients that have residual pain are presented in the seventh column. The numbers of patients and feet can differ slightly from the numbers in the original articles, because only the feet that had enough follow up time according to the original papers are taken into account. The percentage of good clinical results and complications is determined by division the number of pertaining feet by the total number of feet, wheras patient satisfaction is determined by division of the pertaining patients by the total number of patients.

The complications are categorized as early complications and late complications and are presented in the same manner as the results *(Table 3.2.3)*. Early complications include infections and damage to neurovascular structures *(Table 3.2.3)*, because they occur during the operation. Not every author mentions the occurrence of these early complications.

Technical limitations

The limitations of techniques as indicated by authors are presented in Table 3.2.4. A number of authors indicates difficult phases in the procedure for the open as well as the arthroscopic procedure. For the open procedure the main limitations are the difficulty to measure the amount of malalignment or to determine residual deformity, next to wound closure, assessment of radiographic consolidation, removal of cartilage and accurate placement of the fixation screw. A number of authors advises against the use of cortical bone grafts alone. Others suggest that it is not necessary to use a bone graft.

For the arthroscopic technique the limitations are different. Especially the establishment of the portals and the creation of access to the entire surfaces of the subtalar joint are difficult. These limitations, together with the fact that the indication for a subtalar arthrodesis is infrequent, require a highly skilled surgeon. Lastly, it is not possible to perform a subtalar arthrodesis when correction of the hindfoot is needed.

Discussion

This section will discuss each of the operation phases successively. No effort is made to perform a statistical analysis of the results, since there is no uniform evaluation protocol, and even the scales, that are similar, are sometimes interpreted differently by the authors. Instead, factors are identified and trends are derived for each operation phase, that probably are important to

Table 3.2.1
Overview of techniques for open and arthroscopic subtalar arthrodesis subdivided in the proposed operation phases. Only the first author and date of publication are mentioned in the categories. The names printed boldly are papers that present arthroscopic techniques whereas all other papers present open techniques. This table can be used in combination with Table 3.2.2 to derive important factors that influence the outcome of the operation.

pathology	deformities			arthritis	mixed		calcaneal fractures		
authors	Grice [1952]	Dennyson [1976]	Moreland [1986]	[illegible]	Mann [1988]	Bednarz [1997]	[illegible]	[illegible]	[illegible]
	Pollock [1964]	Gross [1976]	Mallon [1989]		Russotti [1988][68]	Mangone [1997][69]	[illegible]	[illegible]	[illegible]
	Seymour [1968]	Ross [1980][73]	Kitaoka [1997]		Scranton [1991]	Mann [1998]	[illegible]	[illegible]	[illegible]
	Engström [1974]	McCall [1985]			Mann [1993]	Sammarco [1998][74]	[illegible]	[illegible]	[illegible]
					Michelson [1996]	Easley [2000]			
misalignment measurement	radiograph (pre/post)				per operative	radiograph both feet (pre and/or post)	goniometers (pre/post)	visually or none	
authors	Gross [1976]	Scranton [1991]	Chan [1997]	Mann [1998]	[illegible]	Ross [1980]	[illegible]	**Lundeen [1994]**	All other authors
	McCall [1985]	Romash [1993]	Fellmann [1997]	Flemister [2000]		Amendola [1996]	[illegible]	**Jerosch [1998]**	or not mentioned
	Hsu [1986]	Amendola [1996]	Kitaoka [1997]			Buch [1996]	[illegible]	**Tasto [1998]**	explicitly in the text
	Moreland [1986]	Buch [1996]	Burton [1998]			Mangone [1997]	[illegible]	**Scranton [1999]**	
	Carr [1988]	Bednarz [1997]	Dahm [1998]			Burton [1998]	[illegible]		
patient position	lateral decubitus		prone	supine with elevated hip					
authors	Carr [1988]	Kitaoka [1997]	[illegible]	Russotti [1988]	Scranton [1999]				
	Buch [1996]	Burton [1998]		Fellmann [1997]					
	Bednarz [1997]	Flemister [2000]		Mann [1998]					
	Tasto [1998]			**Scranton [1999]**					
incision	obliquely over sinus tarsi			longitudinal posterolateral	tip fibula to 4th metatarsal		L-shape	anterior part talar neck	
authors	Grice [1952]	Ross [1980]	Russotti [1988]	[illegible]	Noble [1979]	Mangone [1997]	[illegible]	Seymour [1968]	
	Pollock [1964][10]	Johansson [1982]	Mallon [1989]		Mann [1993]	Mann [1998]	[illegible]	Gross [1976]	
	Thomas [1967]	McCall [1985]	Michelson [1996]		Romash [1993]	Sammarco [1998]	[illegible]	Hsu [1986]	
	Engström [1974]	Hsu [1986]	Dahm [1998]		Amendola [1996]	Laughlin [1999]			
	Dennyson [1976]	Moreland [1986]	Huang [1999]		Fellmann [1997]	Easley [2000]			
					Kitaoka [1997]				
portals	anterior/ middle/ posterior	anterior/ posterior	anterolat. ventral and dorsal / posterolat. ventral	anterior/ middle and dorsal					
authors	**Scranton [1999]**	[illegible]	**Jerosch [1998]**						
distention	soft tissue removal				no distention	lamina spreader			distractor
authors	Grice [1952]	McCall [1985]	Mann [1993]	**Tasto [1998]**	[illegible]	Carr [1988]	Kitaoka [1997]	**Tasto [1998]**	[illegible]
	Pollock [1964]	Hsu [1986]	Romash [1993]		**Seymour [1968]**	Mann [1993]	Burton [1998]		**Buch [1996]**
	Engström [1974]	Moreland [1986]	Amendola [1996]		**Gross [1976]**	Romash [1993]	Dahm [1998]		[illegible]

cartilage removal	partly removal			No	yes			
authors	Thomas [1967] Dennyson [1976] Kalamchi [1977]	Noble [1979] Johansson [1982] Scranton [1991]	Fellmann [1997]	Seymour [1968] Gross [1976] Hsu [1986]	**Lundeen [1994]** **Tasto [1998]** **Jerosch [1998]** **Scranton [1999]**	All other authors or not mentioned explicitly in the text		
bone graft	corticocancellous autograft		cancellous autograft		cortical autograft		allograft	bank bone
authors	Grice [1952] Pollock [1964] Thomas [1967] Kalamchi [1977] Noble [1979] Ross [1980]	Johansson [1982] McCall [1985] Hsu [1986] Mallon [1989] Burton [1998]	Dennyson [1976] Scranton [1991] Romash [1993] Buch [1996] Bednarz [1997] Fellmann [1997]	Easley [2000] Flemister [2000] Jerosch [1998]	Seymour [1968] Gross [1976] Carr [1988] Russotti [1988] Amendola [1996] Buch [1996]	Bednarz [1997] Chan [1997] Sammarco [1998] Scranton [1999] Flemister [2000]	Engström [1974] Moreland [1986] Easley [2000] Flemister [2000]	Pollock [1964] Michelson [1996]
correction	manually		bone removal	bone block in created gap		bone block distraction		
authors	Seymour [1968] Dennyson [1976] Gross [1976] Hsu [1986] Russotti [1988] Scranton [1991]	Mann [1993] Kitaoka [1997] Dahm [1998] Sammarco [1998] Flemister [2000]	Mann [1993] Mann [1998]	Thomas [1967] Kalamchi [1977] Noble [1979] Johansson [1982] Romash [1993]	Buch [1996] Fellmann [1997]	Grice [1952] Pollock [1964] Engström [1974] Ross [1980] McCall [1985]	Moreland [1986] Carr [1988] Mallon [1989] Amendola [1996] Bednarz [1997]	Chan [1997] (2) Burton [1998] Easley [2000] Flemister [2000]
fixation	no screw		screw (cruc. drill guide)	screw (Steinmann pin)	screw (peroperative fluoroscopy or radiograph)		staples	screw
authors	Grice [1952] Pollock [1964] Thomas [1967] Seymour [1968] Engström [1974] Gross [1976] Kalamchi [1977]	Noble [1979] Ross [1980] Johansson [1982] McCall [1985] Hsu [1986] Moreland [1986] Mallon [1989]	[illegible] Bednarz [1997] (2) Kitaoka [1997] Dahm [1998] Mann [1998] Sammarco [1998]	Russotti [1988] Romash [1993] Buch [1996] Fellmann [1997] Burton [1998] **Lundeen [1994]** **Tasto [1998]** **Scranton [1999]**	Carr [1988] (2) Scranton [1991] Romash [1993] Buch [1996] Burton [1998] (2) Scranton [1999] Easley [2000] (2)	Lundeen [1994] Tasto [1998] Scranton [1999]	Mann [1988] Mann [1993] Huang [1999]	Dennyson [1976] Amendola [1996] Chan [1997] Mangone [1997] Flemister [2000] (2) Jerosch [1998]
postoperative care	8 or > weeks nonweightbearing		< 6 w. nonweightb. / 6 w. weight bearing		6 weeks nonweightbearing followed by 6 weeks weightbearing			
authors	Grice [1952] (12) Seymour [1968] (8) Engström [1974] (12) Ross [1980] McCall [1985]	Hsu [1986] (8) Buch [1996] (8) Bednarz [1997] (12) Huang [1999] (8 a 10)	[illegible] Noble [1979] (2) Thomas [1967] (4) Dennyson [1976] (8) Flemister [2000] (partial)	Lundeen [1994] Tasto [1998]	Pollock [1964] Kalamchi [1977] Johansson [1982] Moreland [1986] Carr [1988]	Mallon [1989] Mann [1993] Romash [1993] Amendola [1996] Chan [1997]	Fellmann [1997] Kitaoka [1997] Mangone [1997] Dahm [1998] Burton [1998]	Mann [1998] Scranton [1999] Easley [2000] **Scranton [1999]**

Table 3.2.2
Results mentioned in literature. Only the first author and date of publication are mentioned in the categories.
An asterisk (*) indicates the authors who perform a subtalar arthrodesis together with a tendon transplantation for the majority of their patients.

author	n feet	n patients	clinical result	patient satisfaction	combined scales	residual pain
Grice [1952]*	17	17	88%			
Pollock [1964]*	112	100	64%			
Thomas [1967]	23	21		[illegible]		[illegible]
Seymour [1968]*	27	16	80%			
Engstrom [1974]	27	10	59%			
Dennyson [1976]	48	29	90%			
Gross [1976]	34	34	53%			
Kalamchi [1977]	6	6	100%			[illegible]
Noble [1979]	47	42			91%	[illegible]
Ross [1980]*	113	84	36%			
Johansson [1982]	23	21			95%	[illegible]
McCall [1985]	149	125	54%			
Hsu [1986]	25	19	96%			
Moreland [1986]*	302	255	71%			
Carr [1988]	11	8		[illegible]		[illegible]
Mann [1988]	11	9	73%	[illegible]		[illegible]
Russotti [1988]	45	41	87%	[illegible]		[illegible]
Scranton [1991]	10	10			Angus-Cowell scale 60%	
Romash [1993]	7	7	100% (early results)			[illegible]
Amendola [1996]	15	[illegible]	73%			[illegible]
Buch [1996]	14	14			AOFAS scale 72	[illegible]
Bednarz [1997]	29	28		[illegible]	AOFAS scale 75	[illegible]
Chan [1997]	9	9		[illegible]	AOFAS scale 76	[illegible]
Fellmann [1997]	36	36	78%	61%		[illegible]
Kitaoka [1997]	21	21	76%	[illegible]	AOFAS scale 70	[illegible]
Mangone [1997]	24	24			AOFAS scale 77	[illegible]
Burton [1998]	13	12		[illegible]	AOFAS scale 76	[illegible]
Dahm [1998]	25	24	68%	[illegible]	Angus-Cowell scale 76%	[illegible]
Mann [1998]	48	44	86%	[illegible]	AOFAS scale 89	[illegible]
Sammarco [1998]*	45	43	86%	[illegible]		
Huang [1999]	15	13	73%	[illegible]		
Scranton [1999]	12	12	92%			

achieve a successful subtalar arthrodesis and that could be improved by additional technical support. This implies that from the facts gathered in the tables more conclusions could be derived that are worthwhile to notice, but these are outside the scope of this chapter.

Scoring scales

It is hard to compare the results of different articles and therefore a few remarks about the presentation of the results are appropriate. Till the eighties, the surgeons only used two criteria, consolidation and residual deformity, to rate the results. However, it is doubtful whether radiographic assessment of consolidation is reliable and accurate.[10,14,28] Furthermore, it is unclear how clinical union can be assessed accurately, and how residual deformity should be assessed. Nowadays, a combination scale of patient satisfaction and functional outcome is a more important scale containing better defined and more relevant criteria, and it is widely accepted *(AOFAS-scale)*. Unfortunately, many authors provide only mean values of this AOFAS-scale so that information on its variance is absent. Bednarz et al.[29] have addressed this item and presented the AOFAS-scale in a graph showing the individual improvements, and allows to derive proper conclusions. Another shortcoming in using the AOFAS-scale is that the minimum score corresponding to a satisfactory result is not defined. Flemister et al.[30] are the first ones to define a minimal score of 69 as a satisfactory result.

Patient satisfaction is usually higher than surgeon satisfaction *(Table 3.2.2)*. This can be explained as follows: a patient who has no or less pain after the operation and can do some daily activities or go back to work is probably quickly satisfied, but this does not imply that the operation was performed optimally. Furthermore, the patient is dependent on the surgeon, and therefore giving a satisfying answer could continue a good relationship with their physician. Looking at the results in Table 3.2.2, a number of authors presents a high satisfaction rate, even though a large number of their patients still has some daily pain or residual deformity. In conclusion, the scoring scales do not have clearly defined measures to determine which result is truly satisfactory.

Pathology

Table 3.2.1 shows that a subtalar arthrodesis was primarily indicated to correct foot deformities, and the results of these operations appear to be less satisfactory *(Tables 3.2.2 and 3.2.3)* than results for other disorders. This can be attributed to the fact that deformities are difficult to correct, since not only the shape and relative position of the talus and calcaneus have to be adjusted, but also the balance of muscle forces has to be restored. This requires a thorough understanding of foot and ankle biomechanics to judge whether or not an additional tendon transfer is required. The subtalar arthrodesis procedure is indicated for isolated subtalar disorders in later years and gives more rewarding results *(Table 3.2.2)*. Recently, it became possible to perform the operation arthroscopically, which provides advantages for the patients.[23-26] From the section pathology in Table 3.2.1 and the results in Table 3.2.2, it can be concluded that it is more likely that a subtalar arthrodesis procedure will succeed if the anatomy of the hindfoot is minimally disturbed, the trauma is minimal and if there is no defect in the balance of muscle forces around the hindfoot.

Table 3.2.3 Complications mentioned in literature. Only the first author and date of publication are mentioned in the categories. The authors that are printed bold present complications of arthroscopic techniques.

early complications	author	neurovascular damage	authors	Infections	author	infections
	Noble [1979]	20%	[illegible]	[illegible]	Amendola [1996]	[illegible]
	Johansson [1982]	4%	[illegible]	[illegible]	Buch [1996]	[illegible]
	Carr [1988]	18%	[illegible]	[illegible]	Huang [1999]	[illegible]
	Bednarz [1997]	3%	[illegible]	[illegible]	Easley [2000]	[illegible]
	Burton [1998]	8%	[illegible]	[illegible]	Flemister [2000]	[illegible]
	Mann [1998]	33%	[illegible]	[illegible]	**[illegible]**	[illegible]
	Easley [2000]	9%	[illegible]	[illegible]	**Tasto [1998]**	[illegible]
	Jerosch [1998]	**0%**			**[illegible]**	[illegible]
	Tasto [1998]	**0%**				
	Scranton [1999]	**0%**				
late complications	**author**	**non-union**	**author**	**malalignment**	**author**	**screw removal**
	Pollock [1964]	2%	[illegible]	[illegible]	Dennyson [1976]	10%
	Engström [1974]	33%	[illegible]	[illegible]	Carr [1988]	64%
	Dennyson [1976]	6%	[illegible]	[illegible]	Romash [1993]	43%
	Gross [1976]	41%	[illegible]	[illegible]	Amendola [1996]	7%
	Ross [1980]	11%	[illegible]	[illegible]	Buch [1996]	64%
	McCall [1985]	46%	[illegible]	[illegible]	Mangone [1997]	8%
	Hsu [1986]	4%	[illegible]	[illegible]	Burton [1998]	17%
	Moreland [1986]	5%	[illegible]	[illegible]	Mann [1998]	33%
	Carr [1988]	9%	[illegible]	[illegible]	Huang [1999]	7%
	Russotti [1988]	2%	[illegible]	[illegible]	Scranton [1999]	8%
	Scranton [1991]	30%	[illegible]	[illegible]	Easley [2000]	20%
	Michelson [1996]	9%	[illegible]	[illegible]	Flemister [2000]	19%
	Bednarz [1997]	14%	[illegible]	[illegible]	**Tasto [1998]**	**7%**
	Fellmann [1997]	6%	[illegible]	[illegible]	**Scranton [1999]**	**20%**
	Dahm [1998]	4%	[illegible]	[illegible]		
	Sammarco [1998]*	14%	[illegible]	[illegible]		
	Easley [2000]	16%				
	Flemister [2000]	5%				
	author	**foot instability**	**author**	**Swelling**	**author**	**impingements**
	Mann [1998]	15%	[illegible]	[illegible]	Gross [1976]	9%
	Sammarco [1998]	7%	[illegible]	[illegible]	Ross [1980]	53%

Measurement of malalignment

To be able to fuse the hindfoot in a correct position it is important to measure the amount of malalignment. Apart from this, the surgeon should be able to verify the amount of correction per- and postoperatively. A lateral weightbearing radiograph is often used to determine a couple of variables related to the alignment of the foot *(Table 3.2.1)*. However, these variables are difficult to measure and to reproduce from radiographs *(Table 3.2.4)*. Furthermore, the conditions for taking the radiograph have to be exactly determined, the bony landmarks necessary to measure the variables are not always clear, and the relationship between these variables and the functional outcome is questionable.[30] Flemister et al.[30] found no correlation between the talar declination angle and the AOFAS-score.

None of the authors use the results from the radiographs for accurate preoperative planning of the correction. One of the reasons is that these radiographs are taken in a weightbearing position, whereas during the operation the foot is in a non-weightbearing and different position. Laughlin and Payette[13], Mallon[31], Kitaoka and Patzer[32], and Mann[19] state that it is essential that the forefoot has a certain amount of flexibility to have a successful functional outcome after subtalar arthrodesis. Therefore, it is useful to measure and to compare the range of motion of the forefoot pre- and postoperatively. However, some authors measure only the hindfoot flexibility *(Table 3.2.1)*, whereas forefoot flexibility is not measured quantitatively by any of the authors. Therefore it is unclear how this flexibility is defined and what its range should be. It is also unclear what the ideal configuration is for fusion of the talus and calcaneus. Some authors simply state that the foot deformity has to be corrected. Moreland and Westin[33] indicate that the foot has to be fused in a neutral position, and Lian[8] and Mann[19] suggest that the hindfoot is best fused in 5° valgus, because then the forefoot is flexible. Scranton[34] and Äström[35] state that there exists no such thing as an ideal foot, but it is natural for a human to be symmetric. They suggest that, in establishing correction of the pathologic foot, symmetry has to be sought with the opposite foot, except in cases where both feet are deformed.

In conclusion, a clearly defined quantitative measurement of the degree of malalignment and per- and postoperative correction is not present in the current subtalar arthrodesis techniques. This fact is at least surprising, since one of the main goals is to achieve a good alignment of the hindfoot. A correct foot position is not defined in literature, but it seems logical to aim for a correction in which symmetry with the opposite foot is sought for in a weightbearing position.

Access and cartilage removal

Little attention is paid to the position of the patient in the operation room *(Table 3.2.1)*. This can, however, be an important issue when trying to measure the alignment or amount of correction peroperatively, especially when this is done by visual inspection. With the patient lying in a lateral decubitus position, it is difficult to find an anatomical reference axis to determine the amount of correction.[36] If the patient is lying in a prone position, the opposite leg and foot can be used as reference axis to judge the established correction of the hindfoot.

The necessity to make a large incision when performing an open technique introduces the risk of infections, neurovascular damage, and problematic wound closure *(Table 3.2.3)*.[36,37] In addition to this, surgeons indicate that the access phase is one of the difficult steps in the

Table 3.2.4
Limitations mentioned in literature. Only the first author and date of publication are mentioned in the categories. The limitations mentioned in literature are categorized when this was possible. The techniques that are found difficult mentioned in other articles are placed between brackets in the category limitations (technically demanding: other procedures). In the second part the limitations of arthroscopic techniques are presented.

limitation open	difficult to measure misalignment	bone graft usage	technically demanding: Grice procedure	technically demanding: other techniques or SA in general
authors	Gross [1976] Noble [1979] Moreland [1986] Scranton [1991] * Mann [1998] Huang [1999]	[illegible]	Seymour [1968] Engström [1974] Gross [1976] Ross [1980] graft slippage McCall [1985] Hsu [1986] difficult to fit grafts	[illegible]
limitation arthroscopic	difficult to close incision risk of woundbreakdown	difficult to assess roentgenographic consolidation	difficult to remove cartilage	difficult to position screw accurately
authors	Amendola [1996] Huang [1999]	[illegible]	Buch [1996]	[illegible]
limitation	difficult to establish portals	experienced surgeon Required	correction deformities Impossible	learning curve is very steep
authors	**Tasto [1998]** **Jerosch [1998]**	[illegible]	**Tasto [1998]**	[illegible]

procedure.[15,21] The arthroscopic techniques significantly reduce these complication risks *(Table 3.2.3)*.[23-26] However, for the surgeons this arthroscopic approach is demanding *(Table 3.2.4)*, since the geometry of the subtalar joint is irregular. The Batchelor-technique* can be marked as a minimal access technique. This procedure is supposed to be easier to perform than the Grice-technique** and gives immediate firm fixation of the joint.[38,39] Gross[38] reports a non-union rate of as much as 41% *(Table 3.2.3)* and advises against the use of the Batchelor-technique. The reasons for failure are according to Gross[38]: too short period of non-weightbearing, the use of cortical bone graft, and too little compression force in the subtalar joint. Another major factor could be the fact that the cartilage is hardly removed. If there is no bone-on-bone contact, fusion cannot take place. For the Batchelor- technique, fusion can only take place by means of the bone graft, but since there is only a small bone on bone contact area, the bridge can easily break, even after some time. This is confirmed by Fellman and Zollinger[40] who found that insufficient cortical bone had been removed in their two cases of nonunion. Hsu et al.[41] presented a combination of the Grice- and Batchelor-technique, but the advantages of this combined technique are not evident.
In open surgery, tissue is removed to create workspace. If soft tissue removal is inadequate to inspect the entire joint, a lamina spreader is used, and sometimes a distractor. Excessive distraction can cause nerve damage.[42-44] A method to avoid access to the entire joint and to create extra distraction is the partial removal of the cartilage and subchondral bone of the subtalar joint at the lateral side *(Table 3.2.1)*. However, this method does not enhance quick and solid fusion of the joint *(Tables 3.2.1-3.2.3)*.
In conclusion, firstly, it is favorable to place the patient in a prone position to be able to perform a measurement of alignment in the operation room and use the opposite healthy foot as reference. Secondly, an arthroscopic or minimal access to the subtalar joint has obvious advantages. Thirdly, even though no explicit references could be found, it is derived from the discussion that the feathering of the entire posterior, medial, and anterior facet on the talar and calcaneal sides is an important factor to obtain quick and solid fusion.

Bone graft
A lot of different types of bone graft have been applied and they all have their advantages and disadvantages. A cortical graft is strong and stiff and can be used to correct a deformity, but it does not enhance fusion as well as a cancellous bone graft does. The corticocancellous bone graft seems therefore a good compromise and is used by many authors *(Table 3.2.1)*. Grice[9] and Thomas[45] advise against the use of cortical bone grafts. It can indeed be concluded that surgeons who use only cortical bone grafts report good results, but have more cases of non-union *(Table 3.2.1-3.2.3)*. If there are no deformities, it seems more favorable to use a cancellous bone graft or no bone graft at all, to optimize the conditions for fusion.[23,24,30,32] The main advantage of not using a bone graft is that it reduces the morbidity of the patient, since no additional operation is necessary to obtain a bone graft. The use of an allograft or bank bone also reduces the morbidity for the patient.[30] However, the results for these types of bone graft are mixed. Engström et al.[46] advise against the use of allograft, whereas Michelson and Curl[47], and Easley et al.[14] detected no significant relationships between the type of bone graft that had

** Consists of transfixing the subtalar joint with a fibular graft inserted at the anterior part of the neck of the talus, without removal of cartilage and subchondral bone in the subtalar joint.*
*** Consists of a lateral approach to remove the cartilage and the subchondral bone layers, followed by insertion of bone grafts in the sinus tarsi to perform correction of the hindfoot.*

been used and the results achieved.
In conclusion, solid fusion can be obtained without the use of bone grafts. The authors who present results thereof denude the entire subtalar joint on the talar and calcaneal side. This supports the hypothesis that the removal of cartilage is essential for a solid fusion. When a bone graft is used a cancellous autograft is advised. When correction of a deformity is needed a corticocancellous autograft can be placed.

Correction
Deformity is a primary reason to perform a subtalar arthrodesis. Therefore, correction of the deformity is important, and it is a crucial phase in the operation.[40] Patterson et al.[37] mention that the major cause of failure of a hindfoot arthrodesis was undercorrection of the deformity by the surgeon at the time of operation. It is remarkable that little attention in the literature is paid to methods for correction.
The current correction methods used *(Table 3.2.1)* are inaccurate and unreliable[48,49], since, as it was already pointed out, it is hard to visually judge the degree of correction. Only Easley et al.[14] and Chan and Alexander[50] report measurement of the gap between talus and calcaneus and the size of bone graft. From the analysis of this operation phase, it seems that surgeons lack tools to accurately perform a correction.

Fixation
It is important that the joint is fixated firmly to obtain fusion *(e.g. Gross[38])*. The magnitude of this compression force and how long it is necessary to maintain this force, is not found in literature. Looking at the results and especially the nonunion rates, it can be concluded that fixation with bone grafts alone does not put the joint in enough compression. Seven authors *(Tables 3.2.1 and 3.2.3)* who perform a bone block distraction technique report considerable rates of non-union and malalignment in comparison with results achieved by applying screw fixation.
Nowadays, the arthrodesis is often fixed by positioning a screw in the center of the two joint surfaces. This results in the weakest possible connection between the talus and calcaneus from a mechanical point of view. E.g. when two steel rods are welded to one another, they are fused at the outer circumferential surfaces of the rods, because this results in the highest resistance to bending and torsion. Surgeons have noticed that the fixation with one screw is not always sufficient, and a number of surgeons[14,22,29] solves this problem by using two screws to fixate the joint.[51] Kuwada[52] has adjusted the fixation technique for specific patient groups and Thomas[53] suggests a technique to prevent screw removal. It is, however, questionable if a screw is the most suitable device for fixation, because of the current fixation location, and because the patients often require a second operation for screw removal *(Table 3.2.3)*.
In conclusion, compression of the two bone surfaces of the subtalar joint is important to achieve union. Assessing the conditions for optimal fusion requires a great deal of mechanical engineering background.

Postoperative care

As far as the postoperative care is considered, most authors advocate 6 weeks nonweightbearing cast followed by six weeks of a weightbearing cast. Early weightbearing resulted in a considerable percentage of failures.[38,45,54,55] Buch et al.[15], Bednarz et al.[29] and Huang et al.[56], who present techniques and results for malunited comminuted calcaneal fractures, are more careful with the healing process, because these operations are usually more demanding. The authors presenting an arthroscopic technique tend to let their patient walk at an earlier stage than 6 weeks, because of the already mentioned advantages of less morbidity and reduced damage to neurovascular structures. In conclusion, there seems to be evidence that the more the structures are left intact the faster the patient recovers.

Technical limitations

The subtalar arthrodesis procedure is a demanding technique. One of the reasons is that the indication for subtalar arthrodesis is not frequently made, which impairs surgeons to acquire experience with this procedure. Another reason is that the subtalar joint is very tight and has a geometry that is difficult to reach. An arthroscopic technique is even more demanding, because the access and workspace are more restricted. In conclusion, there is a need for additional technical support to make this procedure easier and more accurate to perform, and to minimize morbidity of the patient.

Conclusions

An analysis of the open and arthroscopic techniques for subtalar arthrodesis reveals that there is a number of limitations using these techniques: no well defined, accurate and reproducible measurement of malalignment and bone correction, difficult access to the subtalar joint, and a weak fixation. In addition to this, factors are derived that are important to achieve a successful arthrodesis: minimal damage to structures, removal of all cartilage and the necessity to compress the joint surfaces to enhance fusion.

3.3 Strategy of a new technique

From Section 3.1 and 3.2, it appears that several factors are important in achieving a successful subtalar arthrodesis. For the patient the important requirements for a new technique are fusion, no residual deformity, no morbidity, no pain and a quick recovery. Therefore, it is chosen to approach the subtalar joint arthroscopically. For the surgeon it is important that he can easily and accurately perform the procedure. It is necessary to assist him by biomechanical analysis and development of additional instruments: a measurement system, an instrument for cartilage removal and a fixation device. In this section, a strategy is presented containing guidelines to optimize the procedure for both the patient and the surgeon, and indicates what instrument should be developed to be able to implement this new technique. The proposed technique is described according to the subdivision in phases presented in Section 3.2: measurement of malalignment, access, removal of cartilage, correction of subtalar alignment and fixation. Each phase will be elucidated.

Measurement of malalignment

To achieve adequate correction of the hindfoot deformity it is necessary to perform a preoperative and a peroperative measurement of any axial deformity. To achieve this it would need the development of a measurement device. The following criteria can be formulated for this device: possibility to measure in weightbearing *(functional situation for the patient)* and nonweightbearing situations *(in the operating room)*, measurement of forefoot flexibility, and determination of the size of a bone graft. Secondly, a quantitative, reproducible measurement that can be determined with sufficient accuracy should be developed. Considerations for this measurement - which will be most likely an angle - are choice of axes that determine this angle, and usage of the opposite healthy leg as a symmetric reference to determine the amount of correction. More criteria will be derived in Section 4.1.

Access

It is chosen to place the patient in a prone position, since this gives good reference possibilities for measurement of correction, because the unaffected contralateral side can be use to seek symmetry. In addition to this, the patient's legs are in a straight position and their axes can also be used as a reference to perform adequate correction of the hindfoot. We feel that it is advantageous to access the subtalar joint by means of an arthroscopic approach. There are portals defined for anterolateral subtalar arthroscopy[26,57-60], but those portals all require the lateral side of hindfoot to be placed upwards, which is contrary to the requirement of the preferred prone position placement of the patient. Recently, a two-portal endoscopic ankle approach with the patient in the prone position has been described that can also be used for access to the subtalar joint.[61]

Removal of cartilage

For a solid fusion, all cartilage has to be removed from both surfaces. Although it is possible to visualize the complete joint[57], it requires skills to remove all cartilage and to create a smooth surface with the current straight instruments, since the joint space is very narrow.

To solve this problem there are two options, namely to create more workspace or to develop a flexible instrument that can follow the contours of the joint and thus makes it possible to reach the entire joint. Furthermore, this instrument can be designed such that it can be used in combination with a routinely used shaver system, which enables easy tissue removal. Creation of more workspace demands more soft tissue resection and ligament release. The more structures are left intact the quicker the patient is likely to recover. It is therefore suggested to develop an arthroscopic instrument that meets the following demands: easy and quick removal of cartilage and subchondral bone, leaving a smooth surface and preserving the shape of the joint.

Correction

Bone correction via an arthroscopic procedure is currently not possible and this is a major disadvantage for the choice of an arthroscopic procedure. Jerosch[26] brings little pieces of bone chips inside the joint. These chips probably are too small to serve as 'bone block'. There are two profitable solutions. The first option is insertion of bone grafts via one of the portals. If the bone grafts are too large, it could be possible to create a larger access portal by removal of fat tissue anterior to the Achilles tendon. The second option is to integrate the correction function in the fixation device. Then, only cancellous bone chips have to be inserted via the portals to enhance fusion. Further investigation is necessary to make a decision.

Fixation

The screws currently used as fixation device do not give an optimal performance. It is necessary to investigate a number of factors to formulate design criteria and specifications: determination of the minimum compression force to create optimal conditions for quick union, determination of the optimal fixation locations, and bone adaptation to the foreign material. The optimal location for fixation could for example be the most loaded area in the subtalar joint during standing or walking.[62-66] It might be advantageous if the screws bear less load when time passes or even dissolve like bioabsorbable materials. This would also prevent an additional operation for screw removal. Lastly, attention should be paid to the integration of the correction and the fixation function into one device.

Subtalar endoprosthesis

The subtalar arthrodesis procedure is commonly used to relief chronic pain complaints in the subtalar joint. In addition to the proposed minimal access to enter the subtalar joint, a step forward would be to replace the joint instead of performing a fusion. The first phases of the proposed technique can also be used for the joint replacement technique.

3.4 Discussion

In this chapter, the clinically driven approach was used only after the engineer had performed a thorough literature study of the current techniques for performing a subtalar arthrodesis. The initiative for starting research in this area came from clinical practice. However, this type of operation is not frequently performed via an open procedure, and not performed via an arthroscopic approach in the Netherlands. Thereto, the engineer had to get acquainted with the topic via literature in order to be able to start a useful interview with experts in the field. From literature, it was possible to set up a new strategy for a minimal access technique, which was mainly due to the fact that the engineer was able to investigate the literature from a different point of view. Seeking for feedback of each idea remained an important step in the process, since surgeons can judge if a new or different step could be possible in clinical practice. The interviews with experts supported the new strategy, and revealed a couple of nuances to the new technique. For example, a new measurement system to determine the hindfoot alignment of a patient will probably be more frequently used in severe cases. It is concluded, that the fact that the interviewer was familiar with the topic and asked detailed questions lead to the gathering of useful information. Analysis from a technical point of view revealed limitations that can be solves by development of simple additional instruments that improve that quality of the procedure.

References

1. Prismant. Internet . 2002. Research, Advise, Information and Education in Health Care, Utrecht. www.prismant.nl.

2. Tuijthof GJM, van Dijk, C. N., and Pistecky PV. Subtalar arthrodesis: current limitations and strategy for a new technique. Submitted to *Foot & Ankle Int.*, 2002.

3. Rockar PA. The subtalar joint: anatomy and joint motion. *J Orthop Phys Ther* 1995; 21: 361-372.

4. Sarrafian SK. Biomechanics of the subtalar joint complex. *Clin Orthop* 1993; 290: 17-26.

5. Isman RE. Inman VT. Anthropometric studies of the human foot and ankle. *Bull Prost Res* 1969; 10: 97-129.

6. Inman VT, ed. *The joints of the ankle*. Baltimore: Williams & Wilkins Company, 1976. ISBN 0-683-04342-0.

7. Perry J. Anatomy and biomechanics of the hindfoot. *Clin Orthop* 1983; 177: 9-15.

8. Lian G. Hindfoot arthrodesis. In: Pfeffer GB, Frey C, eds. *Current practice in foot and ankle surgery*. San Francisco: McGraw-Hill, 1993;262-284

9. Grice DS. An extra-articular arthrodesis of the subastragalar joint for correction of paralytic flat feet in children. *J Bone Joint Surg Am* 1952; 34: 927-940.

10. Pollock JH. Carrell B. Subtalar extra-articular arthrodesis in the treatment of paralytic valgus deformities. *J Bone Joint Surg Am* 1964; 46: 533-541.

11. Mann RA. Baumgarten M. Subtalar fusion for isolated subtalar disorders. *Clin Orthop* 1988; 226: 260-265.

12. Donatto KC. Arthritis and arthrodesis of the hindfoot. *Clin Orthop* 1998; 81-92.

13. Laughlin TJ. Payette CR. Triple arthrodesis and subtalar joint arthrodesis. *Clin Podiatr Med and Surg* 1999; 16: 527-555.

14. Easley ME. Trnka H-J. Schon LC. Nade S. Isolated subtalar arthrodesis. *J Bone Joint Surg Am* 2000; 82: 613-624.

15. Buch BD. Myerson MS. Miller SD. Primary subtalar arthrodesis for the treatment of comminuted calcaneal fractures. *Foot & Ankle Int* 1996; 17: 61-70.

16. Fellman J. Zollinger H. Versteifungseingriffe am unteren Sprunggelenk - wechselnde Konzepte im Wandel der Zeit. *Z Orthop* 1996; 134: 341-345.

17. de Heus JA. Marti RK. Besselaar PP. Albers GH. The influence of subtalar and triple arthrodesis on the tibiotalar joint. A long-term follow-up study. *J Bone Joint Surg Br* 1997; 79: 644-647.

18. Tuijthof GJM. Studiereis USA Bezoek aan orthopedisch chirurgen. Man-machine systems, Department of Design, Engineering and Production, Delft University of Technology, Delft, 2001: 1-31.

19. Mann RA. Arthrodesis of the foot and ankle. In: Mann RA, Coughlin MJ, eds. *Surgery of the foot and ankle.* St. Louis: Mosby, 1993;673-713. ISBN 0-8016-6683-X.

20. Grimbergen CA. Dankelman J. Stassen HG. Man-machine systems aspects of minimally invasive surgery and interventional techniques. The Delft-Amsterdam cooperation. *Min Invas Ther & Allied Technol* 1998; 10.

21. Tuijthof GJM, van Dijk, C. N., Herder JL, and Pistecky PV. Design of arthroscopic instruments: a clinically driven approach. Submitted to the *Journal of Knee Surgery, Sports Traumatology, Arthroscopy,* 2002.

22. Burton DC. Olney BW. Horton GA. Late results of subtalar distraction fusion. *Foot & Ankle Int* 1998; 19: 197-202.

23. Tasto JP, Laimins PD. Recent advances in ankle arthroscopic techniques. In: Parisien JS, ed. *Current techniques in arthroscopy.* New York: Thieme, 1998;181-194. ISBN 0-86577-738-1.

24. Scranton PE. Comparison of open isolated subtalar arthrodesis with autogenous bone graft vs. outpatient arthroscopic subtalar arthrodesis using injectable bone morphogenic protein-enhanced graft. *Foot & Ankle Int* 1999; 20: 162-165.

25. Lundeen RO. Arthroscopic fusion of the ankle and subtalar joint. *Clin Podiatr Med and Surg* 1994; 11: 395-406.

26. Jerosch J. Subtalar arthroscopy - indications and surgical technique. *Knee Surg Sport Tr A* 1998; 6: 122-128.

27. Kitaoka HB. Alexander IJ. Adelaar RS. Nunley JA. Myerson MS. Sanders M. Clinical rating systems for the ankle-hindfoot, midfoot, hallux, and lesser toes. *Foot & Ankle Int* 1997; 18: 187-188.

28. McCall RE. Lillich JS. Harris JR. Johnston FA. The Grice extra-articular subtalar arthrodesis: a clinical review. *J Pediatr Orthop* 1985; 5: 442-445.

29. Bednarz PA. Beals TC. Manoli A. Subtalar distraction bone block fusion: an assessment of outcome. *Foot & Ankle Int* 1997; 18: 785-791.

30. Flemister AS. Infante AF. Sanders RW. Walling AK. Subtalar arthrodesis for complications of intra-articular calcaneal fractures. *Foot & Ankle Int* 2000; 21: 392-399.

31. Mallon WJ. The Grice procedure, extra-articular arthrodesis. *Orthop Clin N Am* 1989; 20: 649-654.

32. Kitaoka HB. Patzer GL. Subtalar arthrodesis for posterior tibial tendon dysfunction and pes planus. *Clin Orthop* 1997; 345: 187-194.

33. Moreland JR. Westin GW. Further experience with Grice subtalar arthrodesis. *Clin Orthop* 1986; 207: 113-121.

34. Scranton PE. Results of arthrodesis of the tarsus: talocalcaneal, midtarsal, and subtalar joints. *Foot Ankle* 1991; 12: 156-164.

35. Astrom M. Arvidson T. Alignment and joint motion in the normal foot. *J Orthop Phys Ther* 1995; 22: 216-222.

36. Lewis G. Biomechanics as a basis for management of intra-articular fractures of the calcaneus. *J Am Podiatr Med Assoc* 1999; 89: 234-246.

37. Patterson RL. Parrish FF. Hathaway EN. Stabilizing operations on the foot: a study of the indications, techniques used, and end results. *Foot & Ankle Int* 1996; 17: 594-607.

38. Gross RH. A clinical study of the Batchelor subtalar arthrodesis. *J Bone Joint Surg Am* 1976; 58: 343-349.

39. Seymour N. Evans DK. A modification of the Grice subtalar arthrodesis. *J Bone Joint Surg Br* 1968; 50: 372-375.

40. Fellman J. Zollinger H. Isolated talocalcaneal interposition fusion: a prospective follow-up study. *Foot & Ankle Int* 1997; 18: 616-621.

41. Hsu LCS. Jaffray D. Leong JCY. The Batchelor-Grice extra-articular subtalar arthrodesis. *J Bone Joint Surg Br* 1986; 68: 125-127.

42. Albert J. Reiman P. Njus G. Kay DB. Theken R. Ligament strain and ankle joint opening during ankle distraction. *Arthroscopy* 1992; 8: 469-473.

43. Casteleyn P-P. Handelberg F. Distraction for ankle arthroscopy. *Arthroscopy* 1995; 11: 633-634.

44. Dowdy PA. Watson BV. Brown JD. Noninvasive ankle distraction: relationship between force, magnitude of distraction end nerve conduction abnormalities. *Arthroscopy* 1996; 12: 64-69.

45. Thomas FB. Arthrodesis of the subtalar joint. *J Bone Joint Surg Am* 1967; 49: 93-97.

46. Engstrom A. Erikson U. Hjelmstedt A. The results of extra-articular subtalar arthrodesis according to the Green-Grice method in cerebral palsy. *Acta Orthop Scand* 1974; 45: 945-951.

47. Michelson JD. Curl LA. Use of demineralized bone matrix in hindfoot arthrodesis. *Clin Orthop* 1996; 325: 203-208.

48. Buckley RE. Hunt DV. Reliability of clinical measurement of subtalar joint movement. *Foot & Ankle Int* 1997; 18: 229-232.

49. Pearce TJ. Buckley RE. Subtalar joint movement: clinical and computed tomography scan correlation. *Foot & Ankle Int* 1999; 20: 428-432.

50. Chan SCF. Alexander J. Subtalar arthrodesis with interposition tricortical iliac crest graft for late pain and deformity after calcaneus fracture. *Foot & Ankle Int* 1997; 18: 613-615.

51. Carr JB. Hansen ST. Benirschke SK. Subtalar distraction bone block fusion for late complications of os calcis fractures. *Foot & Ankle Int* 1988; 9: 81-86.

52. Kuwada GT. Modification of fixation technique for a subtalar joint and triple arthrodesis. *J Am Podiatr Med Assoc* 1988; 78: 482-485.

53. Thomas PJ. Placement of screws in subtalar arthrodesis: a simplified technique. *Foot & Ankle Int* 1998; 19: 416-417.

54. Dennyson WG. Fulford GE. Subtalar arthrodesis by cancellous grafts and metallic internal fixation. *J Bone Joint Surg Br* 1976; 58: 507-510.

55. Noble J. McQuillan WM. Early posterior subtalar fusion in the treatment of fractures of the os calcis. *J Bone Joint Surg Br* 1979; 61: 90-93.

56. Huang P-J. Fu Y-C. Cheng Y-M. Lin S-Y. Subtalar arthrodesis for late sequelae of calcaneal fractures: fusion in situ vs fusion with sliding corrective osteotomy. *Foot & Ankle Int* 1999; 20: 166-170.

57. Frey C. Gasser S. Feder K. Arthroscopy of the subtalar joint. *Foot & Ankle Int* 1994; 15: 424-428.

58. Mekhail AO. Heck BE. Ebraheim NA. Jackson WT. Arthroscopy of the subtalar joint: Establishing a medial portal. *Foot & Ankle Int* 1995; 16: 427-432.

59. Parisien JS. Arthroscopy of the posterior subtalar joint. In: Parisien JS, ed. *Current Techniques in Arthroscopy.* New York: Thieme, 1998;161-168. ISBN 0-86577-738-1.

60. Williams MM. Ferkel RD. Subtalar arthroscopy: indications, technique and results. *Arthroscopy* 1998; 14: 373-381.

61. van Dijk CN. Scholten PE. Krips R. A 2-portal endoscopic approach for diagnosis and treatment of posterior ankle pathology. *Arthroscopy* 2000; 16: 871-876.

62. Sangeorzan BJ. Wagner UA. Harrington RM. Tencer AF. Contact characteristics of the subtalar joint: the effect of talar neck misalignment. *J Orthop Res* 1992; 10: 544-551.

63. Wagner UA. Sangeorzan BJ. Harrington RM. Tencer AF. Contact characteristics of the subtalar joint: load distribution between the anterior and posterior facets. *J Orthop Res* 1992; 10: 535-543.

64. Savory KM. Wulker N. Stukenborg C. Alfke D. Biomechanics of the hindfoot joints in response to degenerative hindfoot arthrodeses. *Clin Biomech* 1998; 13: 62-70.

65. Mulcahy DM. McCormack DM. Stephens MM. Intra-articular calcaneal fractures: effect of open reduction and internal fixation on the contact characteristics of the subtalar joint. *Foot & Ankle Int* 1998; 19: 842-848.

66. Fuller EA. Center of pressure and its theoretical relationship to foot pathology. *J Am Podiatr Med Assoc* 1999; 89: 278-291.

67. Romash MM. Reconstructive osteotomy of the calcaneus with subtalar arthrodesis for malunited calcaneal fractures. *Clin Orthop* 1993; 290: 157-167.

68. Russotti GM. Cass JR. Johnson KA. Isolated talocalcaneal arthrodesis. *J Bone Joint Surg Am* 1988; 70: 1472-1478.

69. Mangone PG. Fleming LL. Fleming SS. Hedrick MR. Seiler JG. Bailey E. Treatment of acquired adult planovalgus deformities with subtalar fusion. *Clin Orthop* 1997; 341: 106-112.

70. Kalamchi A. Evans JG. Posterior subtalar fusion. *J Bone Joint Surg Br* 1977; 59: 287-289.

71. Amendola A. Lammens P. Subtalar arthrodesis using interposition iliac crest bone graft after calcaneal fracture. *Foot & Ankle Int* 1996; 17: 608-614.

72. Dahm DL. Kitaoka HB. Subtalar arthrodesis with internal compression for post-traumatic arthritis. *J Bone Joint Surg Br* 1998; 80: 134-138.

73. Ross PM. Lyne ED. The Grice procedure: indications and evaluation of long-term results. *Clin Orthop* 1980; 194-200.

74. Sammarco GJ. Tablante EB. Subtalar arthrodesis. *Clin Orthop* 1998; 349: 73-80.

75. Johansson JE. Harrison J. Greenwood FAH. Subtalar arthrodesis for adult traumatic arthritis. *Foot Ankle* 1982; 2: 294-298.

76. Platzer W, ed. *Sesam, atlas van de anatomie bewegingsapparaat.* Baarn: Bosch & Keunig, 1998. ISBN 90-414-0252-7.

4. Subtalar arthrodesis: implementation of a new technique

In Chapter 3, a strategy was set up for the performance of a subtalar arthrodesis, including the necessary instruments that have to be developed to implement the technique. In this chapter, design criteria are set up for two of these instruments. For each instrument a prototype is constructed and is evaluated. Section 4.1 concentrates on the development of a measurement system to measure the alignment of the hindfoot pre-, per-, and postoperatively. The second instrument aims at the removal of cartilage and subchondral bone from the joint surfaces of the subtalar joint while preserving the shape of the joint surfaces. Thereto, Section 4.2 presents the set up of a model of the subtalar joint space, and experiments to determine the machining forces of bone and cartilage. These data are necessary to define the actual values for design criteria of the flexible instrument. In Section 4.3, the set up of the design criteria, the conceptual design, and a prototype of the flexible instrument are elucidated. The chapter is concluded with a discussion *(Section 4.4)*.

4.1 Measuring malalignment of the hindfoot

This section is based on the article *Measuring malalignment of the hindfoot*, by G.J.M. Tuijthof, J.L. Herder, P.E. Scholten, C.N. van Dijk, P.V. Pistecky, which will be submitted to the Journal of Biomechanical Engineering.

Keywords: subtalar joint, alignment, clinical evaluation, reliability

Abstract: In about half of the cases where a subtalar arthrodesis is performed, a correction of hindfoot alignment is necessary. To improve the quality of the operation, a measurement system was developed which can measure the hindfoot angle pre-, per-, and postoperatively. This device was evaluated with four observers and eight subjects, for which measurements were performed in standing weightbearing position and in prone nonweightbearing position. The results were compared with hindfoot angles determined by using posterior ordinary photographs. In conclusion, the measurement system measures a clinically relevant hindfoot angle in weightbearing and nonweightbearing positions. The measurement system performs slightly better *(intra SD is 1.3°, inter SD is 1.7°)* in comparison to weightbearing photographs *(intra SD is 1.4°, inter SD is 2.8°)*. Further investigation is necessary to assess if both methods are accurate enough to use them in a clinical setting, since the intertester reliability is poor *(ICC 0.64)*. A strict measurement protocol, in combination with adjustments to the prototype could improve the intertester reliability.

Introduction

In subtalar arthrodesis operations, a correction of the hindfoot alignment is necessary in about half of the cases.[1] In practice, surgeons use pre- and postoperative lateral weightbearing radiographs, and / or peroperative visual inspection to realign the calcaneus with respect to the

leg.[1] This method is not accurate[2], and not reproducible, since the bony landmarks are not always clear on the radiographs. The relationship between variables on the radiographs and the functional outcome is questionable.[3] Furthermore, radiographs are of no use inside the operation room, because during the operation the foot is in a different and nonweightbearing position. Unsatisfactory alignment is obtained in 4% to 21% of the cases after a subtalar arthrodesis.[1,4-17] In addition to this, it is unclear what the ideal configuration is for fusion of the talus and calcaneus. Fusion in a neutral position[11], fusion in 5° valgus[18,19], and fusion where symmetry with the opposite foot is sought[20,21] are all indicated.
A number of studies involves the measurement of subtalar alignment in vivo and in vitro, as well as subtalar motion.[2,22-29] Two subtalar joint positions are used in the measurement of subtalar alignment. For the nonweightbearing subtalar neutral position several definitions are given.[21-23,28,30-33] In this paper, the subtalar neutral position is defined as the position for which the posterior midline of the calcaneus is vertically aligned with the midline of the lower leg.[21,30,33,34] Although the definition is explicit, clinical assessment of this position is unreliable.[21,22,27,30] The weightbearing resting foot position, which is measured relative to the vertical by placing an inclinometer on the midline of the calcaneus[32] or relative to the midline of the calf[21,33], shows a good intratester reliability of 0.85 and a fair intertester reliability of 0.67[21,32].
So far, the systems that have been used to determine subtalar neutral position or range of motion cannot be easily used inside the operating room with the patient in a nonweightbearing prone position.[22,23,27,35-37] An advantage of the prone position in comparison to other positions *(lateral decubitus, and supine with elevated hip)* is that the unaffected contralateral side can be used to seek symmetry when performing the correction. This nonweightbearing prone position is part of a new surgical technique to perform a subtalar arthrodesis *(Chapter 3)*.[1]
The goal of this study is to present the development and evaluation of a measurement system that can be used pre-, per-, and postoperatively to determine the malalignment and correction of the hindfoot in a quantitative, sufficiently accurate and reliable manner. In addition to this, a second method is applied which uses posterior weightbearing photographs in which the hindfoot angle is drawn. A comparison is made between both the methods.

Materials and Method

Conceptual design

From prior study *(Chapter 3)*, it was analyzed that the measurement system should fulfill a number of requirements. Additional requirements are easy in handling, lightweight, sterilizable, and a quick and noninvasive measurement.

Choice of measure

It is assumed that correction mainly takes places in the frontal plane, and that the correction angle has no relation with the anatomical axis of the subtalar joint, since the subtalar joint will be fused. Several options are available to define the hindfoot alignment: angle of the midline calcaneus with a vertically located axis, angle of the midline calcaneus with the midline of the lower leg, or angle of the midline calcaneus with the entire leg axis.[21,32,33] The entire leg axis is preferred as the reference axis, however this is practically difficult to determine from the outside. Therefore, we chose the angle measured in the frontal plane from posterior view between the midline of the calcaneus, and the midline of the lower leg. The latter is defined by a line through the middle between both malleoli and the middle of the knee joint as measured at the level of the joint line which can be palpated quite easily *(Figure 4.1.1)*.[21,33] In case of genu varum or valgum, the surgeon can compensate the to be corrected hindfoot angle accordingly by means of a radiograph of the entire leg. The exact definition to determine the calcaneus axis was not found. Therefore, a logical definition of the calcaneus axis was set up: the midline between two pairs of locations on the calcaneus. Two locations *(Figure 4.1.1: A and C)* are on the medial side of the calcaneus, and two *(Figure 4.1.1: B and D)* on the lateral side as seen posteriorly in the frontal plane. The lowest pair of locations *(A and B)* were chosen at 10 mm above the footsole, and the highest pair *(C and D)* were chosen to be at 25 mm above the first pair, in order to create a large as possible distance between the two pairs.

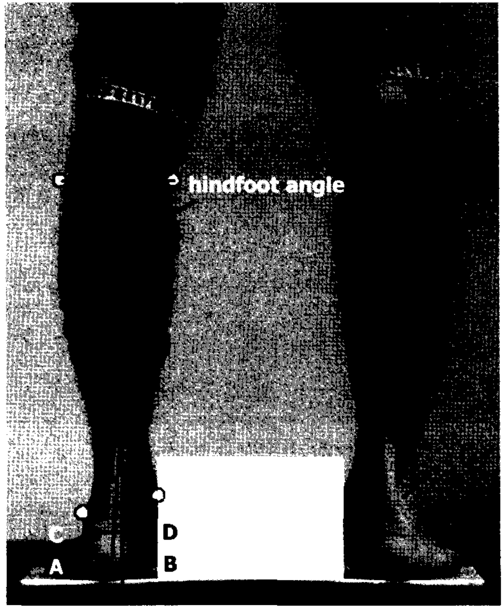

Figure 4.1.1
Photograph of the posterior side of a person.
The locations that are used to determine the midline of the lower leg (white bullets), and calcaneus (black bullets) are indicated.

Weightbearing and nonweightbearing

Measurement in weightbearing position is necessary, since the patient needs a normally aligned hindfoot to stand and to walk properly, whereas a measurement in a nonweightbearing prone position is necessary, since the patient lies nonweightbearing in the operation room.[1] As a consequence, either the standing position has to be imitated in the prone position or an unambiguous regression has to be determined between these two positions. To keep the system simple, it was chosen to determine a relation between the weightbearing and the nonweightbearing positions, and to place the subject's feet on a platform in a fixed distance from each other. The platform can be positioned on a table as well as in 90° rotated fixated to the table *(Figure 4.1.2)*. An average foot distance for the natural resting position was not found, and an average step width seemed too large[38]. Therefore, the foot distance was chosen to be the average shoulder width minus two times the average foot width *(Appendix 4A.1)*. In addition to this, it was found that during weightbearing measurement the knees are in slight flexion, which can also be imitated in the prone position by placement of a cushion underneath the ankles. *(Figure 4.1.2.B)*

Use of system in relation to accuracy

The necessary accuracy is difficult to determine and depends on the use of the measured hindfoot angle. Therefore a couple of options will be discussed. For a unilateral subtalar

Figure 4.1.2
Color illustration see cover.
A) Photograph of a person standing in the measurement system.

B) Photograph of a person lying in prone position in the measurement system. The measurement is performed as follows. The knee joint space is palpated and marked. The subject is positioned in the platform with his medial malleoli placed against the medial black support, and his heel against the edge of the platform at the posterior side. The calcaneal device is positioned in a groove (Figure 4.1.4) and the rods are alternately moved inwardly until the device is fixed to the calcaneus. The lateral malleolus plate is moved medially until it touches the lateral malleolus. The lower leg device is positioned through the ring and the upper rods are positioned on the marks and moved inwardly.

C) The 0°-line is positioned parallel to the lower leg device, and the hindfoot angle can be read on the goniometric scale.

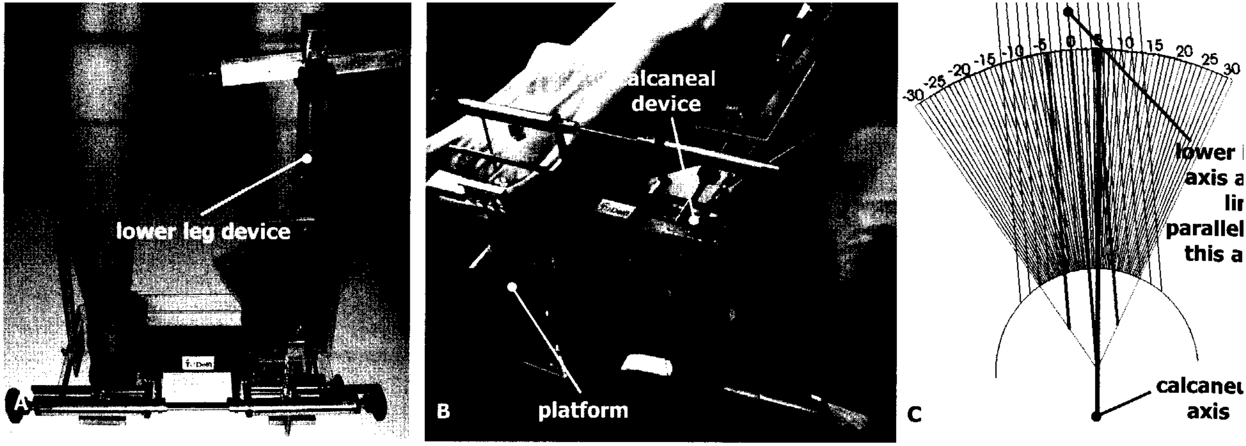

arthrodesis, the surgeon can subtract the preoperatively measured hindfoot angles of both sides to calculate the correction angle. This method assumes symmetry of the left and the right side. However, no data were found to determine if people are sufficiently symmetric, besides when a bilateral subtalar arthrodesis takes place the surgeon cannot use the opposite side. Another method to use the hindfoot angle could be that the surgeon judges the deviations from the ordinary anatomy of the lower extremities. Based on his experience he chooses an optimal hindfoot angle for realignment. The chosen hindfoot angle could be verified after initial fixation of the subtalar joint with a Steinmann pin. Eventually, an option would be to use the measured hindfoot angle to calculate the height of the bone graft when using a bone block distraction technique. With the help of the calculation of the size of the bone graft an estimation of the necessary accuracy can be given *(Figure 4.1.3)*:

$$h_{bonegraft} = 2 \cdot b_{talus} \cdot \sin\left(\frac{\alpha_{correction}}{2}\right) \qquad (4.1.1)$$

Figure 4.1.3
Schematic drawing from the posterior view of the calcaneus and talus to show the relation between the size of the bone graft, the width of the subtalar joint, and the correction angle.

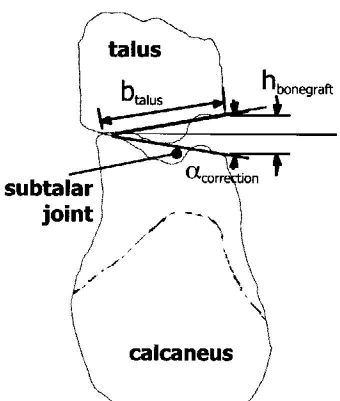

where $h_{bonegraft}$ is the height of the bone graft, b_{talus} is the width of the subtalar joint measured posteriorly in a frontal plane, $\alpha_{correction}$ is the correction angle measured in degrees. An estimation of the accuracy can then be derived, if it is assumed that the size of the bone graft, and the subtalar joint width can be measured with a certain accuracy. With the help of Figure 4.1.3 and Eq. 4.1.1, the equation for the measurement error of the correction angle *($\Delta\alpha_{correction}$)* is derived. Thereto, $\sin\alpha_{correction}$ is linearized with a Taylor-equation.[39] $h_{bonegraft}$ added with an error $\Delta h_{bonegraft}$ is subtracted by $h_{bonegraft}$, and $h_{bonegraft}$ is substituted by Eq. 4.1.1. After assuming that $\alpha_{correction}$ *(in radians)* is small, the equation for the measurement error $\Delta\alpha_{correction}$ is:

$$\Delta\alpha_{correction} = \frac{\Delta h_{bonegraft} - \alpha_{correction} \cdot \Delta b_{talus}}{b_{talus}} \qquad (4.1.2)$$

where $\Delta\alpha_{correction}$ is the error of the correction angle in radians, $\Delta h_{bonegraft}$ is the error of the size of the bone graft, and Δb_{talus} is the error of the subtalar joint width. If it is assumed that b_{talus} and $h_{bonegraft}$ can be measured with ± 1mm, it is calculated that the necessary accuracy of the correction angle should be ± 1°. Notice, that this is merely an indication.

Measurement system

A mechanical prototype of the measurement system was built to determine if the chosen hindfoot angle is a correct measure, and to get a grip on the possible accuracy that can be achieved. Several options are available for the construction: a spring mechanism, a screw mechanism, and a rolling link mechanism. Screw transmissions were implemented in the prototype, which is common in measurement of accurate positions. The prototype of the measurement system consists of three parts: a platform, a lower leg device, and a calcaneal device *(Figure 4.1.2)*. The dimensions of the measurement system were derived from anthropometric data *(Appendix 4A.1 and 4A.2)*.[38,40-43] A subject can stand in the platform with his medial malleoli at a fixed distance against the inner malleoli plates *(Figure 4.1.4)*. The platform can also be attached to a table to measure the patient in prone position *(Figure 4.1.2)*. Rods placed at equal distance from a centre beam determine the midlines of the lower leg and calcaneus *(Figure 4.1.4)*. The rods can be moved simultaneously inwards or outwards with the help of threaded shafts by which accurate motion is achieved. The lower leg device and the calcaneal device can be interchanged between both the extremities, and they are limited to motion in the frontal plane *(Figure 4.1.4)*. The determination of the midline through the calcaneus is performed by two pairs of rods containing a ball at their ends, which are moved inwards until firm fixation is achieved on the calcaneus. Determination of this axis is the most critical factor, since the distance between the two pairs of rods is only 25 mm. This implies that an error of 1 mm results when the midline error is 2°. The measurement system is a non-invasive device, and where possible lightweight materials were used to reduce the weight. Further investigation is necessary to choose materials that can be sterilized. So far, little attention was paid to a quick measurement, but the operation of the system is straightforward.

Evaluation

Systematic errors of the measurement system were determined with the help of photographs taken of the measurement system with an inelastic dummy leg. The hindfoot angle was reconstructed on the photographs using a computer program *(Visio Technical 4.5, 1991-1997)*. No systematic errors were detected for the measurement system.
Three hypotheses were tested with the measurement system:

- There is no difference or a predictable correlation between the hindfoot angle measured in weightbearing standing and in nonweightbearing prone position.
- The accuracy and reliability of the measurement system are sufficient. This implies

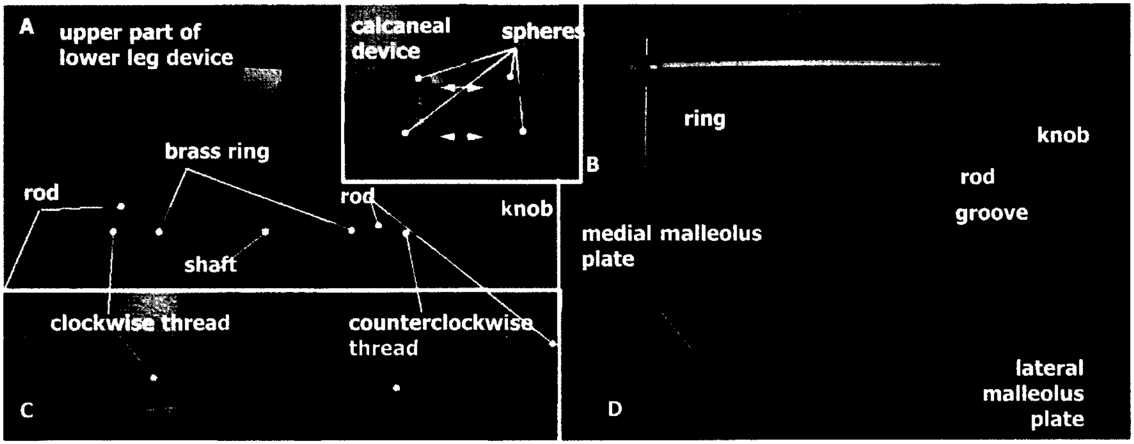

Figure 4.1.4
Photographs to point out a number of details of the measurement system.

A) The shaft of the lower leg device that move the rods inwards and outwards are threaded. On one end the threading is clockwise and the other end counter clockwise. This way the rods can be positioned simultaneously inward or outward, so that the midpoint of the shaft is always halfway between the rods. Clearance is eliminated by pieces of Teflon which are fixed in the brass rings.

B) Frontal view of the calcaneal device, showing the four spheres that indicate the calcaneal axis.

C) Detailed photograph of a threaded shaft of the calcaneus device.

D)Top view of a part of the platform. The calcaneal device is placed in the groove located in the platform to limit its motion to the frontal plane. The calcaneus device rests on a cylinder that allows for sliding and rotation along the groove in the frontal plane. For the lower leg device the limitation of motion to the frontal plane is achieved by a groove that is slid along the pins located in the ring. The ring remains in the middle of the malleoli plates owing to the fact that it moves twice as fast as the lateral malleolus plate.

that it is strived to achieve a standard deviation of 1°, and to achieve an IntraClass Coefficient *(ICC)* of 0.85 or higher for good intratester and intertester reliability.[32,44,45]

- There is a correlation between the hindfoot angle measured with the system and the visual inspection performed by the surgeon.

To evaluate these hypotheses eight healthy subjects *(four males and four females)* were selected that had a hindfoot alignment ranging from valgus feet to varus feet. The average age of the subjects was 25.5 years *(SD 1.5)*, the average length was 1.76 m *(SD 0.1 m)*, the average weight was 69 kg *(SD 13 kg)*; all subjects had a right dominance, and a normal to high activity level. Four observers measured each subject for three conditions: 1) standing position with the measurement system, 2) prone position with the measurement system, and 3) with the help of a photograph taken from the posterior side in standing weightbearing position *(Figure 4.1.1)*. Measurement of the hindfoot angle with posterior photographs was applied before.[21] This condition was added to compare the values of the hindfoot angle measured with the measurement system. In the prone position no extra force was generated to simulate the body weight. Each measurement was performed on the left and right side, and was repeated four times. One of the observers was an experienced surgeon, and the other three had a medical background. The standard deviations as well as the standard error of measurement within observers and between observers were calculated to determine the accuracy of the three conditions. The intraclass coefficients were used to determine the intratester and intertester reliability.[44,45] The hindfoot angle for each foot was determined. The existence of symmetry of the hindfoot angle within a subject was determined with a paired t-test *($p < 0.05$)* as well as possible differences between weightbearing and nonweightbearing measurement. The correlations between the three conditions were determined. With the help of a two-way analysis of variance test for repeated measures *(ANOVA, $p < 0.05$)* significant differences were determined for the hindfoot angle between the conditions *($n = 3$)*, the observers *($n = 4$)*, the left and the right side *($n = 2$)*, the repetitions *($n = 4$)*.

The surgeon who participated was asked to diagnose the alignment of the subjects as is commonly performed by visual inspection, and to classify the feet in five categories *(large varus,*

varus, neutral, valgus, large valgus). In addition to this, another experienced surgeon was asked to do the same by inspection of the posterior photographs of the subjects, where the subjects were placed in the same foot position as in the measurement system. For each category, the range of hindfoot angles was determined by indicating a minimum and maximum value.
Lastly, a simple experiment was done to assess the average natural stance of persons and to determine what the intra-subject standard deviation is for repeated standing in the natural position. Eighteen subjects were asked to stand in their natural resting position and the distance between the medial parts of the calcaneus was measured. This was repeated five times, while the subjects had to walk around in between each measurement.

Results
The chosen dimensions and ranges were such that all subjects could be measured with the measurement system. The ANOVA-test shows no significant differences for the conditions, the observers, and left and right side. For the repetitions there is a significant *($p < 0.05$)* difference, for which the value of the second measurement is always higher for all conditions and observers. The t-tests show that only two subjects had no significant difference between left and right side, whereas the other subjects had a difference of 1° up to 2° between left and right hindfoot angle. This could imply that individuals are sufficiently symmetric to be of use in this application.
Only two subjects had no significant difference between weightbearing and nonweightbearing measurement of the hindfoot angle, which shows that the hindfoot angle in this experiment is significantly different for the two conditions. The correlation between weightbearing and nonweightbearing is also low *($R = 0.48$)*, which rejects Hypothesis 1, so far.
Using the measurement system, the hindfoot angle is measured more accurately in comparison to the usage of photographs *(Table 4.1.1)*. Both methods almost meet the estimated necessary accuracy. The intratester reliability is good for both methods, but the intertester reliability is fair *(Table 4.1.1)*. The intertester reliability improves when taken into account only the first measurements. These results lead to the rejection of Hypothesis 2.
In Figure 4.1.5, the average hindfoot angles per foot are given as classified by the surgeon who

condition	intratester reliability			intertester reliability			intertester reliability*
	ICC	average SD	SEM	ICC	average SD	SEM	ICC
1. weightbearing	0.88	1.3	0.5	0.68	1.8	1.0	0.61
2. nonweightbearing	0.82	1.3	0.6	0.63	1.6	1.0	0.78
3. photographs (weightbearing)	0.9	1.4	0.4	0.63	2.8	1.7	0.66

Table 4.1.1
Reliability coefficients, average standard deviations, and the Standard Error Measurement (SEM) for the three conditions measured with 8 subjects by 4 observers. The interobserver standard deviation was calculated with the average hindfoot angle per observer.

* *Intertester reliability when only the first measurements are taken into account.*

Figure 4.1.5
Diagrams showing the average hindfoot angles of eight subjects. The experienced surgeon categorized the feet qualitatively with the help of the posterior weightbearing photographs. Per category the results of the feet assigned this category are presented. The grey areas indicate the suggested hindfoot angle range for each category: varus (-6° to −2°), neutral (-2° to 2°), valgus (2° to 6°), and large valgus (6° to 10°). Large varus was not indicated within the subject population, but the categories can be logically extended to both sides with ranges of 4°. The three conditions are plotted separately:

A) weightbearing in the measurement system,

B) nonweightbearing (prone position) in the measurement system, and

C) weightbearing photographs.
The average hindfoot angle of the left and right side of each subject is plotted. The given standard deviation indicates the variation between four observers whose average hindfoot angles of four measurements were taken.

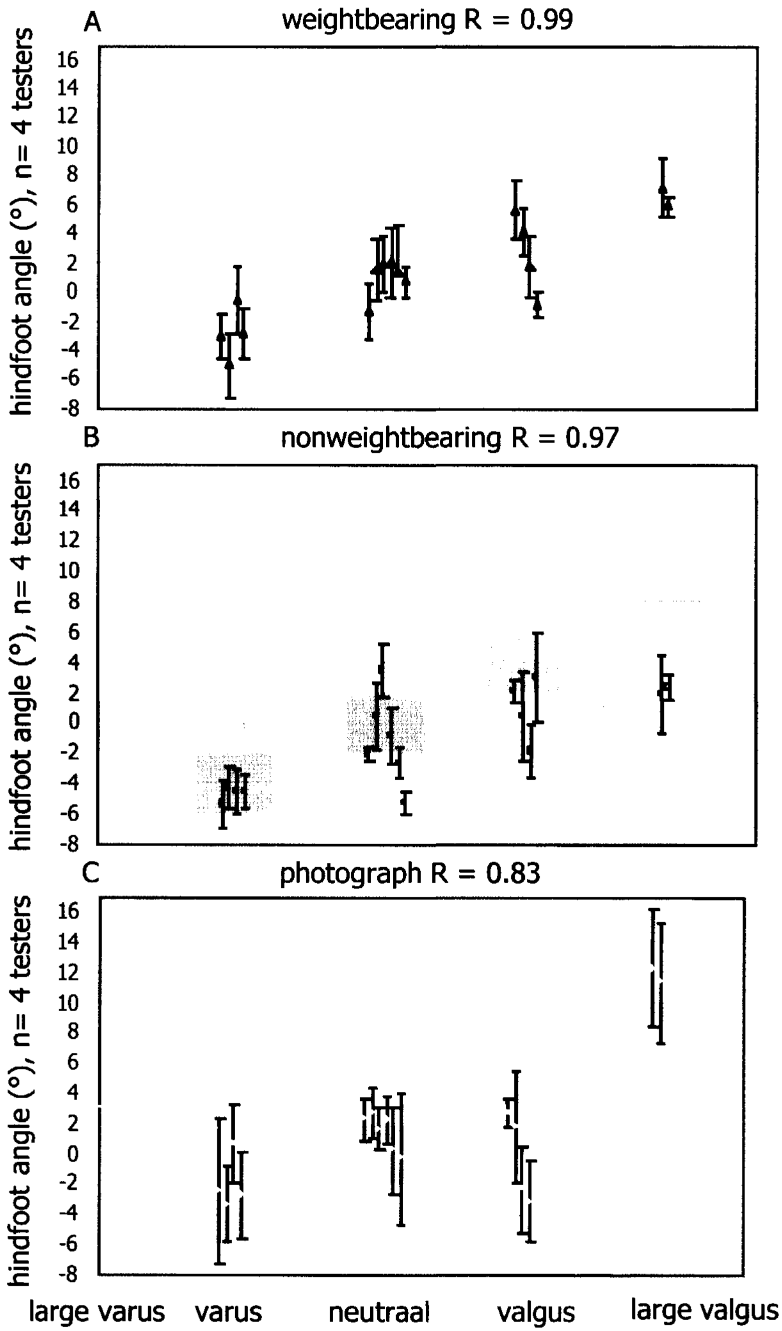

diagnosed the weightbearing photographs. A large correlation is present between the average hindfoot angles of the subjects in each category and the average value of the suggested range per category for all three conditions. The classification of the subjects by the common method of visual inspection showed less correlation with the measured hindfoot angle *(R = 0.7)*. These results are in favour of Hypothesis 3. This result shows that the average distance of the natural stance for eighteen subjects was about 140 mm, which is smaller than the chosen distance *(180 mm Appendix 4A.2)*. The average standard deviation is 22 mm.

Discussion

Both methods, the measurement with the measurement system and the usage of weightbearing photographs, indicate hindfoot angles that are consistent with the common diagnosis performed in clinical practice, and with values found in literature.[21,32] The intratester reliability and intertester reliability are also in the same range as found in literature, whereas the accuracy of the presented methods are slightly better. This holds also for measurements in nonweightbearing prone position, which supports the possible application of this concept in clinical practice. Although the current results do not show a significant correlation between weightbearing and nonweightbearing hindfoot angles, some interesting remarks can be made. In Figure 4.1.5, it can be seen that the hindfoot angles of the varus feet as well as the neutral feet are at least located within the defined ranges, whereas the hindfoot angles of the valgus feet tend to decrease in nonweightbearing prone position. This can be explained by the fact that feet in varus have locked joints and act as a lever that resist the body weight, whereas feet in valgus are flexible and move in eversion on weightbearing. Thus, imitation of weightbearing is especially important for valgus feet in nonweightbearing situation. In the operating room this can be realized by using the tourniquet to create a reaction force on the platform. Ideally the body weight should be applied which could be verified by means of an unster.

The experiment shows that the subjects are not exactly symmetric, but the difference is probably small enough to use the contralateral side as a reference. Thus, the prone position of the patient inside the operation room provides good reference conditions.

The choice of using a fixed distance between the feet results in a high correlation between the hindfoot angle and the visual inspection of the surgeon even though the subjects did not stand in their natural stance. Remarkable is that the correlation with the visual inspection with the actual subjects is lower. The natural stance does apparently also influence the value of the hindfoot angle. A simple experiment was done to establish if individuals can consistently stand in their so-called natural stance. The average standard deviation is rather large, and indicates that persons generally do not stand in one single natural stance. Therefore, either a fixed distance should be chosen, or during the first measurement the natural stance should be documented.

Further investigation and discussions with surgeon should indicate if the current accuracy and reliability are sufficient for use in daily practice. The main cause of the variations within observers is probably caused by the application of the calcaneal device to the hindfoot. This device should therefore be improved to completely eliminate any human aspect in using the device. Another possibility could be to take photographs with a digital camera in combination with a platform to simulate weightbearing and with which for example only the natural stance can be adjusted. The hindfoot angle can be reconstructed on the digital photograph with a simple computer program. This requires a very strict definition of the calcaneal axis and the same camera adjustments for each photograph that is taken. Independently of the method, it is recommended to perform each measurement more than one time, which increases the accuracy. In conclusion, the measurement system has potentials. In a future prototype, attention should be paid to a more ergonomic handling of the system, and the implementation of a mechanism to imitate the weightbearing force in prone position.

4.2 Technical data of the subtalar joint

This section is based on the paper *Technical data of the subtalar joint*, by G.J.M. Tuijthof, J.L. Herder, C.N. van Dijk, P.V. Pistecky, which will be submitted to the Journal of Clinical Biomechanics.

Keywords: subtalar joint, technical characteristics, cadaver material, machine loads, measurement

Abstract: Due to the complex shape of the subtalar joint and its tightness, it is difficult to reach all locations with the conventional straight instruments. To improve the reachability of the subtalar joint, and to facilitate the arthroscopic preparation of the joint for fusion, a new flexible instrument has been developed. This paper presents a method to determine an order of magnitude of the characteristic dimensions of the available subtalar joint space, as well as an order of magnitude of the machining force of bone and cartilage. The data are required to set up design criteria for the flexible instrument. The posterior facet of the subtalar joint space can be modeled as an ellipse shape curved around a cylinder. The average length of the axes of the ellipse are 37 mm and 24 mm. The estimated maximum force to machine bony tissue was experimentally measured to be approximately 50 N for slicing, drilling and milling.

Introduction

This study is part of the development of a complete minimally invasive technique to perform a subtalar arthrodesis.[1] One of the objects of this new technique is to facilitate the minimal invasive preparation of the subtalar joint for fusion. It was chosen to use the two-portal posterior hindfoot approach as is described earlier[46] *(Section 3.3)*. Since the subtalar joint has a curved shape, it was decided to develop a flexible instrument with which the reachability in the subtalar joint would greatly be improved. To start the design process, criteria have to be set up to establish the functions of the flexible instrument, but also to define the geometry, stiffness, and strength of the new flexible instrument. To specify these geometric and load criteria, data are required of the dimensions of the available subtalar joint space as well as the machining forces of bone and cartilage tissue.

In literature, several sets of dimensions of the subtalar joint were found. These include the size of the surface of the posterior, medial and anterior facets[47], the length of the crest line, the crest angle, and the intrafacet angle *(Figure 4.2.1)*[48]. In addition to this, we found that Verdult[49]

presented data on the machining forces to drill human vertebrae. These data are helpful, but not sufficient to quantify the design criteria.
A method is introduced with which the technical characteristics of the subtalar joint can be derived, straightforwardly. These data give an order of magnitude for the geometric and load criteria for the proposed flexible instrument, but could also be used to design other instruments.

Materials and methods

In this paper, the main attention is paid to the geometric dimensions of the posterior facet, since its surface is the largest of the three facets[47] and its curvature gives the boundary condition for the necessary flexibility of the new flexible instrument. It is known that anthropometric dimensions differ greatly.[40-42] This is also true for the surface of the posterior facet of the subtalar joint. Barbaix et al.[47] established an average value of 582 mm^2 and a standard deviation of 103 mm^2. Thus, it can be expected that there is also a variation amongst the other dimensions of the subtalar joint. As a consequence, it is not preferable to measure the data of one subtalar joint accurately. The challenge is to design a flexible instrument that can be used effectively in all subtalar joints. Therefore, in our study orders of magnitude are determined of the dimensions of the subtalar joint. Estimations of maximum and minimum values are used to start the design process.

The machining forces are important to calculate the strength of the mechanism for the proposed flexible instrument. Not only the type of machining process is important in establishing the machining forces, but also the composition of bony tissue. The composition varies with location *(for example cortical bone located at the outside vs. cancellous bone located at the inside).*

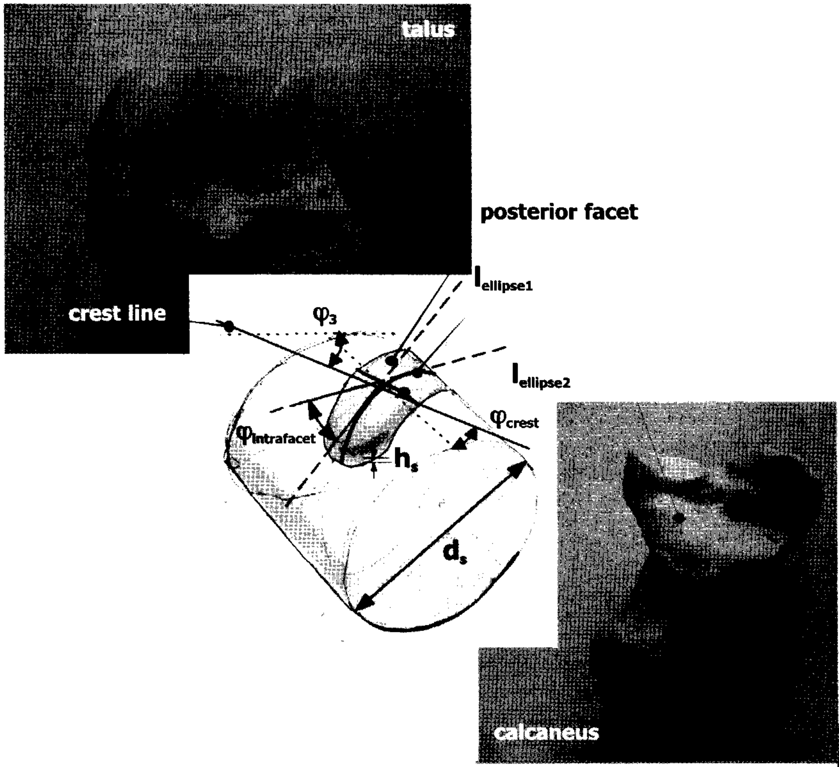

Figure 4.2.1
Anatomic of model of the talus and the calcaneus. The proposed model of the surface of the posterior facet is shown in between the two bones. The dimensions that define the proposed model of the posterior facet are indicated. The crest line (line that divides the posterior facet into a posteromedial and an anterolateral portion), the crest angle (angle between the crest line and frontal plane), and the intrafacet angle (difference between the angles of the surface of the calcaneus of the posteromedial and anterolateral portion in lateral view) defined by Ebraheim et al.[48] are indicated as well. The direction of $l_{ellipse1}$ was chosen parallel to the interosseous ligament (Figure 3.0.1), and its length is the maximum possible distance following the talus or calcaneus contour from one side to the other. $l_{ellipse2}$ is chosen perpendicular to $l_{ellipse1}$.

Dimensions of the subtalar joint and portal location

The geometric criteria *(required stiffness, diameter, and length of the instrument)* are dependent on the available space in the subtalar joint, and the location of portals[46]. Several options are available to document additional anthropometric dimensions of the subtalar joint: subtalar joints of cadaver material, radiographs, MRI-scans, CT-scans, anatomic subtalar joint models, arthroscopic views, and external biomechanical measurements. We chose to perform direct measurements on cadaver material. Furthermore, we used subtalar joint models[50,51] to assess their usefulness in relation to fresh cadaver material.

To define characteristic dimensions of the subtalar joint the available joint space was modeled. The posterior facet was of main interest, and it was modeled as an ellipse with a thickness that is curved around a cylinder *(Figure 4.2.1)*. The important dimensions of this ellipse-shaped model are the two main axes *($l_{ellipse1}$ and $l_{ellipse2}$)* and the thickness of the ellipse *(h_s)*, the crest line[48] *(l_{crest}, indicates the axis of curvature of the ellipse around the cylinder)*, and the diameter of the cylinder *(d_s)*. The latter dimension is believed to be a more suitable measure to determine the instrument's stiffness than the intrafacet angle. To complete the model, the portal locations at the edge of the posterior facet *(ellipse-shaped model)* were necessary to document as well as their orientation in space. Three fresh frozen cadaver ankles were investigated. The actual size of the posterior facet of one of the three ankles was measured and compared with the estimated area of the surface of the ellipse. Each measurement was executed three times. The measurements took place according to the following protocol[52]:

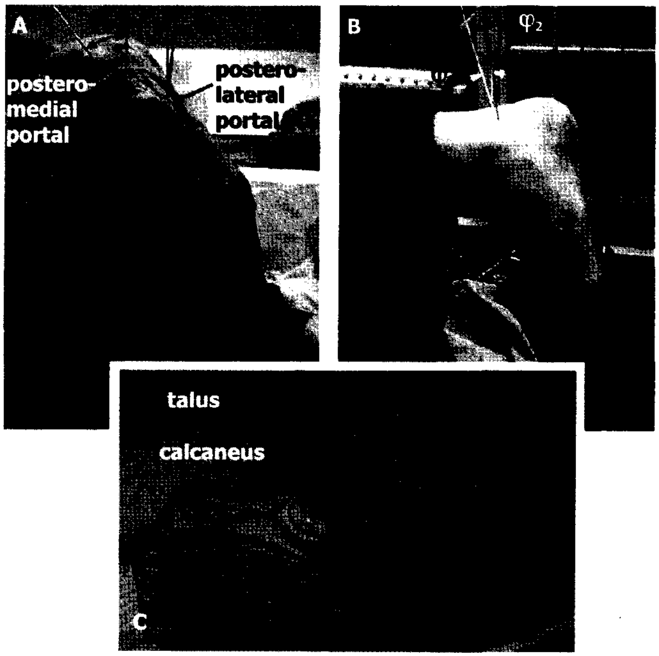

Figure 4.2.2
A) Photograph of a fresh frozen cadaver ankle in the frontal plane indicating the posterolateral and posteromedial portals with Steinmann pins.

B) Photograph of the same ankle in the mediolateral view. The 3D-orientation of the portals is determined by the angle in the transversal plane (φ_1), and the angle in the mediolateral view perpendicular to the longitudinal leg axis and the transversal plane (φ_2).

C) Photograph of the calcaneus and talus constructed with the help of the Visible Human project.[50]

- The posterolateral and posteromedial portals were established with Steinmann pins *(diameter 2 mm)*. The angles φ_1, and φ_2, which were measured with a goniometer *(Figure 4.2.2)*, defined the 3D-orientation.
- The calcaneus and talus bones were dissected.
- The axes of the ellipse *($l_{ellipse1}$ and $l_{ellipse2}$)* were measured with the help of a robe and vernier calipers on the inferior portion of the talus *(Figure 4.2.3)*.
- The crest line was determined on the calcaneus by visual inspection. An alternative crest angle *(φ_3)* was measured with the help of a photograph of the superior calcanei and a computer program *(Visio 4.5) (Figure 4.2.3)*.

- The location of the portals was determined by measuring the distance *(arc)* of a portal along the edge of the posterior facet to the approximated end point of $l_{ellipse1}$ *(Figures 4.2.3).*
- The diameter of the cylinder *(d_s)* was measured by fitting the talus on templates that had different diameters.
- To determine the thickness of the cartilage layers *($h_{cartilage}$)* the talus and calcaneus were cut through the middle. The cartilage thickness was measured by removing a piece of cartilage and by establishing the difference in height at this location with an undamaged part of the cartilage layer.

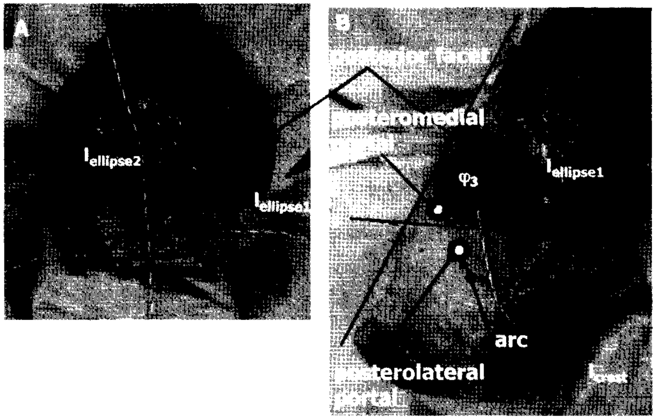

Figure 4.2.3
Color illustration see cover.
A) Photograph of the inferior side of a talus showing the axes of the ellipse ($l_{ellipse1}$ and $l_{ellipse2}$).

B) Photograph the superior side of a calcaneus showing the crest line (l_{crest}), crest angle, and the locations of the portals. The alternative crest angle (φ_3) is defined as the angle between the crest line and the axis along the medial side of the calcaneus.

The same measurements were performed, where possible on an anatomic model of the talus and calcaneus[51], and on a model of the calcaneus and talus derived from the Visible Human project on the Internet[50]. This Visible Human project has made photographs available of a man sliced in pieces of 1 mm. A 3D-model was constructed by cutting the contours of the talus and calcaneus, and piling these photographs *(Figure 4.2.2).* In addition to this, a silicon mould was made of the positive subtalar joint space of one cadaver subtalar joint.[52] The available range of motion of the Steinmann pins in both the portals was assessed for another cadaver ankle.
It appeared to be difficult to reconstruct the proposed model of the subtalar joint space on the computer with the gathered data. Therefore, a paper model was constructed for each cadaver ankle *(Figure 4.2.4).* With the help of these models, a curve from each of the two portals was constructed to three extreme points on the ellipse-shaped surface *(Figure 4.2.4).* Each curve is characterized by two angles *(β_1 and β_2)* and a diameter *(d_c).* In total, 18 curves were obtained this way *(three from each portal times six).* The curve composed of the smallest value for d_c and the largest value of β_2 determines the minimal required flexibility of the shaft of the new instrument as well as the minimal length to reach the entire posterior facet in a wide range of subtalar joints.

Machining forces on cartilage and bone

The load criteria are determined by the machining forces that are necessary to cut cartilage and bony tissue. It was chosen to perform mechanical removal of the subchondral bone in order to generate bleeding contacts. Before an experimental protocol was set up, the tali and calcanei of the three cadaver ankles were machined with existing surgical instruments *(shavers, surgical file, chisel, curette, surgical knife, punch)* as well as ordinary hand tools *(rasp, steel brush,*

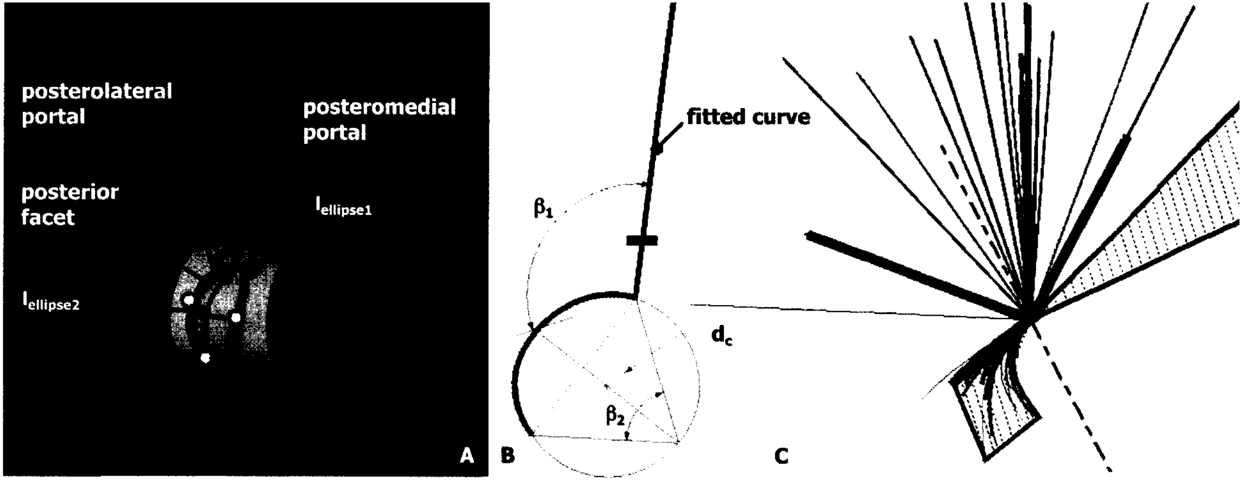

Figure 4.2.4
A) Paper model of one of the three cadaver ankles showing the subtalar joint space including the posterolateral and posteromedial portals (black sticks). With the help of this model curves are reconstructed from each portal along the contour of the subtalar joint space to both end points of $l_{ellipse2}$, and the farthest end point of $l_{ellipse1}$ (white spots).

B) Each curve is characterized by two angles (β_1, and β_2) and a diameter (d_c). β_1 is the angle between the portal and the line through the starting point of the contour of the subtalar joints space and the top of the same contour, β_2 is the angle of the arc of the contour of the subtalar joint space fitted with by a circle, d_c is the diameter of the circle fitted with the contour of the subtalar joint space.

C) Assembly of all curves determined from the three paper models of the subtalar joint spaces. The striped areas indicate the proposed range that has to be reached by the flexible instrument. Most portal lines do not fit in the striped area, which implies that a more suitable portal placement is proposed to access the subtalar joint. The advantage of this portal placement is that less bending of the flexible shaft is necessary.

sandpaper, saw).[52] The instruments were judged qualitatively. It took the least effort to cut the cartilage and the subchondral bone with the surgical knife and the saw. The tali and calcanei were also statically and dynamically penetrated with nails *(diameters ranging from 1.2 to 1.8 mm).*[52] From this initial experiment, it was derived that the supply of dynamic energy caused a greater penetration of the nails than static energy, and an initial value of the machining force of bone was estimated at 75 N.[52]

The machining forces depend on the machining process. In this study, three potential mechanical processes have been investigated in more detail: slicing, drilling, and milling. The condyli of two previously frozen human femur bones were used in this experiment, since this material was readily available and it is expected that the bone structure in the knee joint is about the same as in the subtalar joint. A machining bench constructed by MTO *(AMC, Amsterdam)* was used *(Figure 4.2.5)*. The bench can pull or push with different speeds, and has a force sensor that can measure force in three directions. To simulate the slicing process, a mechanism in which different types of knives could be clipped was attached to the force sensor, and the vertical motion was blocked *(Figure 4.2.5)*. Both cartilage and bone were investigated with the slicing process. Thereto, pieces of different sizes were cut from the condyli to create an as constant as possible cross-section. The influence of a number of variables was studied: slicing velocity *(v = 2, 10, and 20 mm/s)*, width *(b_{bone}, ranging from 3.2 to 4.2 mm)* and thickness *(h_{bone}, ranging from 0.1, to 0.3 mm)* of the sliced bone chip, cutting angle of the blade *(φ_{slice} = 30°, 45°, and 60°)*, and knife type *(Stanley knife, surgical knife, and razor blade) (Figure 4.2.5)*. The sample frequency was adjusted per velocity *(50 Hz for 2 mm/s, 250 Hz for 10 mm/s, and 500 Hz for 20 mm/s)*. The existence of relations between the maximum force and the variables were investigated, if no relation could be found the variable was kept constant at a convenient value. This way, the number of variables that was tested could be decreased. For the slicing process the maximum force per experiment *(F_{slice})* per cross-section *(A_{bone})* was considered. In addition to this, the applied energy was calculated by means of the area underneath the force curve:

$$E_{slice} = \Delta l \cdot \sum_{i=0}^{n} F_{slice,i} \qquad (4.2.1)$$

where, E_{slice} is the applied energy when slicing, Δl is the sample distance, and $F_{slice,i}$ is the slicing force at sample i. With the help of the applied slicing energy *(E_{slice})* per removed volume of bony tissue *(V_{bone})*, and the volume of the entire posterior facet *($V_{postfacet}$)*, a rough estimation can be made of the necessary energy to machine the posterior facet. An estimation of $V_{postfacet}$ can be calculated with the ellipse shaped model:

$$V_{postfacet} = \frac{\pi}{4} \cdot l_{ellipse1} \cdot l_{ellipse2} \cdot 2 \cdot (h_{cartilage} + h_{bone}) \qquad (4.2.2)$$

where, h_{bone} is in this case the thickness of the subchondral bone layer that has to be removed. The value of this thickness was measured to be about 1.5 mm. The power *(P_i)* used per experiment was calculated according to:

$$P_i = \frac{E_i \cdot v}{l_{bone}} \qquad (4.2.3)$$

where v is the slicing velocity, E_i is the necessary energy to machine bone with machining process i, l_{bone} is the length of the bone chip that is machined or the length of the drilled hole. The slicing process showed a stick slip path. Stress was built up against a piece of bone until the ultimate bone stress was achieved, and a piece of bone would break loose. Through the blocking of motion in the vertical direction this effect was partly overcome. The surgical knife and the razor blade were so thin that buckling occurred when slicing the bone, and no further experiments were conducted with these knives.
To study the drilling and milling processes, a drilling device *(Dremel 398, Dremel BV)* was attached to the working bench which supplied the rotational movement for the milling and drilling. The rotational frequency of the drill was kept constant at 5000 rev/min. The push velocity of the working bench that moves the drill forwardly was first set at 2 mm/s *(sample frequency was 50 Hz)*, but this appeared to be to fast for the set up, and was later changed to

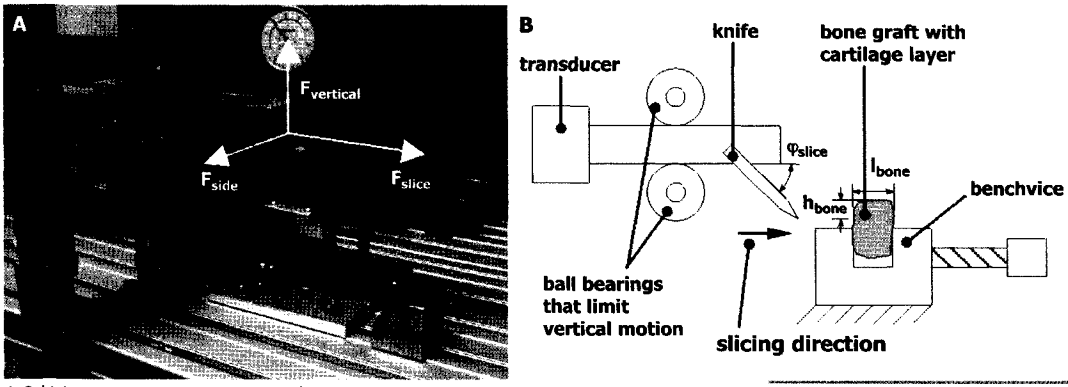

Figure 4.2.5
Experimental set up that was used to measure the machining forces for the slicing process.

A) Photograph of the working bench.

B) Schematic drawing to clarify the experimental set up.

The working bench is limited in vertical direction to ensure the knife to cut straight through the tissue.

0.2 mm/s *(sample frequency was 25 Hz)*. Five drills were tested for drilling, and the three best ones were tested for milling *(Figure 4.2.6)*. The average and standard deviation of the maximum forces required to push the drill through the bone *(F_{drill} or F_{mill})* were documented. The applied energy was calculated according to Eq. 4.2.1 and the power according to Eq. 4.2.3. Since, the condyli had curved surfaces, it was difficult for the milling process to determine the volume of removed bone, accurately.

Results

The results of the measurements of the subtalar joint dimensions, as well as the dimensions of the fitted curves along the portals and posterior facets are shown in Table 4.2.1. The available range of motion in both the portals of one of the cadaver ankles was about 10° for angle φ_1, and 10° for φ_2.

The maximum forces to cut cartilage tissue are about two times lower in comparison to the maximum forces to cut bony tissue, when using the Stanley knife and about four times lower when using a surgical knife. The results show no strong correlation between the machining force and the variables, but a larger slicing angle *(φ_{slice})* tends to increase the maximum force per

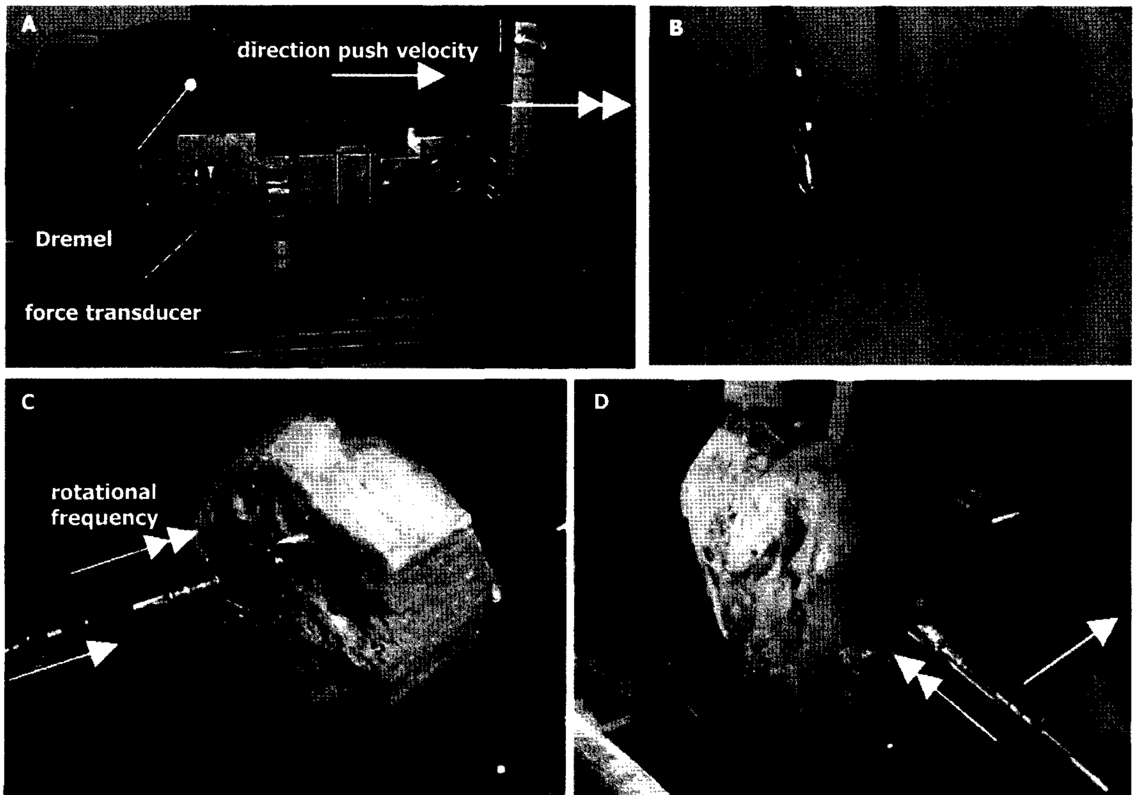

Figure 4.2.6
Color illustration see cover.
A) Photograph of the drilling device clamped onto the working bench to simulate the drilling process. To simulate the milling process the drilling device was clamped at a 90°-angle with the pushing direction of the working bench.

B) Five different drills that were tested. From left to right: standard mill used for the machining of metals (5.5 mm), cylindrical drill of a conventional shaverblade (5.5 mm Stonecutter Acromionizer blade, Smith and Nephew Company, Hoofddorp, the Netherlands), spherical drill (5.5 mm), conical drill (diameter ranging from 2.5 to 5.5 mm), and prototype (5.5 mm). The prototype consists of a hollow tube with a sharp edge.

C) Example of a drilling experiment.

D) Example of a milling experiment.

Table 4.2.1
Results of the geometric measurements of subtalar joint performed on three fresh frozen cadaver ankles, and the two bone models.
All dimensions are given in mm unless mentioned otherwise. For the two bone models the portal directions and thickness of the joint space could not be established. The thickness of the joint space (h_s) is dependent on the amount of tissue that is removed during the procedure and the amount of distention. The Steinmann pins (diameter 2 mm) inserted through the two portals were pushed to the end of the entire posterior facet in one of the ankles.
A silicon mould was fabricated of this configuration. In the lower part the characteristic dimensions of the curves fitted along the contour of the subtalar joint are presented (d_c, β_1, and β_2). For each dimension the average, standard deviation, minimum and maximum value are given. By combining the minimum value of d_c and the maximum value of β_2, a starting criterion is set up for the necessary flexibility of the flexible instrument.

dimension	ankle 1	ankle 2	ankle 3	functional knee joint model[51]	Visible Human[50]	literature[47,48]
$l_{ellipse1}$	40	39	30	39	43	
$l_{ellipse2}$	24	23	21	28	29	
l_{crest}	23.5	22.5	21.7	26	30	21 ± 2
$A_{ellipse}$	767 mm^2	687 mm^2	495 mm^2	851 mm^2	962 mm^2	582 mm^2 ± 103 mm^2
d_s	55	56	34	36	49	
φ_3	45°	67°	76°	67°	69°	72° ± 9° **
$h_{cartilage}$	0.8	0.8	1.0			
h_s	2 to 5	1.6 to 3	1.2 to 2			
$\varphi_{1\ posteromedial}$	15° lateral	20° lateral	30° lateral			
$\varphi_{2\ posteromedial}$	10° plantar	12° plantar	0°			
$\varphi_{1\ posterolateral}$	10° medial	8° medial	15° medial			
$\varphi_{2\ posterolateral}$	15° plantar	4° plantar	5° dorsal			
contour on paper models	**average**	**SD**	**minimum**	**maximum**	**criterion**	**intrafacet angles**
d_c	84	49	24	204	**24**	140° ± 9°
β_1	128°	27°	56°	165°	**170° - 220°**	
β_2	47°	28°	16°	104°	**104°**	

cross-section. The surgical knife gives slightly lower forces per cross-section in comparison to the usage of the Stanley knife. As was expected, the machining forces for slicing cartilage are lower than those for slicing bony tissue. Therefore, no further experiments were performed with cartilage.
The slicing force curves show force peaks that can be as large as 40 N *(Figure 4.2.7, page 63)*. This is consistent with the observation that no slices of constant thickness could be cut for bony tissue. No strong correlations were found between the variables and the maximum forces per cross-section when using the Stanley knife *(Table 4.2.2)*. The slicing angle *(φ_{slice})* is proportional to the maximum force per cross-section *(R = 0.68)*, and the thickness and width of the bone graft that is sliced *(h_{bone} and b_{bone})* are both inversely proportional to the maximum force per cross-section *(R = -0.71, and R = -0.53)*.

***By subtracting the crest angle as defined in Ebraheim et al.[48] from 90°, the alternative crest angle is achieved, so that it can be compared with the results in this paper.*

The results of the average values for the maximum machining forces, the energy per volume and the power of the three machining processes are summarized in Table 4.2.3. In comparison with the slicing process, the maximum forces that occur during drilling with a push velocity of 2 mm/s are higher as well as the used power *(Table 4.2.3)*. The mill, cylindrical drill and spherical drill required the least maximum forces for drilling *(average of 21 N, 53 N, and 54 N, respectively) (Table 4.2.4)*. The mill, cylindrical drill and spherical drill were also tested for milling *(Table 4.2.5)*. The spherical drill required the least maximum forces *(average is 11 N, SD is 9 N)* in comparison to the mill *(average is 22 N, SD is 29 N)* and the cylindrical drill *(average is 31 N, SD is 17 N)*.

When it is assumed that both surface layers of the posterior facet of one of the three cadaver ankles have to be removed, and the relation between the volume and applied energy is linear, it is calculated that the necessary energy is about 6 J.

Discussion

The proposed approximation of the posterior facet by a curved ellipse shape appears to be sufficient in describing the major part of the available joint space in the subtalar joint with a few characteristic dimensions. The actual size of the posterior facet of one of the cadaver ankles is namely 812 mm², which is about 8% larger than the calculated surface of the ellipse, and the variation amongst the cadaver ankles themselves is larger than the error caused by the approximation. The variation of the measured dimensions is within the standard deviation of the values found in literature.[47,48] The dimensions of the two anatomic models were in the same range as those of the cadaver ankles. They can be used also as a start in gathering values for some of the dimensions. The height of the joint space and the cartilage as well as the orientation of the portal placement could not be established for the anatomic models.

Table 4.2.2
Results of the maximum force measured using a Stanley knife for the slicing process and a slice angle (φ_{slice}) of 45°. The velocity and the bone graft size were varied. The results show the average maximum slicing forces (F_{slice}) and the standard deviation are given, as well as the average applied energy (E_{slice}) and the standard deviation for the experiments that were repeated ten times or more. The experiments are presented according to increasing maximum force per cross-section (F_{slice}/A_{bone}). As can be seen the velocity and the width of the bone graft do not seem to have a correlation with the maximum force per cross-section, but the slice thickness has. It is advantageous to cut a larger slice. This can be explained by the fact that once the slice thickness is larger than the knife edge, the force per cross-section does not increase. The applied energy per volume is proportional with the push velocity of working bench (last column).

v (mm/s)	h_{bone} (mm)	b_{bone} (mm)	l_{bone} (mm)	F_{slice} (N)	SD (N)	F_{slice}/A_{bone} (N/mm²)	E_{slice} (J)	SD (J)	E_{slice}/V_{bone} (J/mm³)
2	0.30	4.5	17	24	14	18	0.12	0.06	3.5E-04
10	0.30	3.6	17	32	24	30	0.13	0.1	7.1E-03
2	0.25	4.5	17	38	20	34	0.17	0.07	4.9E-04
2	0.30	3.4	19	36	16	35	0.13	0.06	6.7E-03
20	0.15	3.4	12	23	14	45	0.07	0.06	1.1E-02
2	0.20	3.0	18	28	13	47	0.12	0.06	7.4E-04
20	0.30	3.3	18	48	55	48	0.18	0.23	1.0E-02
2	0.10	3.0	18	16	10	53	0.06	0.03	3.7E-04
2	0.15	3.0	18	28	6	62	0.11	0.03	6.8E-04
10	0.15	3.4	12	34	13	67	0.11	0.08	1.8E-02
2	0.15	3.5	15	47	28	90	0.21	0.14	2.7E-02

process	tissue	item	average	SD
slicing	cartilage	F_{slice}	18 N	8 N
		F_{slice}/A_{bone}	22 N/mm^2	13 N/mm^2
slicing	bone	F_{slice}	31 N	17 N
		F_{slice}/A_{bone}	54 N/mm^2	27 N/mm^2
		E_{slice}	0.013 J/mm^3	0.007 J/mm^3
		P_{slice}	0.043 W	0.078 W
drilling at 2 mm/s	bone	F_{drill}	132 N	26 N
		E_{drill}	0.002 J/mm^3	0.001 J/mm^3
		P_{drill}	0.107 W	0.042 W
drilling at 0.2 mm/s	bone	F_{drill}	52 N	29 N
		E_{drill}	0.001 J/mm^3	0.001 J/mm^3
		P_{drill}	0.003 W	0.003 W
milling	bone	F_{mill}	35 N	11 N
		E_{mill}	0.0003 J/mm^3	0.0002 J/mm^3
		P_{mill}	0.001 W	0.0005 W

Table 4.2.3
Summary of all average values of the maximum machining forces and standard deviations of the conditions per machining process.

For the experiments with the three machining processes a lot of conditions were involved, and often only one experiment per condition was performed. Therefore, this research has to be considered as a pilot study for further investigation in the machining forces of human bony tissue.

The maximum forces that occur during drilling were higher than during slicing. An explanation could be that the slicing experiments were performed on subchondral bone, whereas this was not always feasible for the drilling and milling experiments, where also the harder cortical bone is machined. A disadvantage of slicing is the difficulty to create a smooth surface.

The mill, cylindrical drill and spherical drill require the least maximum forces for drilling. The prototype and the conical drill had probably less sharp cutting blades and also problems with the removal of the cut bone tissue. The conventional mill requires the lowest machining forces and power, which is probably due to the fact that the cutting edges are the sharpest, moreover it has sharp edges at its tip. The spherical drill had obviously a too small cutting blade that disabled sufficient removal of the bone chips. This resulted by a number of experiments in the occurrence of smoke, and burnt tissue. Furthermore, it was difficult to steer the spherical drill in a straight path.

Table 4.2.4
Results of experiments performed to establish the maximum required pushing force to drill bony tissue (F_{drill}) for a given pushing velocity (v). The rotational frequency of the drill was set at 5000 rev/min.

drill type	v (mm/s)	d_{drill} (mm)	l_{drill} (mm)	F_{drill} (N)	E_{drill} (J)	E_{drill}/V_{bone} (J/mm^3)	P_{drill} (W)
mill	0.2	5.5	10.3	22	0.04	1.6E-04	7.8E-04
mill	0.2	5.5	14.3	19	0.06	1.8E-04	8.4E-04
mill	0.2	5.5	11.6	23	0.05	1.8E-04	8.6E-04
cylindrical drill	0.2	5.5	11.3	18	0.07	2.6E-04	1.2E-03
cylindrical drill	0.2	5.5	11.0	20	0.07	2.7E-04	1.3E-03
spherical drill	0.2	5.5	10.8	21	0.07	2.7E-04	1.3E-03
cylindrical drill	0.2	5.5	8.2	54	0.07	3.6E-04	1.7E-03
cylindrical drill	0.2	5.5	9.1	56	0.08	3.7E-04	1.8E-03
spherical drill	0.2	5.5	9.3	25	0.10	4.5E-04	2.1E-03
cylindrical drill	0.2	5.5	7.3	109	0.10	5.8E-04	2.7E-03
spherical drill	0.2	5.5	7.9	64	0.12	6.4E-04	3.0E-03
cylindrical drill	0.2	5.5	2.5	55	0.04	6.7E-04	3.2E-03
prototype	0.2	5.0	3.7	87	0.06	8.2E-04	3.2E-03
prototype	0.2	5.0	2.1	59	0.04	9.8E-04	3.8E-03
spherical drill	0.2	5.5	5.7	51	0.11	8.1E-04	3.9E-03
spherical drill	0.2	5.5	7.4	62	0.18	1.0E-03	4.8E-03
conical drill	0.2	3.0	5.5	79	0.16	4.1E-03	5.8E-03
spherical drill	0.2	5.5	2.7	103	0.17	2.6E-03	1.2E-02
cylindrical drill	0.2	5.5	1.3	59	0.14	4.5E-03	2.1E-02
spherical drill	2	5.5	16.4	86	0.42	1.1E-03	5.1E-02
cylindrical drill	2	5.5	10.2	140	0.41	1.7E-03	8.0E-02
spherical drill	2	5.5	9.3	145	0.50	2.3E-03	1.1E-01
spherical drill	2	5.5	14.8	146	1.02	2.9E-03	1.4E-01
spherical drill	2	5.5	2.6	143	0.21	3.3E-03	1.6E-01

drill type	mill depth (mm)	l_{drill} (mm)	F_{mill} (N)	E_{mill} (J)	E_{mill}/V_{bone} (J/mm^3)	P_{mill} (W)
spherical drill	6	18.2	12	0.05	9.7E-05	5.5E-04
spherical drill	6	18.2	10	0.06	1.2E-04	6.6E-04
cylindrical drill	2.5	20.0	21	0.09	8.7E-04	8.5E-04
cylindrical drill	5	20.0	24	0.10	2.4E-04	9.6E-04
mill	6	20.0	18	0.10	1.7E-04	9.8E-04
mill	6	4.5	26	0.03	2.1E-04	1.2E-03
mill	6	20.0	19	0.13	2.2E-04	1.3E-03
mill	6	20.0	25	0.16	2.8E-04	1.6E-03
mill	6	5.5	26	0.05	3.3E-04	1.9E-03
cylindrical drill	6	15.5	36	0.15	3.3E-04	1.9E-03
cylindrical drill	6	9.8	43	0.10	3.6E-04	2.0E-03

Table 4.2.5
Results of experiments performed to establish the maximum required pushing force to mill bony tissue (F_{mill}) for a pushing velocity of 0.2 mm/s, and a drill diameter of 5.5 mm. The rotational frequency of the drill was set at 5000 rev/min.

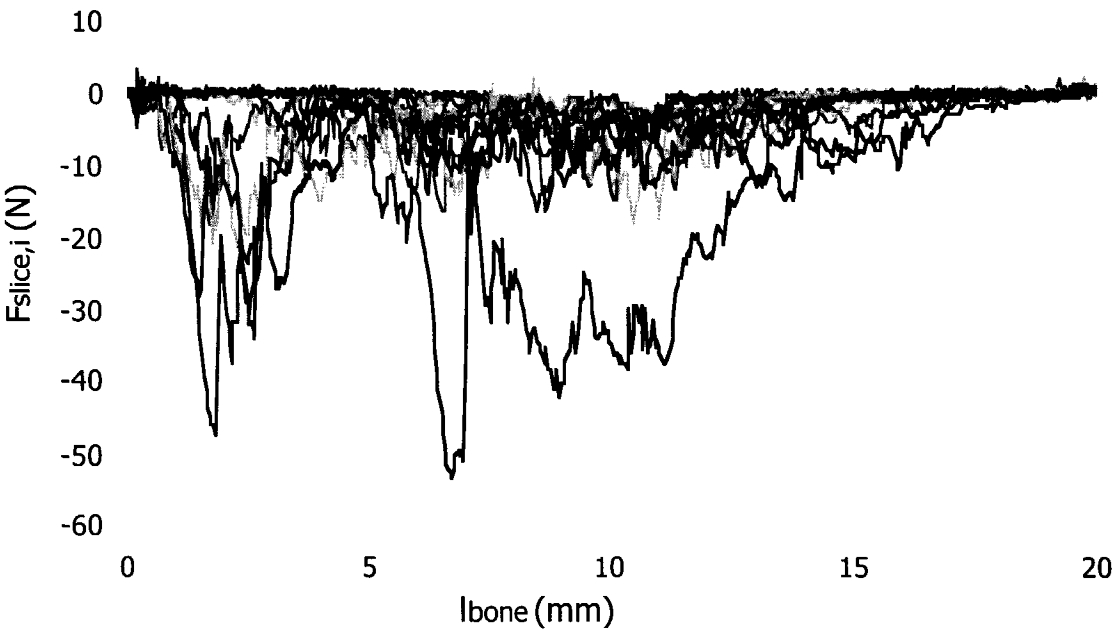

Figure 4.2.7
Slicing force curves of ten experiments performed on bony tissue. The knife that was used was a Stanley knife, v was 20 mm/s, φ_{slice} was 45°, h_{bone} was 0.15 mm, b_{bone} was 3.4 mm, and l_{bone} was 12 mm. In this diagram it is clearly seen that high force peaks can occur. The values of the force are negative, since the force sensor measures pulling forces as positive forces and pushing forces as negative forces.

Conclusions

Considering the results, the following design criteria can be set up:

- It is proposed to create the portals more distally, since this enables a C-shaped entrance of the new instrument to the subtalar joint instead of an S-shaped entrance.
- Length of flexible part of the new instrument *(l_{shaft})* should be at least 50 mm.
- The flexible part should be able to curve around a diameter of 24 mm *(d_c)*, and requires a minimum force to do so.
- Dependent on the choice of the machining process and the location to start the bone removal in the joint, the maximum diameter of the new instrument lies between 1 mm *(smallest joint space)* and 7 mm *(two times the surface layer that should be removed added with the joint space height)*
- The new instrument should be able to apply a maximum cutting force of 50 N, independently of the machining process.
- When a drilling or milling process is chosen, the cutting blades should be large to allow bone chip removal, and should be sharp to decrease the required pushing force.
- When a slicing process is chosen, attention should be paid to the creation of a smooth surface.
- The estimated maximum power is about 0.1 W. This implies that the higher the cutting velocity the lower the cutting forces are, and the lower the pushing force can be to drill or to mill. Furthermore, with the estimated power and the estimated applied energy *(6 J)*, it can be calculated that it should take about 60 seconds to cut the cartilage and subchondral bone in the posterior facet. This is a rough estimation, but the removal with the new instrument is potentially faster than the current method ***(about 15 to 30 minutes)***.

4.3 Flexible instrument to facilitate arthroscopic preparation of a joint for fusion

This section is based on the paper *A flexible instrument for arthroscopic joint fusion*, by G.J.M. Tuijthof, J.L. Herder, C.N. van Dijk, P.V. Pistecky, which will be submitted to the ASME conference.

Keywords: arthroscopy, flexible instrument, subtalar joint, arthrodesis

Abstract: Due to its complex shape and its tightness, it is difficult to prepare the subtalar joint for fusion by means of a minimal invasive access and conventional straight instruments. The preparation implies the removal of the cartilage and the subchondral bone layers of both surfaces to establish bleeding contact. Furthermore, it is desirable to preserve the complex shape of the subtalar joint to create congruent and smooth contact surfaces for optimal fusion. A flexible instrument was designed to facilitate the preparation. The instrument consists of a flexible shaft that is flexible in one direction, to be able to follow the contour of the subtalar joint, and stiff in the other direction, to be able to machine the bony tissue which is done with a drill. The drill is actuated with a flexible steel cable and can be powered by a shaver system. A frame placed in front of the drill allows for passive steering of the instrument and removal of equal portions of each surface. The flexible instrument was tested in cadaver material, and gives promising results, but the design needs fine tuning.

Introduction

Specific problems of arthroscopy are related to the limited workspace in joint cavities, caused by the surrounding bones that are compressed by ligaments, and the limited access to these joint cavities due to overlying neurovascular tissues. This is also true for subtalar joint arthroscopy for which several access portals are available.[53-57] One of the techniques that is being developed for subtalar joint arthroscopy is the subtalar arthrodesis.[56,58-60] The preparation of the subtalar joint to perform an arthrodesis consists of the removal of the cartilage and subchondral bone from both joint surfaces. This way two bleeding bone surfaces are created that will eventually fuse. Four aspects will probably enhance quick and solid fusion of the joint: removal of the subchondral bone and cartilage of the entire subtalar joint surfaces *(Figure 3.0.1)*, establishment of bleeding contact surface areas, preservation of the subtalar joint's shape, and creation of smooth and congruent surfaces that increase the areas of true contact *(Chapter 3)*.[1] Even though several portal options exist to access the subtalar joint, it requires high surgical skills to perform the operation arthroscopically and to satisfy the conditions for optimal fusion. This is due to the complex shape and tightness of the subtalar joint, and the current straight arthroscopic instruments *(Chapter 3)*.[1,58]
The goal of this paper is to present the development of a new flexible instrument that facilitates access to the entire subtalar joint, and with which the four conditions for optimal fusion can be fulfilled. It is expected that if the flexible instrument can reach all locations in the subtalar joint, it can probably also be used in other joints that have a less complex but congruent shape. The conceptual design is presented as well as a prototype which was tested in a cadaver setting.

Materials and methods

Conceptual design

In the introduction, four conditions were already mentioned that probably enhance fusion of the subtalar joint. Apart from the machining of bony tissue other design criteria were taken into account: access, safety, control, time frame, tissue removal, and simplicity of the construction. The requirements for the new flexible instrument are summarized in Table 4.3.1, and they will be elucidated.

It is essential to create bleeding bony contact surfaces, which can be established through mechanical machining of tissue *(Table 4.3.1: Requirement 1)*. The machining force of cartilage was found to be less than the machining force of subchondral bone *(Section 4.2)*. Therefore, the maximum machining force for subchondral bone *(measured to be about 50 N, Section 4.2)* was used as a boundary condition for the strength and stiffness of the flexible instrument. Furthermore, a rough estimation of the necessary power to machine bone tissue was established *(0.1 W, Section 4.2)*. The power is defined as the machining force multiplied by the machining velocity. The machining forces can be kept low when a dynamic component is added. For

Table 4.3.1
Requirements derived for the design of a flexible instrument that facilitates the preparation of the subtalar joint for fusion or implantation. For each requirement the aspect(s) of the instrument that involve the requirement are indicated as well as a choice for the solution. A number of aspects is elucidated in the text.

requirement	aspect	choice
1. Establishment bleeding joint surfaces	Mechanical machining of tissue	Combination of drilling and milling
2. Create smooth surface	Shape of drill	Cylindrical
3. Remove both layers from entire joint surfaces via one access portal	Reachability of joint	Geometry shaft Drill at tip
4. Quicker process than open techniques	Both surfaces simultaneously machined Cartilage layer and subchondral bone layer simultaneously machined	Diameter drill Drill placed centrally to joint surfaces
5. Preserve joint shape	High difference between bending stiffness flexible shaft in two directions	Geometry cross-section Superelastic wire
6. Control	Passive	Joint surfaces used as guidance
7. Tissue removal through instrument	Geometry shaft Suction facility	Bearing of drill at tip Space between cable and shaft wall
8. Safe	Monitor actions Low machining forces No sharp edges	Start at portal High rotational frequency Protection of sharp edges
9. Simplicity	Number of elements	Multiple functions integrated in one element

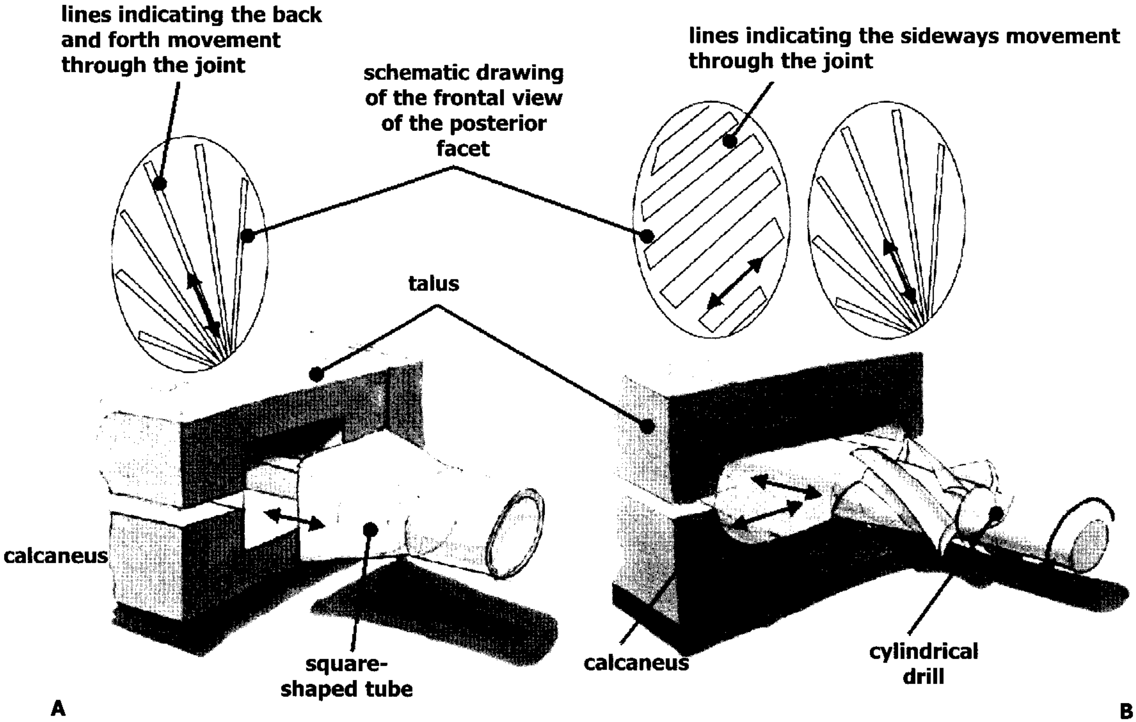

Figure 4.3.1
Sketch showing the two possible machining processes to remove cartilage and bone layers. The blocks represent the subtalar joint.

A) Slicing process, that allows only a back and forth movement in the joint (arrow indicates direction).

B) A combination of drilling and milling process, that allows for back and forth movement and sideways movement in the joint (arrows indicate directions).

example, when a drill is used, the machining force will be lower when the rotational frequency is increased.
After weighing several machining principles *(slicing, drilling, milling, punching, chiseling, sawing)*, two concepts to machine the tissue were further developed *(Figure 4.3.1)*. The first concept machines tissue via a slicing process to which an oscillation component is added for reduction of machining forces. To machine smooth surface *(Table 4.3.1: Requirement 2)* the cross-section of the tube has to be square, since this concept implies machining via a back and forth process for which each machining stroke is performed next to the former *(Figure 4.3.1)*. Few experiments were performed to simulate the oscillation, but this did not give satisfactory results. In addition to this, more research is necessary to design a mechanism to power the oscillation movement. Therefore, this concept was not further developed, so far.
The second concept consists of machining tissue by means of a cylindrical drill. The drill allows for drilling *(back and forth movement)* and milling *(sideways movement through the joint)* *(Figure 4.3.1)*, with which a smooth surface can be created *(Table 4.3.1: Requirement 2)*. It was chosen to further develop this concept, since a conventional cylindrical drill used in existing shaverblades could be initially used, and no further research would be necessary to construct a transmission for actuation of the drill.
From prior research *(Section 4.2)*[52], it was determined that about 3 mm *(cartilage thickness is about 1 mm, and subchondral bone layer is about 2 mm)* should be removed of each surface to

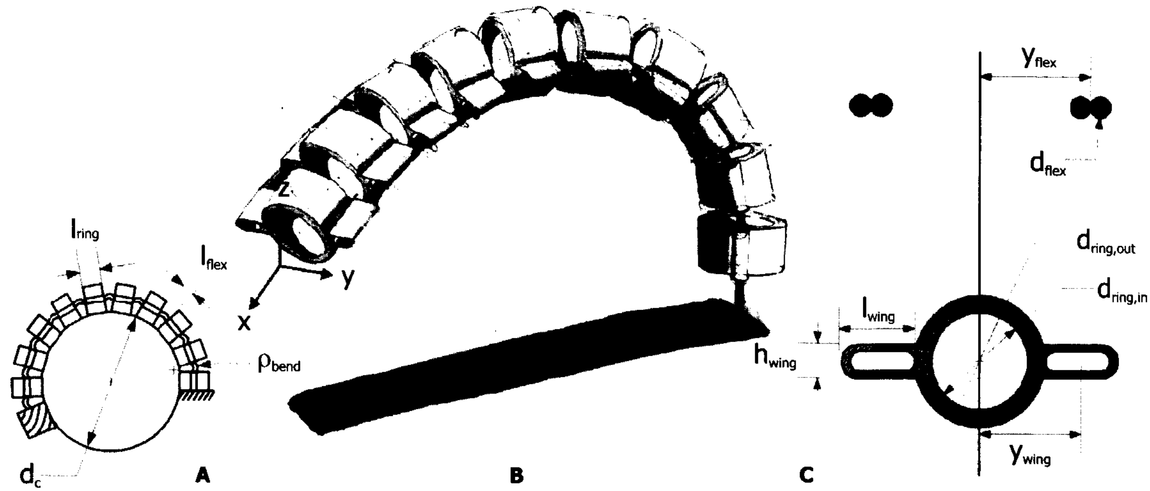

Figure 4.3.2
Sketch showing the configuration of the flexible shaft.

A) To be able to curve the flexible shaft around a circle d_c, the flexible segments have to bend around a circle ρ_{bend}, which is four times smaller. The reason for this is that the rings cannot be bent.

B) 3D-sketch of the flexible shaft showing the directions.

C) Cross-section of the flexible segment and the ring with sidewings.

create bleeding contacts *(Table 4.3.1: Requirement 3)*. To speed up the machining process *(Table 4.3.1: Requirement 4)*, it is preferable to machine both joint surfaces simultaneously. If both layers are machined simultaneously at both joint surfaces this requires a drill diameter of 7 mm, since the subtalar joint space height could be distended upto 1 mm without making use of distraction devices *(Section 4.2)*. This implies that a height of 7 mm is a practical boundary condition for the size of the instrument. The width of the instrument is solely dependent on the size of the access portal and can therefore be set larger at about 15 mm.

To be able to reach the entire subtalar joint, the length of the shaft is important. In Section 4.2, it was determined that if the length of the flexible shaft *(l_{shaft})* is 50 mm the instrument can reach a large range of posterior, medial, and anterior facets. For preservation of the joint's shape *(Table 4.3.1: Requirement 5)*, the new instrument should be able to curve around a circle of 24 mm in one direction *(d_c, Section 4.2)*. However, the shaft should give sufficient support to machine the tissue. Fortunately, the instrument has to be flexible only in the y-direction *(Figure 4.3.2)*, and the joint surfaces can be used to support the instrument in this direction. The stiffness of the instrument in the z-direction should be as high as possible to resist the tissue machining forces *(Figure 4.3.2)*. To achieve this combination of different stiffnesses, the moments of inertia and the configuration of material should be carefully chosen. The construction exists of rings with side-wings through which wires of superelastic alloy are placed *(Figure 4.3.2)*. The rings with side-wings generate a large difference between the moments of inertia in the two bending directions *(Figure 4.3.2)*. The superelastic alloy should allow for large bending. The determination of the number of rings *(k) (equal to the number of flexible segments)*, the length of the rings *(l_{ring})* and the distance between the rings *(l_{flex})* is performed with the help of the maximum allowable radius of curvature of one flexible segment *(ρ_{bend})* *(Figure 4.3.2)*:

$$\rho_{bend} = \frac{y_{max}}{\varepsilon_{max}} = \frac{k \cdot l_{flex} \cdot \frac{1}{2} \cdot d_c}{l_{shaft}} \quad \rightarrow \quad k \cdot l_{flex} = \frac{2 \cdot y_{max} \cdot l_{shaft}}{\varepsilon_{max} \cdot d_c} \qquad (4.3.1)$$

where, y_{max} is the largest distance in y-direction to the neutral axis, and ε_{max} is the maximum allowable strain of the superelastic alloy. Once k and l_{flex} are determined, l_{ring} can be calculated with:

$$l_{ring} = \frac{l_{shaft} - k \cdot l_{flex}}{k} \tag{4.3.2}$$

Three bending stiffnesses were calculated with the help of the superposition principle to determine the size of the diameter of the rings *($d_{ring,in}$, and $d_{ring,out}$)*, the length of the side-wings *(l_{wing})*, and the diameter of the superelastic wires *(d_{flex})*.[61] The bending stiffness of the flexible shaft in y-direction *(K_y)* is calculated assuming no support, but in practice the shaft is supported by the joint surfaces.

The flexible shaft is divided in two types of segments of constant cross-section *(Figure 4.3.2: C)*. The load on each cross-section is determined starting at the end of the shaft, followed by the determination of the amount of deflection for each segment *(Figure 4.3.3: B and C)*. The amount of deflection of each segment consists of a deflection component *(δ_i)* caused by a force *(F)* and a moment *($F \cdot l$)*, and a deflection component consisting of an angle of rotation *(θ_i)* multiplied by the total length of the previous segments caused by the same force and moment. The total deflection of the flexible shaft *(δ_{tot})* is then calculated by the sum of all deflections:

$$\delta_{tot} = \sum_{i=1}^{2k} \delta_i + \sum_{i=1}^{2k} \left(\left(\sum_{i=1}^{2k-1} l_i \right) \cdot \theta_i \right) \tag{4.3.3}$$

where,

$$\delta_i = \frac{F \cdot l_i^3}{3 \cdot E_i \cdot J_i} + \frac{F \cdot \left(\sum_{i=1}^{2k-1} l_i \right) \cdot l_i^2}{2 \cdot E_i \cdot J_i} \tag{4.3.4}$$

and

$$\theta_i = \frac{F \cdot l_i^2}{2 \cdot E_i \cdot J_i} + \frac{F \cdot \left(\sum_{i=1}^{2k-1} l_i \right) \cdot l_i}{E_i \cdot J_i} \tag{4.3.5}$$

E_i is the modulus of elasticity of segment i, and J_i is the moment of inertia of segment i. The length of a segment, the modulus of elasticity, and the moment of inertia are either equal to those of the ring or to those of the flexible segment. Therefore, the Eqs 4.3.3 to 4.3.5 can be simplified to:

Figure 4.3.3

A) Flexible shaft subjected to a load F at the middle of the drill head.

B) Internal forces caused by a force F working on each segment. The first three segments are shown and the last two.

C) Deflection caused by F of the first three segments of the flexible shaft starting at the free end. By making use of the superposition principle the deflections can be determined separately for each segment and than added.

D) Flexible shaft curved around the minimum bending diameter (d_c). The shaft is subjected to a force F, which is directed perpendicular to the plane of bending in this case.

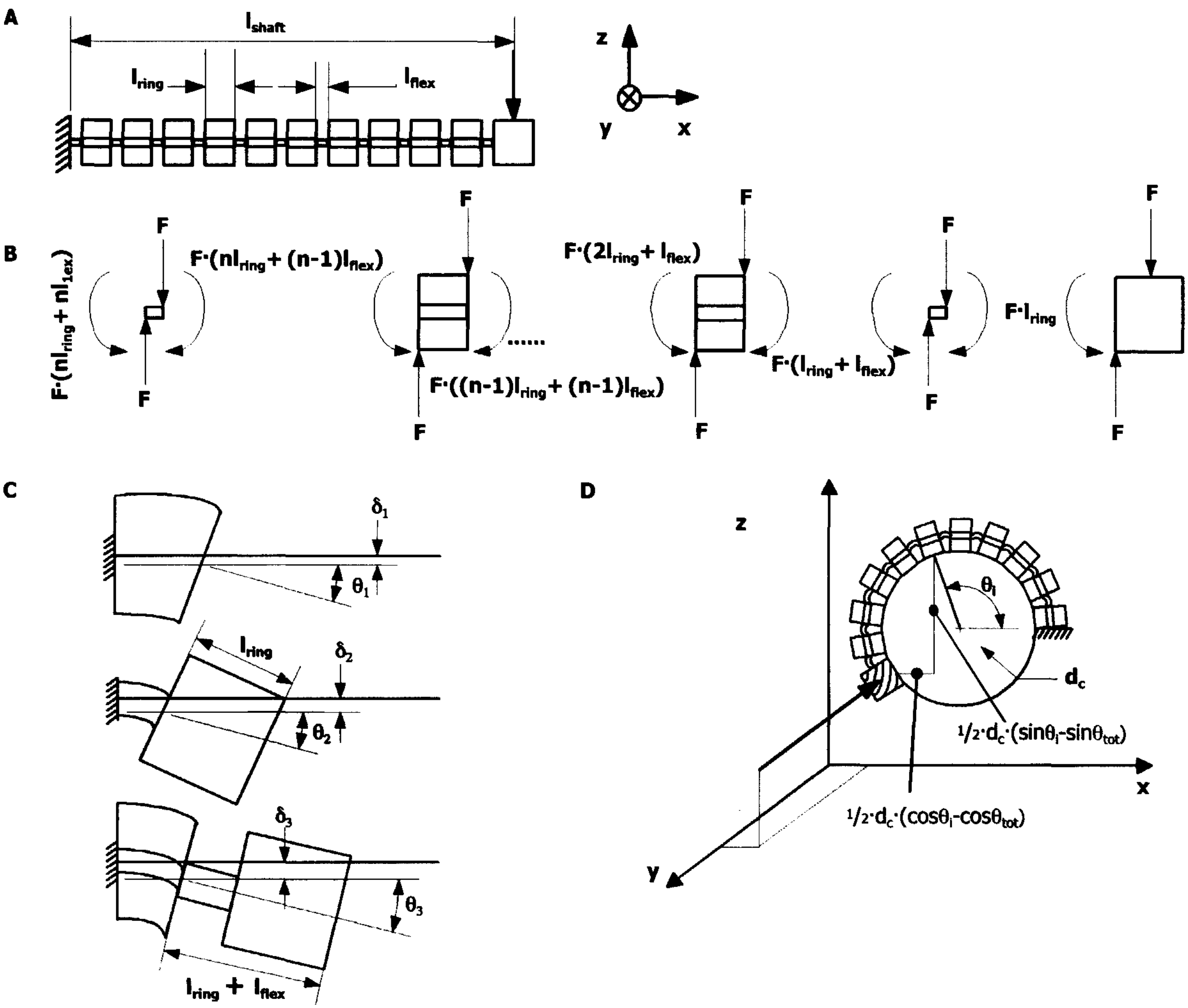

$$\sum_{i=1}^{2k}\delta_i = k\cdot\left(\frac{F\cdot l_{ring}^{3}}{3\cdot E_{ring}\cdot J_{ring,y}}+\frac{F\cdot l_{flex}^{3}}{3\cdot E_{flex}\cdot J_{flex,y}}\right)+\frac{F\cdot l_{ring}^{2}\cdot(l_{ring}+l_{flex})}{2\cdot E_{ring}\cdot J_{ring,y}}\sum_{i=1}^{k}(i-1)$$

$$+\frac{F\cdot l_{flex}^{2}}{2\cdot E_{flex}\cdot J_{flex,y}}\sum_{i=1}^{k}\left(i\cdot l_{ring}+(i-1)\cdot l_{flex}\right) \tag{4.3.6}$$

$$\sum_{i=1}^{2k}\left(\left(\sum_{i=1}^{2k-1}l_i\right)\cdot\theta_i\right)=\frac{F\cdot l_{ring}^{2}\cdot(l_{ring}+l_{flex})}{2\cdot E_{ring}\cdot J_{ring,y}}\sum_{i=1}^{k}(i-1)+\frac{F\cdot l_{flex}^{2}}{2\cdot E_{flex}\cdot J_{flex,y}}\sum_{i=1}^{k}\left(i\cdot l_{ring}+(i-1)\cdot l_{flex}\right)$$

$$+\frac{F\cdot l_{ring}\cdot(l_{ring}+l_{flex})^{2}}{E_{ring}\cdot J_{ring,y}}\sum_{i=1}^{k}(i-1)+\frac{F\cdot l_{flex}}{E_{flex}\cdot J_{flex,y}}\sum_{i=1}^{k}(i\cdot l_{ring}+(i-1)\cdot l_{flex})^{2} \tag{4.3.7}$$

where E_{ring} is the modulus of elasticity of a ring, E_{flex} is the modulus of elasticity of the flexible segment, $J_{ring,y}$ is the moment of inertia of a ring in y-direction, and $J_{flex,y}$ is the moment of inertia of a flexible segment in y-direction *(Figure 4.3.2: C)*:

$$J_{ring,y}=\frac{\pi\cdot(d_{ring,out}^{4}-d_{ring,in}^{4})}{64}+2\cdot\frac{l_{wing}\cdot h_{wing}^{3}}{12} \tag{4.3.8}$$

$$J_{flex,y}=2\cdot\frac{\pi\cdot d_{flex}^{4}}{64} \tag{4.3.9}$$

where h_{wing} is the height of a side-wing.

The stiffness K_y is:

$$K_y=\frac{F}{\delta_{tot}} \tag{4.3.10}$$

The bending stiffness in z-direction *(K_z)* can be calculated with the Eqs 4.3.3, 4.3.6 to 4.3.8, except that the moments of inertia in the z-direction *($J_{ring,z}$ and $J_{flex,z}$)* have to be filled in *(Eqs 4.3.11 and 4.3.12)*.

$$J_{ring,z} = \frac{\Pi \cdot (d_{ring,out}^{4} - d_{ring,in}^{4})}{64} + 2 \cdot \frac{h_{wing} \cdot l_{wing}^{3}}{12} + 2 \cdot (h_{wing} \cdot l_{wing}) \cdot y_{wing}^{2} \qquad (4.3.11)$$

$$J_{flex,z} = 2 \cdot \frac{\Pi \cdot d_{flex}^{4}}{64} + 2 \cdot \frac{\Pi \cdot d_{flex}^{2}}{4} \cdot y_{flex}^{2} \qquad (4.3.12)$$

where y_{wing} is the distance from the neutral y-axis to the y-axis at the centroid of one side-wing, and y_{flex} is the distance from the neutral y-axis to the y-axis at the centroid of half the area of the flexible segment. *(Figure 4.3.2: C)*

Lastly, K_p is the stiffness of the flexible shaft, when curved around a diameter, and is loaded by a force *(F)* that is directed transversally to the plane of bending *(Figure 4.3.3: D)*. K_p was calculated for four conditions: d_c is 24 mm *(θ_{tot} = 244°)*, 32.5 mm *(θ_{tot} = 180°)*, 65.1 mm *(θ_{tot} = 90°)*, and 586 mm *(θ_{tot} = 1°)*. θ_{tot} is the angle between the begin and the end of the shaft. It was expected that K_p for the minimum d_c would be the most critical to resist the maximum machining force of bony tissue. Due to the fact that the shaft is already curved the force (F) causes a bending moment or a twisting couple depending on the location at the shaft. The unit load method for calculating displacements described in Gere and Timoshenko[62] was applied to determine stiffness K_p. This method considers the structure subjected to the actual loads *(in this case F)*, and a unit load in the direction of the displacement to be calculated *(in this case the displacement in the direction of the actual load F is required)*. By equating the work of the unit load and the internal work due to the actual loads, the general equation for δ_p is obtained *(Figure 4.3.3: D)*:

$$\delta_p = \int_{\theta_i}^{\theta_{i+1}} \frac{F \cdot \frac{1}{2}d_c \cdot (\cos\theta - \cos\theta_{tot}) \cdot \frac{1}{2}d_c \cdot (\cos\theta - \cos\theta_{tot}) \cdot \frac{1}{2}d_c}{EJ} d\theta$$

$$+ \int_{\theta_i}^{\theta_{i+1}} \frac{-F \cdot \frac{1}{2}d_c \cdot (\sin\theta - \sin\theta_{tot}) \cdot \frac{1}{2}d_c \cdot (\sin\theta - \sin\theta_{tot}) \cdot \frac{1}{2}d_c}{GJ_p} d\theta \qquad (4.3.13)$$

or,

$$\delta_p = \frac{F \cdot (\frac{1}{2}d_c)^3}{EJ} \left[(\cos^2\theta_{tot} + \tfrac{1}{2})\theta - 2\cos\theta_{tot}\sin\theta + \tfrac{1}{4}\sin(2\theta) \right]_{\theta_i}^{\theta_{i+1}}$$

$$+ \frac{F \cdot (\frac{1}{2}d_c)^3}{GJ_p} \left[(\sin^2\theta_{tot} + \tfrac{1}{2})\theta + 2\sin\theta_{tot}\cos\theta - \tfrac{1}{4}\sin(2\theta) \right]_{\theta_i}^{\theta_{i+1}} \qquad (4.3.14)$$

where, $\frac{1}{2} d_c \cdot d\theta$ is the length of the segment of the flexible shaft, and J_p is the polar moment of inertia which is equal to the sum of the moments of inertia in y- and z-direction. Since, the shaft consists of segments with different moments of inertia and moduli, Eq. 4.3.14 has to be calculated separately by the angle interval $[\theta_i , \theta_{i+1}]$ for each segment. The stiffness K_p is then:

$$K_p = \frac{F}{\delta_p} \qquad (4.3.15)$$

The options to control the instrument in the flexible direction *(Table 4.3.1: Requirement 6)* are active or passive control. It was decided to implement passive control, because the construction can be kept simple, and the surgeon does not have to control an extra degree of freedom. Furthermore, the cartilage layers may be damaged, which offers the opportunity to use the two joint surfaces as a guiding tunnel for passive steering of the flexible instrument.
It would be advantageous, if an existing motorized device, that is already used in arthroscopy, could power the flexible instrument. The shaver system is the first choice, since tissue removal is also possible via this device *(Table 4.3.1: Requirement 7)*. To enable tissue removal through the flexible instrument there should be enough space in between the shaft and the drilling transmission, and no bearings can be placed in the shaft.
Safety is another important issue *(Table 4.3.1: Requirement 8)*. By setting the rotational frequency of the drill as high as possible and using an as sharp as possible drill the machining forces are minimized. This enables easier steering. In addition to this, by machining both joint layers from the beginning of the access portal, the surgeon can monitor his actions. Obviously, the flexible instrument may not have unprotected sharp edges or may not have elements that are sticking out.

Prototype
With the help of the prototype *(Figure 4.3.4)* the solutions that were chosen to meet the requirements are discussed. The dimensions of the parts that were chosen within boundary conditions are shown in Table 4.3.2. Starting at the tip, there is a frame placed in front of the drill which has multiple functions. Passive control is achieved by pushing the frame into the joint space, which requires a height of the frame equal to the joint space height. The flexible instrument is forced to follow the contour of the joint surfaces, since the frame follows the path of least resistance. The central position of the frame in relation to the drill enables simultaneous removal of equal portions of the two joint surfaces. In addition to this, the frame also serves as protection of soft tissue surrounding the joint against the drill. Lastly, since no bearing is allowed in the shaft to enable tissue removal, a bearing axis, that supports the cylindrical drill, was attached to the frame.
A cylindrical drill was chosen as drill head which is currently used in conventional shaverblades *(5.5 mm Stonecutter Acromionizer blade, Smith and Nephew Company, Hoofddorp, the Netherlands)*. The arguments for choosing this drill were that it scored well in drill and mill experiments performed on bone *(Section 4.2)*, was readily available, and was easier to steer

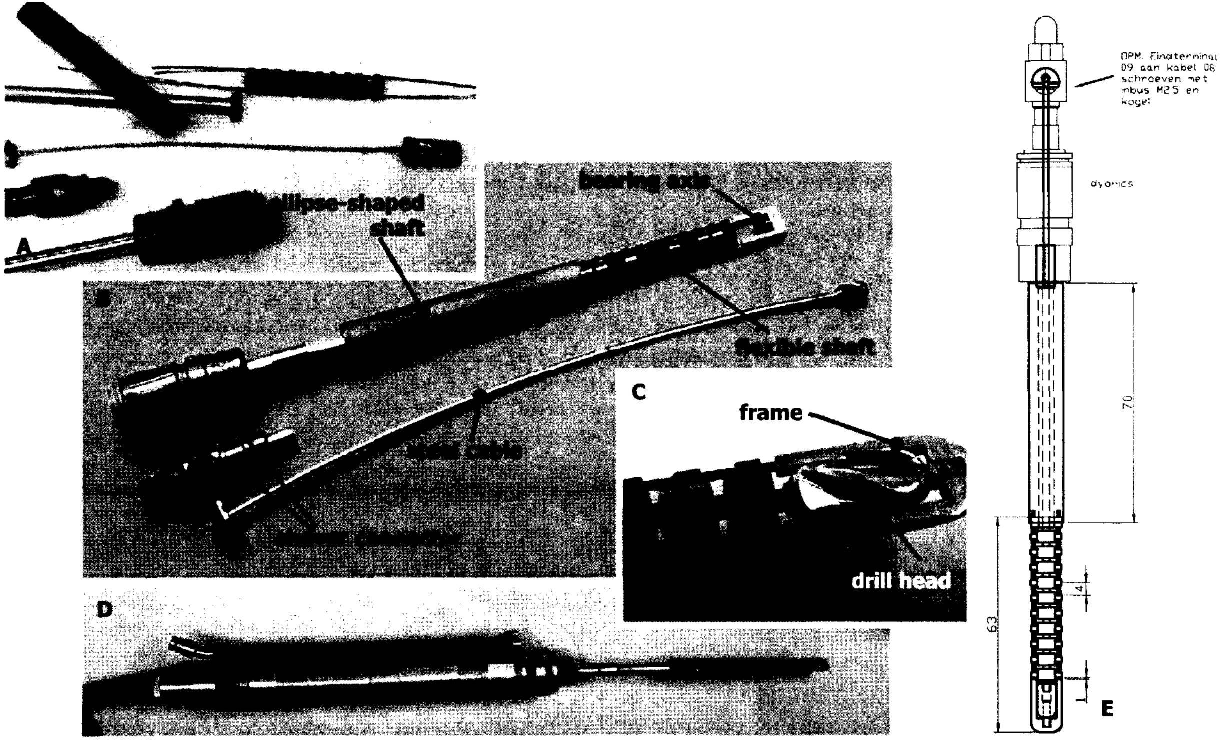

Figure 4.3.4
Color illustration see cover.
Photographs of the prototype.

A) Separate parts of the flexible instrument.

B) Assembled flexible shaverblade.

C) Close up of the tip.

D) Flexible shaverblade inserted in the shaver holder.

E) Construction drawing with the important dimensions.

than a spherical drill. The drill is powered via a steel cable that has the ability to rotate in a curved position of the shaft *(Figure 4.3.4)*. The steel cable can be attached to a normal drilling device, or attached to a shaver system by means of a coupling. A hole was drilled through the axis of the cylindrical drill to allow for bearing and to attach the drill to the steel cable.

The flexible shaft consists of stainless steel rings with side-wings through which superelastic wires *(@medical technologies AMT, Herk-de-Stad, Belgium)* are placed. The side-wings were fabricated by wire electric discharge machining. It was chosen to decrease the width of the side-wings from 3.4 to 2 mm, to be sure that the peak stresses in the wires are minimized. A practical problem was the connection of the wires to the rings. Since, we did not know how the characteristics of the wires would change when they were soldered or welded to the rings, we chose to glue them with Threebond 1373B. Originally, the frame was also glued to the ring at the far end. The available gluing surface appeared to be insufficient. Therefore, two holes of 0.5 mm were fabricated by wire electric discharge machining in each leg of the frame in which the wires were glued *(Figure 4.3.4)*.

The joint surfaces generate the reaction forces to overcome buckling once the flexible shaft is inside the joint. To prevent buckling outside the joint an ellipse-shaped metal shaft was designed that can be pushed over the flexible shaft *(Figure 4.3.4)*. The ellipse-shaped shaft also protects the tissue around the portal against the flexible shaft, and can be pushed over the cylindrical drill when the instrument is inserted. Lastly, the ellipse-shaped shaft is useful for tissue removal, since the flexible shaft with its openings is inappropriate for this task.

Evaluation

Three aspects are important to be tested in order to determine if the flexible instrument fulfills the requirements: A) the preservation of the joint surface contours, B) the removal of sufficient cartilage and bone of both joint surfaces, and C) thecreation of a smooth surface. For the preservation of the joint contour, the passive control has to be tested as well as the flexibility of

item	symbol	value	dimension	remark
height frame		1	(mm)	equal to a small subtalar joint space height
diameter drill		5.5	(mm)	existing size
diameter steel cable		1.6	(mm)	left winded, readily available
minimal diameter of the posterior facet's curvature	d_c	24	(mm)	result of Section 4.2
minimal length of the flexible shaft	l_{shaft}	51.1	(mm)	result of Section 4.2, adjusted for construction
modulus of elasticity of flexible segment	E_{flex}	70	(GPa)	superelastic alloy: assumed value, real value unknown
shear modulus of elasticity of flexible segment	G_{flex}	23.3	(GPa)	superelastic alloy: assumed value, real value unknown
modulus of elasticity of ring	E_{ring}	210	(GPa)	steel
shear modulus of elasticity of ring	G_{ring}	70	(GPa)	steel
maximum allowable strain	ε_{max}	0.06	-	superelastic alloy
diameter of flexible rod	d_{flex}	0.4	(mm)	available dimension
distance between the from the neutral y-axis to the y-axis at the centroid of half the area of a flexible segment	y_{flex}	2.8	(mm)	two wires placed next to each other at both sides
inner diameter of a ring of the flexible shaft	$d_{ring\ in}$	5	(mm)	as large as possible
outer diameter of a ring of the flexible shaft	$d_{ring\ out}$	4	(mm)	smaller than diameter drill
length of one side-wing	l_{wing}	2	(mm)	as large as possible
height of the side-wings of a ring of the flexible shaft	h_{wing}	1	(mm)	equal to a small subtalar joint space height
distance between the from the neutral y-axis to the y-axis at the centroid of the area of the a side-wing	y_{wing}	3.5	(mm)	
inner size ellipse-shaped shaft		9 x 5	(mm)	

Table 4.3.2
Part of the technical specifications of the prototype of the flexible instrument. These dimensions were chosen within the set up boundary conditions.

the shaft. The flexibility of the shaft was firstly calculated with the formulas derived. The practical embodiment of the flexible shaft was tested by curving it around differently sized templates in the y-direction, and by pushing the tip of the instrument on a pair of scales in the z-direction. Aspects A and C, and the passive control were first tested in an experimental set up with artificial bone *(Imbema kunststofchemie, the Netherlands 1991[49])* by means of a drill with a frame without the flexible shaft.
The final prototype was tested in two cadaver ankles where the removal of the entire subtalar joint surfaces was aimed at via the two posterior access portals. For the shaver system used in the tests no active suction device was available. To enable bone chips to be removed the flexible instrument was frequently pulled back. The smoothness of the surface and the assessment of removal of sufficient portions were done by visual inspection. In addition to this, an estimation was made of the thickness of the removed layers by means of a photograph and a probe of which the length was known.

Results

The additional technical specifications of the flexible instrument as well as the calculated stiffnesses of the flexible shaft can be found in Table 4.3.3. The calculations show that K_z is 1000 times higher than K_y. Furthermore, it appears that K_p is approximately equal to K_z for bending around d_c. This is advantageous, since in practice only at the far end of a joint the entire flexible shaft will be curved. Whereas for larger diameters *(d_c)* the flexible shaft will be partly supported by the ellipse-shaped shaft, which results in a larger K_p as was calculated for the entire shaft. The maximal estimated vertical displacement is 2.1 mm. The flexible shaft including the steel cable could be loaded to 30 N with minimal displacement in z-direction, from that point on buckling occurred easily. In practice, K_y is sufficient to curve the shaft around a diameter of even smaller than 24 mm *(Figure 4.3.5)*. However, the stiffness of the steel cable was not taken into account in the calculations, and cannot be neglected as is determined in practice *(Figure 4.3.5)*. Therefore, extra force is needed to curve the shaft.
The initial tests with a straight instrument and a frame at the tip showed that it is possible to passively control the instrument with the frame and that a smooth surface can be achieved at both surfaces *(Figure 4.3.5)*. Tests performed in two cadaver ankles show that both surfaces are equally machined by the drill, and that a smooth surface is created *(Figure 4.3.6)*. The estimated height of the removed tissue was about 2 mm. In addition to this, passive control is possible. However, it was not possible so far with this prototype to follow the entire subtalar joint's contour *(Figure 4.3.6)*. Due to this fact, attempts were postponed to assess if quicker preparation of the joint is possible than the currently used method performed with curettes.
Additional phenomena were noticed during the experiments. The instrument could be inserted through the posteromedial portal by increasing the size of the portal slightly. At insertion, the ellipse-shaped shaft was helpful. It was important to push the ellipse-shaped shaft over the part of the flexible shaft which was not in the joint, since buckling occurred easily. During drilling it was sometimes difficult to keep the ellipse-shaped shaft at its place. The cylindrical drill, which was already used during one operation on a patient, went blunt, quickly. Therefore, more force than expected was needed to push the flexible instrument through the joint. Drilling *(back and*

item	value	dimension	item	value	dimension
k	11	-	K_y	0.03	(N/mm)
l_{flex}	1.1	(mm)	K_z	28.8	(N/mm)
l_{ring}	3.4	(mm)	K_p (θ_{tot} = 244°)	23.4	(N/mm)
$J_{flex,y}$	0.005	(mm^4)	K_p (θ_{tot} = 180°)	25.6	(N/mm)
$J_{flex,z}$	4.0	(mm^4)	K_p (θ_{tot} = 90°)	15.3	(N/mm)
$J_{flex,p}$	4.0	(mm^4)	K_p (θ_{tot} = 1°)	0.7	(N/mm)
$J_{ring,y}$	18.4	(mm^4)	$\delta_{tot,z}$	1.7	(mm)
$J_{ring,z}$	68.5	(mm^4)	δ_p (θ_{tot} = 244°)	2.1	(mm)
$J_{ring,p}$	86.9	(mm^4)			

Table 4.3.3
The calculated dimensions for the flexible shaft. The length of the flexible segments and the rings (l_{flex} and l_{ring}) was calculated assuming a rod of 0.35 mm, in the actual prototype the wires were 0.4 mm. The moments of inertia were calculated with the actual rod diameter.
To calculate the maximum displacement in z-direction the maximum machining force (50 N) determined in Section 4.2 was used.

forth movement) was well possible with the instrument, but milling was very difficult *(sideways movement through the joint)*. The height of the frame in relation to the subtalar joint space height was rather large.

Discussion

In this section, the clinical problem that is addressed is the insufficient arthroscopic preparation of the subtalar joint for fusion. Thereto, requirements defined from clinical practice were translated into technical specifications for the development of a new flexible shaverblade. From this point, the conceptual design of the instrument was started by generating possible solutions for each requirement, and by integrating them to a final concept.

The practical embodiment of the instrument shows that most requirements are met. Smooth bleeding contact areas can be created, equal portions of both surfaces can be removed from the

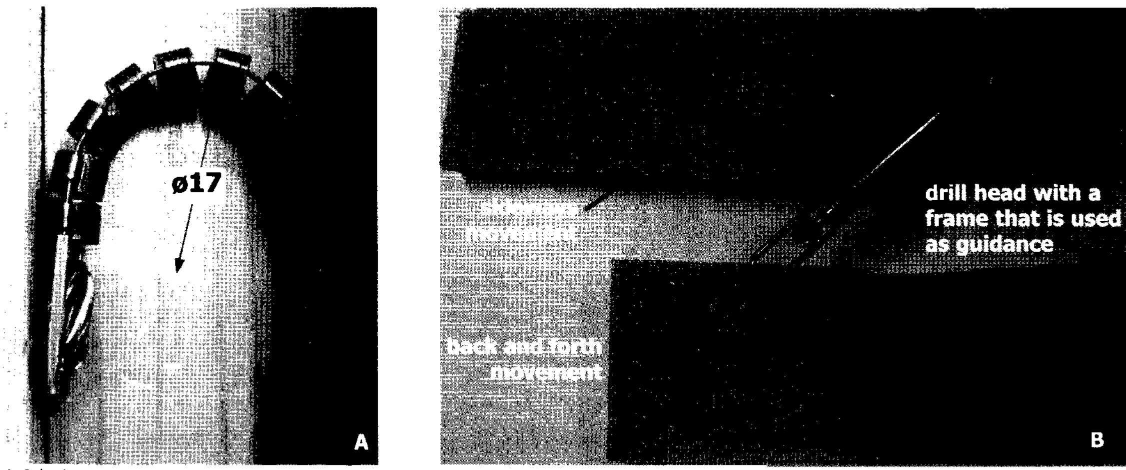

Figure 4.3.5
A) Flexible shaft bent in its most extreme configuration. The flexible shaft including the steel cable could be bent to a diameter of about 30 mm.

B) Photograph of artificial bone material that is machined with a straight drill including a frame.

entire joint *(Figure 4.3.6: A)*, passive control is possible *(Figure 4.3.5)*, tissue removal through the instrument is possible via connection with the shaver system, and the requirements for safety are met. However, the requirement to follow the contour of the joint surfaces is not fulfilled by means of this prototype. The high stiffness of the tip *(frame and drill)* in combination with its relatively large length makes it not possible to curve around the top of the subtalar joint contour. The reaction forces of the joint surfaces forced the instrument to drill into the surface of the calcaneus. Once the subchondral bone is removed on one side, the drill follows the path of least resistance and starts drilling in the softer bone layer underneath the subchondral bone *(Figure 4.3.6: B)*.
In the near future, the following adjustments are foreseen. The length of the combination of frame and drill has to be decreased. Thereto, the length of the frame in front of the drill can be decreased by 1 mm, and the cylindrical drill can be downsized to half of its length including the bearing axis. This implies that the attachment of the steel cable to the drill has to be changed, since too little surface will be left to glue both parts. In addition to this, the drill should have sharper cutting edges. If it has a diameter of 6 or 6.5 mm it is expected that the entire subchondral bone layer is removed. The height of the frame should be decreased to 0.8 mm and care should be taken that the edges are more rounded than currently. A more flexible steel cable should be chosen to decrease the stiffness in flexible y-direction. Furthermore, it is believed that the stiffness of the shaft itself in y-direction may be a bit larger to minimize the occurrence of buckling. Thereto, the width of the side-wings can be kept the same as the width of the rings *(3.4 mm)*. A larger width of the side-wings increases the glue surface of the rings. This is advantageous, since the current attachment of the superelastic wires to the rings is not solid enough. Another option could be to experiment with soldering of the wires.
In conclusion, the concept of the flexible instrument has potential and the prototype meets already a large part of the requirements, but the practical embodiment needs adjustments to make it possible to use the instrument in practice.

4.4 Discussion

To implement the new subtalar arthrodesis technique, the development of additional instruments was started. As was explained in Chapter 1, the anatomic variation of individuals forces the designer to carefully state the exact problem to be solved by the development of a new instrument, the variations that can be assumed constant by suitable approximation, and the variations the instrument should deal with. For the development of the measurement system the difficulty was the presence of variation amongst people in combination with the fact that a correct hindfoot alignment is not clearly defined. This absence of a clear definition was used as a freedom of choice for the design. The definition of the hindfoot alignment is dependent on the position of the person. The question is what position is critical for the definition of a correct hindfoot alignment without actual measurements. Is this the natural stance position or the unilateral position when walking or even another position? It is difficult to determine a suitable position to measure hindfoot alignment. Therefore, guided by practical usage of the measurement system, it was chosen to let all individuals stand in one unambiguously defined position. By choosing this option, the reproducibility of the measurement is emphasized. It is

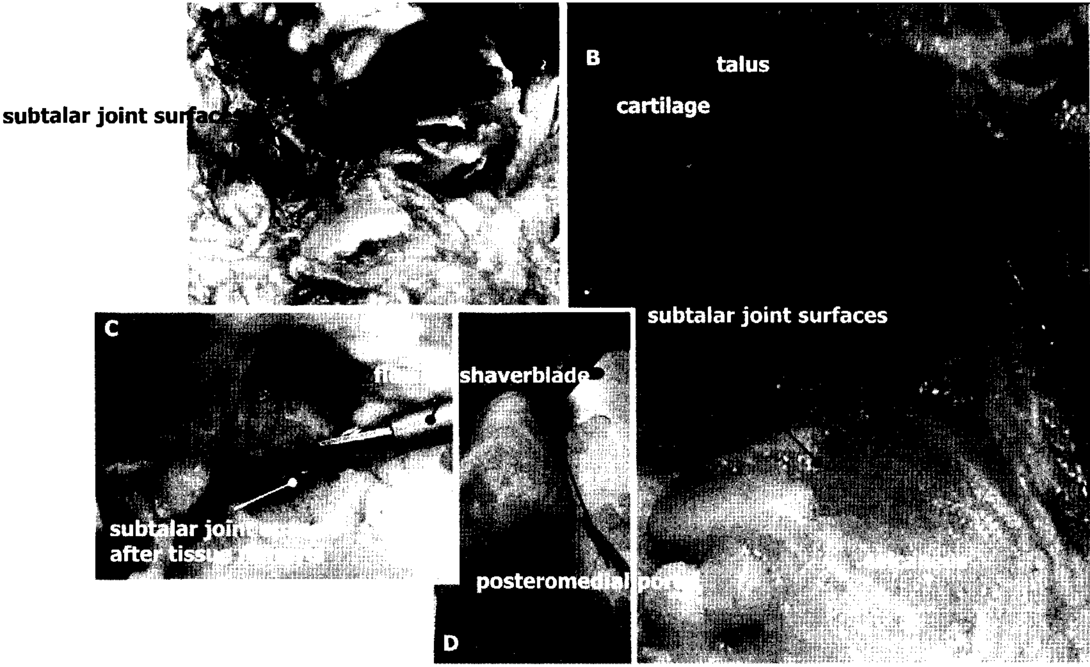

Figure 4.3.6
Color illustration see cover.
A) Photograph of the posterior side of one cadaver ankle showing the posterior facet. Half of the posterior facet (till the top of the joint) is machined with the flexible instrument. This resulted in a smooth surface and equally removed portions of tissue on both surfaces.

B) Photograph of the posterior side of the second cadaver ankle showing the posterior facet. The photograph shows that the major part of the joint surface of the calcaneus is machined, but the majority of joint surface of the talus contains still cartilage.

C) Photograph of the second cadaver ankle, showing the subtalar joint space height after machining the joint with the flexible shaverblade.

D) Photograph of the second cadaver ankle showing the flexible shaverblade inserted in the posteromedial portal.

believed that if the new measurement system can produce reproducible values of the hindfoot alignment, this will be a good start in the search for a definition of hindfoot alignment and an optimal correction of it.
In addition to this, the accuracy is important. How accurate does the measurement has to be, to be useful in clinical practice? How accurate does the measurement has to be, to be of use in search for a proper definition of hindfoot alignment? For this purpose it is probably best to strive for the highest possible accuracy. This can be done by using only one observer, using a large number of repeated measurements per condition, and performing adjustments to the measurement system to minimize human variation. The required accuracy for clinical practice is difficult to assess. Nature can adapt itself well to adjustments. An option would be to start measuring a large population of patients that is going to receive a subtalar arthrodesis, and a population that already has received a subtalar arthrodesis. From these measurements, a boundary angle for correction could be assessed taking into account the accuracy of the measurement system. So far, the first prototype of the measurement system as well as the method making use of posterior weightbearing photographs are a good start for the discussion about the definition of hindfoot alignment. With adjustments, they both could be used in clinical practice.
For the development of a flexible shaverblade, it was important to assess the geometric and the load criteria. The aim was to start fabricating a prototype as soon as possible to verify if the variation amongst individuals was taken into account, sufficiently. Thereto, research was done to assess boundaries for the required criteria by performing simple experiments and by defining a simple model for the subtalar joint space. In practice, the experiments performed to asses the maximum machining force for several machining processes appeared to be difficult to keep in

control, since so many variables influence the machining force. Thereto, this study can be used as a pilot study to start an elaborate study to set up rules of thumb for the machining force of several types of human tissue, as is common in the machining of metals.[63] Since, these data are important for almost every instrument used in removal surgery.[64]
Considering the design of the flexible shaverblade, different functions were tested separately, and proved to work. The combination of functions in the presented prototype needs fine tuning. In addition to this, the opinion of the participating surgeon who used the instrument on a cadaver ankle was positive. The fact that the flexible instrument can be powered by the shaver system is advantageous, since surgeons are familiar with this device, which can lead to easy acceptance of the new shaverblade. Since the currently used shaverblades are disposable *(the drill in the prototype went blunt quickly)*, the possibility exists to make the new shaverblade also disposable. This could be advantageous for the fabrication process, since the flexible shaft could than be fabricated by a moulding process, which is probably cheaper than wire electric discharge machining. The concept of the flexible shaverblade has definitely potentials.

References

1. Tuijthof GJM, van Dijk, C. N., and Pistecky PV. Subtalar arthrodesis: current limitations and strategy for a new technique. Submitted to *Foot & Ankle Int* 2002.
2. McClay I. Bray J. The subtalar angle: a proposed measure of rearfoot structure. *Foot & Ankle Int* 1996; 17: 499-502.
3. Flemister AS. Infante AF. Sanders RW. Walling AK. Subtalar arthrodesis for complications of intra-articular calcaneal fractures. *Foot & Ankle Int* 2000; 21: 392-399.
4. Dennyson WG. Fulford GE. Subtalar arthrodesis by cancellous grafts and metallic internal fixation. *J Bone Joint Surg Br* 1976; 58: 507-510.
5. Carr JB. Hansen ST. Benirschke SK. Subtalar distraction bone block fusion for late complications of os calcis fractures. *Foot & Ankle Int* 1988; 9: 81-86.
6. Grice DS. An extra-articular arthrodesis of the subastragalar joint for correction of paralytic flat feet in children. *J Bone Joint Surg Am* 1952; 34: 927-940.
7. Thomas FB. Arthrodesis of the subtalar joint. *J Bone Joint Surg Am* 1967; 49: 93-97.
8. Seymour N. Evans DK. A modification of the Grice subtalar arthrodesis. *J Bone Joint Surg Br* 1968; 50: 372-375.
9. Engstrom A. Erikson U. Hjelmstedt A. The results of extra-articular subtalar arthrodesis according to the Green-Grice method in cerebral palsy. *Acta Orthop Scand* 1974; 45: 945-951.
10. Gross RH. A clinical study of the Batchelor subtalar arthrodesis. *J Bone Joint Surg Am* 1976; 58: 343-349.
11. Moreland JR. Westin GW. Further experience with Grice subtalar arthrodesis. *Clin Orthop* 1986; 207: 113-121.
12. Russotti GM. Cass JR. Johnson KA. Isolated talocalcaneal arthrodesis. *J Bone Joint Surg Am* 1988; 70: 1472-1478.

13. Amendola A. Lammens P. Subtalar arthrodesis using interposition iliac crest bone graft after calcaneal fracture. *Foot & Ankle Int* 1996; 17: 608-614.

14. Bednarz PA. Beals TC. Manoli A. Subtalar distraction bone block fusion: an assessment of outcome. *Foot & Ankle Int* 1997; 18: 785-791.

15. Dahm DL. Kitaoka HB. Subtalar arthrodesis with internal compression for post-traumatic arthritis. *J Bone Joint Surg Br* 1998; 80: 134-138.

16. Mann RA. Beaman DN. Horton GA. Isolated subtalar arthrodesis. *Foot & Ankle Int* 1998; 19: 511-519.

17. Easley ME. Trnka H-J. Schon LC. Nade S. Isolated subtalar arthrodesis. *J Bone Joint Surg Am* 2000; 82: 613-624.

18. Lian G. Hindfoot arthrodesis. In: Pfeffer GB, Frey C, eds. *Current practice in foot and ankle surgery*. San Francisco: McGraw-Hill, 1993;262-284

19. Mann RA. Arthrodesis of the foot and ankle. In: Mann RA, Coughlin MJ, eds. *Surgery of the foot and ankle*. St. Louis: Mosby, 1993;673-713. ISBN 0-8016-6683-X.

20. Scranton PE. Results of arthrodesis of the tarsus: talocalcaneal, midtarsal, and subtalar joints. *Foot Ankle* 1991; 12 : 156-164.

21. Astrom M. Arvidson T. Alignment and joint motion in the normal foot. *J Orthop Phys Ther* 1995; 22: 216-222.

22. Alexander RE. Battye CK. Goodwill CJ. Walsh JB. The ankle and subtalar joints. *Clinics in Rheumatic Diseases* 1982; 8: 703-711.

23. Ball P. Johnson GR. Technique for the measurement of hindfoot inversion and eversion and its use to study a normal population. *Clin Biomech* 1996; 11: 165-169.

24. Burton DC. Olney BW. Horton GA. Late results of subtalar distraction fusion. *Foot & Ankle Int* 1998; 19: 197-202.

25. Isman RE. Inman VT. Anthropometric studies of the human foot and ankle. *Bull Prost Res* 1969; 10: 97-129.

26. Parenteau CS. Viano DC. Petit PY. Biomechanical properties of human cadaveric ankle-subtalar joints in quasi-static loading. *J Biomech Eng* 1998; 120 : 105-111.

27. Pearce TJ. Buckley RE. Subtalar joint movement: clinical and computed tomography scan correlation. *Foot & Ankle Int* 1999; 20: 428-432.

28. Pierrynowski MR. Smith SB. Rear foot inversion/eversion during gait relative to the subtalar joint neutral position. *Foot & Ankle Int* 1996; 17: 406-412.

29. Siegler S. Chen J. Schneck CD. The three-dimensional kinematics and flexibility characteristics of the human ankle and subtalar joint Part I: kinematics. *J Biomech Eng* 1988; 110: 364-373.

30. Buckley RE. Hunt DV. Reliability of clinical measurement of subtalar joint movement. *Foot & Ankle Int* 1997; 18: 229-232.

31. Lattanza L. Gary GW. Kantner RM. Closed versus open kinematic chain measurement of subtalar joint eversion: implications for clinical practice. *J Orthop Phys Ther* 1988; 9: 310-314.

32. Sell KE. Verity TM. Worrell TW. Pease BJ . Wigglesworth J. Two measurement techniques for assessing subtalar joint position: a reliability study. *J Orthop Phys Ther* 1994; 19: 162-167.

33. Wen DY. Puffer JC. Schmalzried TP. Lower extremity alignment and risk of overuse injuries in runners. *Med Sci Sports Exerc* 1997; 29: 1291-1298.

34. Ryf C, Weymann A, eds. *Range of motion - AO Neutral-0 method.* Stuttgart-New York: Thieme, 1999. ISBN 3-13-116791-2.

35. Brown DN. Method and apparatus for determining the neutral axis of a foot or the like. Patent US4416292 (US19810294307 19810819). Brown DN, United States of America, 22-11-1983.

36. Pearce RF. Foot joint position determination. Patent GB2312754 (GB19960008962 19960429). Pearce RF, United States of America, 5-11-1997.

37. Kovaleski JE. Gurchiek LR. Heitman RJ. Hollis JM. Pearsall AW. Instrumented measurement of anteroposterior and inversion-eversion laxity of the normal ankle joint complex. *Foot & Ankle Int* 1999; 20: 808-814.

38. Hamill J. Bates BT. Knutzen KM. Kirkpatrick GM. Relationship between selected static and dynamic lower extremity measures. *Clin Biomech* 21989; 4: 217-225.

39. Almering JHJ, ed. *Analyse.* Delft: Delft University Press, 1993. ISBN 90-65620788.

40. Jurgens HW, Aune IA, Pieper U, eds. *International data on anthropometry.* Dortmund: Federal Institute for Occupational Safety and Health, 1990. ISBN 92-2-106449-2.

41. Salvendy G, ed. *handbook of human factors and ergonomics.* New Delhi: Wiley, 1997. ISBN 0-471-11690-4.

42. Molenbroek JFM, ed. *Op maat gemaakt, menselijke maten voor het ontwerpen en beoordelen van gebruiksgoederen.* Delft: Delftse Universitaire Pers, 1994. ISBN 90-6275-996-3.

43. Kamp EA vd. Standsbepaling van de calcaneus. Delft University of Technology, department of Design, Engineering, and Production, section Man-Machine Systems, 2001: 1-95.

44. Muller R. Buttner P. A critical discussion of intraclass correlation coefficients. *Stat.Med.* 1994; 13: 2465-2476.

45. Deyo RA. Diehr P. Patrick DL. Reproducibility and responsiveness of health status measures. Statistics and strategies for evaluation. *Control Clin Trials* 1991; 12: 142S-158S.

46. van Dijk CN. Scholten PE. Krips R. A 2-portal endoscopic approach for diagnosis and treatment of posterior ankle pathology. *Arthroscopy* 2000; 16: 871-876.

47. Barbaix E. Roy P van. Clarys JP. Variations of anatomical elements contributing to subtalar joint stability: intrinsic risk factors for post-traumatic lateral instability of the ankle? *Ergonomics* 2000; 43: 1718-1725.

48. Ebraheim NA. Mekhail AO. Yeasting RA. Components of the posterior calcaneal facet: anatomic and radiologic evaluation. *Foot & Ankle Int* 1996; 17: 751-757.

49. Verdult EPHA. *Drilling back.* Delft University of Technology, 1998: 148-152.

50. Visible Human project. Internet. 2002. http://www.nlm.nih.gov/research/visible

51. Somso Modelle. Catalog (A74/1). 1997.

52. Tuijthof GJM. Meetverslag 1: experimenten met kadaverenkels. Man-machine systems, Department of Design, Engineering and Production, Delft University of Technology, Delft, 2001: 1-32.

53. Frey C. Gasser S. Feder K. Arthroscopy of the subtalar joint. *Foot & Ankle Int* 1994; 15: 424-428.

54. Mekhail AO. Heck BE. Ebraheim NA. Jackson WT. Arthroscopy of the subtalar joint: Establishing a medial portal. *Foot & Ankle Int* 1995; 16: 427-432.

55. Parisien JS. Arthroscopy of the posterior subtalar joint. In: Parisien JS, ed. *Current Techniques in Arthroscopy.* New York: Thieme, 1998;161-168. ISBN 0-86577-738-1.

56. Jerosch J. Subtalar arthroscopy - indications and surgical technique. *Knee Surg Sport Tr A* 1998; 6: 122-128.

57. Williams MM. Ferkel RD. Subtalar arthroscopy: indications, technique and results. *Arthroscopy* 1998; 14: 373-381.

58. Tasto JP, Laimins PD. Recent advances in ankle arthroscopic techniques. In: Parisien JS, ed. *Current techniques in arthroscopy.* New York: Thieme, 1998;181-194. ISBN 0-86577-738-1.

59. Scranton PE. Comparison of open isolated subtalar arthrodesis with autogenous bone graft vs. outpatient arthroscopic subtalar arthrodesis using injectable bone morphogenic protein-enhanced graft. *Foot & Ankle Int* 1999; 20: 162-165.

60. Lundeen RO. Arthroscopic fusion of the ankle and subtalar joint. *Clin Podiatr Med and Surg* 1994; 11: 395-406.

61. Gere JM, Timoshenko SP. Deflections of beams. In: Gere JM, Timoshenko SP, eds. *Mechanics of materials.* London: Chapman & Hall, 1993;461-534. ISBN 0412368803.

62. Gere JM, Timoshenko SP. Energy methods. In: Gere JM, Timoshenko SP, eds. *Mechanics of materials.* London: Chapman & Hall, 1993;627-706. ISBN 0412368803.

63. Luttervelt CA van. Scheidende bewerkingen. In: Luttervelt CA van , ed. *Inleiding vervaardigingskunde w53, w56.* Delft: Delft University of Technology, 1993;4.1-4.2

64. Tschatsch H, ed. *Verspaningstechniek.* Schoonhoven: Academic Service, 1997. ISBN 90-395-0465-2.

5. Optimization of arthroscopic view

In this chapter, a problem area is addressed that is related to all arthroscopic operations: insufficient arthroscopic view. A good view on the operation area during arthroscopic operations is essential to perform a procedure safe and fast. Section 5.1 presents more detailed results of the clinically driven approach *(Chapter 2)*. In Section 5.2, the state of the art is summarized on the creation of sufficient view by the irrigation of joints. From Section 5.1 and 5.2, it has been determined that two aspects could supplement the current developments to improve the arthroscopic view. Firstly, the behavior of irrigation systems should be made clear to surgeons who often lack sufficient technical knowledge. This aspect is addressed in Section 5.3 where a model is derived for the most commonly used irrigation systems as well as guidelines for their usage. Secondly, once the factors that influence the joint irrigation are known, the design of a new sheath or cannula that optimizes the joint irrigation can be started. To be able to determine these factors a simplified knee joint model was constructed, which was evaluated with the help of the experiments described in Section 5.3. In Section 5.4, the influence of several factors is investigated, and a new sheath is presented and evaluated. The chapter is concluded with a discussion in Section 5.5.

5.1 Problem analysis

In Chapter 2, it was concluded that the interviewed surgeons agreed that a suboptimal or troubled arthroscopic view was an important problem area. The surgeons were asked to indicate how often the view was impeded in the most common arthroscopic procedure *(Table 5.1.1)*. The main causes for unclear view were malfunction of the arthroscope, the light cable or the camera, malfunction of the irrigation system, and the occurrence of bleedings. Other causes of insufficient view at the operation area are the presence of synovial tissue in front of the arthroscope, and the tightness of joints, especially on the posterior side of the knee joint. Research is started to assess what steps can be taken to optimize the view during arthroscopic procedures.

A summary will be given of observations on arthroscopic view and related items that were performed during 40 arthroscopic operations in 7 different hospitals. These operations include ankle arthroscopy *(11)*, meniscectomy *(13)*, other arthroscopic knee procedures *(11)*, shoulder arthroscopy *(4)*, and wrist arthroscopy *(1)*. All operations were performed with a gravity pump with a separate suction system, except for four operations in which an automated pump was

Table 5.1.1
The number of times that a remark is made on the view during one operation is summarized as a percentage of the total number of observed operations, which was 40.

good view	clear and sharp view	15%
troubled view	tissue in front of the camera	30%
	bleedings and loose tissue parts	25%
	instrument	13%
	operating blindly	10%

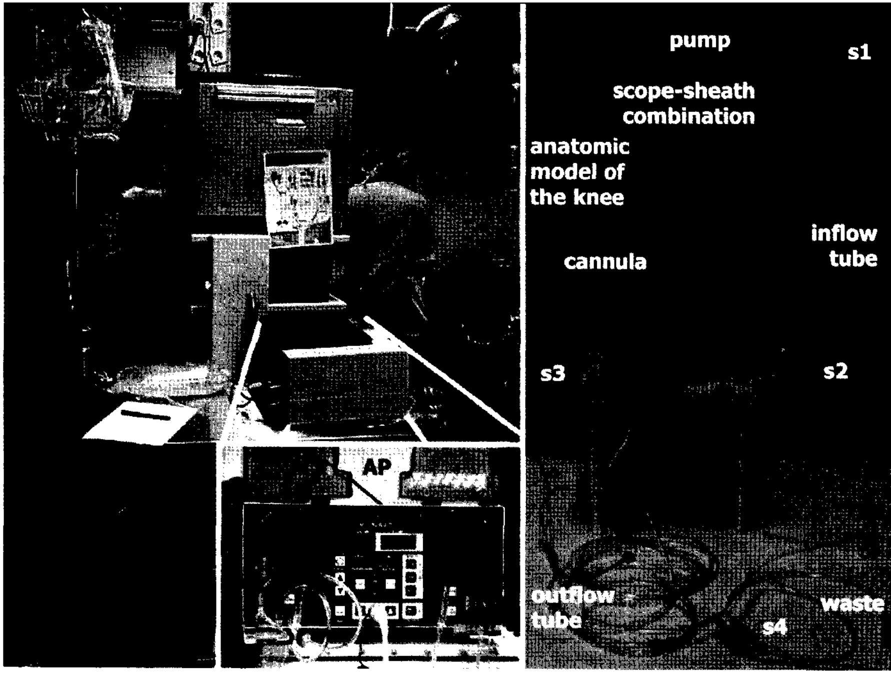

Figure 5.1.1
Color illustration see cover.
To the left: Picture of the gravity pump (GP) on the left side and the automated pump FMS duo+ (AP) in the operation room.

To the right: picture of the tubes connected to the sheath-scope combination, and the cannula. The pressure sensors are also indicated (s1, s2, s3, s4).

used *(Figure 5.1.1)*. From the analysis, it appears that in 15% of the operations the view was optimal during the operation *(Table 5.1.2)*. Furthermore, the configuration of the 30°-arthroscope is useful through its periscope function, and this is sufficient to inspect a large number of joints. This makes it unnecessary to put an effort in developing a flexible arthroscope. However, in about a quarter of the operations the view is troubled in such a way that the surgeon is hampered in performing the operation, and he has to take actions to clarify the view or sometimes perform part of the operation blindly. Furthermore, it was observed that usually when adhesions are present or a joint is heavily damaged, the view is impeded by synovial tissue. It was noticed that during one operation an outflow tube was blocked, and one surgeon used a needle as outflow portal instead of a separate cannula *(Figure 1.1.5)*. About half of the surgeons

view during procedure	always clear	sometimes unclear	always good view	sometimes no view
shoulder arthroscopy	4	6	4	6
elbow arthroscopy	3	4	4	3
wrist arthroscopy	2	3	3	2
diagnostic knee arthroscopy	8	2	6	4
meniscectomy	5	6	3	8
anterior cruciate ligament reconstruction	4	5	7	2
ankle arthroscopy	6	4	5	5

Table 5.1.2
Outcome of a survey in which eleven arthroscopic surgeons were asked for which procedures the view is sometimes impeded. The view is divided into two aspects: clarity (column 2 and 3) and overview (column 4 and 5). Each surgeon was asked to mark one column per aspect. Some surgeons did not perform all types of procedures, therefore the total number of marks differ.

used a third portal through which a separate cannula was inserted for fluid inflow *(only in the knee joint and shoulder joint)*, and the other half used it for fluid outflow. No consensus exists about the choice of inflow- and outflow portal. Furthermore, two surgeons complained of a difficult-to-maneuver connection between the arthroscope and the sheath.

5.2 State of the art

To perform an arthroscopic operation safely and fast, an optimal view is mandatory.[1,2] According to Morgan[1] this can be established by a proper functioning of an optical system and an adequate joint distention. Irrigation systems that pump liquid through a joint during arthroscopic operations are designed for this purpose. The liquid pressure enlarges the available joint space by pushing surrounding soft tissue aside, while the liquid flow removes debris or blood. A clear view in a joint can thus be obtained and maintained. As indicated in Section 1.1 a complete irrigation system exists of a pump, an inflow tube, a scope-sheath combination, a joint, an outflow cannula and an outflow tube *(Figure 5.1.1)*. Two types of irrigation systems have been investigated in this project.[1,2,3,4] The so-called gravity pump *(GP)* is the first and most frequently used irrigation system. This system is open loop controlled and creates a pressure in the complete system due to the hydrostatic pressure difference between a fluid reservoir placed on a certain height and the joint to be operated *(Figure 5.2.1)*. The hydrostatic pressure difference is solely dependent on the height difference.[1,5] When the outflow portal is closed, the flow ceases and the pressure in the joint raises until the pressure gradient is zero.[1] Usually the gravity pump is used in combination with a separate suction device that removes blood and debris from the joint.

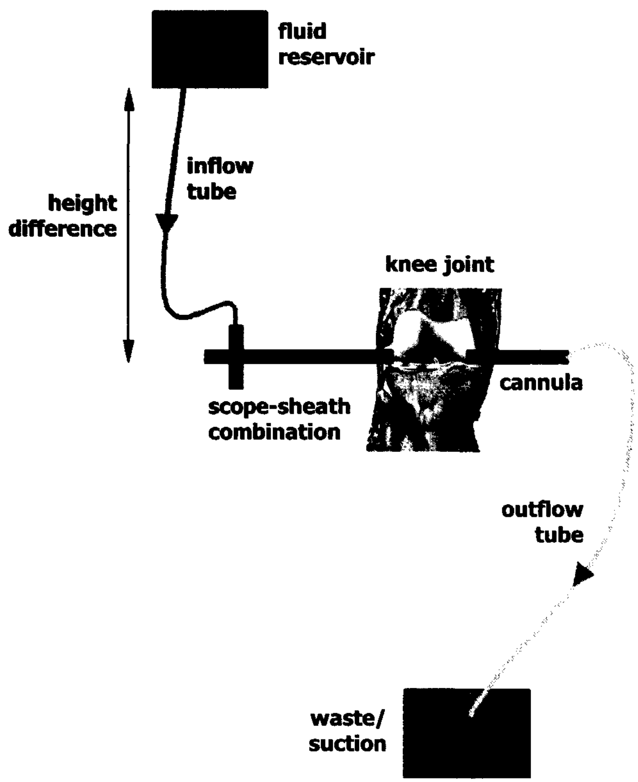

Figure 5.2.1 Schematic drawing of the complete set up in the operating room when using a gravity pump. Due to the difference in height between the fluid reservoir and the joint a pressure difference is generated that causes liquid to flow.

The second irrigation system is an automated pump *(AP)* that can create pressure differences with the help of a roller pump *(= volumetric, or peristaltic pump)* and is controlled by a feedback loop *(Figure 5.2.2)*. In the case of two roller pumps, a constant flow is generated when the two pumps rotate at the same speed, and the value of the flow is dependent on the rotational frequency. Pressure can be built up when the rotational frequency of the inflow roller pump is increased, and the rotational frequency of the outflow roller pump is decreased as opposed to the nominal speed. The impedance of the complete irrigation system determines how quickly the pressure is built up. The value of the pressure is dependent on the duration of the condition for which the roller pumps rotate at different speeds.

The automated pump is controlled by a feedback loop which configuration can vary per brand.[6] Due to the feedback loop automated pumps have the ability to keep the set pressure at a constant level. The pressure is measured at a certain location *(for example at the end of the inflow tube)* in the complete irrigation system. This signal causes the controller to adjust the pump's rotational frequency until the level of the measured pressure is the same as the set pressure. It is possible that the automated pump causes a joint to collapse, if the roller pump in the inflow tube receives pressure measured at a location that does not take into account all restrictions. The controller adjusts the rotational frequency until the pressure equals the sensor pressure. However due to the restrictions that are not included in the control loop the rotational frequency of the inflow pump could be to low to keep up with the rotational frequency at the outflow pump.

A number of these automated pumps has a control function for the flow. This is possible through the second roller pump in the outflow tube, of which the rotational frequency is controlled separately. This suggests that the flow can be controlled independently from the pressure. In Appendix 5A a survey is given of a number of automated pumps that are available on the market.

A number of remarks from literature regarding irrigation are summarized. Then several items important for irrigation are discussed. Substantial pressure gradients and flow rates are advantageous for three reasons: quicker irrigation of blood and debris, the intra-articular pressure may tamponade bleeding vessels, and fat pad or synovial tissue obstructing the visualization will be pushed away preventing unnecessary resection.[7] Optimal rinsing of the joint can be achieved by maximum inflow combined with fully open outflow cannula.[8] Oretrop and

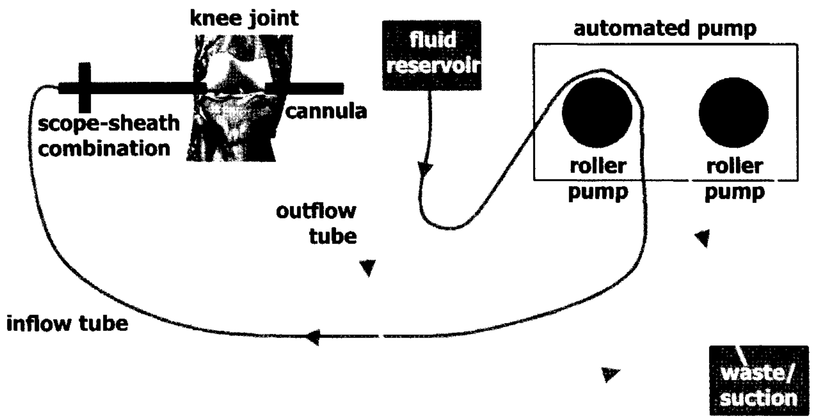

Figure 5.2.2
Schematic drawing of the complete set up in the operating room when using an automated pump. The roller pumps cause a liquid flow. By means of adjusting the rotational frequency of both roller pumps a pressure difference can be generated which is dependent on the restriction of the complete irrigation system.

Elmersson[8] have performed experiments with different diameters of the inflow tube and arthroscope. They found higher flow rates for larger diameters of tube and arthroscope. On the other hand, exceedingly high flow rates create turbulence that can interfere with the visualization.[1] Attention has to be paid when the shaver is used as outflow portal, since in this case the fluid outflow exceeds the capacity of inflow of the system which results in a negative fluid balance causing the joint to collapse.[1,7]

Choice of irrigation system

Advantages of a gravity pump are easy control, cheap and potentially safe. Advantages of an automated pump are the possibility to create more predictable and higher pressure differences and flows, with less risk of a negative fluid balance.[1] Two articles[2,3] present results of experiments done to compare a pump system with only pressure control and a pump system with pressure and flow control. Ogilvie-Harris and Weisleder[2] evaluated the pumps by determining the degree of visualization and technical ease, the degree of soft tissue extravasation *(subjective criteria)* and minimal operation time *(objective criterion)*. They found that using a pressure-flow controlled system reduces the operation time. Ampat et al.[3] used the presence of bleeding vessels, the visual clarity *(subjective criteria)* and the amount of blood loss *(objective criterion)* to compare the systems. They found no differences between the two pump systems for ordinary operations, but complicated and prolonged operations benefited from the more advanced pump system. Oretrop and Elmersson[8] point out that the flow- and pressure-regulating systems are not well understood by the surgeons, because most surgeons have a lack of mechanical engineering background to make optimally use of the irrigation systems.

Optimal intra-articular pressure

Gillquist et al.[9] first reported a minimal intra-articular pressure of 28 mmHg *(3.73 kPa)* for good visualization, because this should be enough to collapse the walls of arterioles and to prevent or to reduce bleeding.[7,8] This is supported by Ewing et al.[4] who measured the intra-articular pressure during 107 arthroscopic knee procedures. They attached a pressure transducer to one of the stopcocks of the scope-sheath combination which was placed in the outflow portal. The pressure was measured during the entire procedure, and the other stopcock of the sheath was only opened on surgical demand. They found that the intra-articular pressures ranged from 0 to 750 mmHg, but usually they were in the range of 70 to 120 mmHg. This latter pressure range was found to be necessary for consistent distention.[4] Bergstrom and Gillquist[7] report that when the outflow cannula is released the pressure never exceeds 60 mmHg. Care must be taken to avoid sudden changes of joint positions, this can cause pressure peaks in the knee, especially when the in- and outflow portals are closed.[1,4,7,10] The knee joint volume is namely greatest at 30° of knee flexion and is much less in extension or in flexion of 90°.[11] Therefore, Morgan[1] advises to operate with a fluid system that is never fully closed. Ewing et al.[4] state that the pressure is affected by a number of factors such as changes in leg position, opening and closing of inflow and outflow portals, and the insertion of tools, especially the shaver. In conclusion, the intra-articular pressure varies widely during a procedure and amongst procedures.[4]

Choice of in- and outflow portal

Two possibilities for the configuration of portals are suggested in literature, each having its advantages and disadvantages. The first configuration is inflow through the sheath that houses the arthroscope *(scope-sheath combination)*. In this manner tissue that obscures the arthroscope can be pushed away, and the direct visual field is cleaned most quickly.[7,10] Furthermore, it is unnecessary to create an extra portal, since outflow can take places through the sheath as well as the shaver.[1] The disadvantage is that the resistance of the sheath-arthroscope combination is very high and causes a significant drop in the flow rate. The second configuration is the use of a separate inflow cannula, and the use of the sheath or the shaver for outflow. The advantage is that higher flow rates can be achieved resulting in a quicker irrigation of the joint. However, this portal often becomes blocked off and can only be used in large joints, because in a smaller joint no possibility exists to create an extra portal.[1,7] Furthermore, outflow via the sheath of the arthroscope implies that all debris passes the visual field.[8] Most surgeons prefer to use the inflow via the sheath of the arthroscope.

Complications

There is always a risk of fluid extravasation.[10,12] Bomberg et al.[13] mentioned a complication rate of 1.4% from fluid extravasation during knee arthroscopy using a pump. Bergström and Gillquist[7] determined the amount of extravasation by measuring the inflow and outflow to the knee joint. They found that in 88% the discrepancy between in- and outcoming fluid volume was smaller than 500 ml under the assumption of no fluid leakage. Ogilvie-Harris and Weisleder[2] also measured the amount of extravasation, but they monitored at the end of the procedure if the patient had a certain amount of swellings. This is a rather subjective and not well quantifiable measurement. They concluded that the use of a more advanced irrigation system decreased the amount of swelling.

Patents

At least six patents *(A-F)*[6,14-18] cover the application of a complete irrigation system consisting of two roller pumps that are controlled via a pressure regulator. Patents B and F[14,18] have one pressure sensor in the inflow line and claim pressure and flow control. Patent F[18] has a three-way valve that can switch between two separate outflow lines. Patents A and E[6,17] also claim pressure and flow control, but their pressure sensors are located differently. For Patent A, this is inside the joint cavity, and for Patent E two sensors are placed, one in the inflow tube and the other in the outflow tube. The irrigation system, described in Patent C[15], controls the outflow with a valve that is controlled by a regulation circuit that receives a signal from a pressure sensor in the inflow tube. Patent D[16] presents a pneumatically driven irrigation system that develops a pulsatile flow, and it is controlled by a pressure regulator.

Other patents claim parts of an irrigation system: a connection of a tube to a pump[19], a special irrigation a tube with compliant sections to reduce variations in fluid pressure[20], tube set with two inflow lines to guarantee continuous flow[21], a new pressure sensor[22], a pressure regulation circuit[23], and a method to determine liquid loss during an operation[24].

Discussion and conclusions

In literature, little attention is paid to the irrigation of joints during arthroscopy. Articles covering the topic of the introduction of active irrigation pumps only give brief descriptions of the systems.[8] Other articles address topics as the choice of irrigation system, the optimal intra-articular pressure, complications, and the choice of in- and outflow portal.[1-3,7,8,10] From these articles no consensus can be derived on optimal conditions for irrigation as will be elucidated.
It can be concluded that an automated pump seems to have more potential in creating a good arthroscopic view, and reducing the risk of extravasation and potential damage to the surrounding soft tissues. Efforts are undertaken to improve the irrigation systems in order to be able to create higher pressure levels and flows. This is evident through the number of patents on irrigation systems.[6] Due to these efforts, the irrigation systems have become more complicated to operate[1], which is a serious problem for surgeons who are missing sufficient technical background.[8] It is for example indicated that a negative fluid balance can occur which can cause a joint to collapse[7], but no guidelines are given to overcome this.
Two options are suggested for the optimal intra-articular pressure.[4,7-9] Care has to be taken to avoid high pressure peaks, since these can cause complications.[1,4,7,10,12] Ewing et al.[4] have performed measurements of the intra-articular pressure during an operation. However, these measurements give only the actual intra-articular pressure in the joint when the outflow portal is closed. When the outflow portal is opened and fluid can flow through the complete irrigation system the scope-sheath combination, which is placed between the pressure transducer and the joint, gives a large pressure drop. Then, the pressure transducer no longer gives a correct measure of the intra-articular pressure. So far, it seems impossible to maintain the optimal intra-articular pressure with the gravity pump without a great number of actions, and it is unclear if the automated pump systems are capable to do so. Furthermore, during the experiment of Ewing et al.[4] the scope-sheath combination is placed in the outflow line, whereas a large number of surgeons uses the scope-sheath combination for inflow. It is also unclear how the pressure measurement takes place when suction is performed with the shaver.
Guidelines are missing for the prevention of the influence of some factors, for example the shaver suction. Lastly, it is unclear what combination of inflow and outflow portals *(including their locations)* is optimal, and it appears to be difficult to set up objective criteria to judge the quality of the arthroscopic view. In conclusion, insight in the behavior of irrigation systems and guidelines for usage of them, and the design of an optimal portal configuration are important steps to achieve optimal arthroscopic view.

5.3 Behavior of arthroscopic irrigation systems

This section is based on the article *Behavior of arthroscopic irrigation systems*, by G.J.M. Tuijthof, L. Dusée, J.L. Herder, C.N. van Dijk, P.V. Pistecky, which is submitted to the *Journal of Arthroscopy*.

Keywords: Arthroscopy, irrigation, intra-articular pressure, descriptive model, clinical experiments

Abstract: Purpose: In literature no consensus exists about optimal irrigation of a joint. The goal of this study is to gain better insight in the behavior of irrigation systems and to derive a number of guidelines to perform optimal irrigation. To this end, optimal irrigation is defined as the steady state of irrigation of a joint in which a sufficient positive intra-articular pressure and a sufficient flow are maintained. **Methods:** Firstly, a model is derived for the complete irrigation system consisting of a pump and restrictions. The main restrictions are the joint, the scope-sheath combination, the cannula, and the in- and outflow tube. With the help of this model a number of hypotheses is proposed. These were evaluated by clinical experiments during ten arthroscopic knee operations in which the pressure at different locations and the flow were measured for several conditions. **Results:** The clinical measurements indicate that the set pressure is always higher than the intra-articular pressure, which varies for different patients and conditions. It appears that the scope-sheath combination is the greatest fluid resistance. Therefore, the scope-sheath combination has the largest influence on the irrigation control. **Conclusions:** The predictions from the model were supported by the clinical results. More measurements are needed since there appeared to be a great variation in the results. Guidelines were derived for the performance of optimal irrigation.

Introduction

To perform an arthroscopic operation in a safe and fast fashion, an optimal view is mandatory.[1,2] According to Morgan[1] this can be established by a proper functioning optical system and adequate joint distention. Irrigation systems that pump liquid through a joint during arthroscopic operations are designed for this purpose. The liquid pressure enlarges the available joint space, while the liquid flow removes debris or blood, and pushes the surrounding soft tissue aside. A clear view in a joint can thus be obtained and maintained.

In the literature, only in the introduction of the field of arthroscopy and the introduction of active irrigation pumps articles address this topic.[1-4,7,8,10] No conclusions can be drawn on the optimal irrigation of joints in order to create a sufficient view.[1,4] This is probably due to the lack of mechanical understanding of the surgeons about the flow- and pressure-regulating systems.[8]

It has been determined that the creation of a clear overview in joints is frequently a problem.[25] The malfunction or complexity of irrigation systems makes them difficult to control, and it is unclear what the optimal intra-articular pressure should be, and whether or not it is possible to maintain it during the operation. In- and outflow of liquid into a joint often takes place through the same cannula, which results in a suboptimal irrigation of the joint. It is unclear what the optimal location of inflow and outflow portal should be. In addition, soft tissues like fat or

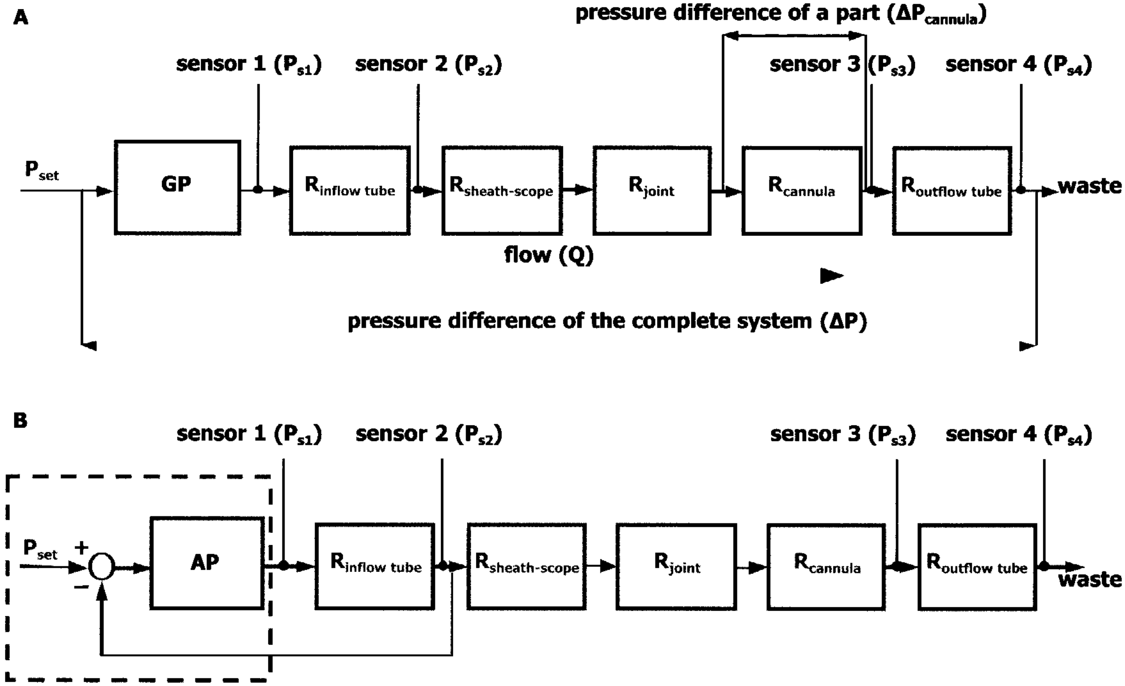

Figure 5.3.1
Model of the complete irrigation system. Two different pumps are modeled and were tested in clinical practice.
A) The gravity pump (GP) is an open loop controlled pump.

B) The automated pump (AP) is a close loop controlled pump for which the location of the pressure sensor depends on the type of automated pump.

The restrictions are located in serial order, and are the inflow tube ($R_{inflow\ tube}$), the scope-sheath combination ($R_{scope\text{-}sheath}$), the joint (R_{joint}), the outflow cannula ($R_{cannula}$) and the outflow tube ($R_{outflow\ tube}$). The liquid flows through the system from the pump to the waste. The pressure drops from the initial pressure to atmospheric pressure. Since the pressure sensors (sensor 1–sensor 4) are placed at an equal height, only hydrodynamic pressure drop takes place.

adhesions often impede the view at the operation field, especially in complex operations. The goal of our investigation is to derive a better insight in irrigation systems behavior and to derive guidelines for the performance of optimal joint irrigation. A model of the complete irrigation system is derived and quantitative measurements are presented of the behavior of the complete irrigation system for several conditions during arthroscopic knee operations. In addition to this, a simplified knee joint model that has been built to perform laboratory tests to optimize the joint irrigation was evaluated.

Methods

In Section A, a model of the irrigation systems is derived and predictions are performed with the help of this model. In Section B, measurements are performed with an experimental set up to determine a number of fluid restrictions, as well as measurements are performed in clinical practice to evaluate both the model and the experimental set up.

A. Derivation of a model

In order to be able to derive guidelines for optimal irrigation, it is defined as the steady state of irrigation of a joint in which a sufficient positive intra-articular pressure and a sufficient flow are maintained. Here, the steady state implies that a constant intra-articular pressure exists and that the fluid balance is in equilibrium. To define a model of the complete irrigation system a number of assumptions is made: minimal extravasation of fluid into the joint and fluid losses are negligible, restrictions are pressure independent, and only steady state conditions are considered. For the latter assumption, the pressure and flow are considered to be constant for a certain amount of time. This implies for example that the dynamic process of a joint enlarging into distention by liquid pressure is neglected, and only the joint's final state of distension is considered. With these assumptions, the complete irrigation system can be modeled as a pump and a number of restrictions which are the inflow tube *($R_{inflow\ tube}$)*, the scope-sheath combination *($R_{scope\text{-}sheath}$)*, the joint *(R_{joint})*, the outflow cannula *($R_{cannula}$)* and the outflow tube *($R_{outflow\ tube}$)* *(Figure 5.3.1)*. The pump and restrictions will be addressed in more detail. The pump creates a certain initial pressure at the beginning of the system. A flow will develop, its magnitude being dependent on the restrictions in the system. Due to the restrictions in the irrigation system the liquid pressure drops at each restriction according to:

$$\Delta P_i = Q \cdot R_i \qquad (5.3.1)$$

where ΔP_i is the pressure difference of a subsystem i, Q is the flow rate, and R_i is the fluid restriction of subsystem i. The pressure difference between the initial pressure and the pressure of the liquid at the end of the system is called the pressure difference of the complete system. The pressure difference of the complete system (ΔP) determines, together with the sum of all restrictions, Q according to the equation:[1,8]

$$Q = \frac{\Delta P}{\sum_{i=1}^{n} R_i} = \frac{\Delta P}{R_{inflowtube} + R_{scope-sheath} + R_{joint} + R_{cannula} + R_{outflowtube}} \qquad (5.3.2)$$

Notice that the pressure difference in this case is solely due to the occurrence of a flow. This is called the hydrodynamic pressure difference. When the pressure sensors *(Figure 5.3.1)* are placed at different heights an additional pressure component, called hydrostatic pressure difference, influences the total pressure difference. This latter component is solely dependent on the height difference between the sensors. The flow is the same at every location in the irrigation system. Only when the outflow is closed, the flow ceases, no hydrodynamic pressure drop takes place and the initial pressure will be maintained.[1] There exists only a hydrodynamic pressure drop if the flow is larger than zero. Furthermore, Eq. 5.3.2 shows that for a defined set of restrictions the flow can only be varied by variation of the pressure difference of the complete system. This implies that change of places of restrictions does not influence the magnitude of the flow of the liquid. However, this interchange can strongly influence the intra-articular pressure, because each restriction causes a different pressure drop dependent on its geometry. Consequently, if the restrictions before the joint are high, the pressure drop before the joint is high, which results in a low intra-articular pressure. If the restrictions before the joint are small, the pressure drop before the joint is low, which results in higher intra-articular pressure.

Pumps

Two irrigation systems are investigated in this project *(Section 5.2).*[1-4] The gravity pump *(GP)* is the first and most frequently used irrigation system *(Figure 5.2.1)*. The gravity pump is modeled as a block that sets a certain initial pressure level *(Figure 5.3.1)*. The second irrigation system is an automated pump *(AP)* that can create a flow with the help of one or two roller pumps *(Figure 5.2.2)*. The automated pumps are modeled as a gravity pump, but with an additional control loop *(Figure 5.3.1)*.

Seven conditions, characterizing important situations involving irrigation were investigated during ten arthroscopic operations *(Table 5.3.1)*. During these measurements the pressure at different locations and the flow were measured. Condition C2 using both types of pumps, and conditions C5 and C6 using only the gravity pump *(Table 5.3.1)* were considered with the help of the proposed model. Condition C2 is compared with C6 for which the standard situation of in- and outflow is inverted, since the choice of inflow and outflow configuration is one of the aspects for which no consensus was found.[1,2,7,8,10]

The pressure that is of most value for the surgeons is the intra-articular pressure. Ideally, an automated pump should therefore control this intra-articular pressure, and should therefore be measured by the automated pump, which is actually used in certain pumps for which a pressure sensor is introduced in the joint.[6] However, this appears practically difficult to conceive, because the sensor can become blocked or the controller can not respond to sudden pressure changes due to changing leg postions.[14,15,17,22,24] Therefore, the effect of the pressure sensing location of an automated pump is analyzed for condition C2.

Table 5.3.1
Seven conditions for which the pressure at different locations and the flow were measured during ten arthroscopic operations. Two different pumps, a gravity pump (GP) and an automated pump (AP), were used. Their pressure levels differed and therefore are indicated explicitly. C1-C3 represent the standard situation with increasing initial pressure, for which inflow takes place through the scope-sheath combination and outflow through a separate cannula. C4 represents the standard situation added with the usage of a probe or a punch, whereas C5 represents the standard situation except that the shaver is used as outflow instead of the separate cannula. C6 represents the inverted standard situation for which the inflow takes place through the separate cannula and outflow through the scope-sheath combination. C7 is the condition for which a bleeding occurs independently of the settings of the irrigation system.

condition	set pressure	inflow portal	outflow portal	instrument
C1	Low: GP 10 mmHg AP 79 mmHg	scope-sheath	cannula	none
C2	Normal: GP 51 mmHg AP 113 mmHg	scope-sheath	cannula	none
C3	High: GP 150 to 250 mmHg AP 146 mmHg	scope-sheath	cannula	none
C4	Normal: GP 51 mmHg AP 113 mmHg	scope-sheath	cannula	probe or punch
C5	Normal: GP 51 mmHg AP 113 mmHg	scope-sheath	shaver	shaver
C6	Normal: GP 51 mmHg AP 113 mmHg	cannula	scope-sheath	none
C7	Occurrence of a bleeding Any pressure level	scope-sheath or cannula	scope-sheath or cannula	probe, shaver, punch or none

Practical values for the restrictions

For the parts of the irrigation system used in the operating room *(in- and outflow tube, scope-sheath combination, and outflow cannula)* the specific pressure drop at a certain flow was determined in the laboratory. The pressure difference was measured by two pressure sensors that were attached at the beginning and at the end of the in- and outflow tube, the scope-sheath combination, and the cannula, respectively. The pressure measured at the beginning was compensated for its hydrostatic pressure difference with the sensor placed at the end. The flow was measured by weighing the mass of fluid using a pair of scales for a certain time. The volume was calculated by means of the fluid's density.

It was determined for each part whether the flow is laminar or turbulent, since this will indicate if the pressure difference is proportional to the flow or to the squared average velocity. This was performed with a the help of the Reynolds number:[5,26]

$$Re = \frac{v_{average} \cdot D}{v} \qquad (5.3.3)$$

where Re is the Reynolds number, $v_{average}$ is the average velocity which is calculated by dividing the flow by the cross-section of a part, D is the inner diameter of a part, and n is the kinematic viscosity of the fluid, which is considered to be constant for these measurements. The sheath-scope combination has an annular cross section. The Reynolds number can still be calculated, but the diameter must be substituted by the hydraulic diameter, which is defined as 4 times the cross-sectional area divided by the wetted perimeter.[5] A rule of thumb is that the flow is laminar, if the Reynolds number is less than 2300. If this is the case the pressure difference is proportional with the flow and the restriction can be calculated with the help of Poiseuille's law:[1]

$$R = \frac{\Delta P}{Q} = \frac{128 \cdot \eta \cdot L}{\pi \cdot D^4} \qquad (5.3.4)$$

where R is the fluid restriction, η is the dynamic viscosity, and L is the length of the part. It can be concluded that the diameter has the greatest influence on the value of the fluid resistance *(Eq. 5.3.4)*, because this is the parameter having the highest power in the equation. If the flow is turbulent *(Re > 2300)* another relation is valid:[5,26]

$$\Delta P = f \cdot \rho \cdot v_{average}^2 \qquad (5.3.5)$$

where f is a constant factor which depends on the tube's geometry and fluid characteristics, and ρ is the density. The factor f cannot be theoretically calculated, but can be derived with the help of experiments in the laboratory in which the pressure difference is measured simultaneously with the flow for each subsystem. To be able to compare the restrictions of all parts, a linear regression was determined with the help of measurements performed in the laboratory and in clinical practice. Oretrop and Elmersson[8] carried out experiments with varying scope diameters and found that higher flows occurred for increasing scope diameter. Thus, it is expected that the scope-sheath combination gives the highest restriction, since its diameter is the smallest in comparison with the other subsystems.

The fluid restriction of a live joint, e.g. the knee joint, cannot be determined easily in the laboratory or in the operating room. Furthermore, experiments to optimize irrigation, and measurements of the intra-articular pressure can be obtained from a physical joint model, in case this joint model has the same restriction as the average knee joint. For this purpose, a physical joint model was constructed that has approximately the same dimensions *(diameter is 95 mm and distension varies from 6 mm to 12 mm)* and the same volume *(64 ml, unpressurized)* as a knee joint[8] *(70 to 90 ml, when pressurized)*. To evaluate this joint model, its restriction was determined in the laboratory, whereas the intra-articular pressure and restriction of the knee joints were roughly estimated from measurements during operations. With the help of Figure 5.3.1 the intra-articular joint pressure can be estimated. In practice, Sensor 2 and Sensor 3 *(Figure 5.1.1)* are not located directly before the sheath and after the cannula, but in the inflow tube and outflow tube, respectively. Therefore, the fluid restrictions of part of the inflow tube and outflow tube have to be taken into account as well. Starting at the inflow side the intra-articular joint pressure *(P_{jointa})* is then estimated with:

$$P_{jointa} = P_{s2} - \Delta P_{inflowtube}(\rho \cdot v^2_{average}) + \Delta P_{scope\text{-}sheath}(Q) \qquad (5.3.6)$$

where P_{s2} is the actual pressure measured at Sensor 2 *(as located in the operating room)*, $\Delta P_{inflowtube}$ is the pressure drop of the inflow tube part between Sensor 2 and the scope as function of $\rho v^2_{average}$, $\Delta P_{scope\text{-}sheath}$ is the pressure drop of the scope-sheath combination as function of the flow. Both functions relate to the linear curve that was determined with the help of the laboratory measurements. Starting at the outflow tube the intra-articular joint pressure *(P_{jointb})* can also be estimated with:

$$P_{jointb} = P_{s3} + \Delta P_{outflowtube}(\rho \cdot v^2_{average}) + \Delta P_{cannula}(\rho \cdot v^2_{average}) \qquad (5.3.7)$$

where P_{s3} is the actual pressure at Sensor 3, $\Delta P_{outflow\ tube}$ is the pressure drop of the tube part between Sensor 3 and the outflow cannula as function of $\rho v^2_{average}$, and $\Delta P_{cannula}$ is the pressure drop of the cannula as function of $\rho v^2_{average}$. From Eqs 5.3.6 and 5.3.7, the intra-articular pressure can be calculated as the average of $P_{joint\ a}$ and $P_{joint\ b}$. The fluid restriction of the patient's knee joints is calculated as the difference between $P_{joint\ a}$ and $P_{joint\ b}$, for which in this case the pressures at Sensors 2 and 3 are compensated for the hydrostatic differences.

In the laboratory, the complete irrigation system using the joint model was built for both types of pumps. A difference with clinical practice was that in the laboratory no separate suction device was available to test it in combination with the gravity pump. For two patients operated with the automated pump the exact settings *(pressure sensors placed at the same height as in the operating room)* were rebuilt in the laboratory using the joint model for which C1-C3 were tested. This was done as an additional test to validate the restriction of the joint model.

B. Set up of clinical experiments

Measurements were conducted during arthroscopic knee operations to analyze the pressure difference of the complete irrigation system and its parts as well as the flow for several situations. Ten patients were involved in this experiment. Six were male, and four were female; the age ranged from 21 to 57 with a mean of 38.6 years. There were four meniscectomies, four diagnostic knee operations, and two arthroscopies for treatment of osteochondral defects. Six patients were operated with a gravity pump, and four with an automated pump *(FMS Duo+©, Arsis Medical BV, De Bilt, The Netherlands) (Figure 5.1.1)*. During the operations with the gravity pump, the outflow tube was connected to a suction device that was set at a constant pressure of -500 mmHg *(33.5 kPa)*. For the experiments the atmospheric pressure *(100 kPa)* was namely chosen as the 0 mmHg level. Through this definition, it was possible that negative pressure can occur. In cases in which an instrument was used the outflow tube of the gravity pump was usually fully closed and outflow took place via leakage alongside the portals.

During an operation the pressure in the complete system was measured at four locations, namely directly underneath the fluid bag when using the gravity pump and directly after the roller pump when using the automated pump *(Sensor 1)*, in the inflow tube as close as possible to the scope-sheath combination *(Sensor 2)*, in the outflow tube as close as possible to outflow cannula or shaver *(Sensor 3)*, and at the end of the outflow tube *(Sensor 4) (Figures 5.1.1 and 5.3.1)*. Sterile pressure sensors *(pressure monitoring kit, Baxter Healthcare Corporation, USA)* were used, since these were easy to use and the accuracy should be enough for this experiment. The pressures measured in the operating room appeared to be significantly more negative than those measured in the laboratory, and were often so low that they dropped below the calibrated range of the pressure sensors. To be sure that the values that were measured were correct, the sensors were calibrated in a range including the large negative pressures, and were found to perform correctly and linearly. The pressure was measured for each condition for a certain amount of times. The pressure signals were recorded by a data acquisition system with a sample frequency of 100 Hz. The flow was measured by measuring the weight of the fluid bag as a function of time using a pair of scales and a stopwatch. Seven conditions were measured for each patient when possible *(Table 5.3.1)*. During each measurement the conditions remained the same.

The average pressure and the standard deviation were calculated for each sensor and measurement. Following this, the average pressure and standard deviation of all measurements of the same condition were calculated for the two pumps. No further statistics were applied, since the aim was to look at trends for several conditions and the number of measurements was too low. To be able to compare the results of the patients, the measured pressures were

Table 5.3.2.
Data of the subsystems of the gravity pump (GP) and FMS duo+ pump (AP) are presented in column one. The length, diameter and Reynolds number can be found in the consecutive columns. As can be seen, only for the scope-sheath combination is a laminar flow present. The proportional factor f between ΔP and $\rho v^2_{average}$ (for turbulent flow), proportional factor R between ΔP and Q (for laminar flow) are given. Lastly, the pressure difference of each subsystem for the average flow, which is calculated from the flows measured during ten operations (98 ml/min), is given. This way the fluid restrictions of the subsystems can be compared. The difference in pressure between inflow and outflow tube of the gravity pump is due to the fact that there are two constrictions in the inflow tube that cause extra resistance.

item	L (m)	D (mm)	Re	f (mmHg·ms²/kg)	ΔP (mmHg
inflow tube GP	2.07	7	3000	0.3721	0.7
outflow tube GP	2.94	7	7000	0.0755	0.1
inflow tube AP	2.59	3.5	3200	0.0786	2.3
outflow tube AP	3.09	5	3300	0.1312	0.9
cannula	0.095	5	9200	0.0055	0.06
		$D_{hydraulic}$ (mm)		R (mmHg·s/m³)	
scope-sheath combination	0.135	0.5	250	$5 \cdot 10^7$	80

compensated for hydrostatic differences. The suggestion is given for C4 using the gravity pump to correct the pressures measured at Sensor 3 to atmospheric pressure, and discard the pressure of Sensor 4, since in this case the outflow tube is blocked and outflow takes place by leakage alongside the portals where the atmospheric pressure exists Thus, in this case, the pressure measured at Sensors 3 and 4 has no relation with the actual irrigation process. The correction was performed in the remainder of this Section.

Results

A. Predictions derived from the model

The pressure differences that were measured in the laboratory at a given flow for each part of the irrigation system are presented in Table 5.3.2. The scope-sheath combination gives the highest pressure difference for the same flow, which is due to its small cross-section *(Table 5.3.2)*.

The results of the predictions derived with the model of the complete irrigation system are shown in Figure 5.3.2. As can be seen, the pressure drops at each subsystem, and will be equal to the atmospheric pressure at the end of the outflow tube. The intra-articular pressure is lower than the initial set pressure due to the pressure drops along the subsystem *(Figure 5.3.2)*.

The interchange of inflow portal has a significant effect on the intra-articular pressure, due to the higher fluid restriction of the sheath-scope combination in comparison to the fluid restriction of the cannula *(Table 5.3.1 and Figure 5.3.2: C2 and C6)*. When a shaver is used, suction takes place at the outflow tube *(Figure 5.3.2: C5)*. Due to the suction the pressure difference of the complete system will be enlarged, which results in a higher flow, but also in a larger pressure drop at each part of the system. The suction causes a lower intra-articular pressure in comparison with C2, assuming that the initial pressure of the pump remains the same.

It can be seen that there is a difference in the pressure course for C2 A and C2 B using the automated pump *(Figure 5.3.2)*. C2 A has a relatively small positive effect on the value of intra-articular pressure, since there is still a large pressure drop before entering the joint due to scope-sheath combination, which is not included in the control loop. In C2 B the restriction of the scope-sheath combination is included in the control loop as is the joint and this results in an intra-articular pressure that is close to the desired initial set pressure.

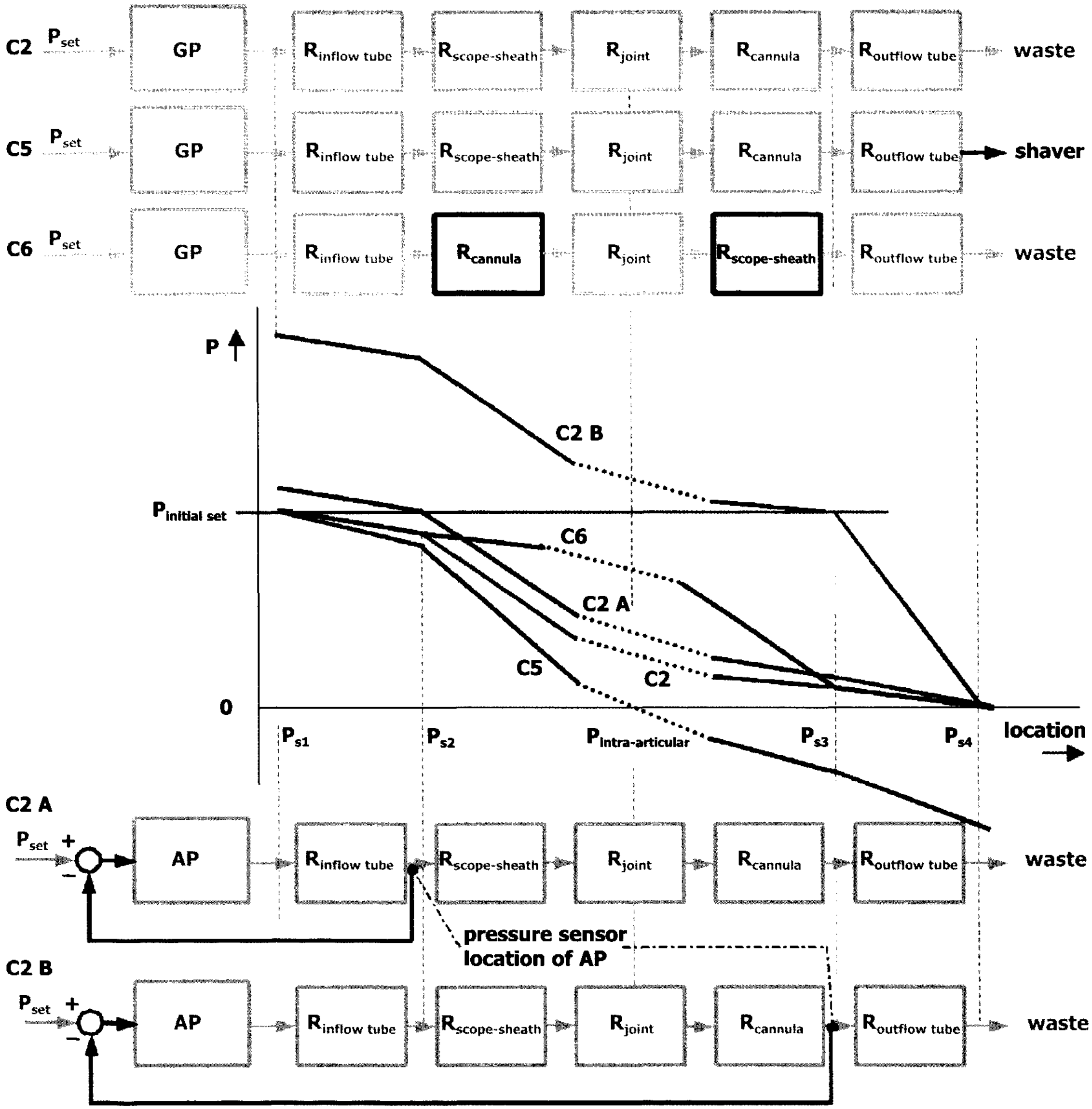

Figure 5.3.2
Pressure course passing through the complete irrigation system for different configurations: C2, C5, C6 using the gravity pump and C2 for two types of automated pumps as indicated in Table 5.3.1. At C2 A the pressure sensor of the pump is located before the scope-sheath combination, and at C2 B the pressure sensor of the pump is located after the cannula. For good comparison it is assumed that for C2 A and C2 B inflow takes place through the scope-sheath combination. For each condition the predicted pressure course is given, which is derived with the help of the practical values for the restrictions. Since the restriction of the knee joint is only estimated, the parts of the graphs indicating the pressure drop for the knee joint are shown by dotted lines. The intra-articular pressure is indicated as well, since this is the important pressure to know, and the initial set pressure is given, because this is the pressure that is set by the surgeon.

B. Measurements in the operating room

Only a few bleedings occurred during the ten operations, which made it not possible to draw conclusions regarding the irrigation system behavior or surgeon's actions for C7. The results of all patients could not be presented in one graph because the flow differed during each procedure. Therefore, the pressure measurements compensated for their hydrostatic differences of one patient for each of the two pumps are shown *(Figures 5.3.3, and 5.3.4)*. The standard deviation for the sampled pressure measurement per sensor is very low *(2 mmHg or less)*, except for Sensor 3 using the automated pump *(1 to 87 mmHg)*. Not all conditions occurred during an operation. Furthermore, for C1-C3, and C6 usually just one measurement was performed per operation. Therefore, the results should be interpreted with care.

The pressures in most cases ranged from -250 mmHg to 200mmHg. The pressure course show a decreasing trend *(Figures 5.3.3 and 5.3.4)*, as was also predicted by means of the model. In Figure 5.3.3, the pressure does not decrease between Sensor 1 and 2, which is probably due to malfunction of Sensor 1. In Figure 5.3.4, the pressure increases between Sensor 3 and 4, which could be due to the working mechanism of the pump that causes large pressure oscillations *(standard deviations up to 87 mmHg)*. The largest pressure drop occurs between Sensor 2 and 3 for all measurements. This is also in agreement with the predictions derived from the model, since the subsystems located between these sensors are the scope-sheath combination, the knee joint and the separate cannula of which the scope-sheath combination causes the largest pressure drop. This indicates that the intra-articular pressure in clinical practice is also lower than the initial pressure. All pressure measurements of Sensor 4 are negative due to the suction at the outflow tube when using the gravity pump *(Figure 5.3.3)*.

The results of experiments performed in the laboratory with the knee joint model using the gravity pump and automated pump *(Figures 5.3.5 and 5.3.6)* are more consistent. The missing suction device in the laboratory setting clarifies some of the differences between the measurements performed with the gravity pump on patients and on the joint model. The results of the measurements performed on two patients for which the exact settings were rebuilt in the laboratory are shown in Figures 5.3.7 and 5.3.8.

In Table 5.3.3, the estimations are presented for the intra-articular pressure per condition and per patient calculated with the help of Eqs 5.3.6 and 5.3.7. Since the fluid restriction of the shaver was not determined, $P_{joint\ b}$ could not be calculated for C5. The measurements of Sensor 3 were only used for the calculations if their values were higher than –250 mmHg. If the pressure is negative using the gravity pump, the outflow tube is squeezed due to the suction, which changes the cross-section of the tube. The variation of the intra-articular pressure in the human knee joints during an operation is large, but trends can be indicated. The intra-articular pressure appears to be higher when the separate cannula is used as inflow portal *(C6)* in comparison with the scope-sheath combination as inflow portal *(C2)*. The adjustment of the initial set pressure seems to have little effect on the intra-articular pressure *(C1-C3)*. When using the gravity pump the initial starting pressure seems to be too low *(C2)*.

The estimated pressure difference of the knee joints and the joint model, as function of the flow, is presented in Figure 5.3.9. There is no consistency in the results, all patients had a different

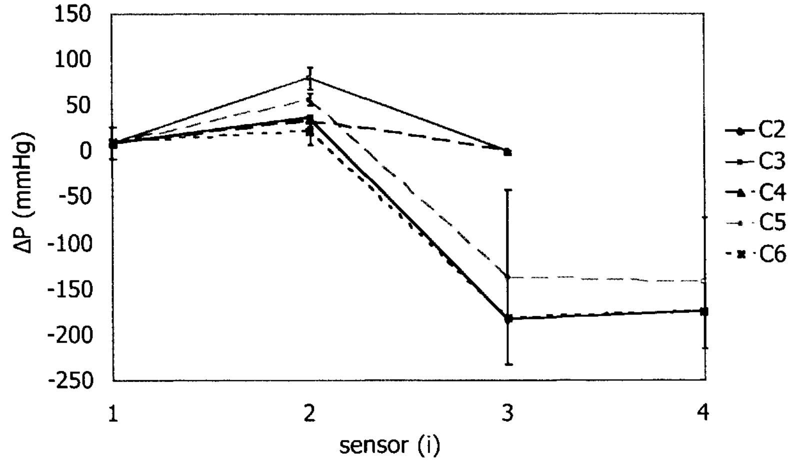

Figure 5.3.3
The hydrodynamic pressure components of the pressure measured during the operation of one patient using the gravity pump (GP) for five conditions (Table 5.3.1). For several conditions the outflow took place via leakage along the portals, whereby the measurements of Sensor 3 and 4 have no meaning and the pressure in the atmosphere is 0 mmHg, as can be seen in the graph. The average flow was 62 ml/min.

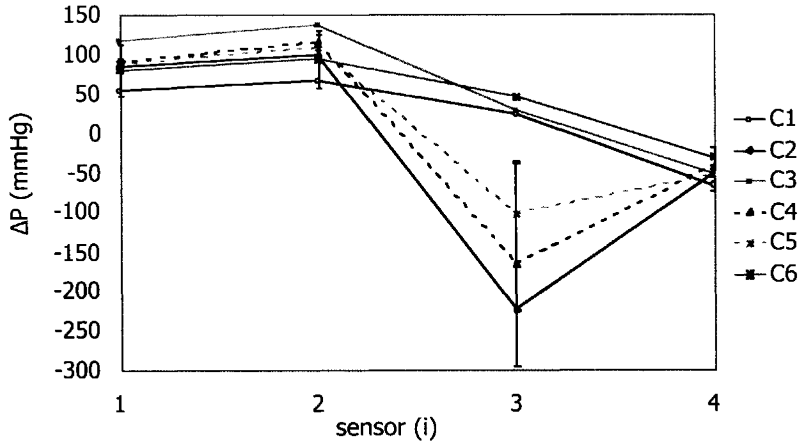

Figure 5.3.4
The hydrodynamic pressure components of the pressure measured during the operation of one patient using the automated pump (AP) for six conditions (Table 5.3.1). The average flow is 114 ml/min.

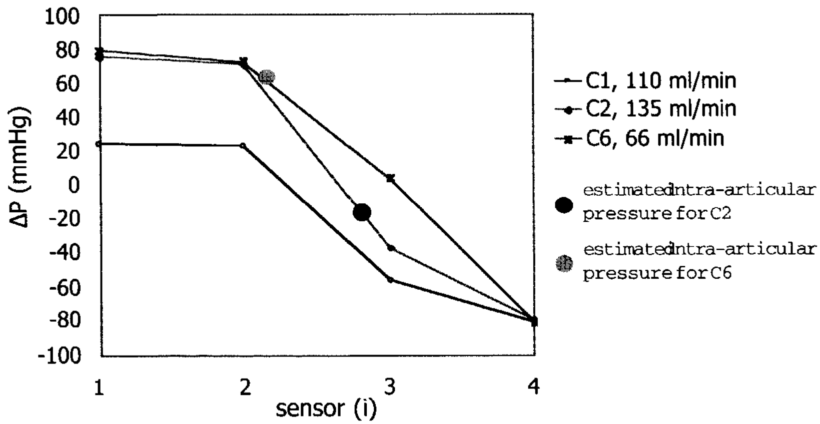

Figure 5.3.5
The results of the pressure measurements done in the laboratory using the gravity pump without separate suction device for C1, C2, and C6 (Table 5.3.1). It can be clearly seen that a higher initial pressure causes a larger pressure drop for each subsystem. Furthermore, when the scope-sheath combination is used as outflow the intra-articular pressure (C6) is significantly higher than the standard situation (C2).

Figure 5.3.6
The results of the pressure measurements done in the laboratory using the automated pump for C1,C2, and C3.

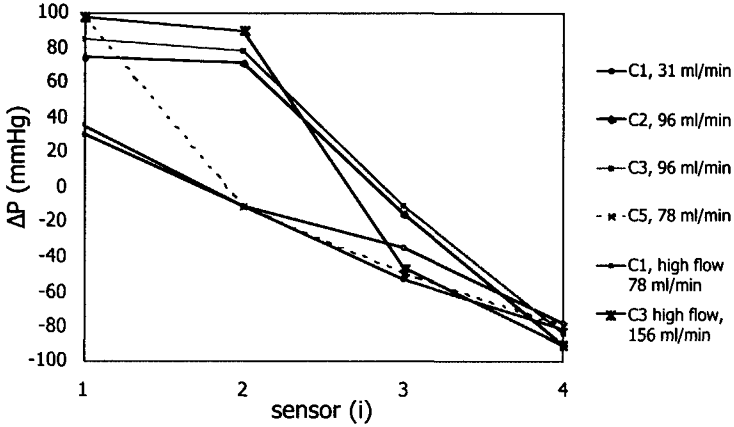

Figure 5.3.7
Pressure measurements of Patient 7 (AP) vs. pressure measurements done in the laboratory with the knee joint model using the same tubes, and the sensors were placed at the same heights as in the operating room.

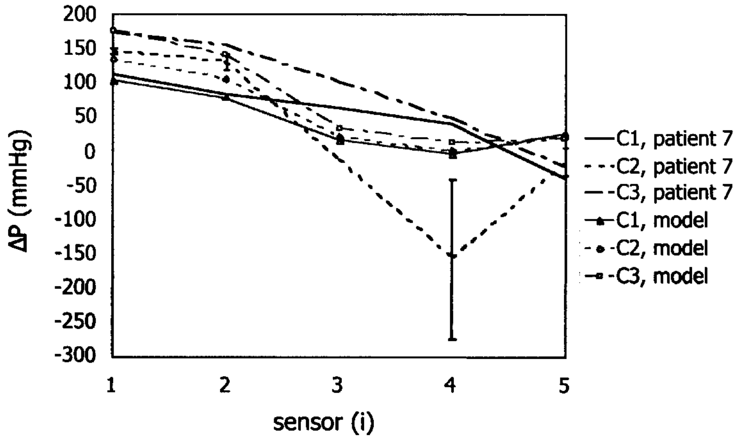

Figure 5.3.8
Pressure measurements of Patient 8 (AP) vs. pressure measurements done in the laboratory with the knee joint model using the same tubes, and the sensors were placed at the same heights as in the operating room.

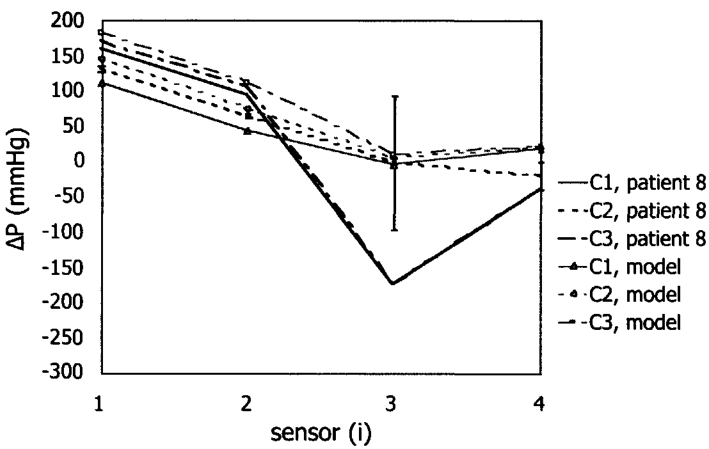

condition	C1		C2		C3		C4		C5		C6	
patient	$P_{joint\ a}$	$P_{joint\ b}$	$P_{joint\ a}$	$P_{joint\ b}$	$P_{joint\ a}$	$P_{joint\ b}$	$P_{joint\ a}$	$P_{joint\ b}$	$P_{joint\ a}$	$P_{joint\ b}$	$P_{joint\ a}$	$P_{joint\ b}$
GP p1			-8		**38**	**0**	**-12**	**0**	**1**		**28**	**0**
GP p2	-18	-9	-78	-9	22	-9					**109**	**125**
GP p3					72	0	**84**	**0**	**31**			
GP p4	**-96**		3	19			**7**	**0**				
GP p5			**-124**				**-149**	0				
GP p6			**-33**		**95**	**0**	**50**	**0**				
Average	**-41**		**-33**		**26**		**-2**		**16**		**66**	
SD	**48**		**51**		**38**		**60**		**21**		**61**	
AP p7			5	11			**39**	**1**	**52**		**126**	**66**
AP p8	-13	42	3		50	48	**42**		**-113**		112	149
AP p9	35		**38**	**35**	46		**-1**	**49**	**-74**		53	59
AP p10	-32		-7		45		7					
Average	**4**		**12**		**45**		**21**		**-45**		**94**	
SD	**42**		**21**		**7**		**25**		**86**		**40**	

Table 5.3.3
The estimation of the intra-articular pressure (mmHg) in the joint is given for each condition (Table 5.3.1) and each patient separately. Six patients (p1-p6) were treated while using a gravity pump (GP), and four patients (p7-p10) were treated with an automated pump (AP). A number of estimations could not be determined. The values that are marked boldly are the average values of a number of measurements.

restriction. The estimations and measurements determined for the restriction of the joint model are in the same range as the human knee joints.

Discussion

The definition of optimal irrigation indicates two items that are important for the surgeon to take into account: intra-articular pressure, and irrigation flow. These two items will be discussed for portal choice, shaver usage, and type of irrigation system, resulting in the definition of guidelines.

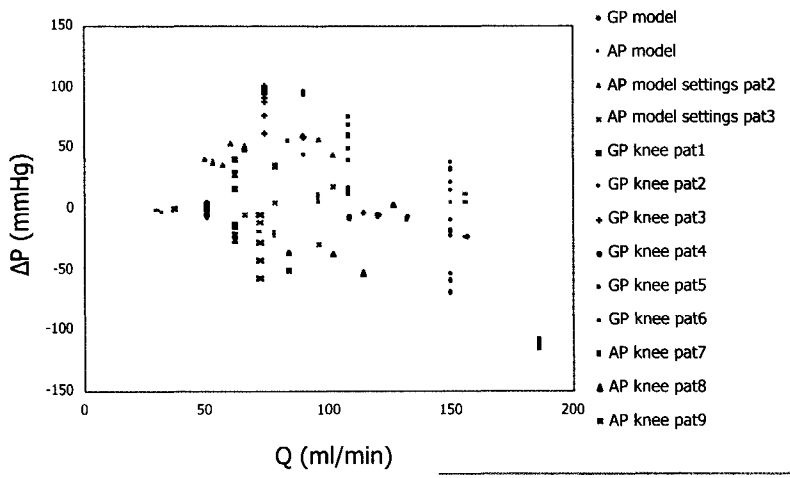

Figure 5.3.9
Estimations of the pressure drop along the knee joints of all patients (black) vs. estimations of the pressure drop along the knee joint model (gray). As can be seen the pressure drop along the knee joint model lies in the range as the human knee joints.

Intra-articular pressure

Ewing et al.[4] have performed measurements of the intra-articular pressure during an operation. They derived that the pressure measurement only equals the intra-articular pressure if the outflow portal is closed and there is no flow. Our results show that if there is indeed a flow, the intra-articular pressure is never the same as the desired initial set pressure *(Figures 5.3.2-5.3.8)*, because the pressure decreases at each restriction. The intra-articular pressure is affected by a number of factors: changes in leg position, opening and closing of inflow- and outflow portals, and instrument and shaver usage.[4] We found that the use of an instrument *(Figures 5.3.3 and 5.3.4)* has little effect on the intra-articular pressure, as well as a change in the initial set pressure of a pump *(Figures 5.3.3 and 5.3.4, Table 5.3.3)*. The latter result is probably due to the fact that in the case of using the gravity pump the suction at the outflow tube is too large.

Portal choice

According to the literature, most surgeons prefer to use the inflow via the scope-sheath combination.[1,7,10] When a separate cannula is used as inflow portal, this often becomes blocked off, debris has to pass the visual field, and a separate cannula can only be used in large joints.[1,7,8] The fact that the debris has to pass the visual field can actually be an advantage, since the debris does not have to travel through the joint before it is removed, moreover it allows the surgeon to monitor the suction and complete removal of debris. From the model and the experiments, it is concluded that using the cannula as inflow portal results in a higher intra-articular pressure than when the scope-sheath combination is used as inflow portal *(Figures 5.3.2-5.3.5, Table 5.3.3)*. This is due to the fact that the restriction of the outflow cannula is about 65 times lower than that of the scope-sheath combination *(Table 5.3.2)*, and therefore cause a much smaller pressure drop.

Shaver usage

Our results verify that if the suction pressure is too high there is a risk that the intra-articular pressure drops below the minimally required level or that even the joint could collapse *(Figures 5.3.2-5.3.4, 5.3.6 and Table 5.3.3)*.[1,7,8]

Type of irrigation system

Oretrop and Elmersson[8] state that an irrigation system should match the following criteria: insert fluid directly into visual field, and high flow in combination with adequate joint distention. When using the gravity pump, the intra-articular pressure is not known by the surgeon. However, the surgeon could derive an estimation of the intra-articular pressure if he knows the value of the restrictions placed in the inflow. Considering the results from the experiments this estimation would be inaccurate and of no use. When an automated pump is used the initial set pressure is maintained within a smaller range. However, it is essential to know the pressure sensing location to control the intra-articular pressure in an optimal way, especially when the large restriction of the scope-sheath combination is placed before the joint *(Figure 5.3.3)*.

Irrigation
According to the literature, increasing the initial pressure results in higher flows, which is advantageous for three reasons.[7] Oretrop and Elmersson[8] state that optimal rinsing of the joint can be achieved by maximum inflow combined with fully open outflow cannula. To increase the flow, the pressure difference of the complete irrigation system has to be increased *(Eq. 5.3.1)*, which can be done by increasing the initial set pressure or by suction at the outflow tube *(Figures 5.3.2-5.3.8)*. Suction at the outflow bears the risk that the intra-articular pressure can become negative which could lead to joint collapse.[1,7] The automated pump *(AP)* has the ability to control the pressure measured at the location of the sensor while increasing the flow *(Figure 5.3.6)*, however a higher flow can also achieved by increasing the pressure difference of the complete irrigation system. Usage of an automated pump with independent flow control can also lead to joint collapse as the results show *(Figure 5.3.4)*. Another option to increase the flow is to decrease the fluid restrictions of the irrigation system. Since, the scope-sheath combination has the largest restriction it will be profitable to reduce the value of this restriction, by the design of a new sheath.

Validation of joint model
It appears from Figures 5.3.7 and 5.3.8 that there are differences between the pressure curves of the patients and the joint model. The measurements in the operating room show larger variations, which can be caused by blocking of the outflow cannula, disturbances due to manipulation of the knee, or a significantly different volume of the knee joint in comparison to the joint model. In some patients, the estimation of the fluid restriction shows a negative value *(Figure 5.3.9)*, which is physically impossible, and could be due to the fact that the estimation was calculated with an averaged flow per patient. Knowing that the estimations of the fluid restrictions are not very accurate, it can however be concluded that the restriction of the joint model is in the same range as that of the human knee joints *(Figure 5.3.9)*. This justifies the use of the joint model for the purpose of optimizing the joint irrigation.

Guidelines
For the gravity pump it is advised to use a separate cannula as inflow portal, because in this configuration the intra-articular pressure will be approximately the same as the initial set pressure. However, for increasing set pressures, the intra-articular pressure will deviate more from the set pressure because of the increasing flow. The intra-articular pressure can be best adjusted by changing the height of the fluid reservoir. It is advisable to start with a low suction level when using a separate suction device. When more suction is necessary, the suction level and the height of the fluid reservoir need to be increased together in order to avoid joint collapse. Another possibility to avoid joint collapse is to manually open and close the outflow portal intermittently by means of a clamp placed at the outflow tube. It was observed that this latter is performed in daily practice for which every surgeon uses its own strategy.
Usage of an automated pump will take fewer actions to achieve sufficient irrigation and the set pressure level is more accurate. When an automated pump is used for which the pressure sensor is located directly after or in the joint while the scope-sheath combination is used as inflow

portal, the intra-articular pressure will be close to the desired initial set pressure of the pump. In this case, the fluid balance is in equilibrium and there is less risk of joint collapse. If the pressure sensor of the automated pump is located in the inflow tube, it is best to use this pump in combination with the separate cannula as inflow portal. Since, cannula causes a relative small pressure drop, which allows the intra-articular pressure to be close to the initial set pressure of the pump.

Conclusions

Our results show that the manner in which the fluid restrictions of the subsystems of an irrigation system are connected, and the location of the pressure sensor of automated pumps greatly influence the intra-articular pressure. The scope-sheath combination has the largest influence on the irrigation control, because of its large restriction. For the gravity pump it is advised to use the separate cannula as inflow portal, and to start with a low suction level when a separate suction device is used. For the automated pump it is advisable to determine the location where the pressure sensor is located to control the pump. Once this is known, a decision can be made to use either the sheath-scope combination or the cannula for inflow. Lastly, it will probably take fewer actions to obtain optimal irrigation control when an automated pump is used. Measurements performed in the laboratory show more consistent results than the measurements performed on patients. The joint model was validated, and it was determined that its fluid restriction is in the range as those of the human knee joints. For an accurate estimation of the restriction of human knee joints it is best to use a gravity pump with outflow in the atmosphere.

5.4 Development of a sheath for arthroscopy

This section is based on the article *Development of a sheath for arthroscopy*, by G.J.M. Tuijthof, J.L. Herder, C.N. van Dijk, P.V. Pistecky, which will be submitted to the *Journal of Arthroscopy.*

Keywords: sheath, flow patterns, experiments, arthroscopy, joint model

Abstract: Purpose: Development of an arthroscopic sheath to improve the joint irrigation for two-portal and three-portal techniques. **Methods:** A simplified joint model was constructed consisting of two circular glass plates positioned parallel to each other. With this model simulations were performed to determine the influence of pressure, flow rate, bleedings, choice of inflow and outflow portals, inflow direction, and the shape of the model on irrigation. This lead to the set up of design criteria for a new sheath. In this device, the inflow and the outflow should take place through separate passages, the diameter of inflow and outflow should be as large as possible, and the inflow should be directed towards the center of a joint. **Results:** A new sheath was designed with a partition that can separate inflow- and outflow taking place through the sheath *(two-portal technique)*. The partition can also be removed to allow only inflow or outflow *(three-portal technique)*. The new sheath was evaluated in a cadaver setting to validate the joint model. **Conclusions:** The new sheath improves irrigation of joints during arthroscopic operations due to its lower fluid restriction, and the addition of a partition in the sheath by which in- and outflow takes place through separate passages. This enables higher flows which results in a quicker cleaning of a disturbed arthroscopic view.

Introduction

To perform an arthroscopic operation safely and fast, an optimal view is mandatory.[1,2] One of the main aspects is the clarity of the view. To accomplish a clear view during arthroscopic procedures the joint is irrigated with liquid that removes debris and blood. However, from our observations during arthroscopic operations it is observed that maintaining a clear view is often difficult due to the following problems: soft tissue in front of the scope[10], suboptimal flow pattern when using a two-portal technique where in- and outflow takes place through a single cannula, inadequate use of irrigation systems which delays the irrigation, and large pieces of debris that cannot be removed without withdrawing the arthroscope.[25] In addition to this, it was determined from prior research that the pressure drop along the scope-sheath combination is considerable, which makes it difficult to control the pressure in a joint during an operation and increases the risk on joint collapse *(Section 5.3).*

In literature, no requirements were found for the design of a sheath or cannula, and patents found on cannula design are of no use in arthroscopy.[27-29] Four patents aim at the integration of multiple functions into one device, including a lens system, a light source, irrigation passages *(possible separate inflow and outflow)*, and an instrument channel.[30-32] A patent presenting a sheath for transurethal inspection has two separate channels for inflow and outflow might be helpful for arthroscopic usage.[33] Another patent[34] consists of a collapsible access channel that could be used as irrigation channel whenever this is needed during the operation. If no irrigation is needed, the channel is flat and does not occupy space.

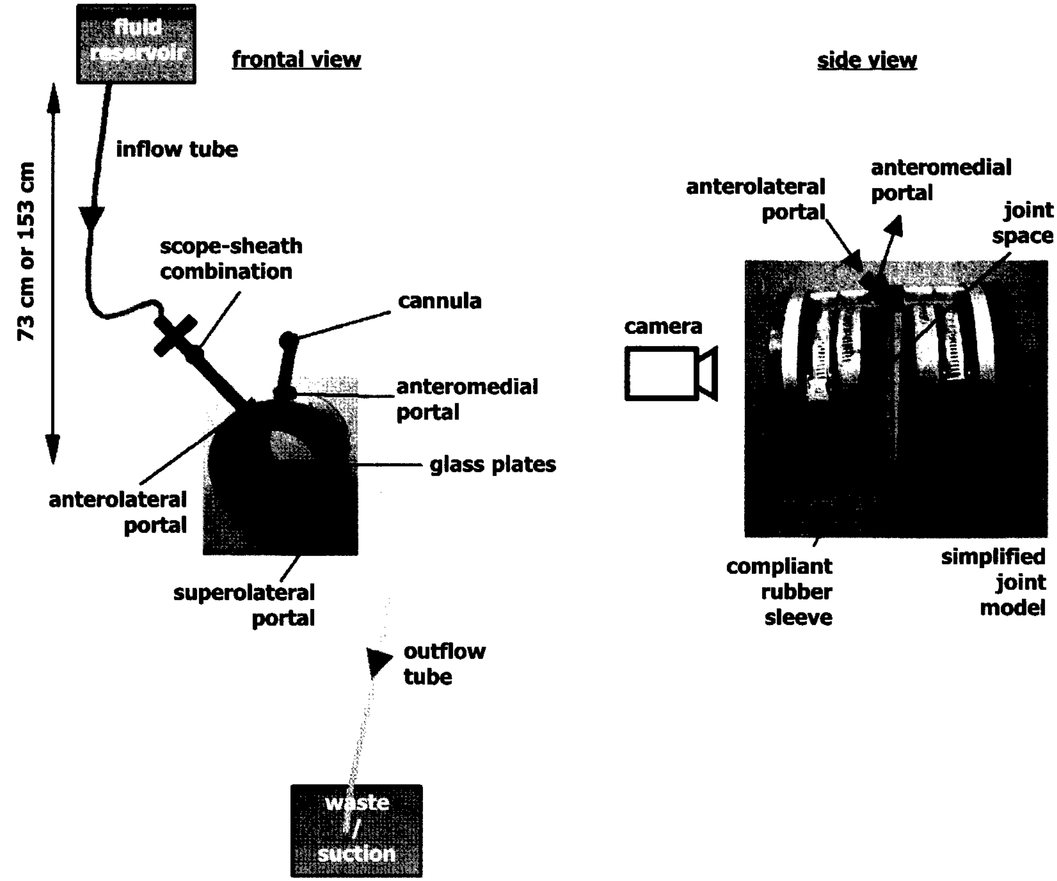

Figure 5.4.1 Frontal view: Schematic set up of the simplified joint model integrated in the gravity pump.

Side view: position of the camera that records the flow patterns as opposed to the joint model. The joint model consists of 2 circular glass plates (diameter 95 mm) positioned at a slight angle to each other which is indicated in the side view. For this position of the glass plates, the joint space height in between the glass plates ranges from 6 mm to 12 mm, which fairly approaches the average knee joint space height. The glass plates are surrounded by a compliant rubber sleeve, which allows the volume of the joint space to increase when the model is pressurized. Two portals are placed at about 30 mm from each other resembling anterolateral and anteromedial portals of knee joint. The third portal placed on the opposite side of the two portals resembles superolateral portal of knee joint.

The goal of this paper is to present the development of a new arthroscopic sheath as well as a new method to determine design criteria for a sheath and to evaluate new designs in comparison with conventional sheaths. Thereto, an experimental set-up was built by means of which the irrigation of joints was simulated and could be visualized. Special attention was paid to the course of the flow through the joint cavity *(called flow pattern)*, since an optimal course will lead to quick irrigation of the joint.

Methods

The experimental set up and objective measures, which were used to assess the influence of several factors on joint irrigation, will be elucidated. With the help of these results design criteria were derived for a new sheath. The conceptual design of the sheath is presented, followed by the evaluation of the new sheath, which was tested in the same experimental set up and in a cadaver ankle.

Physical model of a joint

The flow patterns of the irrigation liquid cannot be visualized in vivo or in vitro joints. Therefore a see-through model of a joint was constructed. The model consists of 2 circular glass plates positioned almost parallel to each other, which enables the visualization of the flow patterns *(Figure 5.4.1)*. The geometry of the knee joint was chosen to assess the size of the simplified model, since most arthroscopic operations are performed on knees.[35] The volume of the joint model is similar *(64 ml, unpressurized)* as was measured for knee joints[8] *(70 to 90 ml, when the knee joint was pressurized with liquid)*. However, the joint model has such a simple configuration that it could also represent other joints such as the ankle joint or the shoulder joint. An advantage of this simple configuration is that differences between conditions can be easier detected and attributed to the variable that is tested *(Figure 5.4.1)*. The joint model's fluid restriction was validated with the help of pressure and flow measurements during ten arthroscopic knee operations *(Figure 5.3.9)*. The joint model has three portals that can be used *(Figure 5.4.1)*.

Objective measures

Objective measures have to be defined to be able to compare the conditions with each other and to determine an optimal configuration. An optimal flow pattern is defined as the flow pattern for which in the shortest time a disturbed arthroscopic view is clear again. The flow patterns were visualized by the injection of blue colored ink in the inflow line near by the inflow portal. Each time 2 ml of blue ink was injected just before the entrance of the inflow cannula. Two irrigation times were defined to be able to compare different conditions: the time till the joint model is completely colored blue *(t_{blue})*, and the time till the joint model is completely clear again *(t_{clear})*. Irrigation time t_{blue} indicates how fast all locations are reached, and was only used in the assessment of design criteria. A small t_{blue} is advantageous, since blood and debris can then be reached quickly at any location. Irrigation time t_{clear} indicates how fast the disturbed view is clear again. The condition for which t_{clear} is the shortest, has an optimal flow pattern, and gives the fastest irrigation of the joint. The irrigation times were measured by visual inspection of digitized films of the recorded flow patterns. The clarity of the liquid in the joint model was initially determined by an observer and with the help of a computer program. This program could determine a clarity value for each sample of the digitized films for which it was important that variation of the clarity value would be only due to the blue ink. With this set up the judgement of the observer was verified. However, the application of this program was later on discarded, since it was difficult to relate changes in the clarity value solely to the blue ink due to varying light conditions during recording. Furthermore, it was not possible to record the arthroscopic view simultaneously with a frontal view of the flow patterns in the joint model due to conflicting light requirements. Thus, the flow pattern in the entire joint space was judged in stead of the flow pattern in the operation field. It was expected that the conclusions derived for the entire joint space based on a frontal view of the joint model are also valid for the operation field, since a fast irrigation of the entire joint will also result in fast cleaning of the operation field. This was later verified by testing the new sheath in a cadaver ankle for which the arthroscopic view was recorded.

Table 5.4.1
The conditions that were varied to determine the influence on the flow patterns during joint irrigation. For all conditions, the automated pump was set as is advised for arthroscopic knee operations (pressure is 113 mmHg and flow is 90 ml/min), except for the condition for which pressure and flow were varied. There were 4 conditions for inflow/outflow combination, 3 for different bleeding locations, 6 for pressure and flow, 3 for direction of inflow, 3 for location of inflow, 2 for disturbance of an instrument, and 2 for a 3D-profile. A picture and sketch are added to show the 3D-profile that was used. The 3D-profile consists of two semi-sphere glasses placed in the centers of each flat glass plate.

inflow / outflow combination	In: scope-sheath 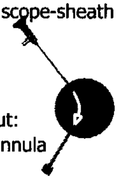 Out: cannula	Out: scope-sheath 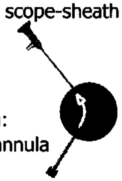 In: cannula	 In & out: scope-sheath	In: scope-sheath  Out: shaver		
bleedings	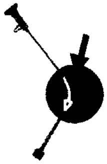	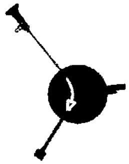	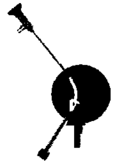			
pressure and flow	68 mmHg 90 ml/min	113 mmHg 90 ml/min	135 mmHg 90 ml/min	180 mmHg 90 ml/min	113 mmHg 200 ml/min	113 mmHg 250 ml/min
direction inflow	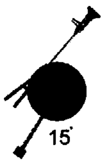		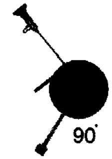			
location inflow			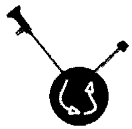			
instrument						
3D-profile		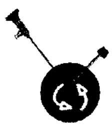	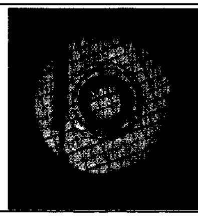	Left: Picture of frontal view showing the actual 3D-profile Right: Picture showing the profiles separately	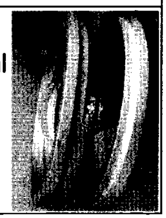	

Design criteria

To be able to determine the conditions that generate an optimal flow pattern, the influence of several factors was investigated. Thereto, the joint model was attached to an automated pump *(FMS Duo+©, Arsis Medical BV, De Bilt, The Netherlands) (Figure 5.4.2)*. The joint model was placed at the same height as the pump. With this automated pump the pressure as well as the flow rate could be kept constant *(advised settings for an arthroscopic procedure were 113 mmHg and 90 ml/min)*, which was advantageous to assess the influence of one factor at a time. A camera was placed in front of the model to record the flow patterns *(Figure 5.4.2)*. The factors that were varied in the laboratory were: combination of inflow and outflow portals, pressure, flow, direction of inflow, location of inflow, disturbance of an instrument, 3D- vs. 2D-dimensional shape of knee joint, and location of bleedings *(Table 5.4.1)*. Each experiment was performed five times. The averaged irrigation times and standard deviations were determined. An ANOVA single factor test *($p<0.05$)* was performed to determine significant differences between the conditions. The flow patterns recorded on video were also evaluated qualitatively. The results of the experiments can be found in Appendix 5B. The conclusions derived from the experiments are given already in the methods section *(Table 5.4.2)*, since they were used to define design criteria for a new sheath. The design criteria are summarized:

- A large cross-section of the inflow cannula *(quick irrigation of joint)*, and a large cross-section of the outflow cannula *(suction of large debris pieces)* are required.
- The inflow stream should be turbulent, the course of the inflow should be directed towards open space, and the inflow stream should reach the entire joint before suction.
- The outflow should be closest to the visual field, because this will push disturbing tissue away from the arthroscope.
- The sheath should have a maximum diameter of 5 mm with a circular shape *(an oval shape is optional but this has to be investigated)*. The sheath should have no sharp edges, should be reusable, should be used with the current obturators, and should have the same connector as the current sheaths.

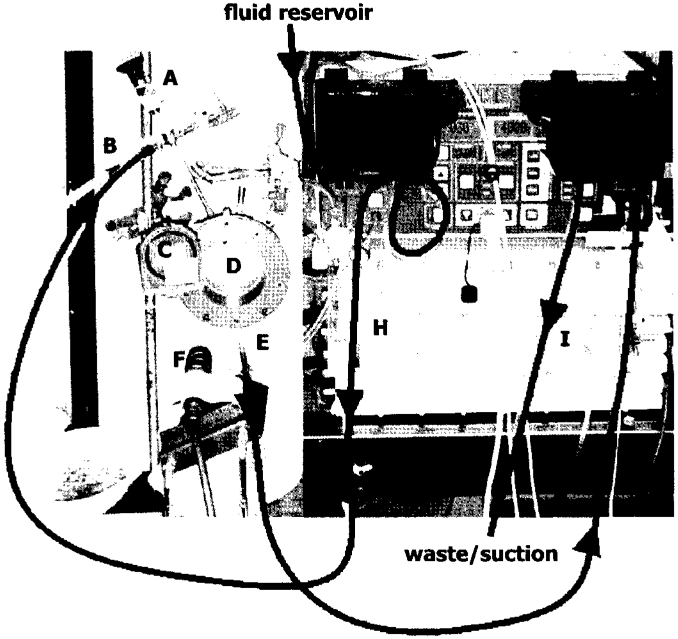

Figure 5.4.2
Picture of the complete experimental set up. In this case the model is integrated with an automated pump. The design criteria were derived with this pump, since the pressure and flow could be kept constant. For the evaluation of the prototypes the automated pump the gravity pump was used (Figure 5.4.1). In the picture the following items can be distinguished: scope-sheath combination (A), injection colored ink (B), stopwatch (C), joint model (D), cannula (E), camera (F), irrigation system (G), inflow tube (H), outflow tube (I).

Table 5.4.2
Overview of conclusions that are derived from the experiments that were done to determine the influence of the factors from Table 5.4.1 on the flow patterns and irrigation times.

conditions	conclusions
inflow/outflow combination	The different in-outflow combinations offer the largest difference in irrigation times in comparison with the other conditions that were varied. The fastest irrigation times occur with inflow via cannula and outflow via sheath-scope followed by using the shaver and inflow via the scope-sheath combination. Inflow and outflow through a cannula without separate passages does not provide an optimal use of the irrigation liquid, since a part of the fluid flow does not enter the joint model.
bleedings	The location of a bleeding does not influence t_{clear}. When a bleeding occurs near the outflow it is slower distributed in the joint model.
pressure and flow	For a quick irrigation of a joint it is favorable to keep the pressure positive (and large). A larger positive effect on the irrigation times than the pressure is the flow rate. With the a number of irrigation systems it is difficult to preserve a positive intra-articular pressure while increasing the flow rate.
direction and location inflow	The fastest irrigation times are reached when the direction of the inflow stream and location of the tip are directed towards the center of the joint model, because then the colored ink is distributed fastest. If the inflow stream bumps into the wall of the joint model, the flow is redirected but is not distributed quickly to the rest of the joint model.
instrument	The disturbance of an instrument in front of the inflow stream has a positive effect on the irrigation times, which become shorter.
3D-shape	The shaped- surface glass plates do not influence the irrigation times.

Furthermore, it is desired to use a two-portal technique instead of a three-portal technique. The reason for this is that a two-portal technique is routinely used when operating on smaller joints, and when operating on larger joints, for which a three-portal technique is routinely used, it will be no longer necessary to create a third portal. To implement the two-portal technique it is required that in- and outflow take place through separate passages in the sheath. An exception of this requirement is the combination for which shaver is used as outflow, since suction takes place through the shaver.

Conceptual design

With the help of the design criteria the patents were analyzed in more detail. Two inventions present solutions for the cleansing of endoscopes that are likely to get foggy during a procedure.[36,37] This is seldom an issue in arthroscopy, but the configuration of the tips of these sheaths offers possibilities to steer the inflow fluid in such a way that the flow patterns in the joint can be optimized. The available cross-section to fulfill each function in the multifunctional sheaths[30-32,38] deserves the main focus. To accomplish sufficient space, two inventions propose a non-circular cross-section.[30,32] From the patent analysis, it can be concluded that attention has to be paid to the cross-section of the flow passages of the sheath. If these passages have an as large as possible cross-section, high flow rates can be achieved for joint irrigation which will result in shorter irrigation times.

From the criteria and patent analysis, the idea arose to start using a 2.7-mm arthroscope in combination with a 4.5-mm sheath instead of the common configuration for which a 4-mm arthroscope is used in combination with the 4.5-mm sheath. This new configuration would triple the cross-section between the sheath and the arthroscope. This will result in a lower fluid restriction which eventually leads to higher flow rates. It is believed that a 2.7-mm arthroscope gives the same picture quality as a 4-mm arthroscope, and with the current developments in camera technology it should be possible to create the same picture size on the monitor. However, for this new sheath there still would be a third portal necessary for in– or outflow. To achieve irrigation through the sheath, the inflow and the outflow should be separated by a partition for which two options were investigated. The first option is a configuration for which the scope is centered in the sheath, and has a partition at each side that divides the cross-section of the sheath in two equal parts *(Prototype 1) (Figure 5.4.3: A)*. The second option is a configuration whereby the scope is placed asymmetrically in the sheath from which one partition extends and divides the cross-section also in two equal parts *(Prototype 2) (Figure 5.4.3: B)*. It was expected that one passage of Prototype 2 would have a lower fluid restriction than one passage of Prototype 1, since the distance between the walls of the wetted perimeter is larger *(Figure 5.4.3)*. Due to this, a larger maximum velocity can be achieved. For both options, simple prototypes were constructed to test this hypothesis. The fluid restriction of one passage of each prototype was determined by measuring the pressure drop of the prototype simultaneously with the flow rate. At a flow of 98 ml/min *(Section 5.3: average flow rate measured during ten arthroscopic operations)*, the pressure drop of Prototype 1 was 16.3 mmHg, and the pressure drop of Prototype 2 was 14.7 mmHg. The hypothesis can be accepted with the notation that the difference is rather small.

A

B

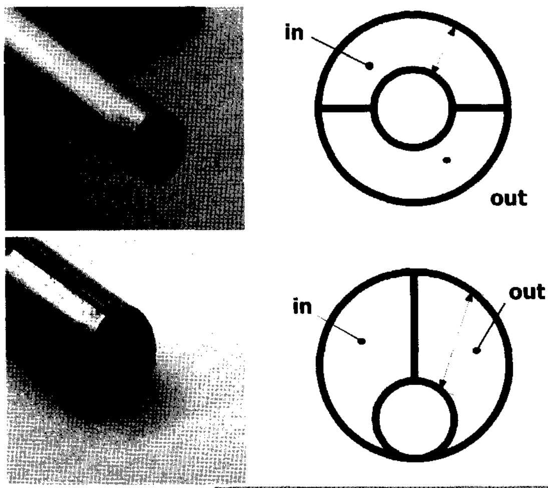

Figure 5.4.3
A) Picture of Prototype 1 showing the symmetric configuration with a partition on each side of the artificial scope.

B) Prototype 2 showing the asymmetric configuration with a partition on one side.

For both prototypes the approximate maximum distance to the walls are indicated. Due to the larger distance for Prototype 2, the maximum velocity will be larger and as a result it is expected that this configuration gives a lower fluid restriction.

Figure 5.4.4
Construction drawing of the new sheath. The stopcocks are positioned in such a way that the least restriction occurs. It would be even better if the stopcocks are placed at a smaller angel than 90°with the shaft. Furthermore, the inner diameter of the stopcocks are slightly larger than the conventional stopcocks. So far, the partition can only be removed by pulling at the tip.

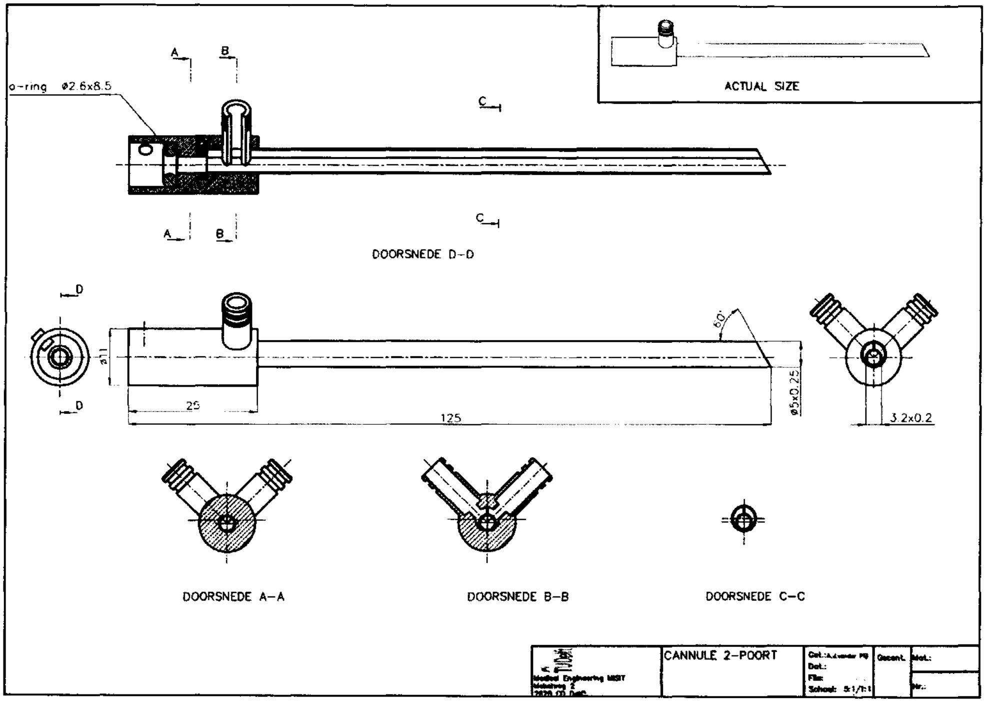

Figure 5.4.5
A) Currently used scope-sheath combination consisting of a 4-mm scope (7200BW, Storz, Germany).

B) Final prototype of the new sheath shown with a 2.7-mm scope (HG 30371, Dyonics, Germany) and a picture without the scope showing the configuration of the stopcocks which are located in such a manner that the flow can pass with the least restriction. Furthermore, close up pictures of the option are presented without partition (B1) and with partition (B2).

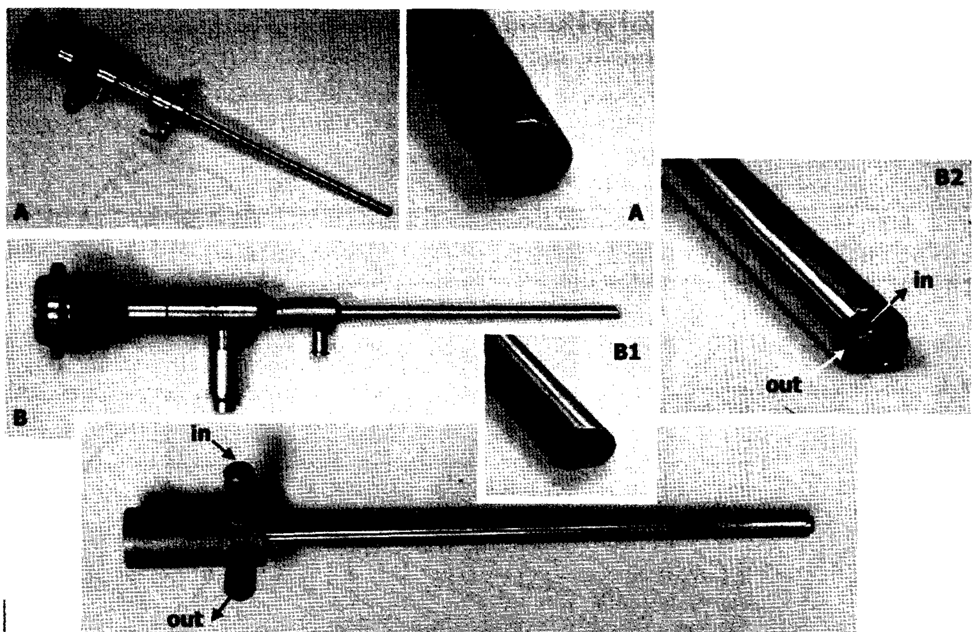

With this knowledge, it was decided to construct a final prototype of a sheath that can actually be used with a 2.7-mm scope *(Figure 5.4.4)*. The scope is placed asymmetrically, and the sheath has a removable partition. This way a surgeon can use the sheath with partition *(inflow and outflow takes place through the separate passages in the sheath)* for operations in smaller joints or soft tissue endoscopy, and remove the partition when he is operating with a three-portal technique or using the shaver. Another option for the three-portal technique is to attach a tube with two connectors. Each connector is then connected to one of the passages of the sheath. Inflow can take place via both passages without removal of the partition.

Evaluation

The final prototype is evaluated in comparison to the currently used scope-sheath combination *(Figure 5.4.5)*. For both scope-sheath combinations the fluid restriction was determined, as well as the irrigation time *(t_{clear})*. t_{clear} was determined in the laboratory set up with the joint model and by means of a cadaver ankle for which the arthroscopic view was recorded. This way it was verified if the irrigation times derived from the joint model had an unambiguous relation with irrigation times documented with the scope view. To asses the fluid restrictions the gravity pump was used instead of the automated pump, to let the flow be solely determined by the fluid restriction and set pressure. For Sheath B the fluid restriction was determined of both passages separately *(Sheath B in and Sheath B out)* as well as both passages together *(Sheath B both)*. The pressure drop along the sheaths was measured by means of two pressure sensors *(pressure monitoring kit, Baxter Healthcare Corporation, USA)*. One sensor was placed just before the sheath, and the other one just after the sheath. The flow was simultaneously measured with a pair of scales and a stopwatch. The pressure measurements took place for each sheath separately at a pressure of 54 mmHg *(is 7.2 kPa)* and 113 mmHg, as well as for each sheath placed in the complete set up of the joint model and the cadaver ankle *(Figure 5.4.1: set pressure is 100 mmHg)*. The pressure at the first sensor was compensated for the difference in height with the second sensor. The Reynolds number[5,26] for each sheath was determined *(Eq. 5.3.3)* to assess if the flow is laminar *($Re < 2300$)* or turbulent *($Re > 2300$)*. For a laminar flow, the pressure drop is proportional to the flow *(Q)(Eq. 5.3.4)*, and for a turbulent flow, the pressure drop is proportional to the squared average velocity *($\rho v^2_{average}$)* *(Eq. 5.3.5)*. For each condition, linear regression lines were determined to assess the proportional factors *(Table 5.4.4)*. For comparison, the pressure drop was calculated for each condition at a flow of 98 ml/min with the help of the regression lines *(Section 5.3)*.
The set pressure of the gravity pump to assess the irrigation times was set at 100 mmHg, and no active suction took place at the outflow *(Figure 5.4.1)*. In the joint model six conditions were measured and in the cadaver ankle only three conditions were measured to validate the assumption that the interpretation of the results for the irrigation of the joint model also hold for the irrigation of the arthroscopic view *(Table 5.4.3)*. Each condition was recorded three times. In the ankle injection was performed with milk instead of blue ink, since milk does not stick into the cadaver tissue. The average and standard deviation of the irrigation times were documented. An ANOVA single factor analysis was performed to determine statistically differences *($p < 0.05$)*.

Table 5.4.3
The conditions for which the irrigation times were measured to compare the currently used scope-sheath combination (Sheath A) with the new configuration (Sheath B). All six conditions were performed with the help of the joint model. Conditions A1, B both 1, and B partition 1 were performed by means of the cadaver ankle.

condition	sheath	inflow	outflow	sketch
A 1	Sheath A	scope	separate cannula	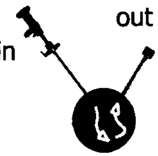
A 2	Sheath A	separate cannula	scope	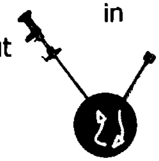
B both 1	Sheath B	both passages scope	separate cannula	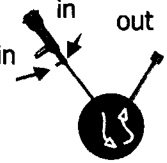
B both 2	Sheath B	separate cannula	both passages scope	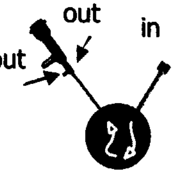
B partition 1	Sheath B	inflow passage	outflow passage	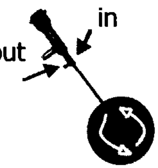
B partition 2	Sheath B	outflow passage	inflow passage	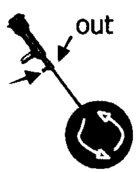

item	L (mm)	$D_{hydraulic}$ (mm)[5]	cross-section (mm^2)	Re	R (mmHg·min/ml)	ΔP (mmHg)
Sheath A	135	0.5	3.34	300	0.82	80
Sheath B right	110	1.2	3.93	1600	0.19	19
Sheath B left	110	1.2	3.93	1900	0.17	17
Sheath B both	110	1.2	7.86	1900	0.11	10

Table 5.4.4
Geometric dimensions of the conventional Sheath A and the new Sheath B. For Sheath B the data are determined for each passage separately as well as for both passage simultaneously. The Reynolds numbers indicate that for both sheaths the flow is laminar, thus the pressure drop is linear with the flow. The proportional factor R between the pressure drop and flow was determined for each item. In the last column the pressure drop is given for a flow of 98 ml/min. This flow is the average flow measured during ten arthroscopic knee operations.

Results

The results of the measurements to determine the fluid restrictions of Sheaths A and B are presented in Table 5.4.4. As was expected the fluid restrictions of Sheath B are smaller than the restriction of the conventional Sheath A. The fluid restriction of both passages is not exactly equal due to the fact that the partition is slightly placed out of center. This is negligible in comparison to the differences with Sheath A. The irrigation times using the joint model as well as the cadaver ankle are shown in Figure 5.4.6. In the graph, it can be seen that there are significant differences in irrigation times. In addition to this, pictures are given of the first seconds of the experiments performed with the joint model *(Figure 5.4.6)*. The results show that evaluation of the irrigation times derived when using the joint model can be used to judge the irrigation in a human joint.

Discussion

The proposed method to assess design criteria as well as to evaluate new prototypes of sheath appears to be a useful tool. The method approaches the clinical practice sufficiently to predict results as appears from the final evaluation test using both the joint model and a cadaver ankle. The joint model can be used as a platform for further investigation on the optimization of arthroscopic view in joints. In the experimental set up conditions can be kept constant to assess the influence of specific variables, which can give more insight in the behavior of the flow patterns. In addition to this, the joint model can be further adapted by making it possible to perform simple operations in the joint and to assess their influence on the irrigation times.
From the results, it appears that decreasing the fluid restriction of a sheath allows for a significant quicker irrigation of the joint at the same initial set pressure. In the case of the three-portal technique the irrigation time is about a factor 10 shorter using the new sheath in the cadaver ankle. When using the two-portal technique, for which in- and outflow take place via the same portal, the irrigation time still reduces by a factor 2 in comparison to the conventional sheath. A reduced fluid restriction in the inflow line is also advantageous for the intra-articular pressure, since the value of this pressure will be closer to the initial set pressure due to the smaller pressure drop.
In the near future, the following developments are foreseen. The new sheath has to be redesigned to allow the 2.7-mm scope with partition to be inserted as one component in the sheath. Then the commonly used obturators can be used in combination with the new sheath. Once this is established the sheath can be sterilized and clinically tested.

Figure 5.4.6
Color illustration see cover.
The irrigation times (t_{clear}) for the conditions indicated in Table 5.4.3 are presented. The experiments are performed by means of a gravity pump and the joint model (white columns) as well as a gravity pump and a cadaver ankle (black columns). It was not possible to test all conditions in the cadaver ankle.
For each condition the average flow is given above each column. To visualize the flow patterns pictures are given of each condition at 1 s, 3 s, 5 s, 10 s, and 15 s after injection of the colored ink using the joint model.

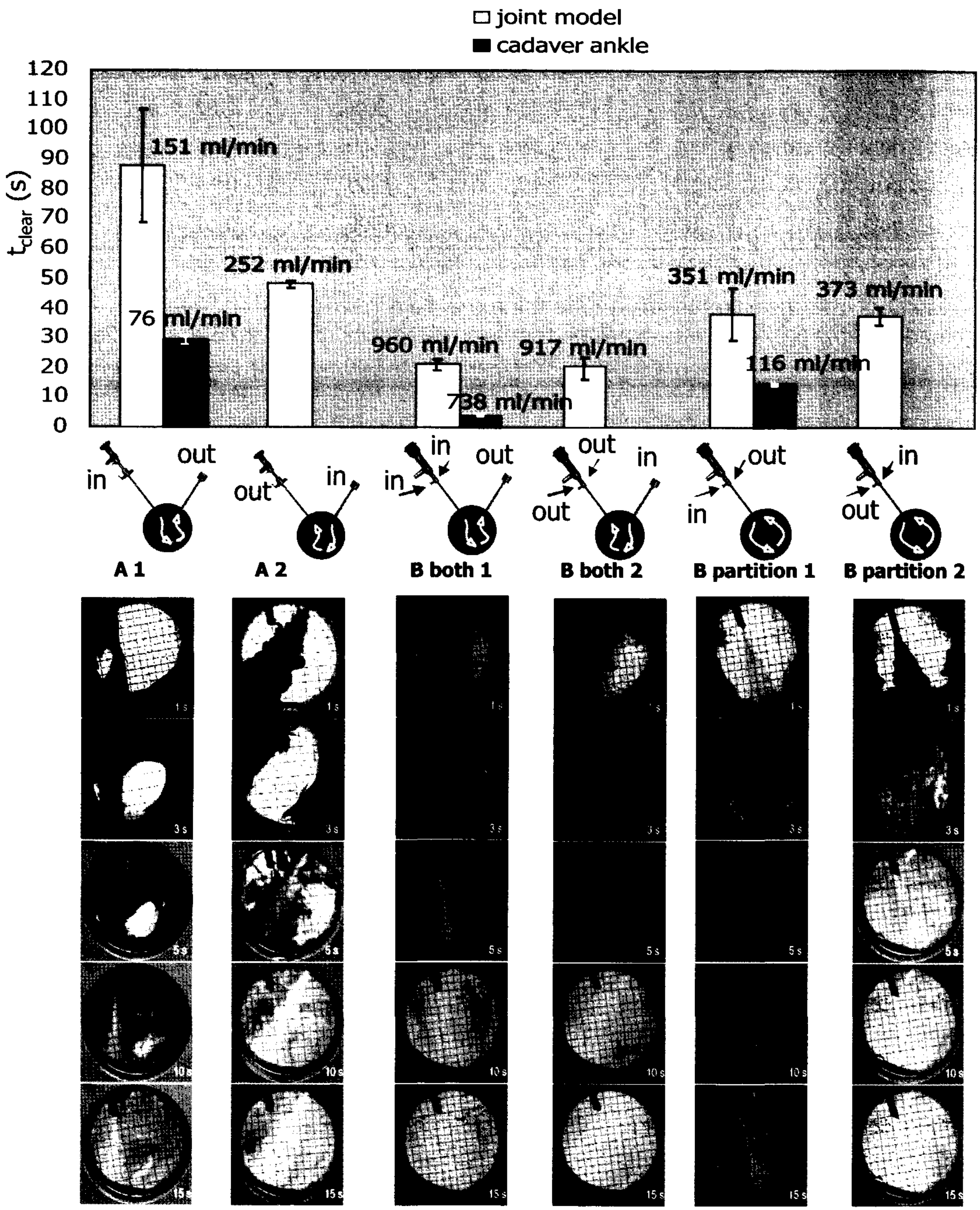

5.5 Discussion

In this chapter, special attention was paid to the clarity of the arthroscopic view during operations. In literature, no clear definitions and requirements were found which involve the optimization of arthroscopic view. An attempt was made to define important aspects as optimal view and flow patterns in order to be able to set up objective measures. This made it possible to start research to assess the conditions to achieve optimal view during operations. In this study, attention was paid to the pressure and the flow in the joint during an operation. Insight in the pressure distribution along the complete set up of irrigation system including tubings and joint was derived from the set up of a system description, as well as experiments performed for constant conditions in an experimental set up. Clinical measurements were performed to validate the model. As could be expected, clinical practice appears to be less predictable than the model, because surgeons act differently in the control of the irrigation, patient sizes are different, and different operative procedures require other actions. Although trends could be distinguished, the variation amongst the operations was too large to support the model unambiguously. It was tried to measure at least some conditions according to a strict protocol, but there were too many variables *(different surgeons, height of the operation table, suction level etc.)* to create a standard. This finding underlines the fact that there is no consensus in achieving sufficient arthroscopic view.

It can be expected that theoretically there is one optimal set up and protocol, which is surgeon independent, and may only be influenced by the volume of the joint that is operated on. By extending the experimental set up with a more elaborate joint model, further research can be done to assess for example the influence of surgical actions on the pressure and flow within the joint as well as the volume of the joint model. This way the clinical practice can be imitated and analyzed step by step. This will lead to well defined guidelines to assess optimal arthroscopic view for different practical situations, as well as design requirements for irrigation systems and sheaths.

This latter item was also further investigated, and the experimental set up could indeed be used to derive design criteria. Furthermore, it was possible to evaluate new sheaths for constant conditions, which proved to be valid for the same conditions measured in cadaver material. The future step should be to evaluate the sheath also in clinical practice. Eventually, when the experimental set is further developed, it can also serve as a platform to test prototypes of new devices involving irrigation. The advantage would be that less cadaver material would be necessary, the set up can be easily adapted, and that it offers good conditions for visualization.

References

1. Morgan CD. Fluid delivery systems for arthroscopy. *Arthroscopy* 1987; 3: 288-291.
2. Ogilvie-Harris DJ. Weisleder L. Fluid pump systems for arthroscopy: a comparison of pressure control versus pressure and flow control. *Arthroscopy* 1995; 11: 591-595.
3. Ampat G. Bruguera J. Copeland SA. Aquaflo pump vs FMS 4 pump for shoulder arthroscopic surgery. *Annals of the Royal College of Surgeons of England* 1997; 79: 341-344.

4. Ewing JW. Noe DA. Kitaoka HB. Askew MJ. Intra-articular pressures during arthroscopic knee surgery. *Arthroscopy* 1986; 2: 264-269.

5. White FM, ed. *Fluid Mechanics.* Boston: McGraw-Hill, 1999. ISBN 0070697167.

6. Patent A: Cassaday EW, Etherington R, Phillips HS, Kane J, Egan MJ, Roundy JS, and Chandler WJ. Fluid management system for arthroscopic surgery. Patent US5830180 (US19960744883 19961108). Aquarius Medical Corp, United States of America, 3-11-1998.

7. Bergstrom R. Gillquist J. The use of an infusion pump in arthroscopy. *Arthroscopy* 1986; 2: 41-45.

8. Oretrop N. Elmersson S. Arthroscopy and irrigation control. *Arthroscopy* 1986; 2: 46-50.

9. Gillquist J. Hagberg G. Oretorp N. Arthroscopy in acute injuries of the knee joint. *Acta Orthop Scand* 1977; 48: 190-196.

10. Noyes FR. Spievack ES. Extraarticular fluid dissection in tissues during arthroscopy. *Am J Sports Med* 1982; 10: 346-351.

11. Funk DA. Noyes FR. Grood ES. Hoffman SD. Effect of flexion angle on the pressure-volume of the human knee. *Arthroscopy* 1991; 7 : 86-90.

12. Sprague NF. Minor and soft tissue complications. In: Sprague NF, ed. *Complications in arthroscopy.* New York: Raven Press, 1989;125-142. ISBN 0-88167-523-7.

13. Bomberg BC. Hurley PE. Clark CA. McLaughlin CS. Complications associated with the use of an infusion pump during knee arthroscopy. *Arthroscopy* 1992; 8: 224-228.

14. Patent B: Fuchs H and Wiest PP. Device for the perfusion of liquids in body cavities. Patent DE3338758 (DE 19833338758 19831021). Fuchs H and Wiest PP, Germany, 9-5-1985.

15. Patent C: Haokanson BH and Andersson P-E. A system for the flushing of a body cavity. Patent WO8600534 (WO1984SE00258 19840711). Gambro AB, Sweden, 30-1-1986.

16. Patent D: Kullas KE. Irrigation system with high flow bypass for use with endoscopic procedure. Patent US5322506 (US19910783845 19911029). Bard Inc.C R, United States of America, 21-6-1994.

17. Patent E: Novak P and Storz K. Device for irrigation of body cavities. Patent US5556378 (US19940308251 19940919). Germany, 17-9-1996.

18. Patent F: Pidoux P, Guignard C, Misse D, and Mathies B. Circulating a liquid through a joint. Patent US4902277 (US19870089740 19870826). United States of America, 20-2-1990.

19. Guignard C. Device for joining a connection piece to peristaltic pump. Patent US5131823 (US19910670864 19910318). Orthoconcept SA, United States of America, 21-7-1992.

20. Dunberger UB, Egan TD, and Kaur H. Irrigation tubing set having compliant sections. Patent US5399160 (US19940233309 19940426). Minnesota Mining & MFG, United States of America, 21-3-1995.

21. Olson DH. Irrigation system for use during arthroscopy. Patent US4940457 (US19870137138 19871223). Snyder Lab Inc., United States of America, 10-7-1990.

22. O'Quinn PS and Donnermeyer DD. Main pump tubing for arthroscopy infusion pump. Patent US5520638 (US19950411508 19950328). Arthrex INC, USA, 28-5-1996.

23. Santangelo JA and Worrick CB. Pressure regulated irrigation system for arthroscopy. Patent US4604089 (US19830523312 19830815). Codman & Shurtleff, United States of America, 5-8-1986.

24. Rodriguez C. Method for determining liquid loss during an operation. Patent WO 99/03518 (PCT/FR98/01496). Future Medical Systems SA, France, 28-1-1999.

25. Tuijthof GJM, van Dijk, C. N., Herder JL, and Pistecky PV. Design of arthroscopic instruments: a clinically driven approach. Submitted to the *Journal of Knee Surgery, Sports Traumatology, Arthroscopy.* 2002.

26. Leijdens H, ed. *Stroming en warmteoverdracht I.* Delft: DUT, 1992.

27. Lajtai G. Aitzetmuller G. Unger F. Orthner E. Half pipe cannula for shoulder arthroscopy. *Arthroscopy* 2001; 17: 224-225.

28. Sidall COR and Savitt RL. Endoscopic disposable sheath. Patent US4741326 (US19860914730 19861001). Fujinon Inc., United States of America, 3-5-1988.

29. Hammerslag JG and Hammerslag GR. Steerable medical device. Patent US5372587 (US19930031810 19930315). Pilot Cariovascular Systems Inc., United States of America, 13-12-1994.

30. Vukovic M. Arthroscope. Patent US4369768 (US19800173952). Vukovic M, United States of America, 25-1-1983.

31. Bonati AO and Ware P. Lumber arthroscopic laser sheath. Patent US5203781 (US19910814185 19911219). Meditron Devices Inc., United States of America, 20-4-1993.

32. Carson RW. Novel arthroscope. Patent US4217891 (US19770861632 19771219). Carson RW, United States of America, 19-8-1980.

33. Iglesias J. Endoscope with continuous irrigation. Patent US3850162 (US19730368186 19730608). Iglesias J, United States of America, 26-11-1974.

34. Jones JS. Collapsible access channel system. Patent US5503616 (US19940177779 19940105). Endomedical Tech Inc., United States of America, 2-4-1996.

35. van Dijk, C. N. Beweegredenen, de patient als bron van inspiratie. Inaugural. 14-3-2002. University of Amsterdam, Amsterdam.

36. Bailey RW. Irrigating laparoscopic cannula. Patent US6017333 (US19950421704 19950413). United States of America, 25-1-0200.

37. Reisdorf D and Donofrio W. Disposable endoscopic sheath. Patent US5989183 (US19980129180 19980605). Xomed Surgical Products Inc., United States of America, 23-11-1999.

38. Ware P and Bonati AO. Arthroscope having five functions. Patent WO9311699 (WO1992US11079 19921217). Meditron Devices Inc., United States of America, 24-6-1993.

6. Meniscectomy: development of steerable punch

In this chapter, the problem area is addressed that is related to the arthroscopic procedure that is performed most frequently: meniscectomy.[1] Optimizing this procedure could therefore benefit a large number of patients. The menisci are located in the knee joint, are composed of cartilage-like tissue, and have a moon-shape form *(Figure 6.0.1)*. Due to their tissue characteristics they play an important role in the lubrication of the knee joint, and the distribution of forces acting on the joint.[2] The menisci can get damaged in case the upper leg rotates with regard to the lower leg when the leg is loaded. In case of a symptomatic meniscal lesion, the damaged part of the meniscus is removed.[3]

Since the knee joint is very tight, a potential problem when performing a meniscectomy is the reachability of the menisci. No literature on this problem area was found. Therefore, the clinically driven approach *(Chapter 2)* was applied to analyze this problem area in detail *(Section 6.1)*. It was concluded that a punch with a side-ways steerable tip could theoretically improve the reachability. The development of this instrument yields two aspects. One aspect concentrates on the design of the instrument tip. In Section 6.2, the design criteria derived from an analysis of the available knee joint space and forces needed to cut meniscal tissue are presented. The other aspect concentrates on the question what the optimal configuration of the handle is from an ergonomic point of view. Therefore, theory on ergonomics concerning the design of hand tools is summarized in Section 6.3. In Section 6.4, a first prototype of a handle is presented with which two degrees of freedom *(cutting and side-ways steering)* can be performed, and that was evaluated. This chapter is concluded with a discussion *(Section 6.5)*.

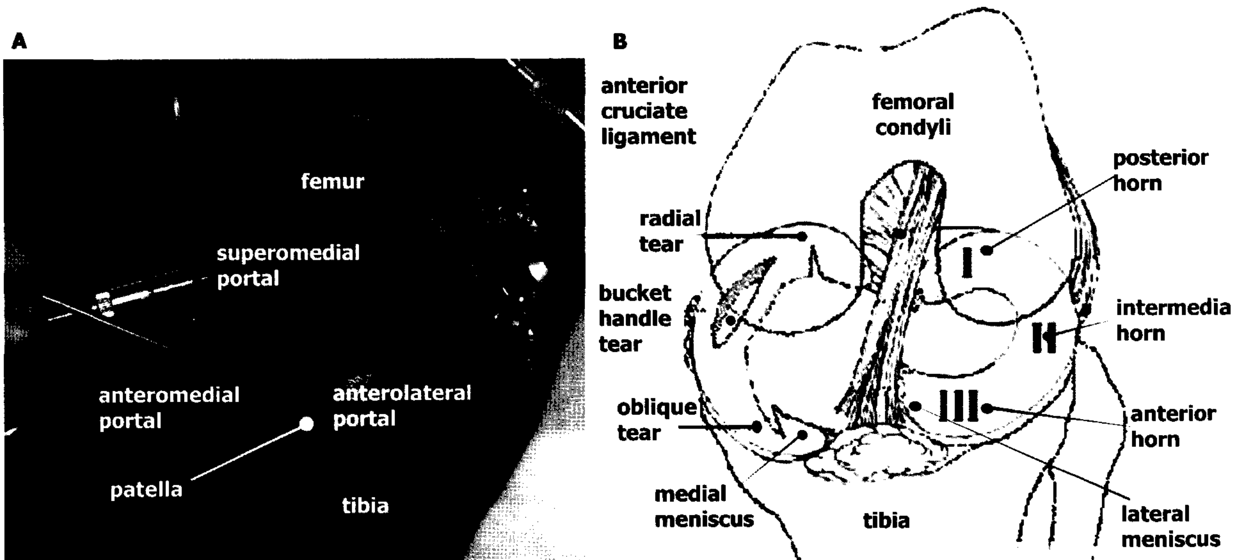

Figure 6.0.1
A): picture of the two routinely used portals to perform knee arthroscopy.

B) Schematic drawing of the frontal side of the knee joint based on Sisk[3]. The menisci are colored gray. The medial meniscus shows three types of tears. The lateral meniscus shows the three zones.

6.1 Problem analysis

Arthroscopic procedures, just as other endoscopic procedures can be clinically demanding due to limited and indirect vision on the operating field, reduced tactile sense and force feedback, and limited degrees of freedom of the instruments which also depends on the location of insertion through the skin.[4] Specific problems are related to the limited workspace in joint cavities, caused by the surrounding bones that are compressed by ligaments, and the limited access to these joint cavities due to neurovascular tissues surrounding the joint. Access to the knee joint is routinely obtained from the anterior side of the joint where two portals are placed at the joint level medially and laterally from the patellar tendon *(Figure 6.0.1)*. Due to this limitation and the convex shape of the femoral condyles, it is difficult to reach the anterior and posterior horn of the menisci with straight instruments *(Figure 6.1.1)*. Due to the convex shape of the condyli of the femoral bone, optimal portal placement is necessary in order to be able to reach the anterior and posterior horn of the menisci with straight instruments. Curved instruments have been developed to facilitate access to all parts of the menisci *(Figure 6.1.2)*. These instruments are called punches *(Section 1.1)*.

Disadvantages current technique

During initial observations of meniscal resections *(Chapter 2)*, it was noticed that often several punches are needed in order to remove a torn meniscus. The use of a large number of these punches has a number of negative aspects. Due to the distinct shape of each punch only a select part of the meniscal tissue can be reached, while most lesions stretch beyond one zone of the meniscus *(Figure 6.0.1)*. This implies that depending on the skills and experience of the individual surgeon and the placement of the portal, differently shaped punches often have to be exchanged a number of times during an operation. Each exchange of instruments is potentially harmful to healthy tissue, because it carries the risk of introducing bacteria into the joint cavity. These well known effects generate unwillingness by the surgeons to exchange less optimally shaped instruments for more suited ones. Therefore, it is frequently observed that surgeons in order to address a complete meniscal lesion with a limited number of instruments have to exert more force than some feel is wise to use on the surrounding structures and the portal in the skin. These applied forces can be so high that bending of instruments might occur, and might in the damage of healthy tissue. In addition to this, the forces are exerted while the surgeon's wrist is in a flexed position, which can cause chronic wrist pain.[5-7] Moreover, a flexed wrist is unsuited for making the grasping finger movements needed for cutting.[8] Lastly, the use of a large number of instruments is expensive.[5]

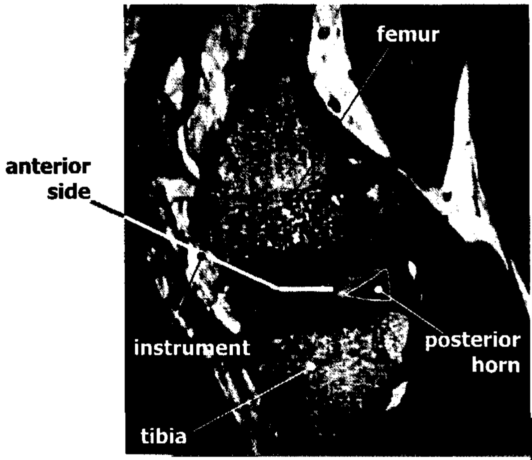

Figure 6.1.1
Picture of a sagittal cross-section of the knee joint. It shows that through the curvature of the condyli it is difficult to reach the posterior side of the knee with the current instruments and portals. Picture based on Pocket atlas of sectional anatomy[55].

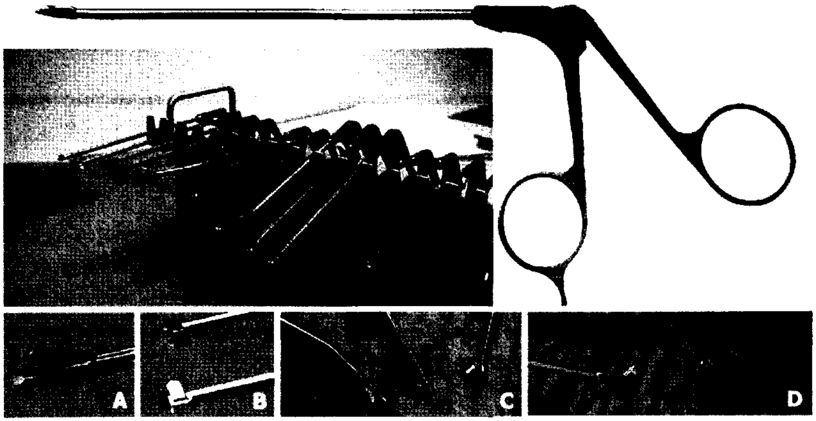

Figure 6.1.2
Differently shaped punches, which are currently available on the market. All punches have a scissors handle.

The punches:
A) straight punch,

B) side-biters,

C) upswept punches, and

D) 45°-angled punches.

Observations and discussions with surgeons

To meet with the disadvantages mentioned above, it was suggested to develop a punch with a steerable tip. In order to avoid the risk of developing a device that is not needed by surgeons, 11 arthroscopic surgeons were questioned about this suggestion in an interview, and they agreed to it as a promising and clinically relevant concept *(Chapter 2)*. In discussions with surgeons it appeared that mechanical dissection of the meniscus is preferred over laser, ultrasone and electronic dissection, because the surgeon can verify the amount of tissue that is going to be cut by initially holding the tissue in the instrument tip. Force feedback, which is important for laparoscopic forceps in which delicate tissues are manipulated, seems to play a

Table 6.1.1
A) The total number of instrument exchanges during 19 meniscectomy procedures. The changes of the same instrument to another portal are also included. In the left column the instrument is given that was used at that moment and this instrument is changed with an instrument shown in the upper row.

B) The total number of times that a type of punch is used in the same 19 operations. An example of each instrument is added.

A to →			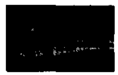			
from ↓	probe	scissors	punch	forceps	suction tube	shaver
probe	1	7	19	4		10
scissors	2	1	4	3		
punch	12	1	23	4	12	10
forceps	5	1	6	1	2	
suction tube	3		8			
shaver	7		9	1		3

B	type of punch		total number of usage during procedures
	straight sheath	tip small or wide	43
	straight sheath	tip angled 15° upwards	14
	straight sheath	side-biter left or right, angled 90° or 45°	11
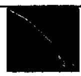	upswept sheath angled 15° to 30°	tip straight	4

minor role. This can be due to the fact that the manipulated tissues in arthroscopy are harder, and that a better visualization of the joint cavity is usually obtained, since it is possible to work in a bloodless field by using a tourniquet placed around the upper leg *(Section 1.1)*.
Additional meniscectomy procedures were observed to define the number and the choice of additional degrees of freedom that give optimal functionality of the steerable punch, and to perform an ergonomic analysis.[9,10] Observations of the operative procedure were performed in three hospitals. A total of 19 meniscectomy procedures were attended, performed by five different surgeons. During the operations the types of the used instruments and the number of interchanges were documented. Furthermore, an ergonomic analysis was conducted of the posture of the upper extremities of the surgeon involved. The average instrument exchange per operation was 11 times *(SD is 9)*. A distinction could be made between standard meniscectomy procedures *(15 operations, operation time: 15 to 20 minutes, instrument changes: average is 7 and SD is 3)*, and more complex meniscectomy procedures *(4 operations, operation time: 35 to 40 minutes, instrument changes: average is 26 and SD is 7)*. The complex operations showed much variation in pathology and method of approach, whereas the performance and pathology of the standard operations were all quite similar.
The results of the observations concerning instrument exchanges are shown in Table 6.1.1. As can be seen, most instrument exchanges occur between punches and the probe, and in-between punches. Most surgeons start the operation with a straight punch, and thus straight punches are used most frequently. Side-biters *(Figure 6.1.2B)* and upswept punches are used at a ratio 11:18 *(Figure 6.1.2C)*. It can be concluded that if all curved instruments are to be integrated into one single instrument, up and down movement of the instrument tip and side-ways movement are necessary to reach all locations in the knee joint. It was observed that surgeons do not continuously hold the punch that is inserted in the joint cavity, since they for example have to adjust the settings of the arthroscope.[9]

joint	excursion	observed average maximum excursion	maximum allowed range of excursion	remarks
shoulder	abduction	30°	60° [11]	The average duration for a meniscectomy is 25 minutes. For this time the allowable abduction range of the shoulder joint is up to 60° [11]
elbow	flexion pronation / supination	135° 45° / 45°	90°-120° [7]	
wrist	fexion / extention	30° / 30°	15° / 15° [12]	Although the maximum force can be exerted with a 20° extended wrist [52] long-term use of a bended wrist can cause chronic complaints[12]
	radial / ulnar deviation	0° / 20°	5° / 15° [12]	

Table 6.1.2
Result of the ergonomic analysis of the posture of surgeons during standard knee arthroscopies. The observed angles were determined by visual inspection of the surgeons during the attended operations. In the third column the observed maximum excursions are presented. In the fourth column the maximum allowable excursions to prevent pain complaints of surgeons are shown.

The results of the ergonomic analysis of the surgeon's posture and actions during a meniscectomy are shown in Table 6.1.2. During routine operations, the joint excursions of the shoulder and the elbow of the surgeon are below the maximum allowed angle[11], however, the wrist excursion exceeds the allowed maximum range.[11,12] This can result in chronic pain complaints in the long run.[6,13,14] Furthermore, an extremely flexed wrist reduces the grasping force of the hand.

All punches on the market have similar scissors handles which can cause ergonomic problems as is known from analyses of laparoscopic instruments *(Figure 6.1.2)*.[5,14,15] The disadvantage of a scissors handle is that the dimensioning of the rings is critical.[16] If they do not fit well, they will cause pain complaints. The observations showed that surgeons hold the scissors handle in two optional grips during the operation. The first is a combined grip consisting of a combination of a two-finger hold grip and an internal precision grip, and the second one is a pistol grip.[7,17]

Choice of degree(s) of freedom of the steerable punch

When analyzing the results in more detail, it becomes apparent that the upward punches and the side-biters are not used within the same operation. This is in correspondence with the anatomy of the knee joint. We therefore decided to develop two punches: one with a side-ways steerable tip to reach the anterior and middle zones, and one with an upwards steerable tip to reach the posterior zone of the menisci. The advantage of this choice is the fact that the instrument tip will be less complex, and the instrument will most likely be less complex to control. In this chapter, the focus is on the development of a punch with a side-ways steerable tip in three fixed positions, for which at first 90°, 0°, -90° were chosen as a starting point. The reason for focusing on a side-ways steerable punch is that the surgeons state that side-biters are likely to cause most damage when inserting them in and extracting them from the joint cavity. Furthermore, fixation of the tip in three positions *(90°, 0°, -90°)* seems enough for the moment, since the skin around the portals also allows a certain level of side-ways movement.

Conclusions

In general, a surgeon is capable to perform a meniscectomy without a large number of instrument exchanges, but in more complex operations the reachability of meniscal tissue is a problem, which can probably be solved by the development of a steerable punch for which design criteria are derived in the next section. A steerable punch will also prevent extreme wrist flexion and extension.

The overall ergonomic judgment of the posture of the surgeon during a meniscectomy is positive. This is mainly due to the short operation time. However, the scissors handle of the punches is not ergonomic, and therefore, in the remainder of this chapter attention is paid to include ergonomic requirements in the design of a new handle for the steerable punch. Lastly, the mechanical removal of meniscal tissue gets high priority, whereas force feedback during the cutting of tissue has a low priority.

6.2 Design criteria for the tip of a steerable punch

This section is based on the paper *Design criteria for the tip of a steerable punch*, by G.J.M. Tuijthof, J.L. Herder, C.N. van Dijk, P.V. Pistecky, which will be submitted to the Journal of Clinical Biomechanics.

Keywords: knee joint, technical characteristics, meniscus, shear stress

Abstract: To overcome the disadvantages of using a large number of punches during a meniscectomy it was decided to develop a side-ways steerable punch. This section presents a method to determine an order of magnitude of geometric characteristic dimensions of the available knee joint space, as well as the required force to cut meniscal tissue. With these data design criteria are set up for the design of the side-ways steerable punch.

Introduction

Specific problems in the field of arthroscopy are related to the limited workspace in joint cavities, caused by the surrounding bones, and the limited access to these joint cavities due to neurovascular tissues surrounding the joint. During observations of meniscectomy procedures, it was noticed that often several punches were needed to perform a meniscectomy *(Table 6.1.1)*.[9,10] The use of a large number of these punches has negative side effects *(Section 6.1)*. Therefore, it was suggested to develop a punch with a side-ways steerable tip.[9,10,18] Mechanical dissection of a meniscal lesion is preferred, since the surgeon can verify the amount of tissue that is going to be cut by initially holding the damaged tissue in the instrument tip *(Section 6.1)*. The goal of this paper is to present technical design criteria for the development of the tip of a side-ways steerable punch. The main design criteria are divided in geometric, and load criteria. The geometric criteria are dependent on the available space in the knee joint and the location of the portals. The load criteria are dependent on the force that is required to cut meniscal tissue. We introduce an efficient method by means of which technical dimensions are derived for the knee joint space. These data give an order of magnitude for the technical criteria that are used as a starting point for the conceptual design of the steerable punch.

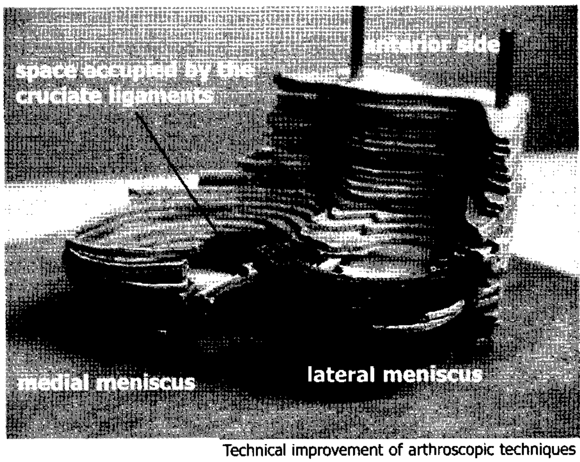

Figure 6.2.1
Model of the available space in the knee joint built up from the pictures of the Visible Human project[25]. The menisci are also shown. In-between the menisci there is no available operation space, since the cruciate ligaments are located there. The space at the anterior side includes fatty tissue that can be removed to create a larger operation space.

Methods

It is known that anthropometric dimensions show variations for which the standard deviations are about 5% to 10% of their average.[19-22] It can be expected that the variation in the size of the knee joints of individuals is about the same. The challenge is to design a steerable punch that can be used effectively in all knee joints. Therefore, characteristic dimensions of the knee joint space were defined for which an order of

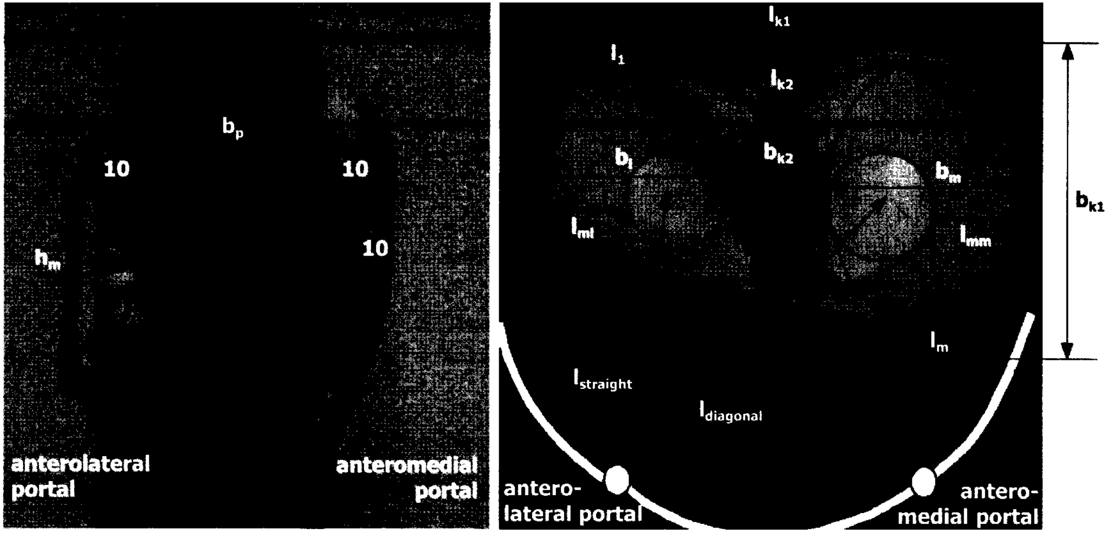

Figure 6.2.2
Two pictures of the functional knee joint model[26] in which the defined dimensions and ellipses are indicated. The portal locations described in literature are indicated as well. The dimensions that are important for the steerable punch design are the distance between the portals (b_p), the horizontal distance of the anterolateral portal to the lateral ($l_{straight}$) and medial ($l_{diagonal}$) meniscus. The values of $l_{straight}$ and $l_{diagonal}$ are approximately the same when they are measured from the anteromedial portal.

magnitude were derived, as well as for the location of the two routinely used portals *(anterolateral and anteromedial)* in a number of specimens *(Figure 6.0.1)*. Maximum and minimum values were used for the design. To our knowledge no data on the cutting force of meniscal tissue are available in literature. However, these data are important to calculate the strength and stiffness of the cutting mechanism. With the help of a simple experiment the shear stress was estimated.

Dimensions of the knee joint

Based on the available space in a knee joint, and the location of the anterolateral and anteromedial portals, an order of magnitude was determined for the shaft length, the orientation of the tip in relation to the shaft, the tip length, and the range for side-ways positioning to reach all locations on both menisci. Furthermore, the optimal portal to access the lateral and medial meniscus was chosen. In literature, descriptions and 2D-sketches of the anatomy of the knee joint are given, which are insufficient for the development of the steerable punch.[23,24] Several options are available to determine anthropometric dimensions of the knee joint: cadaver knee joints, radiographs, MRI-scans, anatomic knee joint models, arthroscopic views, and external biomechanical measurements. We chose a combination of knee joint models, and external

Figure 6.2.3
Two pictures of an arthroscopic view showing the stressed lateral side of a knee joint during an operation, and the stressed medial side of a knee joint during an operation. The probe can be clearly seen on each picture and has tip length is 3 mm by means of which h_k was estimated.

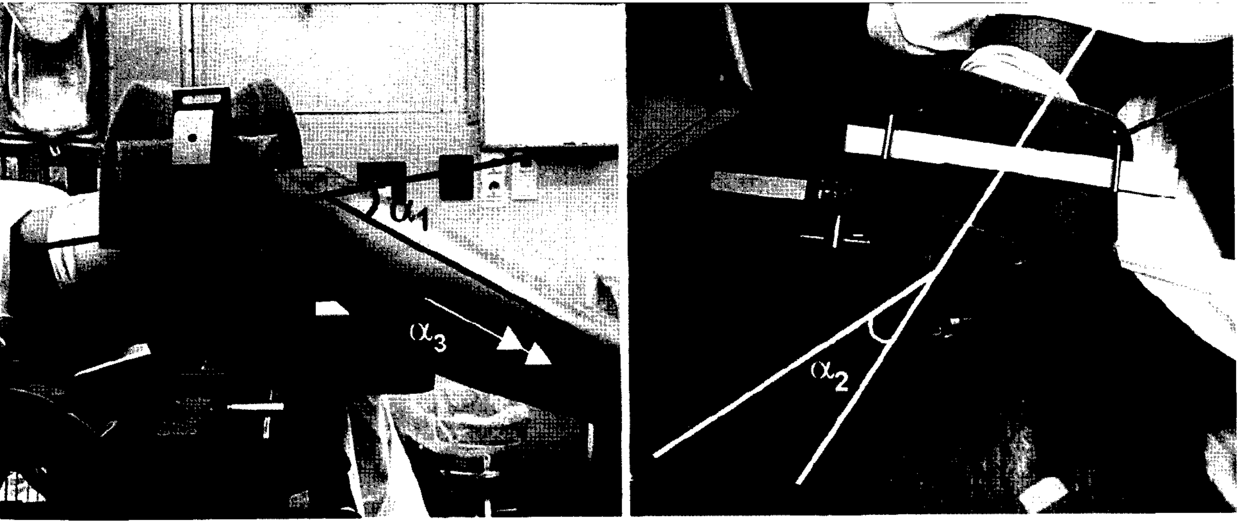

Figure 6.2.4
Two pictures of a stressed knee of a patient during a meniscectomy.
From the pictures the flexion angle (α_1), and abduction angle (α_2) of the lower leg relative to the upper leg were determined. The direction of the rotation angle (α_3) is also indicated.

biomechanical measurements, because this combination was readily available, easy to work with, and made it possible to build a positive model of the available joint space. Furthermore, it was observed that surgeons create more working space during a meniscectomy procedure by medial or lateral distraction of the knee joint, which cannot be documented by means of MRI-scans and radiographs. The use of anatomic joint models was evaluated by measurements on subtalar joints, and found to be accurate enough to determine an order of magnitude of the characteristic dimensions of the joint *(Section 4.5)*.
Two knee joint models were used: a natural size functional anatomic model of the knee joint *(NS 50, Somso)*, and pictures of the Visible Human project.[25,26] Each picture shows a cryosection of a male person which is performed at each mm.[25] With the help of the Visible Human a positive model of the available joint space in the knee was built *(Figure 6.2.1)*. The size of each meniscus *(l is lateral and m is medial)* was characterized by an ellipse with a length *(l_m and l_l)*, and a width *(b_m and b_l)*. From these ellipses a proximally located circle was subtracted having a diameter equal to the meniscus width subtracted by the width of the middle horn *(b_{mm} and b_{ml})(Figure 6.2.2)*. The height at the peripheral rim of the menisci was also defined *(h_m) (Figure 6.2.2)*. The knee joint space was approximated by an ellipse-shaped cylinder which size was determined by the axes of the ellipse *(b_{k1} and l_{k1})*, and the minimal thickness *(h_k)* defined as the minimal available joint opening during an operation *(Figure 6.2.2)*. A smaller ellipse-shaped cylinder was subtracted that is located in the center and represents the space occupied by the cruciate ligaments *(Figures 6.2.1 and 6.2.2)*. This smaller cylinder is characterized by the width and length of the cruciate ligaments *(b_{k2} and l_{k2}) (Figure 6.2.2)*. Furthermore, on top of the ellipse-shaped cylinder a curved triangular beam was placed at the anterior side, which represents the fatty tissue that can be removed to create more working space *(Figure 6.2.1)*. The size of the triangular beam positioned anteriorly is less essential for the dimensions of the punch, and was not specified. h_k was determined by estimating its size by means of the tip of a probe *(tip is 3 mm)* shown at a picture of the arthroscopic view of a medially stressed and a laterally stressed knee *(Figure 6.2.3)*, and by external biomechanical measurements of the leg angles *(Figure*

6.2.4). The flexion angle *(α_1)*, and abduction angle *(α_2)* of the lower leg relative to the upper leg for medial and lateral distraction were determined from pictures of a patient during a meniscectomy *(Figure 6.2.4)*. A knee in distraction is also rotated about its leg axis *(α_3)*. An estimation of this rotation was made with the help of the two other angles, by means of which h_k could be calculated as is described in Cals[10]. The other dimensions were measured by means of vernier callipers.
The location of the anteromedial and anterolateral portals are described in literature[3], and by means of the given instruction the portal locations were determined for both models *(Figure 6.2.2)*. The portals can be created with an accuracy of about 5 mm in the cranial and lateromedial direction. By means of inspection of Figure 6.2.2, it was determined that a straight approach *(lateral portal to reach lateral meniscus or medial portal to reach medial meniscus)* required a range of motion of 180°, for which 0° is defined as the position of the tip parallel to the shaft. Due to this requirement the steering mechanism for the punch would be complex, whereas a diagonal approach did not require backwards cutting. Therefore, it was chosen to propose a diagonal approach for both menisci *(lateral portal to reach medial meniscus, and medial portal to reach lateral meniscus)*. In order to pass the smallest available joint opening *(h_m)*, the orientation of the tip should be in an upward direction relative to the shaft.
With the help of the portal height in the frontal plane *(7 to 13 mm)* and the transversal diagonal distance of the portal to the bottom of the curvature of the condyli *($l_{diagonal}$)* this angle was determined for the dimensions of the 5^{th} en 95^{th} percentile of mature individuals *(Figure 6.2.2)*. With the help of the values for the knee width of the 5^{th} en 95^{th} percentile of mature individuals[19,20] and the construction of a workspace, the total tip length, the bite-size, the shaft length, and the side-ways range of motion were geometrically determined. The values of the knee widths are 76 mm for the 5^{th} percentile, and 128 mm for the 95^{th} percentile, for which the size of the 95^{th} percentile gives the boundary conditions for the dimensions of the steerable punch.[20] The sizes of the menisci and knee joints space that were measured, were scaled to the size of the 95^{th} percentile. Furthermore it was assumed that the bite size of the punch should be at least 3.5 mm, and the distance between the cutting axis and the steering axis should be at least 2 mm to allow the construction of the mechanisms.

Cutting force of meniscal tissue

With the help of the force required to cut meniscal tissue the strength of the force transmission can be determined. The deformation process of the meniscus when punching can be approximated by a punching process for which the force is calculated as follows:[27]

$$F_{meniscus} = \tau \cdot A_{shear} \tag{6.2.1}$$

where $F_{meniscus}$ is the force to cut meniscus, τ is the shear stress of meniscus, and A_{shear} is the circumferential surface along which the tissue is cut. This surface is equal to the circumferential surface of a piece of pie when using a conventional punch, which is determined by the size of the punch tip *(l_{tip} and b_{tip})*, and the maximum opening angle of the tip *(α_{tip}) (Figure 6.2.5)*.[10]

The equation to calculate A_{shear} is:

$$A_{shear} = \alpha_{tip} \cdot l_{tip} \cdot (b_{tip} + l_{tip}) \qquad (6.2.2)$$

The shear stress of meniscal tissue was determined in an experiment in which the tissue was punched with two different equally sized cylinders, one solid cylinder, and one tube with a sharp edge *(Figure 6.2.6)*. The solid cylinder represents a true punching process, and the tube represents the punching process performed with an arthroscopic punch, for which the force is also dependent on the sharpness of the edge.[10] Six samples of fresh *(formerly frozen)* meniscal tissue were used, and each experiment was repeated at least two times on the same sample. The meniscus was placed on a platform which contained a hole through which the cylinders neatly fitted. A cylinder was loaded via a lever construction with gradually increasing load until the tissue was fully punched *(Figure 6.2.6)*. The shear stress is calculated by division of the meniscus force compensated for friction loss and the surface along which the tissue is cut. The average shear stress and the standard deviation were calculated.

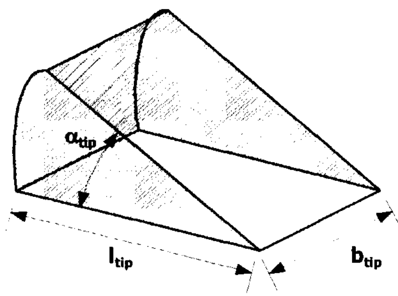

Figure 6.2.5
Schematic drawing of the amount of tissue that can be removed in one cut using an ordinary punch. The hatched surfaces (two triangles and one curved surface) form A_{shear}.

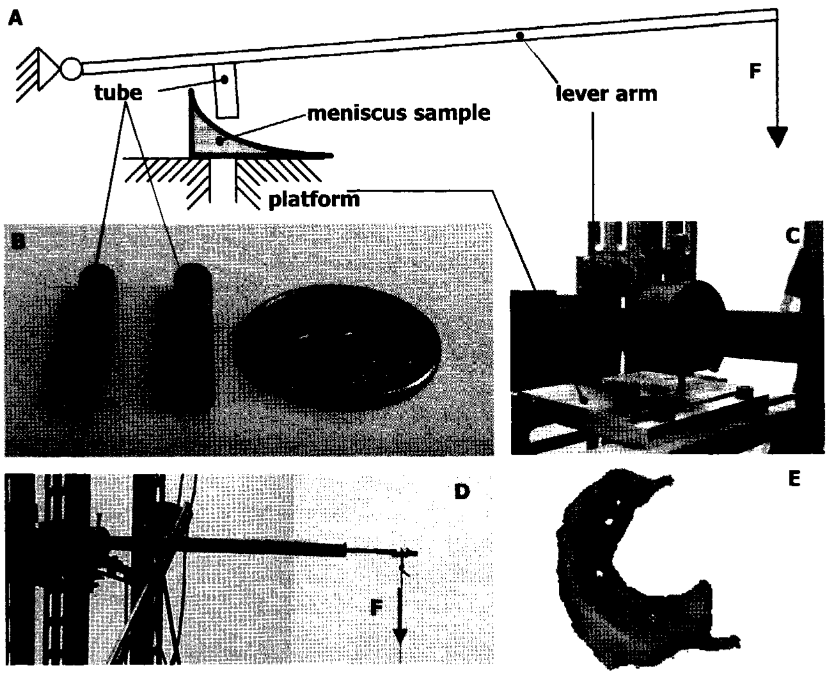

Figure 6.2.6
Pictures of the experimental set up to determine the shear stress of meniscal tissue:

A) Schematic drawing of the experimental set up,

B) The massive cylinder and tube (diameter 3 mm) the diameter of the coin is equal to the diameter of 1 eurocent,

C) Platform with lever construction,

D) The load was applied by adding water in a basket, and

E) Sample of punched meniscal tissue.

Results

In Table 6.2.1 the values of the geometric dimensions are given. The Visible Human is tall in comparison with the data of the functional knee joint model and data derived from literature. During live surgery the soft tissues around the portals allow for about 5 mm of radial movement, which is enough to reach most posterior horns with a fixed upward angle of the tip, since the upward angle for the smallest individual should be 7.7°, and for the largest individual should be 8.4°. In Figure 6.2.7, the workspace is shown for the diagonal approach to both menisci. As can be seen, steering the punch in three fixed positions should be enough to reach the entire menisci. Initially it was thought that the tip should be able to move to −90° and +90° relative to the shaft, but the workspaces show that a smaller range from −55° to 55° will be sufficient. The shear stress of the middle horn is 15% smaller than the posterior horn. The anterior horn seems to have the highest shear stress, however, only three measurements could be performed for this part of the meniscus. The maximum measured shear stress was 20 MPa *($\tau_{massive}$) (Table 6.2.1)*. The maximum shear stress of meniscal tissue is set at the average values plus two times the standard deviation *(21MPa)*. However, the shear stress for punching with an arthroscopic punch is different, and allows for a shear stress that is about 50% lower.

Table 6.2.1
Results of measurements performed on two models of the knee joint, as well as the results of measurements performed on cadaver meniscal tissues. All dimensions are given in mm unless indicated otherwise.

		functional knee joint model	Visible Human	literature			functional knee joint model	Visible Human	literature
medial meniscus	l_m	40	46	35	**lateral meniscus**	l_l	30	34	30
	b_m	25	28	25		b_l	30	32	30
	b_{mm}	12	10			b_{ml}	13	11	
menisci	h_m	7	6	5					
knee joint space					**portals**				
	l_{k1}	78	83			b_p	40	50	
	l_{k2}	53	59			$l_{diagonal}$	56	67	
	l_{k3}	20	24			$l_{diagonal}^{*}$ [p5]	52	$l_{diagonal}$ [p95]	88
patient		**medial**	**lateral**						
	α_1	38°	30°			h_k^{**}		7.8 ± 3	3.2 ± 3
	α_2	23°	35°			h_k^{***}		5	5
	α_3	15°	45°						

dimensions straight punch (S&N)						**shear stress meniscus**			
$\alpha_{tip,max}$	45°	l_{tip}	4	b_{tip}	2.2	$\tau_{massive}$	14.0 ± 3.3 MPa	τ_{hollow}	6.6 ± 1.7 MPa

** Determined with the help of schematic drawings of the transversal view of the knee joint for the estimated 5th percentile and 95th percentile of human individuals.*
*** Determined with the help of the estimated external lower leg angles α_1, α_2, and α_3.[10]*
**** Determined with the help of pictures taken the arthroscopic view of knee joints (Figure 6.2.3).*

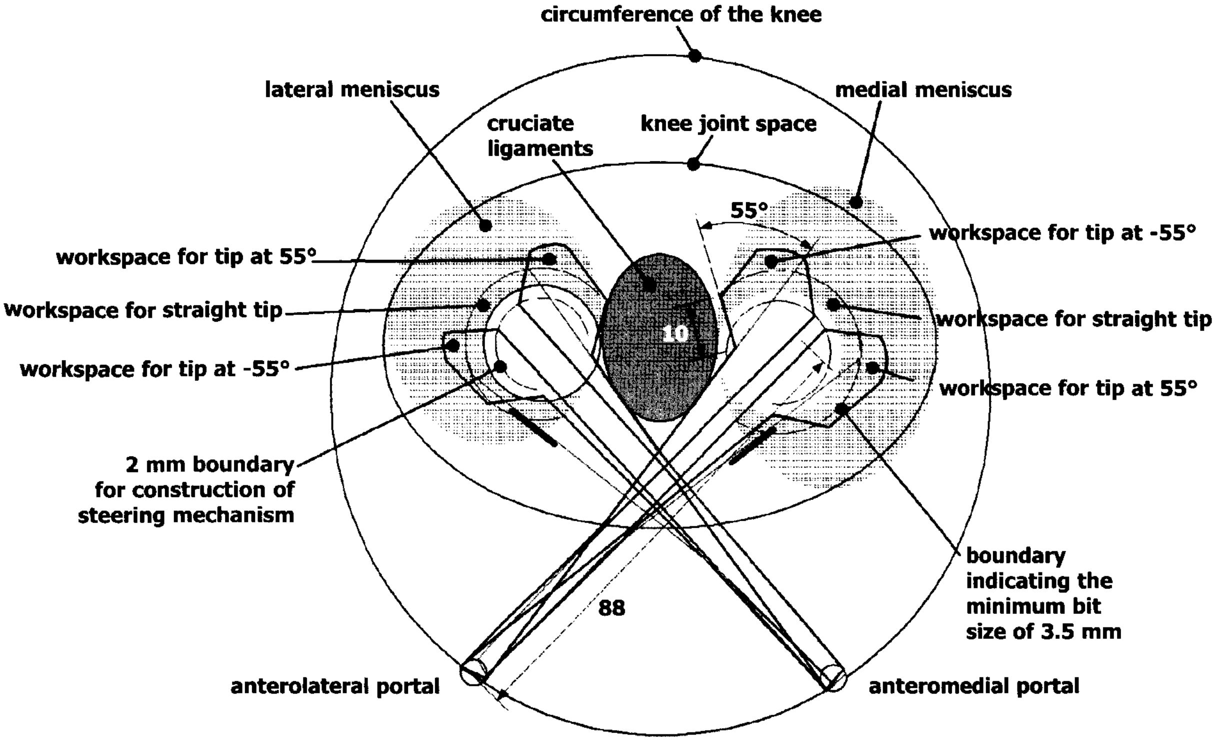

Figure 6.2.7
Transversal view of a schematic drawing of the knee joint which was constructed with the help of the proposed models for the knee joint space and menisci. The size of this knee joint approximates the 95th percentile of human individuals. The diagonal approach was chosen to avoid the steerable punch from becoming unnecessary complex. For each meniscus the two boundary circles are indicated for the minimal required bite-size and the minimal required space for the steering mechanism. The workspace for the punch with a straight tip is indicated by the gray perimeters, whereas the workspaces for a side-ways position of the tip are indicated by the black perimeters. From these workspaces it was derived that the tip length should be about 10 mm, and that the maximum range of motion should be approximately from –55° to 55° to reach all locations on both menisci.

With these results the following design criteria can be formulated:

- The suggestion is given to approach both menisci by a portal that is located diagonally.
- The total tip length should be approximately 10 mm, the bite size should be 3.5 mm, the shaft length at least 130 mm, and the punch should have a maximum diameter of 5 mm proximally, and a maximum diameter of 3.5 mm distally to allow for opening of the tip.
- The side-ways range of motion should be about –55° to about 55°, for which three fixed orientations of the tip are sufficient (-55°, 0°, 55°).
- The tip should have an upward angle of 8°.
- The maximum shear stress of meniscal tissue when punching with sharp edges is about 10 MPa, which results in a cutting force of 190 N, when punching with a routinely used punch.

Discussion

In this section, it was proposed to model the knee joint space by an ellipse-shaped cylinder, and the menisci by part of an ellipse-shaped cylinder. The characteristic dimensions of these models were defined, and an order of magnitude of their sizes was determined by means of two anatomic models. Since, only two models were used, an estimation of the range of variation was derived from the available data for the knee width, which gave the boundary conditions for the dimensions of the steerable punch. For other applications, as for example the set up of biomechanical models, more measurements will be required, preferably on cadaver knee joints. We showed that these measurements are sufficient to determine initial technical design criteria to start the development of an arthroscopic cutter. The feasibility of solutions can be judged with the help of these criteria before a prototype is built.

A substantial part of the current orthopaedic operative techniques involve the removal of tissue. However, data on the required cutting force for human tissues are absent. Usually, only the stiffness and maximum strength of human tissue are presented which are important to set up biomechanical models, but are of no use for the development of cutting instruments. With a simple experiment to determine the shear stress of meniscal tissue a start is made to fill in the missing data.

Another important design criterion that serves attention is the side-ways stiffness of the tip in one of its three orientations. The minimum side-ways stiffness has to be determined experimentally, but for the initial design of the steerable punch it seems reasonable to start with an allowable range of ± 5°.

In conclusion, with a simple method design criteria were set up for the development of a side-ways steerable punch. The design criteria should be complemented with additional criteria on sterilization, manual control of the punch, and robustness. A first prototype tested in cadaver knee joints should ultimately proof the concept.

6.3 Theory on ergonomics of handle design

All products, specifically all hand tools, have a certain functionality, which can be described as how suitable the tool is for its purpose; the possibility of achieving the goal with the instrument for which it was designed.[9,28] Functionality can be divided into two aspects: the first is usefulness, which deals with all aspects considering the working principle *(Table 6.3.1)*. The other aspect is usability, which takes the user into account who has to operate the product, and it covers therefore the user-friendliness of the product.[15] The characteristics of good handle design according to the theory are summarized in Table 6.3.1.[9,12,29,30] These characteristics were specified for the design of the handle of a steerable punch, and will be elucidated in this section.

Usefulness

In this study, relevant aspects for usefulness are positioning *(reachability)* and safety. The ability to position an instrument is determined by its geometry and the number of degrees of freedom the tip can be operated with inside the joint cavity. Earlier in this chapter, it was concluded that the current instruments lack degrees of freedom to reach the pathological tissue without instrument changes. Our observations pointed out that the reachability of the menisci can be improved with about 40% *(Table 6.1.1B)* when the tip of a punch is side-ways steerable and in an upward direction. The side-ways steerable tip could also increase the safety of an operation, because it is no longer necessary to exert large forces at the portal to reach the meniscal tissue. In addition to this, the problems that arise when inserting and extracting side-biters can be overcome, since the steerable tip can be placed in a straight position for insertion and extraction.

aspects considering handle design			requirements
functionality	usefulness	reachability	The locations are reached faster Less inter punch exchanges take place
		safety	Less tissue damage Smaller movements of shaft at incision resulting in less forces at the incision
	usability: cognitive ergonomics	self explaining	Learning curve is steeper than conventional instruments Working principle is understood by visual inspection The position of the tip is known by the position of the lever
		safety	Little mistakes in operating the handle The mental effort to operate the handle is low
	usability: physical ergonomics	support	The wrist excursions remain within the allowable region Holding the handle is more comfortable
		ergonomic control	The operation of the handle is more comfortable
	usability: sensorial ergonomics	force feedback	The transmission mechanism has a higher efficiency The operating force is within the most sensitive range

Table 6.3.1
Characteristics of good handle design are shown.[9,12,15,29,30] *A well-designed handle is adjusted to the cognitive, physical and sensorial aspects of the user in such a way that it prevents mistakes. In the right column, requirements are presented derived from the general criteria for ergonomic handle design for which it is expected that this leads to a good handle once these are fulfilled.*

Usability

The usability of an instrument consists of three elements: cognitive ergonomics, physical ergonomics and sensorial ergonomics.[15]

Cognitive ergonomics

The aim of cognitive ergonomics is to keep the mental effort low, by designing an instrument that is self-explaining in the environment in which it is used.[31] The self-explaining abilities of the instrument are subject to the appearance of that instrument. A well-designed instrument serves as an external memory by exchanging information with the user. The mental effort of the user is kept low due to the external memory.[32] To be effective as an external memory the control of an instrument should be simple, because the amount of functions that the instrument supports, determines how complex it is to operate.[33] The theory of external memory is applied to the steerable punch introduced in this study. This implies that the fewer degrees of freedom the surgeon has to control, the less complex the instrument can be, and the lower the mental effort of the surgeon has to be when operating the handle. This supports the choice to develop two steerable punches with each having only one additional degree of freedom that has to be controlled. When an instrument is self-explaining it ideally causes no human errors and therefore improves the safety of the clinical operation.[30]

The design of the handle also has to be in accordance with the knowledge and experience of the surgeon. This implies that the handle should be designed such that the functions are operated with the same working principle as the surgeon is used to or should be operated completely differently, since then the surgeon starts a new learning process to control the handle instead of having to adjust his routinely control of the handle.[34] This way, mistakes in controlling the handle are avoided assumed that the learning process of a completely new handle is intuitive and short. For example, if the control of the new handle is in accordance with the control of the current instruments, but the effect of the action is different, the surgeon may automatically act wrongly, because he is used to the effect resulting from the control of the old instrument.[34] Therefore, the design should have the same scissors type handle with an extra lever to operate the side-ways movement, or completely different control levers. Furthermore, care has to be taken with the subject selection when testing a new handle in comparison with conventional handles, because the user's experience in using the conventional handle could bias the test results.[34]

Physical ergonomics

The aim of physical ergonomics is to offer physical comfort while controlling the instrument. This means that the size of the interface between surgeon and instrument has to match the anthropometric data of the surgeon, and the control of the instrument has to be in accordance with the movability of the upper extremities of the surgeon.[7,19,20,35,36] The shoulder, arm, and hand support the instrument. To prevent fatigue the joint excursions must be kept within the allowable ranges as shown in Table 6.1.2, and the weight of the instrument should be low.[6,6,14] Since, the instrument is sometimes not supported when inserted in the joint cavity, its center of mass should be at the portal to keep it in balance. This implies that the handle should have a low mass by using lightweight materials and as little material as possible.

The sort of grip used to hold the instrument largely influences the ability to position and to control the instrument. A distinction can be made between a power grip, a contact grip and a pinch grip or seizing grip, which can be further subdivided.[16,37,37] A pistol grip is advised for the positioning of the side-ways steerable punch, because this allows accurate manipulation of the instrument, but it also allows exertion of force.[38] In addition to this, a pistol grip supports the observed practice of positioning the shaft of the instrument accurately by placing the index finger along the shaft. In order to guarantee comfortable manipulation, no pressure should be exerted on the dorsal side of the hand, since it will lead to degeneration of the skin and underlying structures.[7] To control the instrument the index finger and the thumb are most suitable.[7]

Sensorial ergonomics

Sensorial ergonomics deals with the human senses and human perception.[15] The main sensorial interaction between the surgeon and a device during endoscopic surgery is the image display.[15] This aspect is not studied in this project. It is assumed that the surgeon normally has sufficient arthroscopic view during the operation. Force feedback is another subject in the field of sensorial ergonomics. Due to the usage of an instrument the force feedback is reduced, which is due to the force transmission characteristics of the instrument, and not so much due to the handle. Furthermore, it was observed that force feedback is of minor importance when performing a meniscectomy. There is one aspect that should be taken into account for both the handle design and the tip of the instrument. That is the force needed to cut meniscal tissue. When the value for the cutting force is known, the strength of the instrument, and the transmission ratio from tip to handle can be calculated. The allowable force when controlling the lever with the thumb ranges from 28 to 48N.[39] As a start, we determined an operating force of about 16N with the current straight punch that has a scissors handle and a lever arm of 75 mm, when cutting is performed in fixed cadaver meniscal tissue.[9]

Conclusions

From literature, a number of guidelines is determined for the design of an ergonomic handle. Most information is obtained from general ergonomics on hand tools design and from the design of laparoscopic handles for which it was previously recognized that the instrument handles are unergonomic. In Section 6.4, it is shown that the general ergonomic requirements were integrated in a new handle for the suggested side-ways steerable punch.

6.4 Ergonomic handle for an arthroscopic cutter with a steerable tip

This section is based on the paper *Ergonomic handle for an arthroscopic cutter*, by G.J.M. Tuijthof, S.J.M.P. van Engelen, J.L. Herder, R.H.M. Goossens, C.J. Snijders, C.N. van Dijk, Minimally Invasive Techniques and Allied Technologies, 12 (1/2), 2003.

Keywords: arthroscopy, ergonomics, handle, steerable tip, experiment

Abstract: From an analysis of the routinely performed meniscectomy procedures, it was concluded that a punch with a side-ways steerable tip would improve the reachability of meniscal tissue. This potentially leads to a safer and more efficient meniscectomy. Furthermore, the current scissors handles of arthroscopic punches are ergonomically not sufficient. An ergonomic handle is designed with one lever that enables opening and closing of the instrument tip, and side-ways steering of the instrument tip. The design of the handle complies with ergonomic guidelines that were found in literature. To evaluate this handle in comparison to conventional handles it was necessary to add a model of the instrument tip. Experiments were performed with a knee joint model, and both objective and subjective criteria were used. The results show that the concept of a side-ways steerable punch is promising, since faster task times are achieved without increasing the risk on damaging healthy tissue. The current design of the ergonomic handle incorporates two degrees of freedom in an intuitive way, is more comfortable to hold, and is easy to control. The external memory capabilities of the new handle could be improved. Further development of this handle and the addition of a sufficient instrument tip and force transmission are recommended.

Introduction

Access to the knee joint is routinely obtained from the anterior side of the joint where two portals are placed at the joint level medially and laterally from the patellar tendon.[3,40] Due to the convex shape of the condyli of the femoral bone, optimal portal placement is necessary in order to be able to reach the anterior and posterior horn of the menisci with straight instruments. Curved instruments have been developed to facilitate the access to all parts of the menisci *(Figure 6.1.2)*.

During observations of meniscectomy procedures, it was noticed that often several punches were needed to perform the operation *(Table 6.1.1)*.[9,10] The use of a large number of these punches has a number of negative side effects *(Section 6.1)*.

To meet with the disadvantages mentioned above, it was suggested to develop a punch with a steerable tip, which was positively received by surgeons.[18] It appears that the upward punches and side-biters are used as frequently, but they are not used within the same procedure. In order to prevent the handle from becoming too complex to control, it was decided to develop a punch with a side-ways steerable tip and a punch with an upwards steerable tip. We focused on the punch with a side-ways steerable tip, because the side-biters are likely to cause most damage when inserting and extracting them from the joint cavity. In literature, no attention is paid so far to the design of handles for arthroscopic instruments.

In this paper, we present results of an experiment performed with a prototype of a new

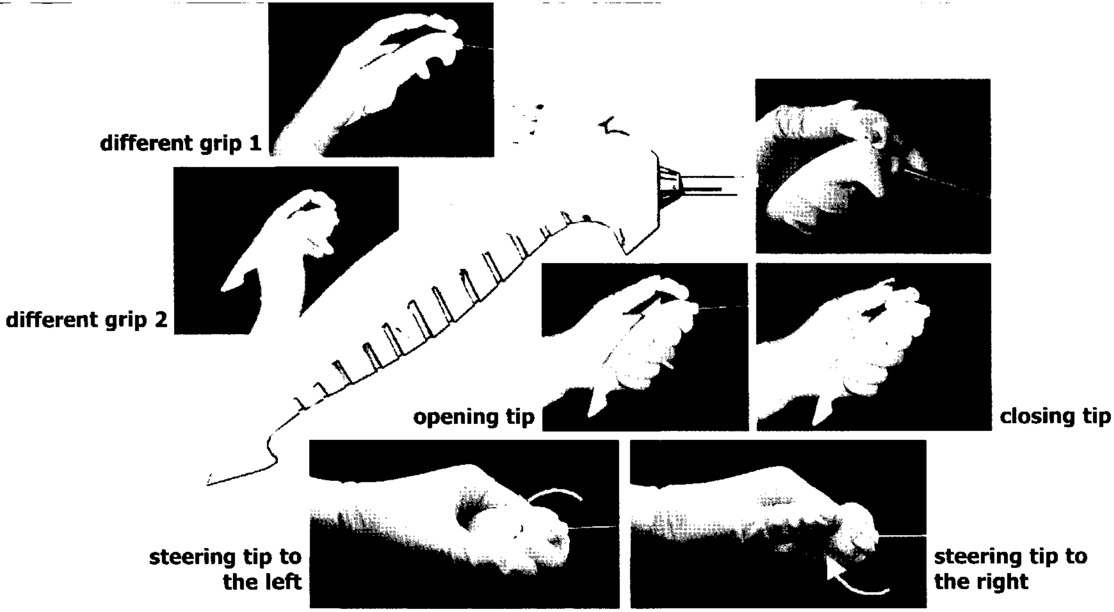

Figure 6.4.1
Color illustration see cover. Design of the ergonomic handle. In the picture a drawing of the concept is presented as well as the working principle of the lever. It is shown that the handle can be held and operated with different grips.

ergonomic handle for a punch that bears the capability to control of two degrees of freedom, which are up and down movement *(cutting of tissue)*, and side-ways movement *(steering of the tip)*. Evaluation of the side-ways movement was performed in a simulated clinical setting. A complete model of the steerable punch consisting of the handle and an end-effector was used, since the functionality of the handle depends on its relation with the end-effector, and evaluation of its perfomance should thus take place with a complete instrument.

Materials and Methods

Handle design

With the help of the presented analysis of the clinical practice *(Table 6.1.1)*, and guidelines from ergonomics[7,12,15,16,19,30,37,41] specific requirements were derived for the design of the handle:

- The handle should have two control options; one for opening and closing the tip, and one for side-ways positioning.
- Self explaining[30]: the instrument should show its possible control options. the instrument should indicate its tip position by means of the handle.
- The handle should be controlled with one hand, which can be either the left or the right hand; the surgeon holds the arthroscope in the other hand.[7]
- Control switches of the handle should be within reach of the thumb or the index finger to be able to operate the handle while maintaining a stable grip.[7,20]
- The design of the handle should fit the hand sizes.[7,35-37]
- The joint excursions during the operation should be within allowable ranges *(Table 6.1.2)* while operating the handle.[7,11,12]

Furthermore, there are additional restrictions concerning reliability, reusability, and maximum pressure on the hand during operating the steerable punch.[7] After considering several potential designs, the concept presented in Figure 6.4.1 was chosen. The concept consists of a pistol shaped handle with one lever for both opening and closing of tip, and side-ways positioning *(Figure 6.4.1)*. When the lever is moved to the left, the instrument tip moves to the right, and when the lever is moved upwards, the instrument tip is opened. The shape of the handle enables a stable position in the hand, prevents pressure peaks on the skin, and enables operating the handle with different grips thereby giving the surgeon freedom to control it as he/she likes

Table 6.4.1 Requirements as derived from ergonomics[9,12,15,29,30] that are made operational to judge the functionality of the new ergonomic handle in comparison with the current handles used for punches. The requirements that are printed in italics could not be tested adequately with the used experimental set up.

requirements	objective	subjective
1. The locations are reached faster	Task times (sec.)	
2. *Less inter punch exchanges take place*	*Number of exchanges (n)*	
3. Less tissue damage	Number of unallowed tissue contact (n)	
4. *Smaller movements of shaft at the incision resulting in less forces at the incision*	*Range of shaft rotation at incision in transversal plane (°)*	
5. Learning curve is steeper than conventional instruments	Slope of regression line fitted through the average of the six trial times	
6. Working principle is understood by visual inspection		Question (Good or False)
7. The position of the tip is known by the position of the lever		Question (Good or False)
8. Little mistakes in operating the handle	Number of mistakes (n)	
9. The mental effort to operate the handle is low		Mental score (percentage)[44]
10. *The wrist excursions remain within the allowable region*	*Angles see table 6.1.2 (°)*	
11. Holding the handle is more comfortable		Question (True or False)
12. The operation of the handle is more comfortable		Question (True or False)

(Figure 6.4.1).[37] The shape of the lever is designed such that it allows sufficient information feedback to the surgeon *(the position of the handle indicates the position of the tip)*, makes it possible to control the lever with different grips and is easy to produce. The length of the lever is large enough to allow the surgeon to apply a sufficient moment with his/her thumb to cut meniscal tissue *(20 mm)*. This length was determined with the help of the allowable force when controlling the lever which ranges from 28 to 48N[38,39], a reasonable contact area *(114 mm²)*, and the required moment to cut meniscal tissue *(0.68 Nm)*[9,42]. The moment for cutting meniscal tissue was measured in a simple experiment with a conventional punch and an unster.[9] Both the handle and the lever are dimensioned according to the anthropometric data of the hand.[19,35,36]

Experiments

A combination of objective and subjective evaluation criteria is commonly used in handle evaluation, and this is also applied in this study.[6,14] The specified requirements for ergonomic handle design *(Table 6.3.1)* were also used to assess the functionality of the handle in comparison with the conventional handles of the punches *(Table 6.4.1)*. The handle is considered to have potential if it scores better in comparison with the currently available arthroscopic handles.

Objective measurements

To evaluate the new handle's usefulness, it was attached to a model of the instrument tip of the steerable punch *(Figure 6.4.2)*, and with this instrument a meniscectomy was performed in an experimental model of the knee. It was decided to add a model of the instrument tip, since no mechanism was available that was suitable for usage in an experimental clinical setting. The shaft of the instrument model has a diameter of 5 mm, and has a side-ways steerable tip which is 11 mm long. Both the shaft and the tip are slightly larger than the average conventional punches *(diameter 3.4 mm and tip length 8 mm)*. A transfer mechanism between the handle and the tip consists of four wires that enable opening and closing of the tip, and side-ways positioning of 90° to the right and 90° to the left. The original handle design was slightly changed to incorporate the mechanism for steering the tip *(Figure 6.4.1-6.4.2)*. Due to the provisional mechanical embodiment, it was not possible to exert cutting forces with this instrument model *(Figure 6.4.2)*. The focus of the experiment was on positioning of the instrument tip, and control of the handle.

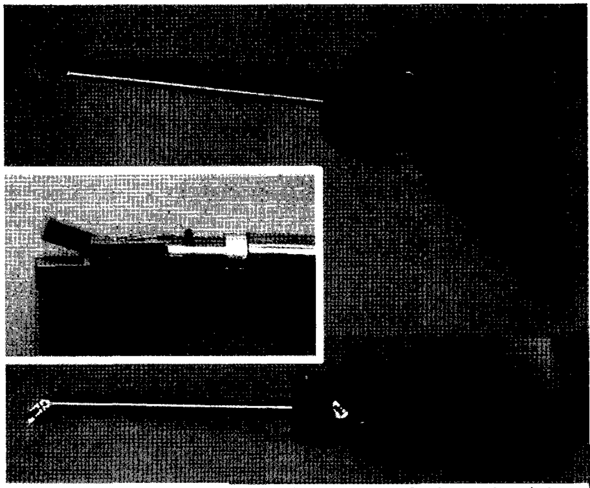

Figure 6.4.2
Picture of the model of the ergonomic handle including a shaft and a steerable tip. The appearance is slightly different compared to Figure 6.4.1 due to constructive demands for the transmission device from handle to tip. The tip is part of the experimental set up, which implies that this is not a realistic appearance of the final design of the steerable punch, but its function is sufficient to test the handle.

The experimental set up included an artificial model of a right knee joint, three conventional punches *(two side-biters (type 010913 and 010912) and one straight punch (012044), Smith & Nephew BV,*

Figure 6.4.3
Pictures of parts of the experimental set up.

A) Picture that is seen on the monitor of the computer. It shows the menisci with the colored contacts and the arrow that indicates the contact that has to be touched.

B) The knee joint model. The inner side contains the menisci with five colored contacts that are electrically connected to the computer.

C) Iron gauze shaped in the form of the femur condyli.

D) The circles indicate the three portals: a medial portal where the arthroscope is inserted, and two lateral portals, of which one is ideally placed (1), and the other one is more medially placed (2).

E) Camera to record the movements inside the joint. Although these portals are located close to each other, their locations influence the reachability inside the joint greatly.

F) A device that transmits the electric signals from the knee model to the computer.

G) Model of the instrument with steerable tip.

H) The three conventional punches (two side-biters, and one straight punch). The tips of the four instruments were isolated in such a way that only the front of the tip could make electrical contact with the colored electrical contacts on the menisci.

I) Computer.

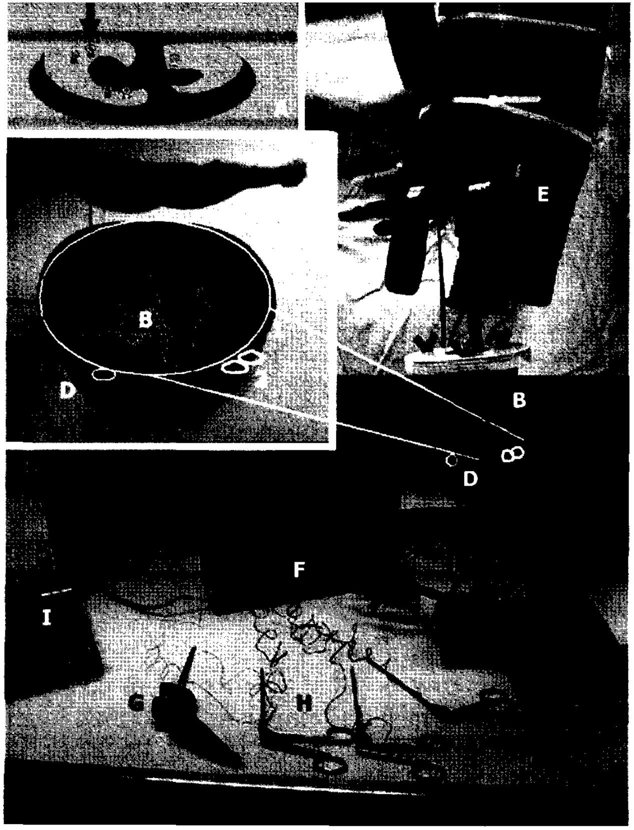

Hoofddorp, The Netherlands), an arthroscope, a monitor, a computer, a video camera, and the handle with the model of the instrument tip *(Figure 6.4.3)*. The removal of tissue was simulated by electrical connection of an instrument tip and an electrical contact on the menisci. The electrical signals were transmitted to a computer. In the knee joint model three portals were made: a medial portal and two lateral portals, of which one was ideally placed *(Figure 6.4.3: Portal 1)*, and one placed more medially *(Figure 6.4.3: Portal 2)*. The tibia and femur were constructed of metal gauze which was also electrically connected to the computer *(Figure 6.4.3)*. The gauze represents the vulnerable cartilage layers that can easily be damaged. On each gauze contact with one of the punches, one unallowed tissue contact was recorded, which imitated possible cartilage damage caused by an instrument.

Sixteen orthopaedic trainees participated in the experiment. They were asked to perform a meniscectomy on the knee joint model. Their arthroscopic experience ranged from 0-25 arthroscopic procedures per year. Performing a simulated meniscectomy consisted of positioning instruments along a trajectory of the colored contacts on the menisci randomly generated by the computer. The arthroscope is placed in the medial portal. There are four conditions: C1) conventional instruments with Portal 1, C2) conventional instruments with Portal 2, C3) steerable punch with Portal 1, and C4) steerable punch with Portal 2 *(Figure 6.4.3)*. Each condition was performed three times, after which a second session with all conditions was started. The subjects were given the opportunity to practice before the actual experiment was started. The Latin square method was used to eliminate the learning effect for statistical analysis.[43] The task given to each subject was to perform a trajectory as fast as possible with as few unallowed tissue contacts as possible. For each trajectory the trial time *(Table 6.4.1: Requirement 1)*, and the number of unallowed tissue contacts *(Requirement 3)* were recorded. Significant difference between the trial times and the number of unallowed tissue contact for the four conditions was determined by a two-way analysis of variance test *(ANOVA, $p < 0.05$)*. The learning curve for each condition is determined by a linear regression line fitted through the averaged task times of the six trials per condition *(Requirement 5)*. The slope of these curves is a measure for

learning speed. The movements of the instrument tips as well as the hand movements of the subjects are recorded by a video camera. The number of operation errors when using the new handle were assessed by analysis of the video *(Requirement 8)*.
Due to the experimental set up three evaluation criteria could not be tested adequately *(Table 6.4.1 printed in italics)*. Requirements 2 and 4 were already incorporated in the set up, since the subjects were forced to interchange with the conventional punches in order to reach the contacts. No attempts were undertaken to reach a contact with a less suitable punch. The knee joint model allowed to reach all contacts with the steerable punch without interchanges. Lastly, Requirement 10 could not be tested, since opening and closing of the handles was not allowed during the tests, and therefore the handles of the conventional punches were held differently than is commonly done during actual operations.

Subjective measurements
The sixteen subjects were asked a number of questions to assess the usability of the handle, and to document suggestions for improvement of the handle. The self-explaining capacities of the new handle were tested by asking the subjects how they expected the steerable punch would operate *(Requirement 6)*. A memorability test was performed in-between two sessions for which the new handle with instrument model was placed in a certain orientation in the knee joint model, and the subject had to indicate the tip orientation by visual inspection of the handle *(Requirement 7)*. The mental effort of the four conditions was tested by six questions concerning level of activity, force to position the tip, time pressure, success, fatigue, and frustration *(Requirement 9)*. This test scores the mental effort to perform the task of which the instrument

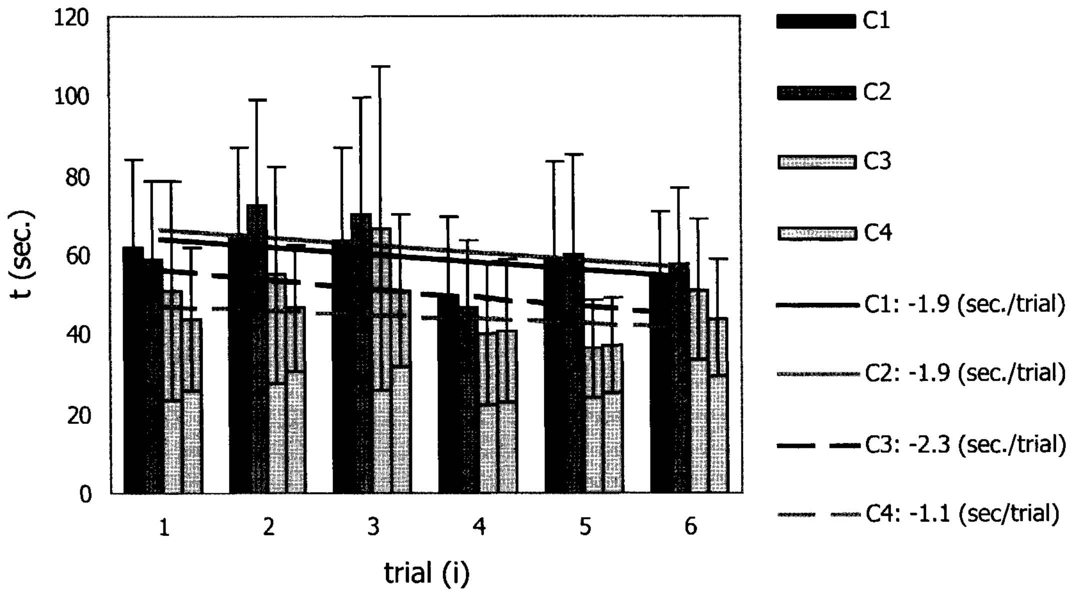

Figure 6.4.4
Results of the trial times for performing the artificial meniscectomy for the four conditions. C1: conventional instruments with Portal 1 (Figure 6.4.3), C2: conventional instruments with Portal 2 (Figure 6.4.3), C3: steerable punch with Portal 1, C4: steerable punch with Portal 2. The columns give the average task times of the sixteen trainees, thus the variation indicated is due to the differences among the subjects. For each condition the learning curve is added, and the proportional factor between the trial and the trial times is given.

Figure 6.4.5
Results of the numbers of unallowed tissue contact, when performing the meniscectomy on the knee joint model.
C1: conventional instruments with Portal 1 (Figure 6.4.3), C2: conventional instruments with Portal 2 (Figure 6.4.3), C3: steerable punch with Portal 1, C4: steerable punch with Portal 2.

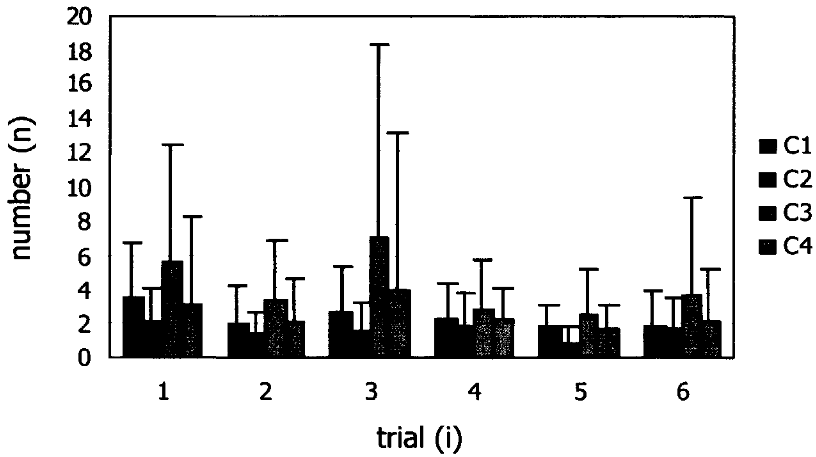

is a part. The NASA-TLX method was applied to score the mental effort on a scale of 10 cm, in which the full scale corresponds to 100% mental effort.[44] Thus, a higher percentage corresponds to higher mental effort. The average percentage of each question per condition was calculated.

Results

The trial times for the steerable punch are significantly lower than for the conventional punches, *F(1,16)*=23.16, $p<0.05$, and accounted for a meaningful proportion of the variance, ω^2=60.7% *(Figure 6.4.3)*. There is no significant difference between the two instrument portals *(Portals 1 and 2)*, however, there is a significant difference for the combination of a portal and an instrument *(F(1,16)=7.66, p<0.05)*, in favor of the steerable punch. The slopes of the learning curves for the conventional instruments are alike *(Figure 6.4.4)*. The slope of C3 *(steerable punch, Figure 6.4.3: Portal 1)* is the steepest, whereas the slope of C4 *(steerable punch, Figure 6.4.3: Portal 2)* is the flattest. The curves of C3 and C4 are located below the curves of C1 and C2. Considering the number of unallowed tissue contacts *(Figure 6.4.5)*, there is no significant difference between the conventional instruments and the steerable punch, but there is a significant difference between the two portals *(F(1,16)=5.58, p<0.05)*, in favor of the Portal 2, the more medially placed portal. During the tests it has been noticed that four persons operated the handle of the steerable punch wrongly once or twice, thereby steering the instrument tip into the wrong direction.

The answers to the questions of the subjective criteria are summarized in Table 6.4.2. The answers to the mental effort scale for each condition show a large variation for each question and condition *(standard deviation from 15% to 29%)*. The mental effort test shows that the task was probably not very difficult to perform. The more experienced subjects apparently lost their concentration, because the task could probably be too simple. This is supported by increasing trial times where one might expect decreasing trial times. Furthermore, it is difficult to relate the results of the mental effort test specifically to the use of the instruments, since the NASA-TLX method scores the entire task of which the handling of the instruments is a part.

A number of suggestions is given to improve the handle. Most subjects prefer more than three possible orientations of the tip to be able to follow the contour of a meniscus lesion more accurately. The orientations should ideally be adjusted continuously. All subjects have been able to mention the potential advantages of the side-ways steerable tip, and some indicate that less instrument changes would lead to a more unperturbed progression of the operation as an additional advantage.

	subjective criteria	score				
6	Working principle is understood by visual inspection	open tip	close tip	steer tip to left	steer tip to right	
	Percentage correct	75%	75%	69%	69%	
7	The position of the tip is known by the position of the lever	Tip positioned to the left				
	Percentage correct	77%				
9	The mental effort for each condition	Condition 1	Condition 2	Condition 3	Condition 4	No preference
	Activity level	40%	34%	41%	38%	
	Force to position	14%	17%	17%	17%	
	Time pressure	15%	21%	17%	18%	
	Rate of success	42%	52%	51%	52%	
	Rate of fatigue	29%	26%	28%	28%	
	Rate of frustration	17%	23%	31%	23%	
	Which condition is the most difficult to perform? (percentage of subjects)	19%	25%	19%	13%	25%
11	Which handle is more comfortable to hold?	conventional handle	new handle	No preference		
	(percentage of subjects)	25%	56%	19%		
12	Which handle is more comfortable in control? (percentage of subjects)	19%	69%	13%		
	Which operation would you prefer?	1 lever, 1 finger	2 levers, 1 finger	2 levers, 2 fingers		
	(percentage of subjects)	63%	6%	31%		

Table 6.4.2
Results of the subjective criteria for sixteen trainees who performed 384 trajectories in total. A high percentage of the mental effort corresponds to a high mental effort.[44]

Discussion

From the results, it can be concluded that the functionality of a steerable punch is potentially good, since the use of this instrument leads to quicker trial times in comparison to conventional punches, while not increasing the number of unallowed tissue contacts in comparison to conventional punches. When placed in a slight malposition of the access portal the steerable punch performs better. This is important, since it is obvious that ideal portal placement is difficult to obtain for every patient. It is dependent on the individual anatomy of the patient and the experience of the surgeon. The model of the steerable punch has a thicker shaft and a larger tip in comparison to the conventional punches. Despite its larger size no significant increase in unallowed tissue contact was detected using the model of the steerable tip. This is an encouraging result, since it is expected that evolution of the design to the same geometry could be accompanied by even less undesired contacts, and an improved arthroscopic view. The learning curves of the new ergonomic handle compare favorably with the conventional handles, since those curves are located below the curves of the conventional handles. Furthermore, they are flat which indicates that no learning is required to control the new ergonomic handle.

Ideally, a handle is well designed when the user understands the working principle of the handle immediately as by intuition.[30,45] 11 of the 16 trainees understood the working principle of the handle by visual inspection only *(Requirement 6)*, and 12 of the 16 trainees memorized the working principle *(Requirement 7)*. Therefore, the appearance of the handle could be improved to enlarge the external memory capabilities. The number of subjects who prefer the new handle is twice the number who prefer the conventional handle *(Requirement 11)*. The main reasons are the greater comfort, and the fact that no attention has to be paid to hold the handle. The new handle resulted in quicker positioning while no exchanges were needed to perform a complete meniscectomy, which enabled the trainees to view the operation area continuously. The possibility to control both functions of the steerable punch with one lever and one finger was received positively. This did not only result in a quicker performance, but also in a more effective use of the handle as an extension of the body *(Requirement 12)*.[30,45] The mental effort test *(Requirement 9)* showed no significant difference between the four conditions, which is supported by the variety in answers to the question which was the most difficult condition. The question is if this mental effort test is suitable for this for this type of experiment. A set up resembling the clinical practice more realistically and causing more stress might detect a distinction between the four task conditions, however this first has to be tested.

Problems we encountered were related to the side-ways stiffness of the model's tip in one of the three fixed positions. This stiffness was barely sufficient, yet appeared to be essential to control the tip. This finding has to be included in the actual design of the tip, and the force transmission.

In conclusion, the new handle scores also better in comparison with the conventional instruments considering the subjective evaluation criteria.

Another aspect that needs further attention is the size of the force that the surgeon has to apply in order to meniscal tissue. Estimations indicate that the current configuration of the lever is sufficient to apply the required cutting force. However, tests have to be performed to verify whether or not the force can be applied easily in every position of the lever, and still can be controlled intuitively. Force feedback is probably of minor importance for good functioning of the

handle, since meniscal tissue is not as delicate as for example bowel tissue, and most often the operative field can be adequately inspected by direct vision which provides visual feedback *(Section 6.1)*.
The overall conclusion is that the concept to develop a side-ways steerable punch is promising, and could lead to a safer and more efficient performance of a meniscectomy. The current design of the ergonomic handle appears to incorporate two degrees of freedom in an intuitive manner. The major advantage of the new handle in comparison to the conventional handles is the improved comfort. However, the external memory capabilities could be improved. Further development of this handle and the addition of a sufficient instrument tip and force transmission are recommended.

6.5 Discussion

With the help of the clinically driven approach, an analysis was performed of the current available techniques of performing meniscectomy procedures. It was concluded that a punch with a side-ways steerable tip could improve the reachability of meniscal tissue, which prevents instrument exchanges with the current straight punches, and which reduces the maximum excursions of the wrist. Design criteria were formulated, in which distinction was made between criteria for the control and ergonomics of the handle, and criteria for the instrument tip. This is an important step in the development of an instrument, since the verbal description of an idea or requirement has to be translated into technical, quantifiable dimensions. Performing this process enables a continuous focus and redefinition of the final result that has to be reached. In this case, the goal is an as safe and an as fast as possible operative procedure with the least damage to healthy tissue, which enables the surgeon to focus entirely on the procedure itself. Furthermore, careful analysis with the operative goal in mind can offer simple solutions. For example, it appeared that the upswept punches and side-biters were not used during the same operation. This made it possible to drop an extra degree of freedom making the control and construction of the punch less complex. Another example is the determination of the tip length. It was first determined that the length should vary with the orientation angle. However, after realizing that during surgery in humans the portals have a certain amount of flexibility, and the shaft can be positioned along its longitudinal axis, it was concluded that a variable tip length was unnecessary.
The challenge of the steerable punch is the integration of a steering function that is perpendicular to a cutting function within a diameter of 5 mm, and the integration of a large range of motion and a high workload. If only attention is paid to the steering function, several mechanisms can be found in literature.[46-51] With the design criteria each mechanism can be judged on its feasibility.
Since the conventional scissors handle is far from optimal, and an additional switch to control the side-ways movement had to be integrated, theory on the ergonomics of hand tools were specified for the steerable punch. To test the use of this ergonomic handle a prototype was made. The results were in favor of the prototype, and revealed a number of additional requirements of the surgeons participating in the experiment.
The next step will be the integration of all design criteria into a complete design of the side-ways

steerable punch including a handle, a force transmission, and an instrument tip, that can be tested in cadaver knee joints, and subsequently in human beings.

References

1. van Dijk, C. N. Beweegredenen, de patient als bron van inspiratie. Inaugural, 14-3-2002. University of Amsterdam, Amsterdam.

2. Kelly MA, Fithian DC, Chern KY, Mow VC. Structure and function of the meniscus: basic and clinical implications. In: Mow VC, Ratcliffe A, Woo SL-Y, eds. *Biomechanics of diarthrodial joints.* New York: Springer-Verlag, 1990. ISBN 0-387-97378-8.

3. Sisk TD. Arthroscopy of knee and ankle. In: Crenshaw AH, ed. *Campbell's operative orthopedics.* St. Louis: CV Mosby Company, 1987;2547-2608. ISBN 0-8016-1065-6.

4. Breedveld P. Stassen HG. Meijer DW. Jakimowicz JJ. Manipulation in laparoscopic surgery: overview of impeding effects and supporting aids. *J Laparoendosc.Adv.Surg Tech.A* 1999; 9: 469-480.

5. Van Veelen MA. Goossens RHM. Jakimowicz JJ. Snijders CJ. Jacobs JJ. Meijer DW. New ergonomic guidelines for laparoscopic instruments. *Min Invas Ther & Allied Technol* 2001; 10: 163-167.

6. Berguer R. Forkey DL. Smith WD. Ergonomic problems associated with laparoscopic surgery. *Surg Endosc* 1999; 13: 466-468.

7. Matern U. Principles of ergonomic instrument handles. *Min Invas Ther & Allied Technol* 2001; 10: 169-173.

8. Stuchin S. Biomechanica van de pols. In: Snijders CJ, Nordin M, Frankel VH, eds. *Biomechanica van het spierskeletstelsel, grondslagen en toepassingen.* Utrecht: Lemma BV, 1995. ISBN 90-5189-278-0.

9. Engelen SJPM van. Ontwerpvoorstel voor een stuurbare arthroscopische operatietang met ergonomische bedieningsinterface. Product & Systems Ergonomics, Department of Design, Engineering and Production, Delft University of Technology, 2000: 1-113.

10. Cals RHH. Design criteria for a steerable instrument used for meniscectomy (S 888). Delft University of Technology, department of Design, Engineering, and Production, section Man-Machine Systems, 2001: 1-41.

11. Greenberg L, Chaffin D B. Workers and their tools: a guide to ergonomical design of hand tools and small presses. In: Buurman R den, Boersema KH, Christiaans HHCM, eds. *Ontwerpergonomie IDE230.* Delft: TU Delft, 1995;

12. Hedge A. Design of hand-operated devices. In: Stanton N, ed. *Human factors in consumer products.* London: Taylor & Francis, 1998;203-222. ISBN 0748406034.

13. Nguyen NT. Ho HS. Smith WD. Philipps C. Lewis C. De Vera RM. Berguer R. An ergonomic evaluation of surgeons' axial skeletal and upper extremity movements during laparoscopic and open surgery. *Am J Surg* 2001; 182: 720-724.

14. Matern U. Eichenlaub M. Waller P. Rückauer K-D. MIS instruments, An experimental comparison of various ergonomic handles and their design. *Surg Endosc* 1999; 13: 756-762.

15. Goossens RHM. Van Veelen MA. Assessment of ergonomics in laparoscopic surgery. *Min Invas Ther & Allied Technol* 2001; 10: 175-179.

16. Bullinger HJ. Ergonomische arbeitsmittelgestaltung I-Systematik. In: Buurman R den, Boersema KH, Christiaans HHCM, eds. *Ontwerpergonomie IDE230.* Delft: TU Delft, 1995;

17. Moes CCM. Ontwerpen van handwerktuigen; bedieningsmotoriek. In: Buurman R den, Boersema KH, Christiaans HHCM, eds. *Ontwerpergonomie IDE230.* Delft: TU Delft, 1995;

18. Tuijthof GJM, van Dijk, C. N., Herder JL, and Pistecky PV. Design of arthroscopic instruments: a clinically driven approach. Submitted to *Knee Surgery, Sports Traumatology, Arthroscopy.* 2002.

19. Molenbroek JFM, ed. *Op maat gemaakt, menselijke maten voor het ontwerpen en beoordelen van gebruiksgoederen.* Delft: Delftse Universitaire Pers, 1994. ISBN 90-6275-996-3.

20. Tilley AR, Henry Dreyfuss Associates, eds. *The measure of man and woman.* New York: John Wiley & Sons, Inc., 2002. ISBN 0471099554.

21. Jurgens HW, Aune IA, Pieper U, eds. *International data on anthropometry.* Dortmund: Federal Institute for Occupational Safety and Health, 1990. ISBN 92-2-106449-2.

22. Salvendy G, ed. *handbook of human factors and ergonomics.* New Delhi: Wiley, 1997. ISBN 0-471-11690-4.

23. Putz R, Pabst R, eds. *Sobotta, atlas van de menselijke anatomie.* Houten: Bohn Stafleu Van Loghum, 1994. ISBN 90-313-1733-0.

24. Platzer W, ed. *Sesam, atlas van de anatomie bewegingsapparaat.* Baarn: Bosch & Keunig, 1998. ISBN 90-414-0252-7.

25. Visible Human project. Internet. 2002. http://www.nlm.nih.gov/research/visible

26. Somso Modelle. Catalog (A74/1). 1997.

27. Luttervelt CA van. Scheidende bewerkingen. In: Luttervelt CA van , ed. *Inleiding vervaardigingskunde w53, w56.* Delft: Delft University of Technology, 1993;4.1-4.2

28. *Telematica ide 432.* Delft: Faculty of Industrial Design, Delft University of Technology.

29. Sperling L. Dahlman S. Wikstrom L. Kilbom A. Kadefors R. A cube model for the classification of work with hand tools and the formulation of functional requirements. *Appl Ergon* 1993; 24: 212-220.

30. Gibson JJ, ed. *The ecological approach to visual perception.* Boston: Houghton Mifflin, 1979. ISBN 0-395-27049-9.

31. Voorhorst F. Affording action, implementing perception-action coupling for endoscopy. Delft University of Technology, 1998.

32. Kirlik A. Requirements for psychological models to support design: toward ecological task analysis. In: Flach J, Hancock P, Caird J, eds. *Global perspectives on the ecology of human-machine systems.* New Jersey: Lawrence Erlbaum Associates, 1995;68. ISBN 0-8058-1381-0.

33. Warren WH. Constructing an econiche. In: Flach J, Hancock P, Caird J, eds. *Global perspectives on the ecology of human-machine systems.* New Jersey: Lawrence Erlbaum Associates, 1995. ISBN 0-8058-1381-0.

34. Kanis H. Producten: functioneren en gebruik. In: Buurman R den, Boersema KH, Christiaans HHCM, eds. *Ontwerpergonomie IDE230.* Delft: TU Delft, 1995.

35. Fox JS. Bell GR. Sweeney PJ. Are orthopaedic surgeons really gorillas? *BMJ* 1990; 301: 1425-1426.

36. Barrett DS. Are orthopaedic surgeons gorillas? *BMJ* 1988; 297: 1638-1639.

37. Patkin M. A checklist for handle design. Ergonomics Australia On-Line. 1997. http://www.nlm.nih.gov/research/visible

38. An KN, Chao EY, Cooney WP, Linscheid RL. Forces in the normal and abnormal hand. In: Snijders CJ, Nordin M, Frankel VH, eds. *Biomechanica van het spierskeletstelsel, grondslagen en toepassingen.* Utrecht: Lemma BV, 1995. ISBN 90-5189-278-0.

39. Wagner D, Birt JA, Snyder M, Duncanson JP. Anthropometry and biomechanics. In: Wagner D, Birt JA, Snyder M, Duncanson JP, eds. *Human factors design guide.* Springfield, Virginia: National Technical Information Service, 1996;45.

40. Norman Scott W, Insall JN, Kelly MA. Arthroscopy and meniscectomy: surgical approaches, anatomy and techniques. In: Insall JN, Windsor RE, Kelly MA, Norman Scott W, Aglietti P, eds. *Surgery of the knee.* New York: Churchill Livingstone, 1993;165-216. ISBN 0-443-08734-2.

41. Buurman R den, Boersema KH, Christiaans HHCM, eds. *Ontwerpergonomie IDE230.* Delft: TU Delft, 1995.

42. Cals RHH. Design of a steerable cutting instrument for meniscectomy. Delft University of Technology, department of Design, Engineering, and Production, section Man-Machine Systems, 2002: 1-67.

43. Wagenaar WA. Note on the construction of digram-balanced latin squares. *Psych Bull* 1969; 72: 384-386.

44. Hart SG. Standard development of NASA-TLX. In: Hancock PA, ed. *Human factors psychology.* Amsterdam: Noord-Holland, 1987. ISBN 0-444-70319-5.

45. Simpson DC. The choice of control system for the multimovement prosthesis: extended physiological proprioception. In: Herberts P, Kadefors R, Magnusson R, Petersen I, Charles C, eds. *The control of upper-extremity prostheses and orthoses.* Springfield, Illinois: Thomas, 1974;146-150. ISBN 0-398-02869-9.

46. Griffiths JR. Surgical instrument with steerable distal end. Patent US5766196 (US19960739924 19961030). TNCO Inc., 16-6-1998.

47. Herder JL and Berg FPA van den. Statically balanced compliant mechanisms (SBCM's), an example and prospects. DETC2000/MECH-14144. 10-9-2000. Baltimore, Maryland, Proc. ASME DETC'00.

48. Jaeger JC. Surgical instrument with adjustable angle of operation. Patent US4763669 (US19870093009 19870904). Jaeger JC, United States of America, 16-8-1996.

49. Mukherjee R. Minor M. Song G. Satava R. Optimization of an articulated instrument for enhanced dexterity in minimally invasive therapy. *Min Invas Ther & Allied Technol* 1998; 7: 335-342.

50. Peirs J, Reynaerts D, and Brussel H van. Shape memory micro-mechanisms for medical applications. 155-160. 1997. IEEE, ICAR.

51. Poncet P and Dyk K van. Surgical device. Patent US5254130 (US19920867649 19920413). Raychem Corp, United States of America, 19-10-1993.

52. Volze RG, Lieb M, Benjamin J. Biomechanics of the wrist. In: Snijders CJ, Nordin M, Frankel VH, eds. *Biomechanica van het spierskeletstelsel, grondslagen en toepassingen.* Utrecht: Lemma BV, 1995. ISBN 90-5189-278-0.

53. Insall JN, Kelly MA. Anatomy. In: Insall JN, Windsor RE, Kelly MA, Norman Scott W, Aglietti P, eds. *Surgery of the knee.* New York: Churchill Livingstone, 1993;1-20. ISBN 0-443-08734-2.

54. Arnoczky SP. Structure and biology of the knee meniscus. In: Mow VC, Ratcliffe A, Woo SL-Y, eds. *Biomechanics of diarthrodial joints.* New York: Springer-Verlag, 1990;177-190. ISBN 0-387-97378-8.

55. Moeller TB, Reif E, eds. *Pocket atlas of sectional anatomy.* New York: Thieme, 2000. ISBN 0-86577-813-2.

7. Conclusions and future research

7.1 Conclusions

The research presented in this thesis aims at the improvement of arthroscopic techniques and instruments. An important issue in this research is the philosophy that surgeons as users of the products have to be closely involved in the assessment of problem areas and the design of new instruments.

Clinically driven approach

To achieve the involvement of surgeons, a method called clinically driven approach was used and further developed. Observations during operations *(Chapter 2)* as well as literature studies *(Chapter 3)* give the engineer sufficient knowledge to communicate with a surgeon. The observations in combination with discussions lead to the identification of six clinically relevant research topics in the arthroscopic field. These are optimization of a clear view during operations, development of soft-tissue endoscopy, development of a minimal access technique for subtalar arthrodesis, optimization of the treatment of osteochondral defects, development of multifunctional instruments, and development of criteria and instruments to determine the quality of the procedure. To avoid fulfilling the specific needs of only one surgeon, the research topics were reconsidered by a larger population of experts in an interview. In general, surgeons are reasonably satisfied with the current techniques. However, it was pointed out that the current straight instruments give limited access to locations which are difficult to reach, and the limitations of equipment results in a sub-optimal view in joints. Problem areas that have priority are the optimization of the treatment of osteochondral defects, and the design of a steerable punch. Expansion of the arthroscopic techniques is not encouraged, but new techniques will be accepted if they show good results and if they are not significantly more difficult to perform.

Based on the clinically driven approach, it was decided to focus on a minimal access technique for subtalar arthrodesis, the optimization the view in joints and the development of a sideways steerable punch.

Each of the three topics was further analyzed by means of a specific literature study, additional observations, and discussions with surgeons *(Chapter 3, 5 and 6)*. This leads to the definition of the following problems, limitations and important factors for each topic:

Subtalar arthrodesis (Chapter 3)

- To analyze the subtalar arthrodesis techniques systematically, the procedure was divided into the following phases: measurement of malalignment, access, removal of cartilage, correction of subtalar alignment and fixation.
- The limitations of the current techniques for subtalar arthrodesis are: no well defined, accurate and reproducible measurement of malalignment and correction of the hindfoot, difficult access to the subtalar joint, and a weak fixation.

- Important factors to achieve a successful arthrodesis are: minimal damage to healthy tissues, removal of the cartilage and subchondral bone layers of the entire joint, and the compression of the joint surfaces to enhance fusion. It was concluded that it is important that a new technique provides for a fusion, no residual deformity, no morbidity, no pain and a quick recovery. Therefore, it is chosen to approach the subtalar joint arthroscopically. For the surgeon it is important that he can easily and accurately perform the procedure.

Arthroscopic view (Chapter 5)

- The creation of a clear overview in a joint is frequently a problem due to the malfunction or complexity of irrigation systems, suboptimal rinsing of the joint caused by inadequate sheath design, and soft tissues like fat or adhesions often impede the view at the operation field, especially in complex operations.
- There is no consensus on the optimal intra-articular pressure and combination of inflow- and outflow portal, and guidelines are missing to control the irrigation systems such that optimal view is achieved.
- No clear definition was found on optimal view.

Meniscectomy (Chapter 6)

- In more complex operations the reachability in the knee joint is a problem and leads to a large number of unnecessary instrument exchanges with the current straight instruments. These exchanges are potentially harmful to healthy tissue, whereas it carries the risk of introducing bacteria into the joint cavity.
- The upward punches and the side-biters are not used within the same operation. This is also in correspondence with the anatomy of the knee joint, and allows for the design of two instruments *(one instrument with an upward steerable tip and one instrument with a sideways steerable tip)* instead of one more complex instrument.
- The overall ergonomic judgement of the posture of the surgeon during a meniscectomy is positive. This is mainly due to the short operation time. However, the scissors handle of the punches is not ergonomic, and attention should be paid to include requirements for an ergonomic handle in the design.
- The mechanical removal of meniscus tissue is preferred, and force feedback during the cutting of tissue does not seem to be of great importance.

In conclusion, each individual problem area was thoroughly analyzed independently of a solution from a technical point of view, via a systematic approach. This revealed starting points for the improvement of certain techniques. Since a lot of effort was put in the analyses, it was possible to simplify the design of new instruments, or to establish merely guidelines for the usage of devices. Examples are the steerable punch for which the requirement of upwards steering and side-ways steering could be separated, and the usage of irrigation systems for which only guidelines had to be set up, instead of developing a complete new irrigation system.

Design process and design criteria

Requirements were set up for each research topic to improve the limitations and to incorporate the important factors derived in the analysis *(Chapter 4, 5 and 6)*. Technical data that were not available, but important to dimension the new instruments were experimentally determined. The available joint space of the subtalar joint and the knee joint were modeled by simple geometric shapes, for which the dimensions were measured. This approach was useful to determine an order of magnitude of the geometric boundary conditions. Furthermore, data on the machining force of meniscal tissue, cartilage and bone were measured as well as an order of magnitude of the fluid restriction of knee joints. All requirements were put together for each topic:

New technique to perform subtalar arthrodesis (Chapter 3)

The new technique for minimal access subtalar arthrodesis implies:

- A posterior arthroscopic approach with the patient lying in prone position.
- Determination and verification of an adequate correction peroperatively with the help of a new measurement device.
- Removal of cartilage and subchondral layers by means of a new instrument that preserves the complex joint shape, and that creates smooth bleeding contact surfaces to enhance optimal fusion.
- Temporary fixation by means of a new fixation device that is placed in the optimal fixation location, and that transfers its fixation function gradually to the fusion bridges of the bone.

The main focus was on the development of the measurement system and the instrument to remove cartilage *(Chapter 4)*. Important requirements for the measurement system are: measurement in weightbearing standing and in nonweightbearing prone position, the measurement should be quantitative, accurate, and reliable. In addition to this, it should be easy in handling, lightweight, sterilizability, and a quick, and noninvasive measurement are required. The hindfoot angle that was chosen is the angle between the midline of the calcaneus and the midline of the lower leg, when the patient is placed in a fixed position.

For the development of the instrument to remove cartilage and subchondral bone, it was derived that four aspects will enhance quick and solid fusion of the joint: removal of the subchondral bone and cartilage of the entire posterior facet, establishment of bleeding contact surface areas, preservation of the subtalar joint's shape, and the creation of smooth surface areas that increase the locations of true contact.

Optimization of arthroscopic view (Chapter 5)

- A descriptive model of two types of complete irrigation system was derived and validated with experiments performed in an set up including a physical joint model.
- A method was developed to determine design criteria for a sheath that improves joint irrigation, and to evaluate new designs in comparison with conventional sheaths.
- The design criteria for a new sheath include that the in- and outflow should take place through separate passages in the sheath, and that the cross-section of the passages should be as large as possible.

Steerable punch for meniscectomy (Chapter 6)
To improve the reachability during meniscectomy procedures, a sideways steerable punch was developed for which the following requirements hold:

- The menisci are approached from the portal located diagonally to the traumatized meniscus.
- The instrument should have a mechanism for sideways steering of the tip with three fixed orientations and opening and closing of the tip. The stiffness and strength of the tip should be sufficient in all three positions to cut the meniscus tissue.
- The handle should be self-explaining, controlled with one hand, should fit the hand sizes, and should keep the joint excursions within allowable ranges while operating the handle.

The translation from medical requirements to technical specifications was hampered, since no technical data were available of the dimensions of joint spaces and machining forces of tissues. A start was made to derive these data with simple experiments. Although the data merely gave boundary conditions, this appeared to be sufficient to dimension the concepts for the two cutting mechanisms, which were previously defined.
For the measurement system the first step was to define the angle to be measured. Eventually it was chosen to use simplicity of the mechanism and reproducibility as starting points. Thereto, the individuals were all measured in the same fixed position, and the hindfoot angle was determined with axes defined by bony landmarks that are easy to palpate. The choice was made for a mechanical device, since although telemanipulators might be more accurate than a mechanical device, they are likely to be more time-consuming, it will take more preparation to measure the angle inside the operation room, and they cannot be easily moved from one place to another. Since, the subtalar arthrodesis is a procedure that is not frequently performed surgeons are probably not willing to acquire an expensive system.
To optimize arthroscopic view, joint irrigation was investigated as a starting point. This lead to improved arthroscopic view, which was demonstrated by experiments. Results show that taking into account simple guidelines the irrigation systems can be used optimally, and a redesign of an arthroscopic sheath is required, since this causes the main limitation in current joint irrigation.

Prototypes and guidelines

The solutions developed to improve the investigated procedures were verified by means of prototypes. This resulted in the following conclusions.

Measurement system (Chapter 4)
The dimensions of the prototype of the measurement system were chosen adequately, since all subjects fitted in the system. The measurement system proves to be able to measure hindfoot angles that are consistent with the clinical diagnosis, and with values found in literature. It allows for measurement in weightbearing standing and nonweightbearing prone position. The intratester reliability and intertester reliability were in the same range as found in literature, whereas the accuracy of the measurement system is slightly better. It is derived that the hindfoot

angles of subjects are symmetric within a range of 2°, which is probably sufficient to use the opposite leg as reference for performing correction. This supports the possible application of this concept in clinical practice.

Instrument to prepare the subtalar joint arthroscopically for fusion (Chapter 4)
The practical embodiment of the instrument consists of a drill actuated by a steel cable, which can be passively controlled. The cable is placed in a shaft that is flexible in one direction, which makes it possible to follow the contour of the joint surfaces. The shaft is stiff in the other direction to resist tooling forces of the drill. A frame at the tip allows for passive control of the instrument. The instrument can be used on combination with conventional shaver systems. Experiments prove that most requirements are met, but the combination of functions in the prototype needs fine tuning.

Guidelines for usage of irrigation systems (Chapter 5)
It is advised for the gravity pump to use the separate cannula as inflow portal, and to start with a low suction level when a separate suction device is used. For the automated pump it is advisable to determine the pressure sensor location that provides the feedback signal with which the pump is controlled. Once this is known, care should be taken to include the sheath-scope combination in the feedback control loop of the automated pump.

Arthroscopic sheath (Chapter 5)
The prototype of the new sheath consists of a tube with a removable partition that has to be used in combination with a 2.7-mm arthroscope which is placed asymmetrically in the tube. The new scope-sheath combination demonstrates to have a 4 times lower fluid restriction, which allows for a significantly quicker irrigation of the joint. In the case of the three-portal technique the irrigation time is about a factor 10 shorter when the new sheath is used. When using the two-portal technique, for which in- and outflow take place via the same portal, the irrigation time is reduced by a factor 2 in comparison to the conventional sheath.

Handle of steerable punch (Chapter 6)
The prototype of the steerable handle consists of handle that can be held with several different grips, and incorporates one lever with which opening and closing of the tip as well as side-ways steering can be controlled. The concept to develop a sideways steerable punch is promising, and could lead to a more safe and efficient performance of a meniscectomy. The current design of the ergonomic handle appears to incorporate two degrees of freedom in an intuitive way. The major advantage of the new handle in comparison with the conventional handles is the greater comfort. However, the external memory capabilities could be improved. Further development of this handle and the addition of a sufficient instrument tip and force transmission are supported by surgeons.

All the prototypes met the assumptions and requirements that were derived from prior analysis. Although further development is necessary, no conceptual changes are to be foreseen.

7.2 Future research

In this thesis a research line is set up for which three topics were addressed in more detail. A lot of material is left to continue improvement of arthroscopic techniques and instruments in order to facilitate the procedures and improve safety. In addition to the possible research topics that were identified but not further explored, some loose ends remain for the topics that were addressed.

Technical data of joints

The assessment of the geometric dimensions of the joints and the machining forces of different human tissues are important for the design of any instrument that is used to machine the human tissues. Surprisingly, these data are missing in literature. Therefore, research should be started to set up a complete overview of technical data for joints. To simplify the measurement of dimensions, a model for each type of joint space can be set up. To determine machining forces a lot of experiments have to be done, since the forces are not only dependent on the machining processes, and dimensions of the tools, but also on the tissues, which usually have an inhomogeneous structure. Specific machining forces and rules of thumb can be set up as is common for the machining of materials in the industry. The set up of tissue models could probably help to assess the sensitivity of different variables, which helps to focus on the most important variables. The results presented in this thesis can be used as a pilot study.

Irrigation

The irrigation process of joints appeared to be difficult to capture. This topic needs further investigation to explore the situations that occur during an operation, and to extend the current experimental set up to assess the influence on joint irrigation of additional conditions, that are more related to the clinical practice. Thereto, the physical joint model needs to be rebuilt to obtain a more realistic representation of a joint. It is expected that this approach will eventually lead to one protocol and configuration of the complete irrigation system to achieve optimal arthroscopic view for all operative procedures.

Subtalar joint

The proposed technique to perform subtalar arthrodesis via a minimal access approach needs to be further developed. No attention was paid so far to the optimal temporary fixation. The part of the technique that was developed so far could eventually be adapted for the placement of a subtalar implant. In the changing health care, the patient might no longer be satisfied when a joint is fused. A proper functioning subtalar prosthesis has not been developed so far. A sequel research proposal has been submitted for the development of a subtalar prosthesis.

Appendix 4A.1:

Anthropometric data that were used to determine the dimensions and range of motion of the measurement device. The values are given in mm.

author	[illegible]		[illegible]		[illegible]		[illegible]		[illegible]	
population	[illegible]		[illegible]		Dutch Students (age 18-25)		[illegible]		[illegible]	
	[p5]	[p95]	[p5] female	[p95] male	[p5] female	[p95] male	[p5] f/m	[p95] f/m	min	max
foot length (mm)	250	300	224	292						
foot width (mm)			82	110						
knee width (mm)					97	124				
buttock-knee length - buttock heel length (mm)			102	121	102	139	101	107		
knee height (mm)	505	600	474	606	436	561				
lower leg length (popliteal height) (mm)	410	505	351	476			369	491		
lateral malleolus height (mm)			52	76	65	86			61	83
medial malleolus height (mm)									73	96
shoulder width biacromial (mm)	360	430			317	432	336	438		
malleoli width (mm)									60.5	77

author	[illegible]	
population	[illegible]	
	[p5]	[p95]
angle of gait (degrees)	7.7	9.7
step width (mm)	210	530

Appendix 4A. 2:

Dimensions for the measurement system derived from the anthropometric data of Appendix 4A.1. The values are given in mm.

required dimensions derived from anthropometric data	average	min	max	dimensions for measurement device	length part of construction	range of motion
width of foot position (mm)	194			distance between medial malleoli	180	
				width of platform	415	
foot length (mm)	267	224	300	length platform	300	
lower leg length (mm)	434	351	505	lower leg device	510	100
knee width (mm)	112	97	139	location rods lower leg device	160	50
height lateral ankle malleoleus (mm)	70	52	86	size plate lateral malleoli	40	70 +/-20
height medial ankle malleoleus (mm)	85	73	96	size plate medial malleoli	40	80 +/-20
malleoli width (mm)	68	60.5	77	location plates		68 +/- 20

Appendix 5A:

Overview of automated arthroscopy irrigation systems that are currently on the market.

Brand	Type	Patent	Pressure range (mmHg)	Maximum flow rate (ml/min)	Location pressure sensor	Independent flow control	Special features	Remarks
Aesculap	PG 030 Fluid2		0 to 500	1000	?	?		
Apex	Universal Irrigation System	US 5460490	20 to 150	2000	scope-sheath or cannula	yes		Can also be used without pressure sensor
Davol Inc.	HydroFlex AD	US 5322506	0 to 300	2500	?			
Dyonics/ S&N	Data could not be found							
FMS	FMS DUO +	amongst others EP 0306445, US 4902277	23 to 338	1000	inflow tube	yes		
Karl Storz	Arthropump plus		0 to 200	1000	?	yes	Optional external pressure transducer for intra-articular pressure measurement	
Linvatec	87k Fluid Control System		5 to 100	1350	scope sheath or cannula	yes		
Richard Wolf	Data could not be found							

Appendix 5B:

Results of experiments to determine influence factors on irrigation.

Results of measurements performed to determine the influence of several factors *(Table 5.4.1)* on the flow pattern in a joint. The measurements were performed with an experimental set up that included a physical joint model. For each factor the results are presented and discussed.

Different combinations of inflow and outflow portal (Figure 5B.1)

- With the help of an ANOVA single factor test *($p < 0.05$)* it was calculated that the irrigation times of different inflow and outflow combinations are significantly different.
- Column 2 gives the fastest t_{blue} and t_{clear}. The difference between this combination and others is that the diameter of the cannula, which is used as inflow, is larger than the effective diameter of the scope-sheath combination, which is used as inflow for the other configurations. Due to this fact the inflow velocity is at least six times lower than for the other in-outflow combinations. The low velocity causes the kinetic energy of the inflow stream to be low, which results in the fact that the direction of this flow can be easier influenced, leading to a faster distribution of the blue ink. Furthermore, the pressure in the joint model at the inflow location for Column 2 is higher than the pressure in the joint model at the outflow, which causes a flow from inflow towards outflow portal.
- Leakage of the joint model occurred during experiments of Column 2 *(leakage mainly along the clamps of the joint model (Figure 5.4.1))*, and Column 4 *(mainly between shaver and sleeve)*.
- The irrigation times of Column 3 are actually incomparable with the rest of the combinations, because there is no partition in the sheath housing the scope. This causes a part of the colored ink to flow directly through the sheath without entering the joint model. Thus, less ink is introduced in the joint model. It is difficult to estimate the fraction of colored ink that does not enter the model, but the fraction is assumed to be approximately 30%. If this is the case then the irrigation times of Column 3 are about the same is for Columns 1 and 4.
- Column 1 is a regularly used setting in clinical practice, and scores the worst.
- From the results, it can be concluded that the diameter of the inflow is an important factor for the design of a new sheath. It appears that the increasing cross-sections result in faster irrigation times.

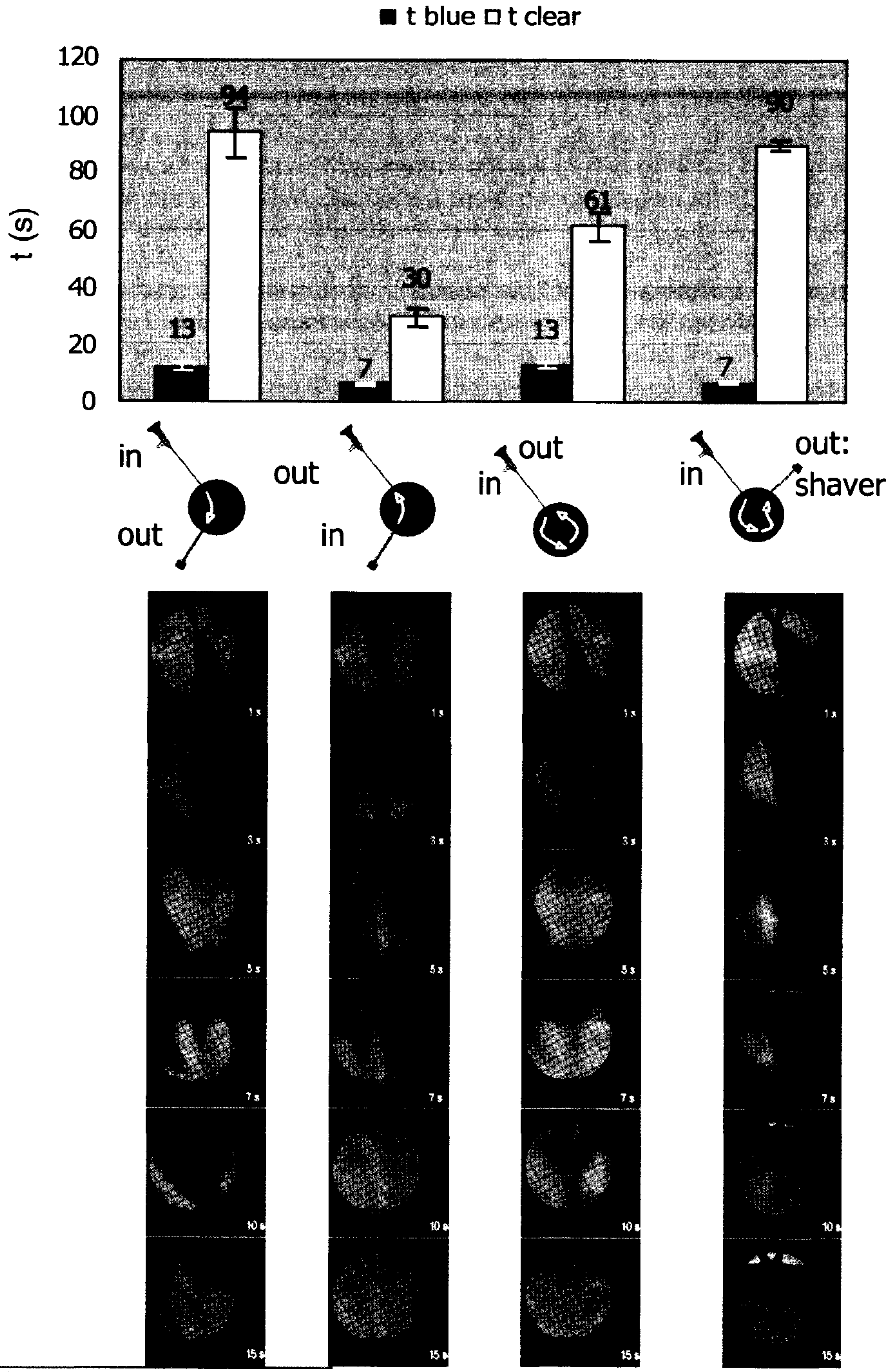

Figure 5B.1
Irrigation times for different inflow and outflow combinations (Table 5.4.1).

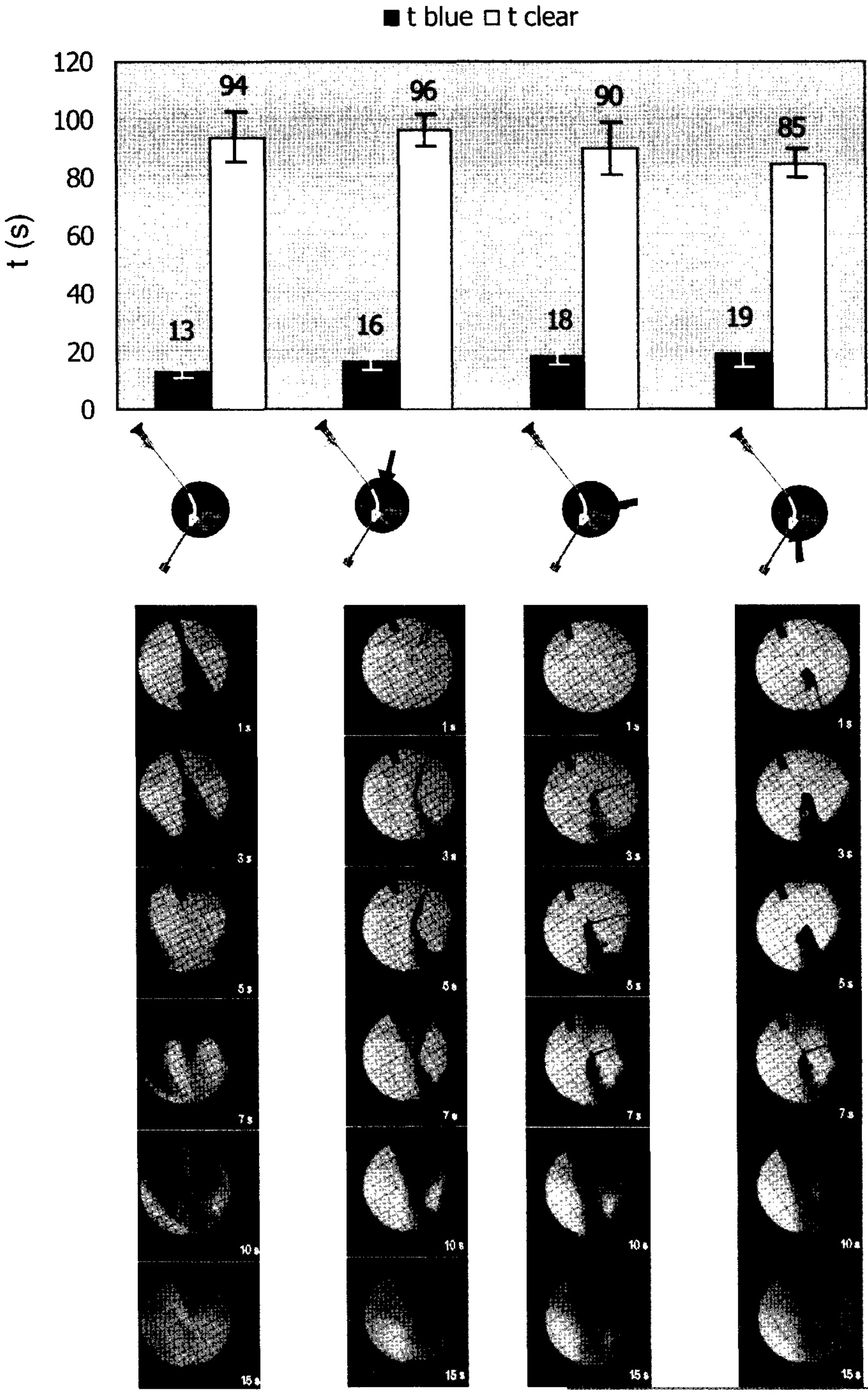

Figure 5B.2
Irrigation times for bleedings occurring at different locations (indicated by arrows) vs. no bleeding (column one) (Table 5.4.1).

Different locations of bleedings (Figure 5B.2)

- With the help of an ANOVA single factor test *($p < 0.05$)* it was calculated that the irrigation times of different bleeding locations are significantly different for t_{blue} and not significant for t_{clear}.
- When a bleeding takes place near the inflow portal *(Column 2)* the blood *(ink)* spreads quickly, because it is carried along with the main inflow stream. For the two other conditions *(Columns 3 and 4)* the blood stream is pushed backwards by the dominant inflow stream.
- t_{clear} is not significant which implies that the surgeon can freely choose the position of the outflow cannula in order to remove the blood.

Different pressure and flow combinations (Figure 5B.3)

- With the help of an ANOVA single factor test *($p < 0.05$)* it was calculated that the irrigation times of different pressure and flow combinations are significantly different. However, Columns 1 and 2, Columns 3 and 4, and Columns 5 and 6 do not differ significantly.
- This division of the pressure and flow combinations in three groups can be explained as follows. At the first group *(Columns 1 and 2)* initial set pressures are too low to create a good flow pattern. At the second *(Columns 3 and 4)* the initial set pressure creates at least a positive pressure in the joint model, which causes the irrigation times to decrease with approximately 30%. In the third group *(Columns 5 and 6)* the flow rate is increased and accordingly the irrigation times are further decreased. This outcome was expected *(Section 5.3)*. There is one disadvantage when suction is performed using this automated pump. During suction with an increased flow rate, the pressure in the knee joint model decreases significantly and can reach underpressures of 200 mmHg. This willlead to the joint collapse, and is highly undesirable.

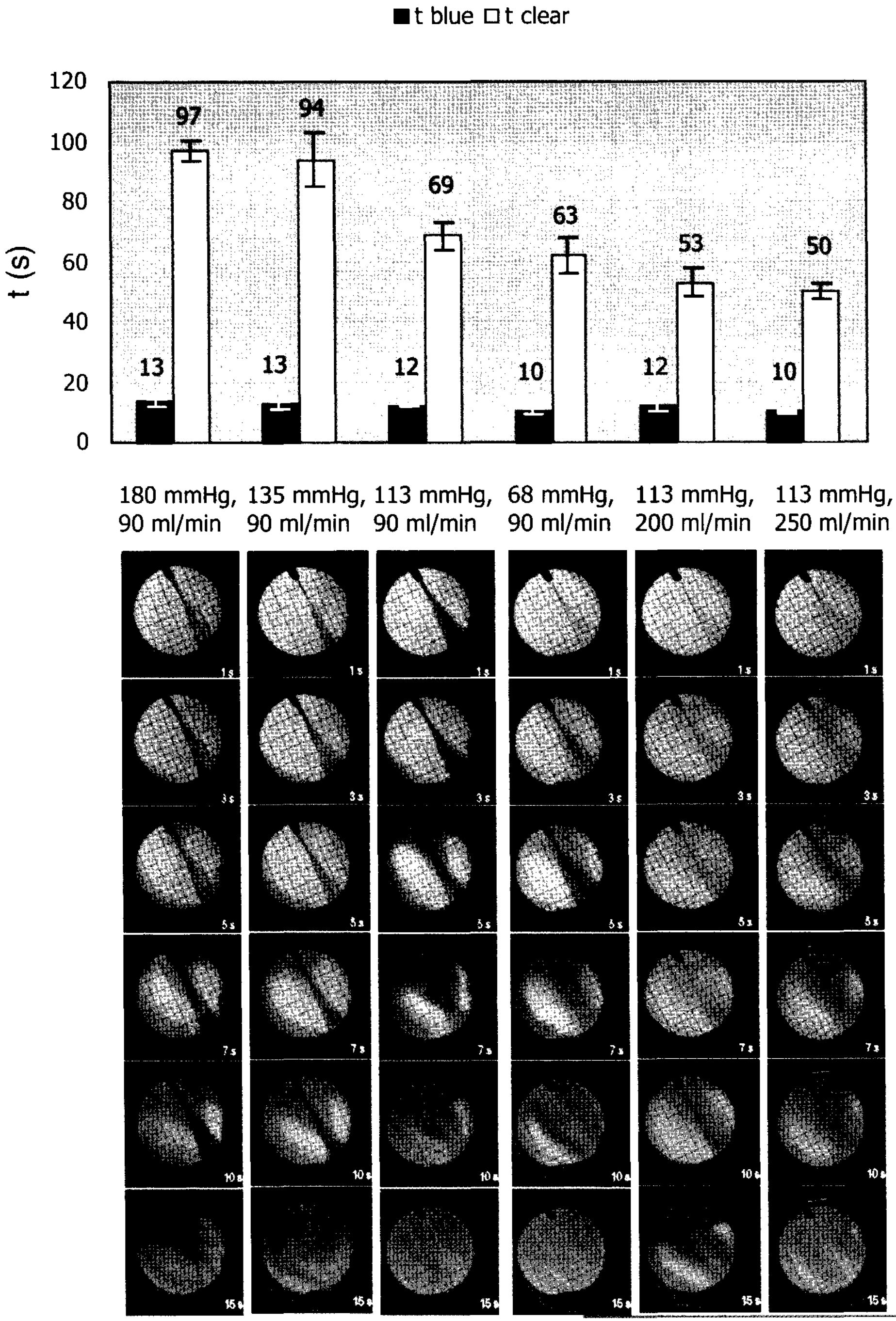

Figure 5B.3
Irrigation times for different pressures and flows (Table 5.4.1).

Figure 5B.4
Irrigation times for different conditions using a shaver as outflow portal (Table 5.4.1).

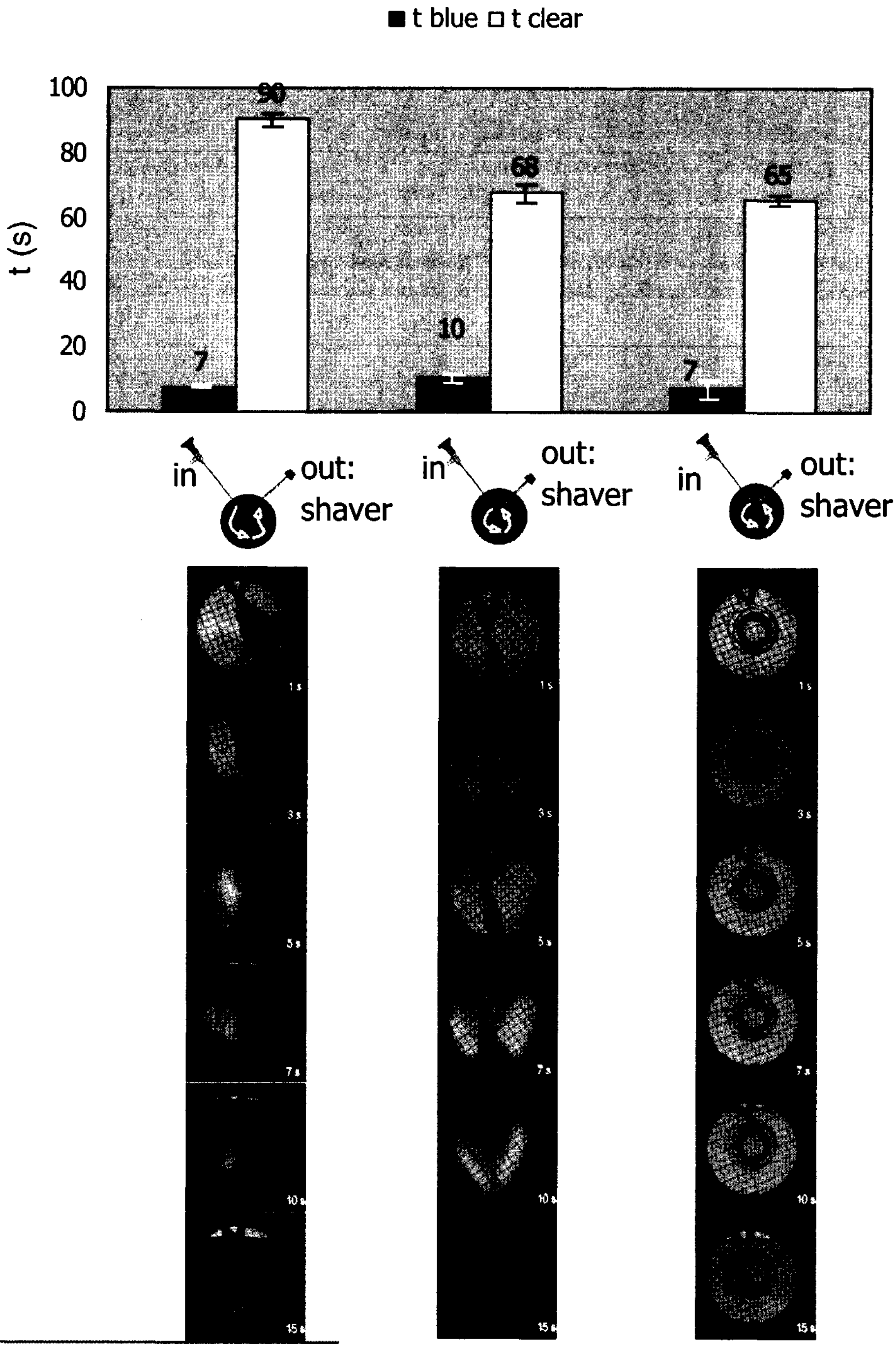

Different conditions when using the shaver as outflow portal (Figure 5B.4)

- With the help of an ANOVA single factor test *($p < 0.05$)* it was calculated that the irrigation times of the different shaver conditions are significantly different, accept for Column 2 in comparison with Column 3.
- The usage of the 3D-profile does not give a significantly different result. This implies that the configuration of the joint model is sufficient so far to test several factors.
- When the shaver is used as outflow, leakage occurs along the shaver and sleeve. This together with the occurrence of underpressure in the joint model enables air to be sucked into the knee joint model. This causes the water level to drop to the position of the shaver tip. This effect influences the flow pattern.

Different directions of inflow stream (Figure 5B.5)

- With the help of an ANOVA single factor test *($p < 0.05$)* it was calculated that the irrigation times of the different directions of the inflow stream are significantly different.
- The configuration in Column 3 *(90°)* produces the fastest irrigation times. This is probably due to the fact that the tip of the sheath-scope combination for this configuration is located towards the center of the joint model. The inflow stream at the 90° location is less influenced by the walls of the sleeve *(Figure 5.4.1)* than it is in the other configurations, and therefore the inflow stream looses its kinetic energy at a slower speed.
- The inflow angle of 15° is a configuration that surgeons do not often use for treatment. For this condition, the inflow stream is directed along the wall of the rubber sleeve *(Figure 5.4.1)* and only mixes slowly to reach the entire joint model.
- With the results if these tests, it can be concluded that the inflow direction has influence on the irrigation of joints. This leads to the requirement that the inflow should take place towards the open space in a joint.

Figure 5B.5
Irrigation times for different angles of the inflow portal (Table 5.4.1).

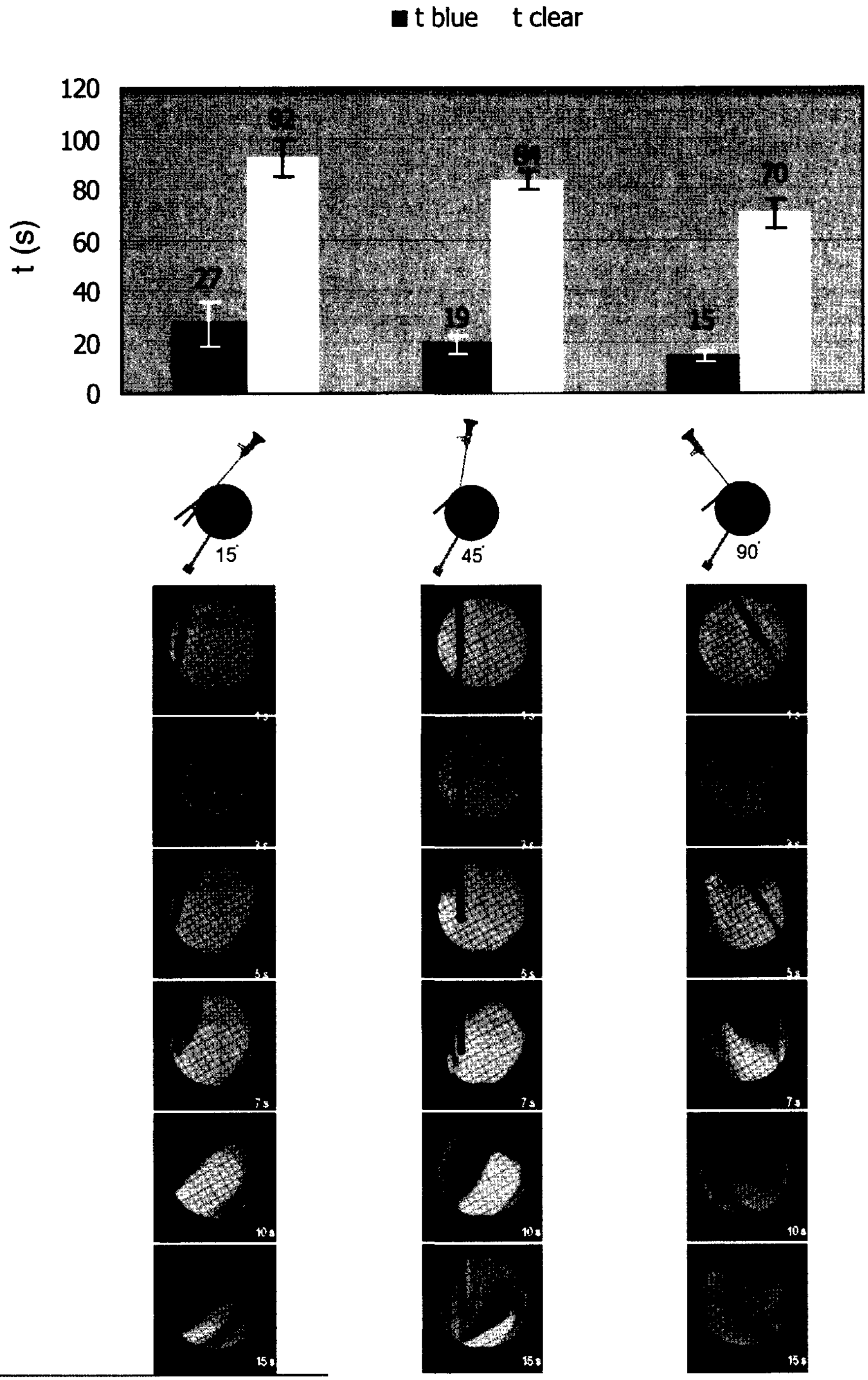

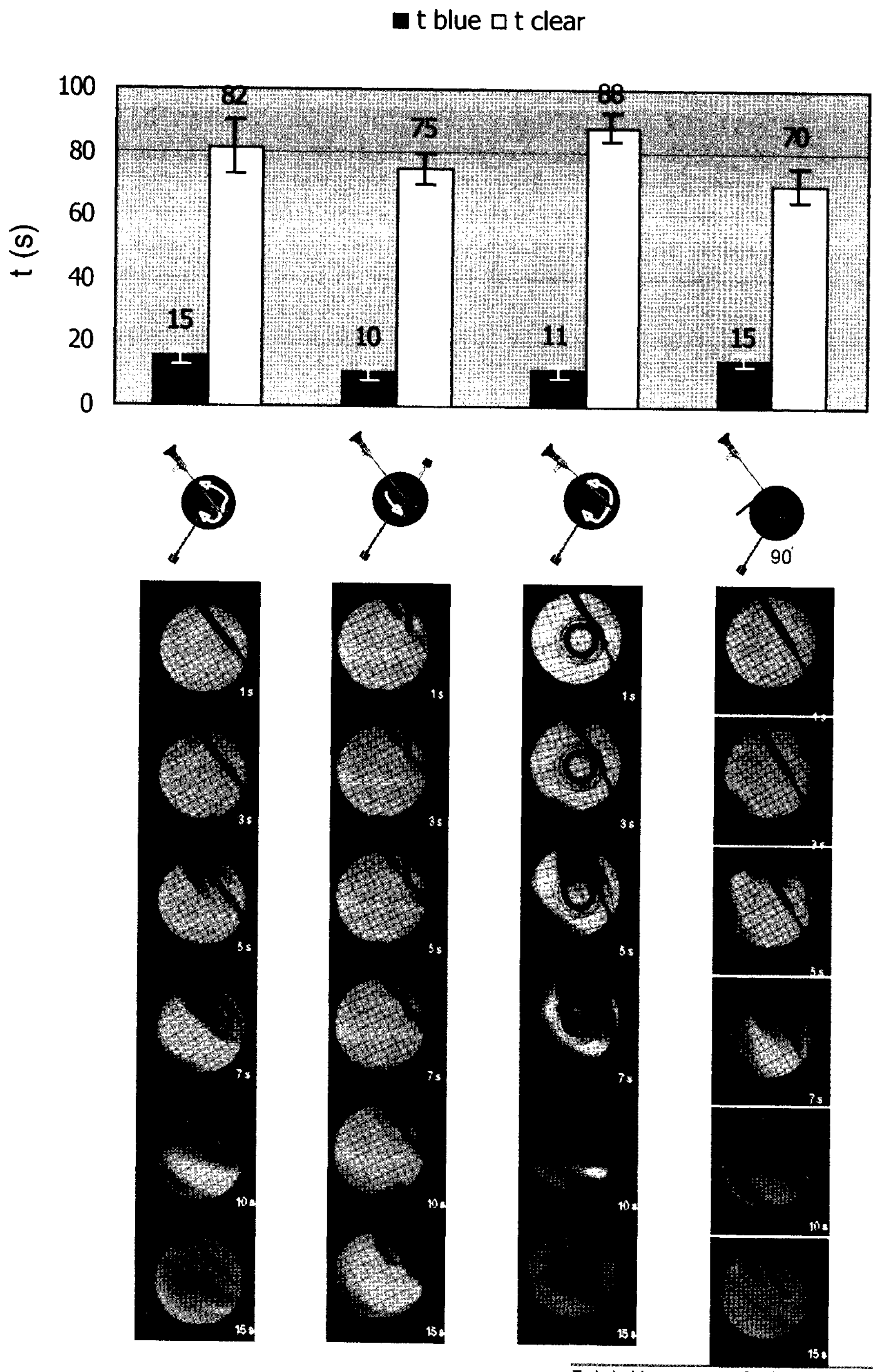

Figure 5B.6
Irrigation times for different conditions (Location 1, Instrument, 3D-profile, Inflow angle at 90°) when the inflow portal is located at Location 1 (Table 5.4.1).

Different effects in location 1 (Figure 5B.6)

- With the help of an ANOVA single factor test *($p < 0.05$)* it was calculated that the irrigation times of the different conditions at Location 1 in the joint model *(Table 5.4.1)* are significantly different, except for the comparison of Column 1 with Column 3.
- The scope-sheath combination of the configuration with an instrument placed in front of the scope-sheath combination is at a slightly different position in the joint model. It appears that the presence of an instrument in front of the tip of inflow sheath has a positive effect on the irrigation time. This is due to the fact that the inflow stream is redirected towards the center of the joint model which causes the colored ink to mix faster. This result is clinically important, because it often happens that an instrument is used in front of the camera.
- For Columns 1 and 4, the scope-sheath combination location differed only slightly, but the average irrigation times are significantly different. An explanation could be that the scope-sheath combination in Column 1 is so close to the wall of the rubber sleeve *(Figure 5.4.1)* that this greatly influences the mixing of colored ink in the entire joint model.
- The presence of a 3D-profile does not effect the irrigation times.

Different effects in location 2 (Figure 5B.7)

- With the help of an ANOVA single factor test *($p < 0.05$)* it was calculated that the irrigation times of the different conditions at Location 2 in the joint model *(Table 5.4.1)* are not significantly different.
- A closer look at the results shows that the presence of an instrument in front of the inflow stream has positive effect on the irrigation times.
- For Columns 1 and 4, the location of the scope-sheath combination differs slightly, which results in a difference of 10 seconds in the average irrigation time t_{clear}. Since this result is consistent with the result found for different conditions tested in Location 1, it strengthens the argument that the inflow stream is greatly influenced by when it comes into contact with the wall of the sleeve.
- If the results of Location 1 and 2 are compared *(Figures 5B.6 and 5B.7)*, the following aspects become apparent:
  1. The irrigation times at Location 2 are about 20 seconds larger. Therefore, Location 2 is not favorable. This is due to the fact that in this location the distance between the glass plates is smaller than for Location 1 and the sheath-scope tip is closer to the wall of the sleeve.
  2. The location of the inflow stream influences the flow patterns and irrigation times. Care should be taken in the design of a new sheath that treatments take place in different operating areas in a joint.

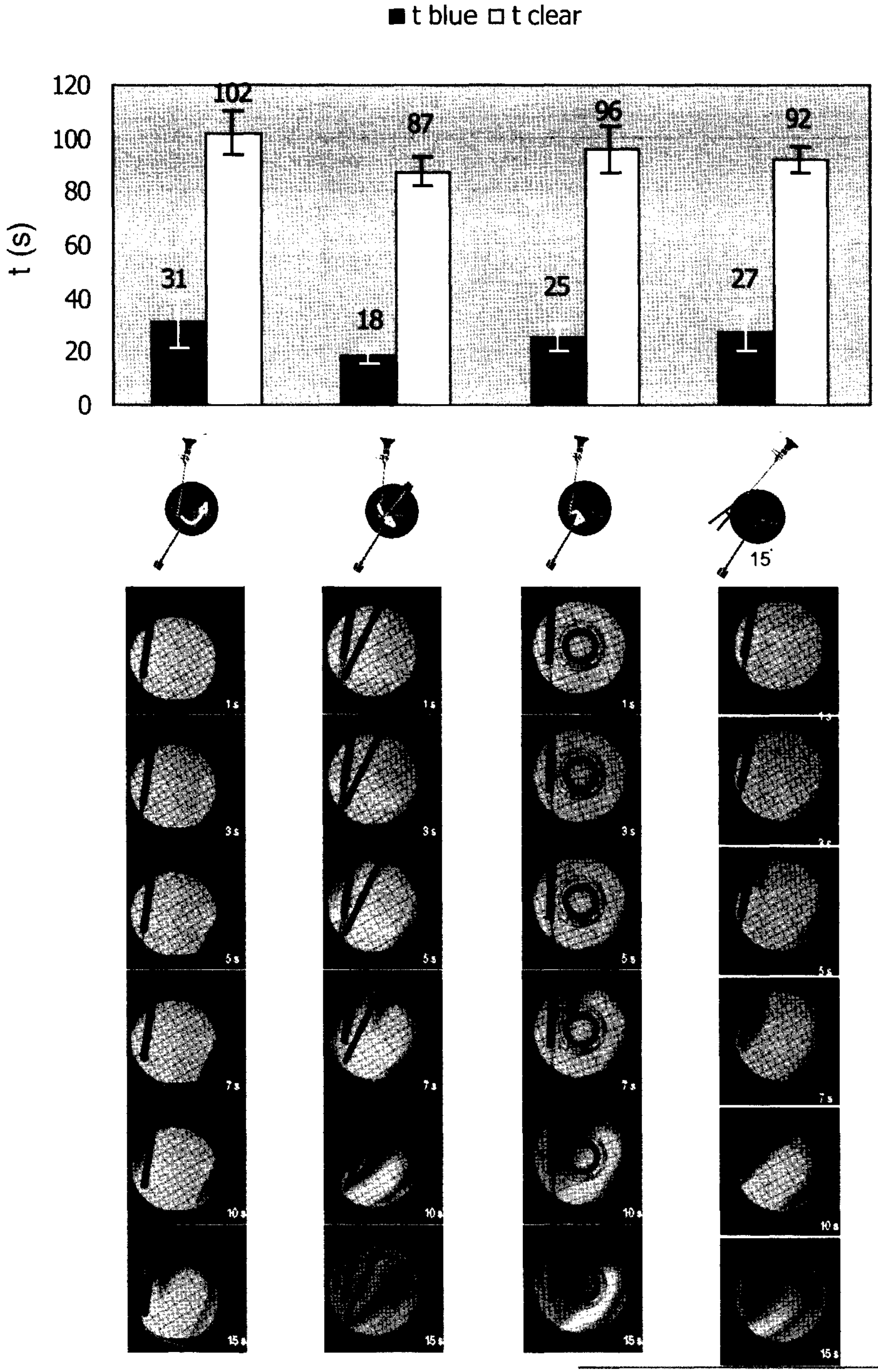

Figure 5B.7
Irrigation times for different conditions (Location 2, Instrument, 3D-profile, Inflow angle at 15°) when the inflow portal is located at Location 2 (Table 5.4.1).

List of terms

Arthrodesis	The surgical fixation of a joint by a procedure designed to accomplish fusion of the joint surfaces by promoting the proliferation of bone cells
(Articular) cartilage	A flexible, somewhat elastic, semitransparent substance with an opalescent bluish tint on the articular surface of bones in synovial joints
Acromioplasty	Surgical removal of the anterior hook of the acromion to relieve mechanical compression of the rotator cuff during movement of the shoulder joint
Allograft	A graft of tissue between individuals of the same species but of disparate genotype
Anterior	Situated in front of an organ
Anthropometry	The science which deals with the measurement of the size, weight, and proportions of the human body
Arthritis	Inflammation of a joint
Arthroscope	An endoscope for examining the interior of a joint and for carrying out diagnostic and therapeutic procedures within the joint (Figure 1.1.2)
Arthroscopy	Examination of the interior of a joint with an arthroscope
Autograft	A graft of tissue derived from another site in the body of the organism receiving it
Calcaneocuboid joint	Joint between the calcaneus and cuboid bone
Calcaneus	Heel bone, the irregular quadrangular bone at the back of the tarsus (Figure 3.0.1)
Cancellous bone	Spongy or lattice-like structured bony tissue
Cannula	A tube for insertion into a joint (Figure 1.1.5)
Carpal tunnel release	Cutting of the passage for the median nerve and the flexor tendons in the wrist
Concave	Resembling the hollowed inner surface of a segment of a sphere
Condyle	A rounded projection on a bone usually for articulation with another bone
Convex	Resembling a segment of the external surface of a sphere
Contralateral	Situated on or affecting the opposite side
Cortical bone	Bone of the nature of a cortex or bark
Cruciate ligament	A cross shaped ligament with the knee joint (Figure 6.0.1)
Curette	Spoon-shaped instrument for removing material from the wall of a cavity or other surface (Figure 1.1.3)
Debridement	Mechanical removal of tissue, usually sharp dissection
Ergonomics	The science relating to man and his work, embodying the anatomic, physiologic, psychologic, and mechanical principles affecting efficient use of human energy
Eversion	Consists of elevation of the lateral border of the foot and depression of the medial border of the foot (Figure 3.1.1)
Feedback loop	Causes the system to take corrective action if the output signal deviates from the input signal
Fibula	The outer and smaller of the two bones of the leg (Figure 3.0.1)
Fluoroscopy	Examination by means of a device used for inspection of deep structures by means of x-rays
Force	The action of one body on another, whereby the force tends to move a body in the direction of its action
Frontal	Denoting a longitudinal plane of the body at right angles to the sagittal plane
Hydrodynamic pressure	Pressure which is solely the result of the presence of flow
Hydrostatic pressure	Pressure caused by differences in height between two locations
Intraclass coefficient	A coefficient that is used to assess agreement of quantitative measurements in the sense of consistency and conformity
Inversion	Consists of elevation of the medial border of the foot and depression of the lateral border of the foot (Figure 3.1.1)
Ipsilateral	Pertaining to the same side, as opposed to contralateral
Irrigation system	System that pumps liquid through a joint for irrigation during arthroscopy (Figure 1.1.4)
Lateral	Denoting a position farther from the midline of the body or of a structure
Lateral decubitus	Lying on the side

Ligament	A band of fibrous tissue that connects bones or cartilages, serving to support and strengthen joints
Malleolus	The rounded processes of the tibia and fibula on either side of the ankle joint
Medial	Denoting a position closer to the midline of the body or of a structure
Meniscectomy	Excision of an intra-articular meniscus as in the knee joint
Meniscus	A crescent-shaped disk of fibrocartilage attached to the superior articular surface of the tibia (Figure 5.0.1)
Neurovascular	Pertaining to both nervous and vascular elements
Osteochondral defect	Damage to a bone and its cartilage
Ovoid	Egg-shaped
Peroperative	Occurring during a surgical operation
Posterior	Situated in the back part of a structure
Postoperative	Occurring after a surgical operation
Preoperative	Occurring before a surgical operation
Probe	Instrument used to examine tissue (Figure 1.1.3)
Prone	Lying face downward
Punch	Instrument used to cut soft tissue (Figure 1.1.3)
Reflex sympathetic dystrophy	A series of changes caused by the sympathetic nervous system following muscle sprain, bone fracture or injury to nerves or blood vessels
(Fluid) Restriction	Resistance to flow
Rotator cuff	A musculotendinus structure about the capsule of the shoulder joint, providing mobility and strength to the shoulder joint
Sagittal	Denoting any vertical plane that passes through the body and divides the body in left and right portions
Shear stress	Stress cause by forces trying to cut through material
Sheath	A tube for insertion into a joint that projects the arthroscope (Figure 1.1.5)
Soft tissue endoscopy	Surgery performed via small incisions in artificial cavities created in the body
Steinmann pin	A long slender rod for the fixation of the ends of fractured bones
Stiffness	The ability of a structure to resist changes in shape
Subchondral bone	Bone beneath a cartilage
Subtalar joint	Joint between the calcaneus and talus located in the hindfoot (Figure 3.0.1)
Supine	Lying with the face upward
Synovia	A transparent alkaline viscid fluid, resembling the white of an egg, secreted by the synovial membrane, and contained in joint cavities
Talonavicular joint	Joint between the talus and the navicular bone
Talus	Ankle bone, the highest of the tarsal bones and the one which articulates with the tibia and the fibula to form the ankle joint (Figure 3.0.1)
Tibia	The inner and larger bone of the leg below the knee (Figure 3.0.1)
Tourniquet	An instrument for the compression of a blood vessel by application around an extremity to control the circulation and prevent the flow of blood to or from the distal area (Figure 1.1.7)
Unilateral	Affecting but one side
Valgus	Denoting a deformity in which the angulation of the part is away from the midline of the body
Varus	Denoting a deformity in which the angulation of the part is toward the midline of the body

List of symbols and abbreviations

α_1	(°)	Flexion angle of lower leg (Figure 6.2.4)
α_2	(°)	Abduction angle of lower leg (Figure 6.2.4)
α_3	(°)	Rotation angle of the lower leg (Figure 6.2.4)
$\alpha_{correction}$	(°)	Difference between the measured hindfoot angle and the required hindfoot angle (Figure 4.1.3)
α_{tip}	(°)	Maximum opening angle of steerable punch
β_1	(°)	Angle between the portal and the line through the starting point of the contour of the subtalar joints space and the top of the same contour (Figure 4.2.4)
β_2	(°)	Angle of the arc of the contour of the subtalar joint space fitted with by a circle (Figure 4.2.4)
δ_i	(mm)	Deflection of a segment i of the flexible shaft (Figure 4.3.3)
δ_p	(mm)	Displacement of the curved flexible shaft out of the plane of curvature (Figure 4.3.3)
Δl	(mm)	Distance per sample (Section 4.2)
ΔP_n	(mmHg)	Pressure difference over part n
ε_{max}	-	Maximum allowable strain of the superelastic alloy
η	(kg/ms)	Dynamic viscosity
φ_1	(°)	Portal angle in transversal plane (Figure 4.2.2)
φ_2	(°)	Portal angle in mediolateral view (Figure 4.2.2)
φ_3	(°)	Crest angle: angle between the crest line and the axis along the medial side of the calcaneus (Figure 4.2.1)
φ_{slice}	(°)	Slicing angle of the blade (Figure 4.2.5)
υ	(m^2/s)	Kinematic viscosity
θ_i	(rad)	Angle of a segment of the flexible shaft when it is in a curved position (Figure 4.3.3)
θ_{tot}	(rad)	Angle of the flexible shaft when it is in a curved position (Figure 4.3.3)
ρ	(kg/m^3)	Density
ρ_{bend}	(mm)	Radius of curvature of one flexible segment of the flexible shaft (Figure 4.3.2)
τ	(MPa)	Shear stress
$\tau_{massive}$	(MPa)	Shear stress resulting from punching with a massive tube
$\tau_{meniscus}$	(MPa)	Shear stress resulting from punching with a hollow sharp edged tube
A_{bone}	(mm^2)	Cross-sectional area of a bone chip that is sliced
AP	-	Automated pump (Figure 1.1.4)
A_{shear}	(mm^2)	Circumferential surface along which tissue is punched with the tip of a punch
b_{bone}	(mm)	Width of a bone or cartilage chip that is sliced (Figure 4.2.5)
b_{k1}	(mm)	Shortest axis of the ellipse that covers the size of the knee joint in the transversal plane (Figure 6.2.2)
b_{k2}	(mm)	Shortest axis of the ellipse that covers the size of the cruciate ligaments in the transversal plane (Figure 6.2.2)

b_l	(mm)	Width of lateral meniscus (Figure 6.2.2)
b_m	(mm)	Width of lateral meniscus (Figure 6.2.2)
b_{ml}	(mm)	Width of the middle horn of the lateral meniscus (Figure 6.2.2)
b_{mm}	(mm)	Width of the middle horn of the medial meniscus (Figure 6.2.2)
b_p	(mm)	Distance between two knee portals in frontal plane (Figure 6.2.2)
b_{talus}	(mm)	Width of the talus at the subtalar joint height (Figure 4.1.3)
b_{tip}	(mm)	Width of a punch tip
D	(mm)	Diameter of a tube
d_c	(mm)	Fitted diameter of the curved contour from a portal to a point on the subtalar joint surface (Figure 4.2.4)
d_{flex}	(mm)	Diameter of the superelastic wire of the flexible shaft (Figure 4.3.2)
$D_{hydraulic}$	(mm)	Hydraulic diameter of a noncircular tube
D_{in}	(mm)	Inner diameter of a tube
D_{out}	(mm)	Outer diameter of a tube
$d_{ring\ in}$	(mm)	Inner diameter of a ring of the flexible shaft (Figure 4.3.2)
$d_{ring\ out}$	(mm)	Outer diameter of a ring of the flexible shaft (Figure 4.3.2)
d_s	(mm)	Diameter of the cylinder which is part of the model for the subtalar joint surface (Figures 4.2.1)
E_{flex}	(GPa)	Modulus of elasticity of the flexible segments of the flexible shaft
E_i	(GPa)	Modulus of elasticity of a material i
E_{ring}	(GPa)	Modulus of elasticity of a ring of the rings of the flexible shaft
$E_{slice/drill/mill}$	(J)	Applied energy to work tissue according to the working process of slicing, drilling or milling
f	(mmHg·s/m3) or (mmHg·min/ml)	Constant restriction factor which is dependent on the geometry and fluid characteristics
F	(N)	Force applied to the end of the flexible shaft with which the bending stiffness are calculated
F_{drill}	(N)	Maximum force needed to drill tissue
$F_{meniscus}$	(N)	Force needed to punch meniscus tissue
F_{mill}	(N)	Maximum force needed to mill tissue
F_{slice}	(N)	Maximum force needed to slice tissue
G_{flex}	(GPa)	Shear modulus of elasticity of the flexible segments
G_{ring}	(GPa)	Shear modulus of elasticity of the rings
GP	-	Gravity pump (Figure 1.1.4)
h_{bone}	(mm)	Thickness of a bone or cartilage chip that is sliced (Figure 4.2.5)
$h_{bonegraft}$	(mm)	Height of the bone graft that is placed in the subtalar joint to establish hindfoot correction (Figure 4.1.3)
$h_{cartilage}$	(mm)	Thickness of the cartilage of the subtalar joint
h_k	(mm)	Minimal height of the knee joint space during surgery
h_m	(mm)	Height of the peripheral rim of the menisci

h_s	(mm)	Height of the subtalar joint space
h_{wing}	(mm)	Height of the side-wings of a ring of the flexible shaft (Figure 4.3.2)
$J_{flex,y}$	(mm^4)	Moment of inertia of the flexible segments of the flexible shaft in y-direction
$J_{flex,z}$	(mm^4)	Moment of inertia of the flexible segments of the flexible shaft in z-direction
$J_{flex,p}$	(mm^4)	Polar moment of inertia of the flexible segments of the flexible shaft
$J_{ring,y}$	(mm^4)	Moment of inertia of the rings of the flexible shaft in y-direction
$J_{ring,z}$	(mm^4)	Moment of inertia of the rings of the flexible shaft in z-direction
$J_{ring,p}$	(mm^4)	Polar moment of inertia of the rings of the flexible shaft
k	-	Number of rings of the flexible shaft, which is equal to the number of flexible segments
K_y	(N/mm)	Bending stiffness of the flexible shaft in y-direction (Figure 4.3.2)
K_z	(N/mm)	Bending stiffness of the flexible shaft in z-direction (Figure 4.3.2)
K_p	(N/mm)	Bending stiffness of the flexible shaft, which is firstly bent to its required maximum in y-direction and than is bent in the transversal direction (Figure 4.3.3)
l_{bone}	(mm)	Length of a bone or cartilage chip that is sliced or length of hole that is drilled in tissue (Figure 4.2.5)
l_{crest}	(mm)	Length of the crest line on the posterior facet. The crest line is the line that divides the posterior facet of the subtalar joint in a posteromedial and an anterolateral portions (Figure 4.2.3)
$l_{diagonal}$	(mm)	The horizontal distance of anterolateral portal in the knee joint to the medial minimum thickness of the knee joint space (Figure 6.2.2)
$l_{ellipse1}$	(mm)	Largest axis of the ellipse with which the posterior facet of the subtalar joint is modeled (Figure 4.2.1)
$l_{ellipse2}$	(mm)	Smallest axis of the ellipse with which the posterior facet of the subtalar joint is modeled (Figure 4.2.1)
l_{flex}	(mm)	Distance in between the rings of the flexible shaft (Figure 4.3.2)
l_i	(mm)	Length of segment i of the flexible shaft (Figure 4.3.3)
l_{k1}	(mm)	Largest axis of the ellipse that covers the size of the knee joint in the transversal plane (Figure 6.2.2)
l_{k2}	(mm)	Largest axis of the ellipse that covers the size of the cruciate ligaments in the transversal plane (Figure 6.2.2)
		Width of the space in between the two menisci that contains the cruciate ligaments in the knee (Figure 6.2.2)
l_l	(mm)	Length of the lateral meniscus (Figure 6.2.2)
l_m	(mm)	Length of the medial meniscus (Figure 6.2.2)
L_n	(m)	Length of a part n
l_{ring}	(mm)	Length of a ring of the flexible shaft (Figure 4.3.2)
l_{shaft}	(mm)	Length of the flexible part of the new instrument (Figure 4.3.2)
$l_{straight}$	(mm)	The horizontal distance of anterolateral portal in the knee joint to the lateral minimum thickness of the knee joint space (Figure 6.2.2)
l_{tip}	(mm)	Length of a punch tip

l_{wing}	(mm)	Length of one side-wing
$P_{slice/drill/mill}$	(J/s)	Power required to work tissue with the working process of slicing, drilling or milling
P_n	(mmHg)	Actual pressure at a location n
Q	(m^3/s)	Fluid flow
Re	-	Reynold's number
R_n	(mmHg_min/ml)	Fluid restriction of a part n
SD	-	Standard deviation
t_{blue}	(s)	Time until view is completely colored blue
t_{clear}	(s)	Time until view is completely clear
$v_{average}$	(m/s)	Average velocity of fluid
v	(mm/s)	Slicing velocity or push velocity of working bench for drilling and milling
V_{bone}	(mm^3)	Volume of removed bone
$V_{postfacet}$	(mm^3)	Total volume of cartilage and subchondral bone that has to be removed from the posterior facet
y_{flex}	(mm)	Distance between the from the neutral y-axis to the y-axis at the centroid of half the area of a flexible segment (Figure 4.3.2)
y_{max}	(mm)	Largest distance in y-direction to the neutral axis
y_{wing}	(mm)	Distance between the from the neutral y-axis to the y-axis at the centroid of the area of the a side-wing (Figure 4.3.2)

Summary

In the past twenty-five years orthopaedic surgery has made tremendous progress by means of the development of arthroscopy, which implies that the operation is performed by means of small incisions in the skin. Surprisingly, in the development of arthroscopic instruments sufficient communication between the users and the developers or manufactures is often missing, leaving unsolved problems or leading to the development of less functional instruments. The point of attention in this thesis is the improvement of the techniques and instruments in the field of arthroscopy. To achieve improvements, the philosophy is emphasized that developments should be guided by clinical practice and requirements of surgeons. A thorough analysis of requirements and inconveniences will lead to the development of useful and simple instruments that can be straightforwardly controlled.

To achieve the involvement of surgeons, a method called clinically driven approach was used and further developed. Observations during operations as well as literature studies give the engineer sufficient knowledge to communicate with a surgeon. Observations in combination with discussions with a small group of surgeons lead to the identification of six clinically relevant research topics in the arthroscopic field. These are optimization of a clear view during operations, development of soft-tissue endoscopy, development of a minimal access technique for subtalar arthrodesis, optimization of the treatment of osteochondral defects, development of multifunctional instruments, and development of criteria and instruments to determine the quality of a procedure. By means of an interview with a larger population of surgeons, and other criteria, it was decided to focus on a *minimal access technique for subtalar arthrodesis, the optimization of the view in joints, and the development of a sideways steerable punch (cutter for meniscus tissue).*

For the subtalar arthrodesis *(fusion of the joint in the hindfoot)* current limitations were determined with a thorough literature study from a technical point of view, and discussion with surgeons. This lead to the proposal of a new technique that consists of A) a posterior minimal access approach with the patient in prone position, B) determination and verification of an adequate correction peroperatively with the help of a new measurement device, C) removal of cartilage and subchondral layers by means of a new instrument that preserves the complex joint shape and creates smooth bleeding contact surfaces to enhance optimal fusion, and D) temporary fixation by means of a new fixation device that is placed in the optimal fixation location and transfers its fixation function gradually to the fusion bridges of the bone. Two new instruments were developed to start the implementation of this new technique. The first instrument is a measurement system with which the amount of anatomic correction of the hindfoot can be determined pre-, per- and postoperatively, with adequate accuracy and reproducibility. The second instrument is a flexible drill that can be passively steered through the subtalar joint. To be able to dimension this instrument, technical data of the subtalar joint were determined experimentally. The prototype needs fine tuning to meet all requirements.

To improve the arthroscopic view during operations two aspects were investigated. Insight in the behavior of two types of irrigation systems was established by the formulation of a descriptive model of the complete irrigation system consisting of pump, tubes and joint, as well as

experiments were performed with an experimental set up including a physical joint model. This lead to the set up of guidelines for usage of the irrigation pumps. Furthermore, design criteria were assessed for the development of a new sheath to improve irrigation of the joints during an operation. A prototype of the new sheath proves that the irrigation times are significantly decreased.
To improve the reachability in the knee joint, a new arthroscopic cutter was developed that has a sideways steerable tip. Attention was paid to both the tip and the handle of the instrument. To dimension the tip, technical data of the knee joint and cutting force of meniscus tissue were determined. For the handle design, theory on ergonomics was applied. Experiments with a prototype of the handle support the concept of a sideways steerable punch and show that the new handle increases comfort.
In conclusion, a new design approach was set up to improve the arthroscopic techniques and instruments. The requirements and solutions that were derived with this new approach appear to be useful for usage in clinical practice.

Samenvatting

In de afgelopen vijfentwintig jaar heeft de orthopedische discipline een grote vooruitgang geboekt door de ontwikkeling van arthroscopie, waarbij operaties aan gewrichten plaatsvinden via kleine incisies in de huid. Het is dan ook verbazingwekkend dat in de ontwikkeling van instrumenten voor deze arthroscopische technieken voldoende communicatie tussen chirurg en ontwerper ontbreekt, waardoor klinische problemen niet worden opgelost of minder functionele instrumenten worden ontwikkeld. In deze dissertatie wordt de aandacht gericht op de verbetering van arthroscopische technieken en instrumenten. Om dit te bereiken worden ontwikkelingen in gang gezet die gestuurd zijn door vragen uit de klinische praktijk en behoeften aangegeven door chirurgen. Een uitgangspunt daarbij is dat analyse van de behoeften en ongemakken van chirurgen zal leiden tot de ontwikkeling van functionele en eenvoudige instrumenten die gemakkelijk te bedienen zijn.

Om the betrokkenheid van de chirurgen te waarborgen is de zogenaamde klinisch gedreven aanpak gebruikt en verder ontwikkeld. Observaties en literatuurstudies geven de ontwerper voldoende kennis om te kunnen communiceren met de chirurg. Observaties in combinatie met discussies gevoerd met een kleine groep chirurgen heeft er toe geleid zes klinisch relevante probleemgebieden aan te duiden. Deze zijn de optimalisatie van het zicht tijdens operaties, de verdere ontwikkeling van weke-delen-endoscopie, de ontwikkeling van een minimaal invasieve techniek voor de subtalaire arthrodese procedure, de optimalisatie van kraakbeenbehandeling, de ontwikkeling van multifunctionele instrumenten, en de ontwikkeling van methoden om de kwaliteit van de operatie te kunnen controleren. Gebaseerd op een interview met een grotere populatie chirurgen, en andere criteria, is besloten drie klinische probleemgebieden verder te onderzoeken: *de ontwikkeling van een minimaal invasieve techniek voor de subtalaire arthrodese procedure, de optimalisatie van het zicht tijdens operaties, en de ontwikkeling van een zijwaarts stuurbare kniptang.*

Voor de subtalaire arthrodese *(fusie van het gewricht in de achtervoet)* zijn de huidige beperkingen in kaart gebracht door middel van een literatuurstudie gedaan vanuit een technisch perspectief en discussie met chirurgen. Dit leidde tot het opzetten van een nieuwe techniek voor de subtalaire arthrodese, die bestaat uit A) toegang via een twee-portal achterste enkelbenadering waarbij de patiënt in buikligging is geplaatst, B) bepaling en verificatie van een correcte anatomische uitlijning van de achtervoet ten opzichte van het onderbeen peroperatief met behulp van een nieuw meetsysteem, C) verwijdering van kraakbeen en subchondrale botlaag door middel van een nieuw flexibel instrument dat de gewrichtsvorm in stand houdt en gladde contact oppervlakken creëert voor optimale vergroeiing, en D) tijdelijk fixatie tot vergroeiing door middel van een nieuw fixatiemiddel dat geplaatst wordt in een optimale locatie en verliest zijn functie naarmate de vergroeiing vordert.

Twee nieuwe instrumenten zijn ontwikkeld om een begin te maken met de implementatie van deze nieuwe techniek. Het eerste instrument is een meetsysteem waarmee de mate van correctie van de achtervoet bepaald kan worden pre-, per-, en postoperatief. Daarnaast geeft het meetsysteem voldoende nauwkeurigheid en reproduceerbaarheid ten opzichte van de huidige meettechniek. Het tweede instrument is een flexibel boortje dat passief gestuurd kan

worden door het gewricht, en vanwege zijn flexibiliteit alle locaties in het gewricht kan bereiken. Om dit instrument te dimensioneren zijn technische gegevens over het subtalaire gewricht experimenteel bepaald. Beide prototypen verdienen nog enige aanpassingen om aan alle eisen te voldoen, maar er zijn geen conceptuele veranderingen nodig.
Om het zicht tijdens operaties te verbeteren zijn twee aspecten bestudeerd. Inzicht is verkregen in het gedrag van de twee veelgebruikte spoelsystemen door middel van het opstellen van een beschrijvend model bestaande uit de pomp, de inflow- en uitflowslang, de canule, de scope en het gewricht. Daarnaast zijn ook experimentele metingen met een eenvoudig gewrichtsmodel en klinische metingen gedaan. Dit heeft geleid tot het opstellen van richtlijnen voor het gebruik van de verschillende spoelsystemen, en het opstellen van ontwerp criteria voor de ontwikkelingen van een nieuwe canule. Testen met het prototype van de nieuwe canule laten zien dat ongeveer twee keer zo snel gespoeld kan worden dan met de huidige configuratie.
Om de bereikbaarheid in het kniegewricht te verbeteren is een nieuwe kniptang ontworpen die een zijwaarts stuurbare tip heeft. Aandacht is besteed zowel aan de ontwikkeling van de tip als aan de ontwikkeling van een nieuw handvat. Om de instrumenttip te dimensioneren zijn technische gegevens van het kniegewricht en de benodigde snijkracht experimenteel bepaald. Voor het ontwerp van het handvat zijn theoretische richtlijnen uit de ergonomie toegepast. Experimenten ondersteunen het concept van de stuurbare kniptang en laten zien dat het nieuwe handvat comfortabel is.
Concluderend is een nieuwe ontwerp aanpak toegepast ten behoeve van het verbeteren van arthroscopische technieken en instrumenten. Ontwerpeisen en de daaruit volgende oplossingen blijken functioneel te zijn voor gebruik in de klinische praktijk.

Acknowledgement

Ofcourse this thesis could not have been created without the support, the contributions, the help and the love of colleagues, friends and family. Therefore, it is no more than logical that I would like to express a few words of sincere thankfulness.
Starting with the MISIT-4 group, my nearest colleagues: Peter Pistecky, Just Herder, Petr Havlik, Hans de Visser, Wouter Sjoerdsma and Albert van der Pijl. It was so inspiring to work with you guys. You taught me about setting up and performing scientific research in combination with the design components, which were characteristic for our type of discipline. Peter, our Daddy, was always around when I needed you. You were so committed to get the best out of us with all your sharp comments and suggestions, your experience and your belief that we are really working on something important. Indeed, you were sometimes a bit of a father figure also in the personal communication. I am honoured to have worked with you, and thank you so much for our last retreat at the Final Czech. Just man, in what direction would I have gone without your knowledge, intelligence and endless support. I could have imagined a better mentor and friend in one person than you. You encouraged me to stay, and start research, and I must say in those four years I have grown a lot. Thank you.
Hans and Petr, we jumped in this adventure together as three freshmen at the same time. Our mutual stimulation and a little bit of competition, I think, brought us a higher level. Petr, I have great respect for you, and Hansie: catch me if you can. Albert, you joined our team later in the process, and after a challenging start, we managed to work in pleasant cooperation together. Without your work, I could not have done as much experiments, and construct actual prototypes to test al the ideas. Wouter unfortunately you chose to leave our little group. I have great memories being with you and Hans all over the country to visit surgeons.
The magic hands and practical advices of John Dukker made it possible to actually fabricate the instruments, which were sketched sometimes on just a piece of paper. Leo Brinkman always tried to take care that all the facilities were present for us in order to work optimally. It was a great pleasure to work in such a unique group, the Man-Machinesystems group, with so many intelligent and funny colleagues especially Mark, Jules, Martijn, Richard, Karen, Evelien and Stepan. Mark and Dirk Jan, thanks for your advices concerning statistics.
Thanks to the endless talks and meetings and discussions with Prof. van Dijk I quickly was introduced in the field of arthroscopy. I eagerly have learnt from your knowledge and experience, which were of key importance in many stages of my project. Thanks is given to the ORCA group of the Orthopaedic Department in the Academic Medical Center (AMC) in Amsterdam. Especially to Marga Lammerts and Leendert Blankevoort who introduced me in the AMC, and made sure that all facilities and material to perform experiments were available. It was a very pleasant and efficient cooperation. In addition to this I would like to thank Peter Scholten for his medical advice and participation in several of the experiments.
Frits de Vries, Joris Jaspers, Petro Broekhuizen en Ron van Driel from the MTO did a perfect job in the construction and fabrication of prototypes and additional supplementary devices.
Ofcourse, I could not have done so many projects without the help and inspiration of many students. Susanne and Roger, you both set up de basic concept for a steerable arthroscopic

cutter. With a few more steps to be taken to implement the instrument. Leonie, you came as an unexpected change in my life. We had a challenging project to work, especially because of the tide schedule and the number of people involved, when performing measurements in the operating room. You were an eye opener to many aspects in life, and we became close friends. Thank you for your humor and amazing viewpoints, I hope to share many more good moments with you. Lizette, Martin and Job, cofounders, of the already famous measurement system, your enthusiasm and fascination for musculoskeletal structures started many interesting discussions. Furthermore, I would like to thank Hans Lambrechts from Smith and Nephew BV and Freek Kroneman from Arsis Medical BV for making available arthroscopic cutters and an automated irrigation system, respectively. Special thanks to the surgeons who offered me the opportunity to observe their operations and discuss their techniques: dr. M. Myerson (Baltimore, USA), dr. R.O. Lundeen (Indianapolis, USA). dr. Tasto (San Diego, USA), dr. J.H. Barentz (Alkmaar), dr. A.F.W. Barnaart, (Amersfoort), dr. C.M. Douw (Maastricht), dr. W.F. Draijer (Sittard), dr. E.R. Hammacher (Nieuwegein), dr. M.P. Heijboer (Rotterdam), dr. T. Hogervorst (Amsterdam), dr. T.V.S. Klos (Eindhoven), dr. D. van der Schaaf (Nijmegen), dr. M. Schaffroth (Amsterdam), dr. J.L. Schoen ('s Hertogenbosch), dr R.L. Te Slaa (Delft), dr. H.M. Schüller (Leiden), dr. B. verbiest (Capelle a/d Ijssel), dr. H. Verburg (Delft), dr. M. Wijbenga (Nijmegen), dr. D.B. Wouters (Tilburg),

All the subjects who participated in the experiments to test the prototypes are thanked as well especially, Peter Scholten, Job, Lizette, Leonie, Mark, Hanneke, Leonne, Jan Willem, Tessa, Theo, Eveline, Saskia, and Susanne.

Special thanks go to Hans Dusée who was so brave to agree to do the lay out of this thesis, which has cost him many hours of work. The effort was worth it as can be seen.

Lastly, I would like to thank my family and friends who were always there to support me in any kind of way. Mum and dad, thank you for your stimulation to explore and improve my capabilities and for leading me in the right direction. I never say it in such words, but I love you guys. My sister, Michelle, always there at a slight distance, but clear as crystal. My closest friends, Leonie, Lianne, Just, Marte and Suus, how lucky I was to met all of you who give me such depth and joy in life. I hope, I can be a good friend to all of you as you are to me.

Curriculum Vitae

20 October 1975	Born in Teheran, Iran.
1987-1993	Gymnasium-B attended at the Stella Maris college in Meerssen.
1993-1998	MSc study Mechanical Engineering at the Delft University of Technology. Graduated with honours at the Man-machine Systems and Control group, headed by Prof. dr. ir. H.G. Stassen. Title of MSc-thesis: Design, actuation and control of an anthropometric robot arm.
1998-2003	PhD study at the Man-machine Systems and Control group, as a part of the MISIT (Minimally Invasive Surgery and Interventional Techniques) program, which is performed in cooperation with the Department of Orthopedics at the Academic Medical Center, headed by Prof. dr. C.N. van Dijk.

Figure 5.1.1

To the left: picture of the gravity pump (GP) on the left side and the automated pump FMS duo+ (AP) in the operation room.

To the right: picture of the tubes connected to the sheath-scope combination, and the cannula. The pressure sensors are also indicated (s1, s2, s3, s4).

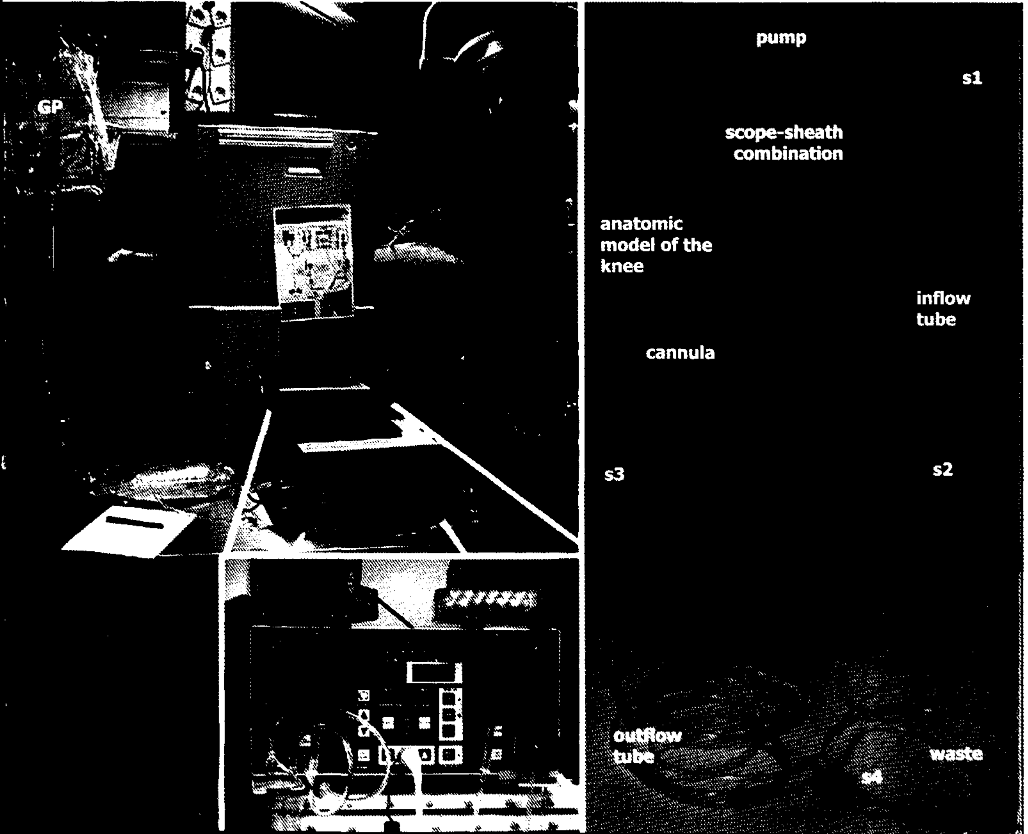

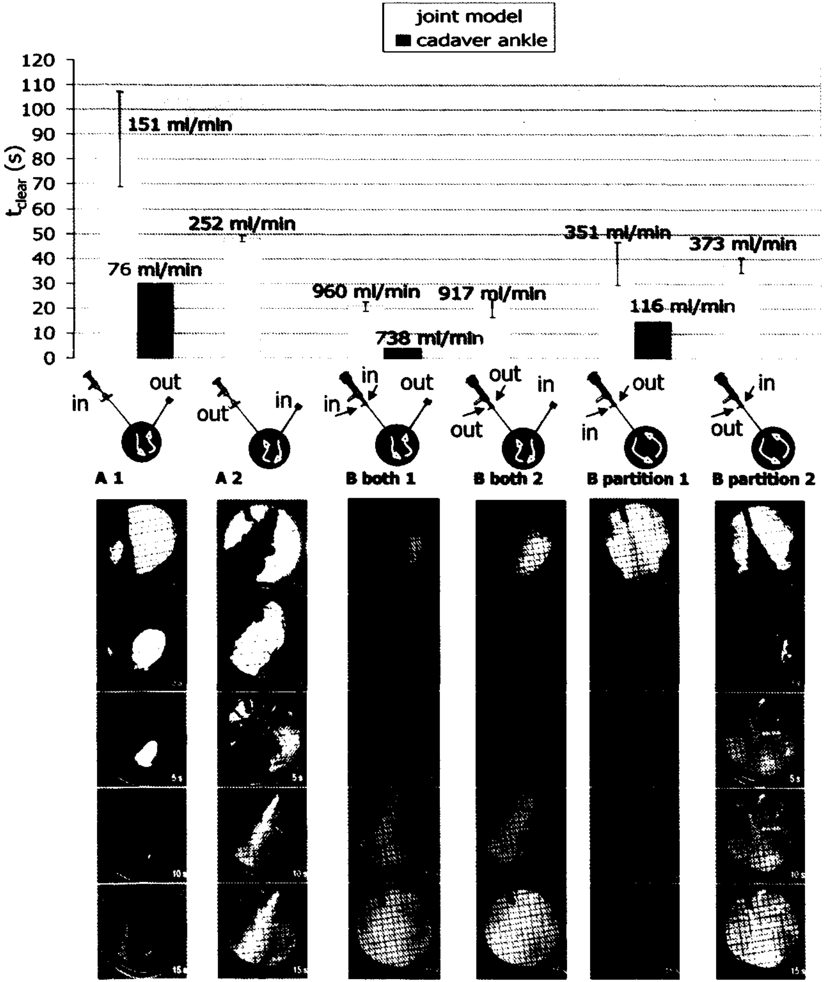

Figure 5.4.6

The irrigation times (t_{clear}) for the conditions indicated in Table 5.4.3 are presented. The experiments are performed by means of a gravity pump and the joint model (white columns) as well as a gravity pump and a cadaver ankle (black columns). It was not possible to test all conditions in the cadaver ankle. For each condition the average flow is given above each column. To visualize the flow patterns pictures are given of each condition at 1 s, 3 s, 5 s, 10 s, and 15 s after injection of the colored ink using the joint model.

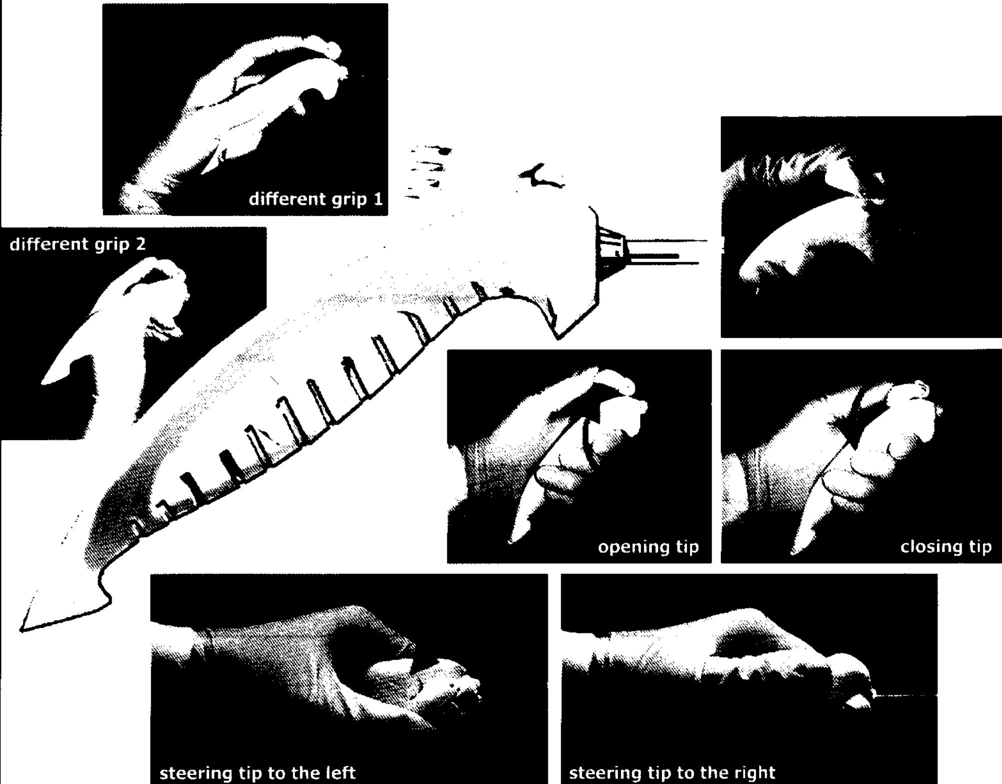

Figure 6.4.1

Design of the ergonomic handle. In the picture a drawing of the concept is presented as well as the working principle of the lever. It is shown that the handle can be held and operated with different grips.

ISBN 90-370-0200